ORSAY
N° d'ordre : 2564

THESE

PRESENTEE

A L'UNIVERSITE DE PARIS SUD
CENTRE D'ORSAY

POUR OBTENIR

LE GRADE DE DOCTEUR ES SCIENCES PHYSIQUES

par

Jean-Michel NEUMANN

ETUDE PAR RESONANCE ET RELAXATION MAGNETIQUES NUCLEAIRES DE LA CONFORMATION ET DE LA STRUCTURE DYNAMIQUE DE MONO-, OLIGO-, ET POLYNUCLEOTIDES EN SOLUTION AQUEUSE

Soutenue le 26 mars 1982, devant la Commission d'Examen

MM.	HELENE	Président
	ROQUES	
	SAUZADE	
	GUERON	Examinateurs
	PAILLOTIN	
	TRAN DINH	

ORSAY

N° d'ordre : 2564

THESE

PRESENTEE

A L'UNIVERSITE DE PARIS SUD

CENTRE D'ORSAY

POUR OBTENIR

LE GRADE DE DOCTEUR ES SCIENCES PHYSIQUES

par

Jean-Michel NEUMANN

ETUDE PAR RESONANCE ET RELAXATION MAGNETIQUES NUCLEAIRES DE LA CONFORMATION ET DE LA STRUCTURE DYNAMIQUE DE MONO-, OLIGO-, ET POLYNUCLEOTIDES EN SOLUTION AQUEUSE

Soutenue le 26 mars 1982, devant la Commission d'Examen

MM.	HELENE	Président
	ROQUES	
	SAUZADE	
	GUERON	Examinateurs
	PAILLOTIN	
	TRAN DINH	

UNIV.
LEIDEN
BIBL.

REMERCIEMENTS

Cette thèse a été préparée au Département de Biologie du Centre d'Etudes Nucléaires de Saclay, dans le service de Biophysique. Je remercie MM. J. COURSAGET et G. PAILLOTIN de m'avoir accueilli dans leurs laboratoires.

MM. C. HELENE, B. ROQUES et M. SAUZADE m'ont fait l'honneur d'examiner ce travail, qu'ils en soient vivement remerciés.

J'adresse mes remerciements à M. M. GUERON qui a accepté d'être le rapporteur de ce travail et dont l'aide, ainsi que celle de ses collaborateurs du laboratoire de Biophysique de l'Ecole Polytechnique ont été précieuses.

Mes remerciements vont tout particulièrement à M. S. TRAN-DINH qui est à l'origine de ce travail et dontl'appui et les conseils ont été constants.

Je voudrais exprimer ici ma reconnaissance à MM. T. HUYNH-DINH et J. IGOLEN ainsi qu'à leurs collaborateurs de l'Unité de Chimie Organique de l'Institut Pasteur et à MM. S.K. KAN et G. SIMMONOT de l'Institut d'Electronique Fondamentale du centre d'Orsay pour leur collaboration très fructueuse.

Je suis reconnaissant à tous ceux qui, dans le département de Biologie, m'ont aidé, en particulier M. J. THIERY et mon collègue de laboratoire M. J. BORREL.

Enfin, que tous ceux qui ont contribué à la réalisation matérielle de ce mémoire, en particulier Mme BONGUET, trouvent ici l'expression de mes remerciements.

Digitized by the Internet Archive
in 2026

https://archive.org/details/IA41547306_0045

TABLE DES MATIERES

Pages

INTRODUCTION 1

Chapitre I - GENERALITES 11

A. Structure et conformation des acides nucléiques 13

A.I. Conformation des nucléosides et nucléotides 13

A.II. Structure et conformation des acides nucléiques 16

B. Méthodes de RMN appliquées à l'étude de la conformation et de la structure dynamique des acides nucléiques en solution 21

B.I. Déplacement chimique 22

B.II Couplage scalaire spin-spin 25

B.III. Relaxation longitudinale des spins 1/2 27

Chapitre II - ETUDE DE LA CONFORMATION ET DE LA FLEXIBILITE DES MONO- et DINUCLEOSIDES MONOPHOSPHATES EN SOLUTION 45

A. Comparative conformations of Uridine and Pseudouridine and their derivatives, Neumann, J.M., Bernassau, J.M., Guéron, M. and Tran-Dinh, S. (1980) Eur. J. Biochem. 108, 457. 47

Pages

B. Conformation and flexibility of GpC and CpG in neutral aqueous solution using ^{1}H-NMR and relaxation times measurements, Neumann, J.M., Guschlbauer, W. and Tran-Dinh, S. (1979) Eur. J. Biochem. 100, 141. 65

C. ^{1}H-NMR comparative studies of dinucleoside monophosphates. Influence of different factors on the conformational equilibria of nucleoside and dinucleoside monophosphates in aqueous solution, Tran-Dinh, S., Neumann, J.M. and Borrel, J. (1981) Biochim. Biophys. Acta 655, 167. 81

Chapitre III - ETUDE DE LA CONFORMATION ET DE LA STRUCTURE DYNAMIQUE DES OLIGONUCLEOTIDES EN SOLUTION 109

A. Methods for the assignment of DNA fragment proton resonances. ^{1}H-NMR spectra of dApTpGpT and dApCpApTpGpT, Tran-Dinh, S., Neumann, J.M., Huynh-Dinh, T., Igolen, J. and Kan, S.K. (1982) Org. Mag. Res. 18, 148. 111

B. ^{1}H-NMR and relaxation studies of dApTpGpT in neutral aqueous solution, Neumann, J.M., Huynh-Dinh, T., Kan, S.K., Genissel, B., Igolen, J. and Tran-Dinh, S. (1982) Eur. J. Biochem. 121, 317. 121

C. ^{1}H-NMR studies of helix-coil transition, conformation and dynamic structure of the self-complementary deoxyhexanucleotide dApCpApTpGpT in aqueous solution, Tran-Dinh, S., Neumann, J.M., Huynh-Dinh, T., Genissel, B., Igolen, J. and Simmonot, G. (1982) Eur. J. Biochem. (sous presse). 139

Pages

Chapitre IV - ETUDE DE LA CONFORMATION ET DE LA STRUCTURE DYNAMIQUE DES POLYNUCLEOTIDES EN SOLUTION 167

A. Conformation and dynamic structure of Poly I in neutral aqueous solution by ^{1}H, ^{2}H, ^{13}C and ^{31}P NMR spectroscopy, Neumann, J.M. and Tran-Dinh, S. (1981) Biopolymers 20, 89.

B. ^{1}H-NMR comparative studies of polynucleotides : conformation and dynamic structure of Poly U and Poly C in neutral solution, Neumann, J.M. and Tran-Dinh, S. (1982) Biopolymers 21, 383. 197

CONCLUSION 223

INTRODUCTION

Les acides ribonucléiques (ARN) et déoxyribonucléiques (ADN) constituent avec les protéines les éléments essentiels de la vie cellulaire ; ils assurent i) le stockage et la transmission de l'information génétique (réplication de l'ADN), ii) le décodage de cette information réalisé par l'intermédiaire des ARN. Rappelons que ces macromolécules sont des polymères linéaires formés de l'enchaînement de résidus nucléotides, eux-mêmes constitués de trois unités : base, sucre (ribose dans les ARN, 2'-déoxyribose dans les ADN) et phosphate.

La compréhension de leurs fonctions biologiques est étroitement reliée à la connaissance de leur structure moléculaire et depuis les travaux de Watson et Crick [1], dont le modèle en double hélice de l'ADN rend compte de la possibilité d'autoduplication, les études physicochimiques de la conformation et de la structure des acides nucléiques ont pris un essor considérable.

La structure des fibres d'acides nucléiques a fait l'objet de travaux en diffusion des rayons X de plus en plus raffinés [2-4] et parallèlement, la structure des monocristaux de nucléosides et nucléotides a été abondamment étudiée par diffraction des rayons X [5-7]. Dans ces derniers, il a été observé que le cycle du sucre (ribose ou déoxyribose) présente deux conformations principales, soit la forne N (C_3, endo), soit la forme S (C_2, endo) et que la base est en général, orientée en *anti* par rapport au sucre. L'étude des fibres

d'acides nucléiques a révélé deux grandes familles de structure en double hélice droite, appelées A et B. Dans la première, le cycle du sucre a la conformation N et l'hélice contient onze paires de base par tour, dans la seconde le cycle a la conformation S et l'hélice contient dix paires de base par tour ; dans les deux cas, les bases sont orientées en *anti* par rapport au sucre et appariées par liaisons hydrogènes suivant le modèle de Watson et Crick. Récemment, des structures hélicoïdales différentes des formes standards A et B ont été observées : en particulier, le fragment d'ADN $d(GC)_3$ cristallise sous forme d'une double hélice gauche, appelée forme Z, dans laquelle les résidus G adoptent les conformations *syn*, N et les résidus C les conformations *anti*, S [8]. Ce résultat, avec d'autres [9, 10] montrent qu'il existe une plus grande variété de conformations qu'on ne le soupçonnait auparavant. Par ailleurs, les structures bicaténaires ne sont pas les seules observées ; il existe un certain nombre d'ADN et d'ARN (de virus en particulier) sous forme monocaténaire et dans les ARN de transfert, qui ne comptent qu'une centaine de résidus et dont la structure est l'une des plus connue à l'heure actuelle [11, 12] on rencontre, outre des structures bicaténaires de type A, des boucles et des terminaisons monocaténaires.

En solution, la conformation et la structure des acides nucléiques et de leurs constituants sont moins bien connues ; les mouvements moléculaires compliquent singulièrement la tâche. Cependant, durant ces dernières années, les techniques de spectroscopie se sont rapidement développées et en particulier les études en résonance magnétique nucléaire (RMN) prennent une extension importante. La mesure des couplages entre les protons du sucre permet d'étudier sa conformation et leur analyse montre que le cycle du sucre des nucléosides et nucléotides isolés n'est pas rigide mais qu'il existe un équilibre entre les deux formes N et S dont on peut mesurer les proportions relatives [13-15]. Dans le même temps, la détermination de l'orientation de la base par rapport au sucre, dans ces mêmes molécules, fait l'objet

de nombreuses études utilisant des techniques de RMN diverses : déplacements chimiques des protons du sucre [16, 17], couplage J[^{13}C-^{1}H] [18, 19] effet des ions de terre rare [20] et relaxation magnétique (effer Overhauser [21-23] et temps de relaxation T_1 [24, 25]). A l'exception de la relaxation, ces méthodes mesurent des effets indirectement liés à la conformation, ce qui rend leur interprétation délicate ; leurs conclusions sont en faveur de l'orientation en *anti* de la base, probablement influencées par les conformations observées à l'état cristallin. Cependant, les mesures de l'effet Overhauser [21-23] mettent directement en évidence la flexibilité de la base par rapport au sucre et montrent que la conformation *syn* existe en solution. L'étude de l'équilibre *syn/anti* par effet Overhauser et T_1, avec et sans deutération sélective, se poursuit dans notre laboratoire et constitue une partie importante de ce travail. Pourtant ce n'est que petit à petit que les résultats obtenus par les méthodes indirectes évoquées plus haut sont interprétés en terme d'équilibre *syn/anti* [26-28] et il faut attendre l'exemple spectaculaire de l'orientation en *syn* des résidus G dans le fragment d'ADN $d(GC)_3$ cristallisé (voir ci-dessus et réf. 8) pour que le consensus se fasse autour du principe de l'équilibre *syn/anti* des nucléotides en solution.

La mise en évidence de la flexibilité des nucléotides en solution, inhérente aux mouvements N$\rightleftharpoons$S et *syn* $\rightleftharpoons$ *anti* (ainsi qu'à la rotation autour du groupe phosphate) conduit à se demander quelles sont les conformations prédominantes, comment et dans quelles circonstances varient les proportions des conformations en équilibre, comment se modifient les conformations et la flexibilité de ces composés lorsqu'ils sont insérés dans des chaînes de plus en plus longues dont la structure secondaire va de la pelote statistique aux complexes multicaténaires, quel est le type de structure réalisée en solution. Sans doute, les variations de conformations et de flexibilité constituent un mode d'expression de l'information biologique et interviennent dans les mécanismes de reconnaissance protéines-acides nucléiques.

Pour répondre à ces questions et à cause de la complexité des molécules d'acides nucléiques, nous avons choisi de travailler sur des composés modèles que l'on peut grouper en trois familles : les mono- et dinucléotides, les oligonucléotides et les polynucléotides synthétiques.

L'étude des mono- et dinucléotides a pour but de connaître toutes les possibilités de conformation des unités qui composent ARN et ADN et constitue une base préalable pour étudier des molécules plus complexes. Elle comporte la détermination des conformations prédominantes et des facteurs qui influencent l'équilibre conformationnel : structure chimique (nature de la base, du sucre, position du groupe phosphate) et conditions physicochimiques (température, pH, concentration, force ionique).

Le deuxième groupe, les oligonucléotides, concerne des composés qui ne comportent pas plus d'une dizaine de résidus et dont la séquence peut être auto-complémentaire, ce qui les rend susceptibles de former des structures bicaténaires. Ces molécules modèles permettent d'une part d'étudier en fonction de la nature de la séquence, le processus de formation-dissociation des complexes bicaténaires et le type de structure formé en solution et d'autre part d'étudier la conformation (base, sucre) et la flexibilité de chaque résidu de la chaîne suivant sa place, la séquence de la chaîne et sa longueur, en relation avec l'état mono ou bicaténaire (les bases dans ce dernier cas sont bloquées dans une orientation bien définie pour assurer les liaisons hydrogènes).

Enfin, les polynucléotides synthétiques, dont la séquence est la répétition de un ou deux résidus et dont le poids moléculaire dépasse 10^5, constituent des systèmes très intéressants pour étudier la conformation et la flexibilité locale du résidu nucléotidique dans des chaînes de longueur comparable à celle d'acides nucléiques naturels, en relation avec la structure des chaînes qui va de la pelote statistique aux complexes multi brins.

Pour cette étude de conformation et de structure dynamique des acides nucléiques et de leurs composants en solution, la RMN bien qu'étant une technique relativement complexe, est à notre avis la plus adaptée : i) parce qu'elle permet par la mesure des couplages ^{1}H-^{1}H la détermination de la conformation du sucre dont on sait qu'elle est directement reliée à la structure des chaînes (A, B, Z) et par les mesures de relaxation longitudinale des protons (effet Overhauser, T_1) l'étude de la conformation de la base par rapport au sucre ; ii) parce que l'observation des signaux de résonance et de leurs variations (par exemple avec la température) des protons échangeables des groupes NH et NH_2 engagés dans les liaisons hydrogènes (mais aussi ceux des protons non échangeables et du ^{31}P) nous renseigne sur la structure secondaire et le mécanisme de formation-dissociation des complexes bicaténaires en solution ; iii) parce que la relaxation magnétique du ^{1}H, ^{13}C, ^{31}P et d'autres noyaux est directement liée aux mouvements moléculaires et donc à la mobilité des résidus et des chaînes.

Pour obtenir le maximum d'informations concernant les propriétés physicochimiques des acides nucléiques et de leurs constituants, dans ce travail, la conformation et la structure dynamique de mono-, oligo- et polynucléotides ont été étudiées par résonance et relaxation magnétiques nucléaires des protons et dans certains cas d'autres noyaux (^{31}P, ^{13}C, ^{2}H), à des fréquences de résonance différentes et dans différentes conditions expérimentales de température, concentration, pH etc ...

Le chapitre II (3 articles réfs 29, 30 et 31) comprend l'étude des conformations de l'uridine et de la pseudouridine, et de leurs dérivés et celle des conformations et de la flexibilité des diribonucléosides monophosphates. Cette étude comparative nous permet d'établir quels sont les différents facteurs au niveau de la structure chimique et des conditions physicochimiques qui influencent l'équilibre conformationnel des mono- et dinucléosides monophosphates. Le chapitre III (3 articles réfs 32, 33 et

34) traite de la conformation et de la structure dynamique des oligo déoxy-ribonucléotides dApTpGpT et dApCpApTpGpT, ce dernier composé réalisant grâce à sa séquence auto-complémentaire un complexe bicaténaire en solution ; le processus de dissociation du complexe est étudié par différentes méthodes et analysé. Le dernier chapitre (IV) (2 articles réfs 35 et 36) est consacré à l'étude comparative de la conformation et de la structure dynamique des homopolynucléotides poly rU, poly rI et poly rC.

Au cours de ces travaux, diverses méthodes ont été développées pour lever les difficultés rencontrées en particulier dans l'attribution des raies de résonance des spectres ^{1}H des oligonucléotides et le traitement de la relaxation magnétique. Nous présentons dans le premier chapitre quelques généralités sur les méthodes de RMN utilisées dans l'étude de la conformation et de la structure dynamique. Au début de ce chapitre, dans le souci de faciliter la lecture et la compréhension de cette étude, nous rappelons brièvement les principales caractéristiques structurales des acides nucléiques et de leurs constituants.

REFERENCES

1. WATSON, J.D. and CRICK, F.H.C. (1953) Nature 171, 737 et 964.

2. RICH, A., DAVIES, D.R., CRICK, F.H.C. and WATSON, J.D. (1961) J. Mol. Biol. 3, 71.

3. ARNOTT, S., DOVER, S.D. and WONACOTT, A.J. (1969) Acta Cryst. 25, 2192.

4. ARNOTT, S., HUKINS, D.W.L., DOVER, S.D., FULLER, W. and HODGSON, A.R. (1973) J. Mol. Biol. 81, 107.

5. SAENGER, W. (1973) Angew. Chem. Intern. Edit. 12, 591.

6. SUNDARALINGAM, M. (1969) Biopolymers 7, 821.

7. SUNDARALINGAM, M. (1975) Ann. N.Y. Acad. Sci. 255, 3.

8. WANG, A.H.J., QUIGLEY, G.J., KOLPAK, F.J., CRAWFORD, J.L., Van BOOM, J.H., Van Der MAREL, G. and RICH, A. (1979) Nature 282, 680.

9. CRAWFORD, J.L., KOLPAK, F.J., WANG, A.H.J., QUIGLEY, G.J., Van BOOM, J.H., Van Der MAREL, G. and RICH, A. (1980) Proc. Natl. Acad. Sci. USA 77, 4016.

10. VISWAMITRA, M.W., KENNARD, O., JONES, P.G., SHELDRICK, G.M., SALISBURY, S., FAVELLO, L. and SHAKKED, Z. (1978) Nature 273, 687.

11. SUSSMAN, J.L. and KIM, S.H. (1976) Biochem. Biophys. Res. Commun. 68, 89.

12. SCHEVITZ, R.W., PODJARNY, A.D., KRISHNAMACHARI, N., HUGHES, J.J., SIGLER, P.B. and SUSSMAN, J.L. (1979) Nature 278, 188.

13. ALTONA, C. and SUNDARALINGAM, M. (1973) J. Am. Chem. Soc. 95, 2333.

14. DAVIES, D.B. and DANYLUK, S.S. (1974) Biochemistry 13, 4417.

15. GUSCHLBAUER, W. and TRAN-DINH, S. (1975) Nucl. Acids Res. 2, 585.

16. SCHWEIZER, M.P., BROOM, A.D., TS'O, P.O.P. and HOLLIS, D.P. (1968) J. Am. Chem. Soc. 90, 1042.

17. DANYLUK, S.S. and HRUSKA, F.E. (1968) Biochemistry 7, 1938.

18. LEMIEUX, R.U., NAGA BHUSHAN, T.L. and PAUL, B. (1972) Can. J. Chem. 50, 773.

19. DELBAERE, L.T.J., JAMES, M.N.G. and LEMIEUX, R.U. (1973) J. Am. Chem. Soc. 95, 7866.

20. BARRY, C.D., NORTH, A.C.T., GLASEL, J.A., WILLIAMS, R.J.P. and XAVIER, A.V. (1971) Nature 232, 236.

21. HART, P.A. and DAVIS, J.P. (1971) J. Am. Chem. Soc. 93, 753.

22. TRAN-DINH, S., GUSCHLBAUER, W. and GUERON, M. (1972) J. Am. Chem. Soc. 94, 7903.

23. GUERON, M., CHACHATY, C. and TRAN-DINH, S. (1973) Ann. N. Y. Acad. Sci. 222, 307.

24. CHACHATY, C., ZEMB, T., LANGLET, G., TRAN-DINH, S., BUC, H. and MORANGE, M. (1976) Eur. J. Biochem. 62, 45.

25. NEUMANN, J.M., BORREL, J., THIERY, J.M., GUSCHLBAUER, W. and TRAN-DINH, S. (1977) Biochim. Biophys. Acta 479, 427.

26. JORDAN, F. and NIV, H. (1977) Biochim. Biophys. Acta 476, 265.

27. DOBSON, C.M., GERALDES, C.F.G.C., RATCLIFFE, G. and WILLIAMS, R.J.P. (1978) Eur. J. Biochem. 88, 259.

28. LEE, C.H. and SARMA, R.H. (1976) J. Am. Chem. Soc. 98, 3541.

29. NEUMANN, J.M., BERNASSAU, J.M., GUERON, M. and TRAN-DINH, S. (1980) Eur. J. Biochem. 108, 457.

30. NEUMANN, J.M., GUSCHLBAUER, W. and TRAN-DINH, S. (1979) Eur. J. Biochem. 100, 141.

31. TRAN-DINH, S., NEUMANN, J.M. and BORREL, J. (1981) Biochim. Biophys. Acta 655, 167.

32. TRAN-DINH, S., NEUMANN, J.M., HUYNH-DINH, T., IGOLEN, J. and KAN, S.K. (1982) Org. Mag. Res. 18, 148.

33. NEUMANN, J.M., HUYNH-DINH, T., KAN, S.K., GENISSEL, B., IGOLEN, J. and TRAN-DINH, S. (1982) Eur. J. Biochem. 121, 317.

34. TRAN-DINH, S., NEUMANN, J.M., HUYNH-DINH, T., GENISSEL, B., IGOLEN, J. and SIMMONOT, G. (1982) Eur. J. Biochem. (sous presse).

35. NEUMANN, J.M. and TRAN-DINH, S. (1981) Biopolymers 20, 89.

36. NEUMANN, J.M. and TRAN-DINH, S. (1982) Biopolymers 21, 383.

CHAPITRE I

GÉNÉRALITÉS

A. STRUCTURE ET CONFORMATION DES ACIDES NUCLEIQUES.

B. METHODES DE RMN APPLIQUEES A L'ETUDE DE LA CONFORMATION ET DE LA STRUCTURE DYNAMIQUE DES ACIDES NUCLEIQUES EN SOLUTION.

A. STRUCTURE ET CONFORMATION DES ACIDES NUCLEIQUES.

Les acides nucléiques sont des polymères linéaires formés de l'union de résidus nucléotides reliés les uns aux autres par des liaisons phosphodiesters. Les nucléotides sont constitués eux-mêmes de trois unités : base, sucre, phosphate. On appelle nucléoside l'union d'une base et d'un sucre. Le sucre est le ribose dans les ARN, le 2'déoxyribose dans les ADN ; il comporte un cycle à cinq atomes et un groupe exocyclique $-CH_2O-$ lié au carbone 4' du cycle. Les bases puriques, adénine (A) et guanine (G), sont présentes dans les ARN et les ADN, les bases pyrimidiques, cytosine (C) et uracile (U), se trouvent dans les ARN tandis que la thymine (T) remplace l'uracile dans les ADN. Hormis ces cinq bases principales, un certain nombre d'autres bases dites atypiques se rencontrent, en particulier dans les ARN de transfert.

A.I. CONFORMATION DES NUCLEOSIDES ET NUCLEOTIDES.

La conformation d'un nucléoside, illustrée par l'exemple de la cytidine (Fig. 1), est déterminée par :

i) l'orientation de la base par rapport au sucre, qui peut être *anti* ou *syn* suivant que l'atome H_6 de la base (pour les pyrimidines ; H_8 pour les purines) se trouve ou non au-dessus du cycle du sucre ; la définition de l'angle de rotation T (ou χ), du sens de rotation et des domaines *syn* et *anti* sont données dans la figure 1.

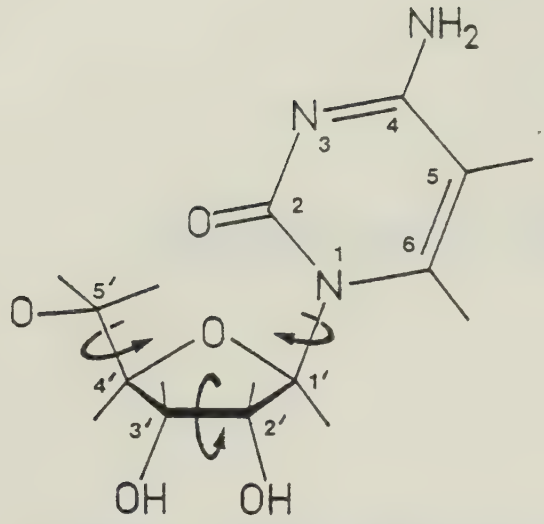

Figure 1

Conformation d'un nucléoside : la cytidine.

La conformation d'un nucléoside est déterminée par :

1- l'orientation de la base par rapport au sucre : définie par l'angle diédral T (H_1'-C_1'-N_1-C_6) autour de la liaison C_1'-N_1. Le sens de rotation et les domaines *syn/anti* sont définis par [1] :

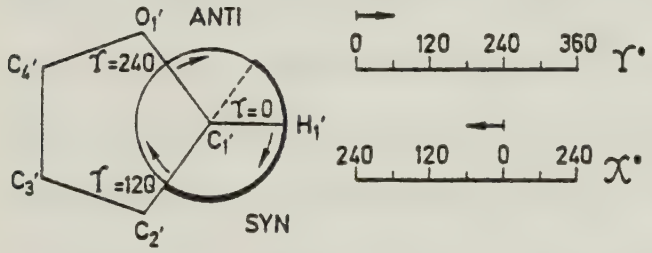

χ est la notation due à Sundaralingam [2] et correspond à l'angle O_1'-C_1'-N_1-C_2

2- la conformation du sucre ; les deux principales sont :

C_3'-endo (N) 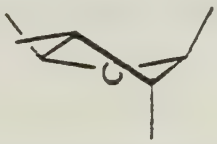 ; C_2'-endo (S)

3- la conformation autour de la liaison C_4'-C_5' ; les trois conformations décalées sont :

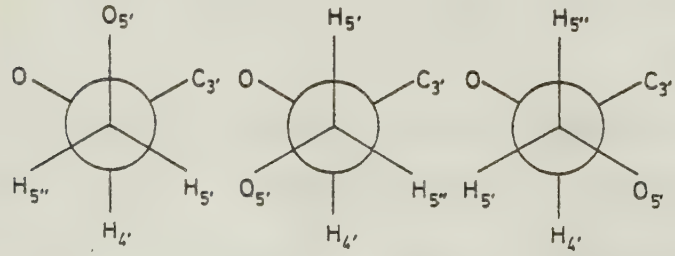

gauche-gauche gauche-trans trans-gauche

Ces trois conformations sont aussi appelées rotamères

ii) la déformation du cycle du sucre par rapport au plan moyen des cinq atomes ; chaque atome du cycle peut être déplacé en position endo (vers le haut) ou en position exo (vers le bas) (Fig. 1).

iii) la conformation du groupe exocyclique autour de la liaison $C_{4'}$-$C_{5'}$; les trois conformations principales (décalées) sont appelées : gauche-gauche (gg), gauche-trans (gt) et trans-gauche (tg) suivant la position relative des atomes $H_{5'}$ et $H_{5''}$ par rapport à $H_{4'}$ (Fig. 1).

Les nucléotides sont les esters phosphoriques des nucléosides. L'estérification peut avoir lieu en 2', 3' et 5' pour les ribonucléosides, en 3' ou 5' pour les 2'déoxyribonucléosides.

La structure cristalline de nombreux nucléosides et nucléotides a été étudiée par diffraction des rayons X [3]. Les deux conformations principales du cycle du sucre que l'on rencontre sont soit la forme $C_{3'}$, endo appelée forme N et la forme $C_{2'}$, endo appelée forme S (Fig. 1). Dans la plupart des composés, le groupe exocyclique a la conformation gg et la base est orientée en *anti* par rapport au sucre.

En solution, les études en RMN-^{1}H ont montré que les nucléosides et nucléotides isolés sont des molécules flexibles : il existe un équilibre rapide entre les conformations *syn* et *anti* de la base [4, 5], entre les formes N et S du cycle du sucre [6] et entre les rotamères gg, tg et gt du groupe exocyclique. Les proportions des conformations en équilibre dépendent de la structure chimique et des conditions physicochimiques (voir le chapitre II).

A.II. STRUCTURE ET CONFORMATION DES ACIDES NUCLEIQUES

Dans les acides nucléiques, les nucléotides sont reliés entre eux par une liaison 3'-5' phosphodiester (Fig. 2). Les molécules les plus petites comportent moins d'une centaine de résidus (ARN de transfert), les plus importantes ont un poids moléculaire qui dépasse plusieurs millions.

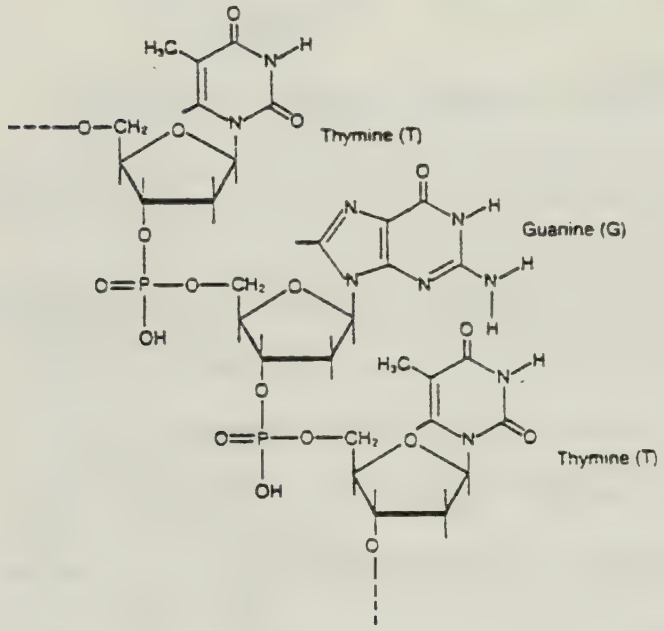

Figure 2

Enchaînement des résidus nucléotides par des liaisons 3'-5' phosphodiesters.

Un des éléments déterminants de la structure des acides nucléiques est la propriété qu'ont les bases de s'apparier par l'intermédiaire de liaisons hydrogènes grâce à leur structure complémentaire : les appariements inter-bases s'établissent, en général, d'une part entre l'adénine et la thymine ou l'adénine et l'uracile avec deux liaisons hydrogènes et d'autre part entre la cytosine et la guanine avec trois liaisons hydrogènes (Fig. 3).

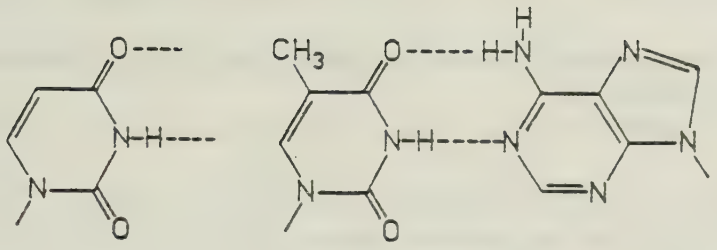

Uracile ou Thymine avec Adénine
(ARN) (ADN)

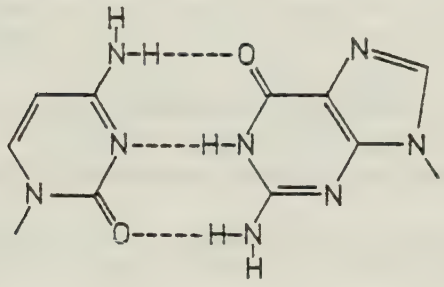

Cytosine avec Guanine

Fig. 3 - Appariements inter-bases par liaisons hydrogènes dans le modèle de Watson et Crick.

La plupart des structures proposées sont dérivées de l'analyse aux rayons X de fibres d'acides nucléiques naturels et depuis peu de monocristaux de fragments d'ADN ou d'ARN synthétiques (oligonucléotides à séquence auto-complémentaire). Le Tableau I résume les caractéristiques principales de ces structures.

Les deux familles de structure appelées A et B qui sont issues du modèle, maintenant familier, de Watson et Crick [7] (double hélice droite, dans laquelle chaque hélice est reliée à l'hélice complémentaire par des appariements inter bases du type présenté ci-dessus) se distinguent, au niveau de la conformation des résidus, principalement par la forme adoptée par le cycle du sucre : forme N dans les structures A, forme S dans les structures B. Dans les deux cas, les bases sont orientées en *anti* par rapport au sucre.

Tableau I - Caractéristiques principales des différents modèles de structure bicaténaire.

Acides nucléiques étudiés et références. Dénomination de la structure	Organisation générale des brins	Conformation des résidus	
		Base	Sucre
Type A fibres d'ADN [8] (faible humidité) fibres d'ARN [8]	Double hélice droite 11 paires de base/tour Pas de l'hélice : 28 Å inclinaison des bases⁂ : 19°	*Anti*	N
Type B fibres d'ADN [9] (forte humidité)	Double hélice droite 10 paires de base/tour Pas de l'hélice : 34 Å inclinaison des bases⁂ : 6°	*Anti*	S
Type Z $d(GC)_3$ cristal [10]	Double hélice gauche 12 paires de base/tour Pas de l'hélice : 45 Å inclinaison des bases⁂ : 7°	*Anti* (dC) *Syn* (dG)	S(dC) N(dG)
$d(AT)_2$ cristal [11]	2 doubles hélices droites segmentaires	*Anti*	S(dA) N(dT)

⁂ Angle entre le plan des bases et le plan perpendiculaire à l'axe de l'hélice.

Les deux fragments d'ADN $d(AT)_2$ et $d(GC)_3$ présentent des structures bicaténaires singulièrement différentes des formes A et B. Dans la structure de $d(AT)_2$, les deux segments AT d'un brin forment chacun une mini-double hélice droite avec la séquence complémentaire de l'autre brin (la présence d'un coude entre les deux segments empêche la formation du duplex à 4 paires de bases) et le cycle du sucre des résidus A adopte la conformation N tandis que celui des résidus T adopte la conformation S. La molécule $d(GC)_3$ offre une structure hélicoïdale encore plus différente des formes A et B : ce fragment d'ADN cristallise sous forme d'une double hélice gauche (appelée forme Z) dans laquelle la base des résidus G est orientée en *syn* avec le sucre en conformation N alors que la base de résidu C est orientée en *anti* avec le sucre en conformation S. Dans tous les cas, les appariements inter-bases sont du type Watson-Crick.

La présence de conformations N et S au sein d'une même molécule se rencontre également dans les ARN de transfert. L'étude raffinée en diffraction des rayons X d'ARN-t [12] montre que si leur structure comprend principalement des parties bicaténaires de type A et des boucles monocaténaires dans lesquelles le sucre adopte la forme N, il existe cependant des replis dans les chaînes et des intercalations de base qui peuvent être associés à des changements de conformation du ribose (de N à S).

Cette présentation rapide des caractéristiques principales de la structure et de la conformation des acides nucléiques montre en particulier que la connaissance de la conformation du sucre et de l'orientation de la base des résidus nucléotidiques permet de caractériser le type de la structure.

B. METHODES DE RMN APPLIQUEES A L'ETUDE DE LA CONFORMATION ET DE LA STRUCTURE DYNAMIQUE DES ACIDES NUCLEIQUES EN SOLUTION.

La RMN s'est révélée être une des techniques les plus efficaces et les plus complètes d'étude conformationnelle des molécules en solution. L'augmentation de l'intensité des champs magnétiques disponibles et l'utilisation des techniques de transformée de Fourier ont amélioré la résolution et la rapidité des mesures.

Les méthodes d'analyse conformationnelle par RMN reposent sur l'étude des déplacements chimiques des signaux de résonance et des couplages scalaires entre spins, et sur l'étude de la relaxation magnétique. Dans le cas des acides nucléiques et de leurs composants, les noyaux les plus couramment observés sont le proton, le carbone ^{13}C et le phosphore ^{31}P, tous les trois de spin 1/2. Les deux premiers sont présents sur la base et sur le sucre ; leur étude est donc susceptible de nous renseigner sur les conformations et la flexibilité du sucre et de la base par rapport au sucre. Cependant le rapport gyromagnétique du ^{1}H est environ quatre fois plus élevé que celui du ^{13}C et surtout l'abondance isotopique du ^{1}H avoisine les 100% tandis que celle du ^{13}C n'est que de 1% (Tableau I) ; par conséquent, la RMN ^{1}H est la technique la plus sensible. C'est celle qui est la plus utilisée dans ce travail et la plus grande partie de cette section y est consacrée. Toutefois la relaxation magnétique du ^{13}C qui présente un intérêt particulier dans l'étude de la structure dynamique a également été utilisée dans ce travail et est traitée dans la partie consacrée à la relaxation. Dans cette même partie,

la relaxation du ^{31}P qui nous a permis d'obtenir des informations sur la conformation et la mobilité autour du groupe phosphate est également traitée.

Tableau I - Abondance isotopique, rapport gyromagnétique γ et fréquence de Larmor ν (dans un champ de 23,5 kG) de ^{1}H, ^{31}P et ^{13}C.

Noyau	Abondance isotopique (%)	γ (CGS)	ν (MHz)
^{1}H	99,9	26 753	100
^{31}P	100	10 840	40,5
^{13}C	1	6 728	25,15

B.I DEPLACEMENT CHIMIQUE

L'environnement électronique d'un noyau (liaisons chimiques, densité électronique locale, etc ...) écrante le champ magnétique auquel il est soumis et modifie la position de son signal de résonance. Cette variation ou déplacement chimique permet en premier lieu de distinguer les noyaux de même nature suivant leur position dans une molécule. Ainsi, dans les spectres de RMN des protons non échangeables dans D_2O des acides nucléiques, les protons aromatiques ont les déplacements chimiques les plus importants (effet d'écran dû au nuage d'électrons π des bases) qui se situent en général dans la région comprise entre 7 et 8 ppm environ (par rapport à TMP). Ensuite, par ordre décroissant de déplacement chimique, on trouve les signaux des protons des groupes CH (1', 3', 4' et 2' (pour les riboses seulement) entre 4 et 6 ppm) ceux des groupes CH_2 (5', 5" (entre 3,8 et 4,2 ppm) et 2', 2" (pour les déoxyriboses seulement entre 1,9 et 3,0 ppm)) et enfin les protons des groupes CH_3 (de la thymidine par exemple).

Par ailleurs, l'important effet d'écran des bases et son caractère fortement anisotrope sont à l'origine de nombreuses applications dans l'étude de la structure et de la conformation, dont la plus courante est l'étude des interactions base-base dans les mono-, oligo- et polynucléotides sous forme mono brin. En effet les interactions hydrophobes favorisent l'empilement des bases ("stacking") et peuvent provoquer l'aggrégation des molécules (interactions intermoléculaires) et/ou la formation d'une structure secondaire plus ordonnée (interactions intramoléculaires). Cet empilement des bases induit des déplacements importants des signaux de résonance et la mesure des déplacements chimiques en fonction de la température et de la concentration, en particulier, permet de distinguer les effets intra- et intermoléculaires et de les étudier. Dans ce travail, de telles mesures ont été effectuées pour les dinucléotides (Section C du chapitre II), les oligonucléotides (Section B du chapitre III) et les polynucléotides (Section B du chapitre IV).

Pour l'étude de la structure en solution des acides nucléiques et des oligo et polynucléotides capables de former des complexes bicaténaires, la RMN-^{1}H dispose avec l'observation des raies de résonance des protons engagées dans les liaisons hydrogènes d'un outil très efficace. En effet, si en général, en solution aqueuse, les protons des groupes NH et NH_2 s'échangent suffisamment rapidement avec ceux de l'eau pour que la RMN ne puisse les détecter, par contre lorsque ces protons sont impliqués dans des liaisons hydrogènes, la vitesse d'échange devient suffisamment lente pour que leurs signaux de résonance soient observables. L'observation de ces signaux apportent la preuve de la formation des appariements inter-bases et permet de connaître le nombre de liaisons hydrogènes formées, et d'étudier, par exemple en variant la température, la cinétique de dissociation et le processus de "débobinage" du complexe multibrins. C'est ce qui a été réalisé dans ce travail sur un oligodéoxynucléotide à séquence autocomplémentaire (Section C du chapitre III). Avec ces composés modèles ne comportant pas plus d'une dizaine

de résidus, la transition hélice-pelote statistique peut être également étudiée en suivant les variations de déplacements chimiques des protons non-échangeables à condition que l'attribution des résonances soit réalisée ; cette étude a d'autant plus d'intérêt que les signaux des protons échangeables disparaissent souvent à des températures relativement basses (parfois à température ambiante). Il est ainsi possible d'étudier la transition sur un intervalle de température plus important et d'évaluer les paramètres thermodynamiques associés à la transition plus simplement, c'est-à-dire sans avoir à prendre en compte l'échange avec le solvant comme dans le cas des protons des groupes NH et NH_2 (voir Section C du chapitre III).

La mesure des déplacements chimiques est également utilisée pour étudier la conformation de la base par rapport au sucre (voir la Section A de ce chapitre). Cette application découle du fait que les déplacements chimiques des protons du sucre varient avec l'orientation de la base. Ces variations ont été calculées théoriquement en fonction de l'angle de torsion autour de la liaison base-sucre [13] et analysées expérimentalement sur des ensembles de nucléosides et nucléotides [14-16]. En principe, pour une famille de composés, il est ainsi possible de déterminer la prépondérance de l'un ou l'autre des domaines d'orientation *syn* ou *anti* de la base. Cependant cette méthode n'apporte aucun renseignement sur le mouvement de la base et en pratique, le nombre de facteurs susceptibles d'influencer les déplacements chimiques est tel (structure chimique des bases, conformation du sucre, effet du solvant, etc ...) que leur interprétation en terme d'orientation de la base est très difficile et doit être considérée avec précaution. Ainsi des études basées sur cette méthode ont conclu à l'orientation *anti* de la base dans les nucléosides et nucléotides isolés en solution [14] alors que l'observation des effets Overhauser proton-proton (voir la troisième partie de cette section) a mis directement en évidence la flexibilité de la conformation par rapport au sucre dans ces molécules et l'existence d'un équilibre *syn/anti* [4, 5].

Après les déplacements chimiques, le second paramètre observable sur les signaux de résonance en RMN est le couplage scalaire spin-spin dont les applications à l'étude conformationnelle sont très importantes.

B.II. COUPLAGE SCALAIRE SPIN-SPIN

Les interactions scalaires entre spins par l'intermédiaire des électrons des liaisons chimiques sont responsables de la structure en multiplet des signaux de résonance et la mesure des constantes de couplage est un outil important pour l'analyse spectrale.

En RMN-^{1}H des oligonucléotides, on observe des couplages géminaux (deux liaisons séparent les noyaux) entre $H_{5'}$ et $H_{5''}$, $H_{2'}$ et $H_{2''}$ et des couplages vicinaux (à trois liaisons) entre les protons portés par les carbones successifs du sucre qui déterminent un ensemble de cinq constantes de couplage $J_{1'2'}$, $J_{2'3'}$, $J_{3'4'}$, $J_{4'5'}$, $J_{4'5''}$ pour le ribose, auxquelles il faut rajouter $J_{1'2''}$ et $J_{2''3'}$ pour le déoxyribose. On peut observer également des couplages scalaires entre les protons de la base comme par exemple dans l'uridine entre H_5 et H_6.

Si les couplages géminaux n'apportent aucune information sur la conformation, par contre les couplages vicinaux dépendent des angles de torsion autour des liaisons chimiques. La constante de couplage J_{ij} entre les protons H_i et H_j, portés par les carbones C_i et C_j (reliés par une liaison simple) varie suivant l'équation de Karplus [17] avec l'angle ϕ_{ij} entre les plans $(H_iC_iC_j)$ et $(C_iC_jH_j)$:

$$J_{ij} = A\cos^2\phi_{ij} + B\cos\phi_{ij} + C \qquad (1)$$

A, B et C sont des constantes.

La première application de la mesure des constantes de couplage, concerne l'étude de la conformation du cycle du sucre. Il a été montré que le cycle du sucre des nucléosides et des nucléotides isolés en solution est

flexible et qu'il existe un équilibre rapide entre les deux formes N et S (voir la section précédente). Les constantes de couplage vicinal J_{ij} observées entre les protons du cycle représentent les valeurs moyennes entre les constantes J^N_{ij} et J^S_{ij} associées aux deux formes N et S :

$$J_{ij(obs)} = x_N J^N_{ij} + x_S J^S_{ij} \qquad (2)$$

avec $x_N + x_S = 1$; x_N et x_S sont les proportions respectives des formes N et S. En raison de la géométrie des conformations N et S (les ϕ_{ij}) et de leur symétrie, $J^N_{1'2'} \sim J^S_{3'4'}$ et $J^S_{1'2'} \sim J^N_{3'4'}$ de sorte que $J_{1'2'(obs)}$ et $J_{3'4'(obs)}$ varient en sens inverse avec pratiquement la même amplitude quand le rapport x_N/x_S varie et la somme $J_{1'2'} + J_{3'4'}$ reste constante.

Le calcul des constantes A, B et C de l'équation (1) [6] montre que cette somme vaut environ 10 Hz. La mesure du rapport $J_{1'2'}/(J_{1'2'} + J_{3'4'})$ donne ainsi une estimation de x_S et donc des proportions relatives des conformations en équilibre.

Avec le déoxyribose, on dispose de deux constantes de couplage vicinal supplémentaires $J_{1'2''}$ et $J_{2''3'}$ dont on peut remarquer pour des raisons de symétrie qu'elles sont pratiquement égales respectivement à $J_{2'3'}$ et $J_{3'4'}$. La forme S étant souvent prédominante dans les fragments d'ADN, le couplage entre les protons $H_{2''}$ et $H_{3'}$ est alors faible (si $x_S \sim 70\%$, $J_{3'4'} \sim J_{2''3'} \sim 3$ Hz) et constitue un critère pour distinguer les signaux de résonance des protons $H_{2'}$ et $H_{2''}$ (le détail de cette procédure est rapporté dans la section A du chapitre III).

La seconde application de la mesure des constantes de couplage a pour objet la conformation du groupe exocyclique du sucre autour de la liaison $C_{4'}$-$C_{5'}$ (voir la section A de ce chapitre). Comme précédemment, les constantes $J_{4'5'}$ et $J_{4'5''}$ observées représentent chacune une moyenne des trois constantes associées à chacune des trois conformations principales du groupe exocyclique

$$J_{4'5'(obs)} = p_{gg}J_g + p_{gt}J_g + p_{tg}J_t \quad (3)$$

$$J_{4'5''(obs)} = p_{gg}J_g + p_{gt}J_t + p_{tg}J_g \quad (4)$$

avec

$$p_{gg} + p_{tg} + p_{gt} = 1 \quad (5)$$

p_{gg}, p_{tg} et p_{gt} sont les proportions relatives des trois conformations gg, tg et gt autour de la liaison $C_{4'}$-$C_{5'}$. Les constantes J_g et J_t qui sont associées respectivement aux positions gauche et trans de $H_{5'}$ ($H_{5''}$) par rapport à $H_{4'}$, peuvent être calculées à partir de l'équation (1) et les trois relations (3), (4) et (5) permettent d'évaluer les fractions p_{gg}, p_{gt} et p_{tg}.

Ce type de méthode ne peut être appliqué à l'étude de la conformation de la base par rapport au sucre en raison de l'inexistence de couplage vicinal entre les protons de la base et ceux du sucre.

La troisième technique importante utilisée en RMN est l'étude de la relaxation, qui nous permet en particulier d'obtenir des informations sur l'orientation des bases et sur les mouvements moléculaires dans les acides nucléiques. La section suivante est consacrée en totalité à la relaxation longitudinale, la plus étudiée dans ce travail bien que pour certaines applications, la relaxation transversale ait été exploitée - mesure des largeurs de raies en RMN-^{1}H et -^{2}H (les détails des procédures utilisées dans ces deux cas sont rapportés dans les sections A et B du chapitre IV).

B.III. RELAXATION MAGNETIQUE LONGITUDINALE DES SPINS 1/2.

La relaxation longitudinale est le processus de retour vers leur valeur d'équilibre, le long de la direction du champ magnétique Oz, des aimantations d'un ensemble de spins lorsque celles-ci ont été perturbées. Dans la plupart des cas, pour les spins nucléaires 1/2, les fluctuations de l'interaction dipolaire entre ces spins, dues à la rotation des vecteurs internucléaires (mouvement brownien) sont essentiellement responsables de la relaxation longitudinale.

En RMN-^{1}H, l'interaction dipolaire homonucléaire ^{1}H-^{1}H est la plus efficace alors qu'en résonance du ^{13}C et du ^{31}P c'est l'interaction hétéronucléaire avec les protons (^{13}C-^{1}H et ^{31}P-^{1}H) qui l'emporte (dans les molécules que nous étudions). Il en résulte que le traitement de la relaxation longitudinale du ^{1}H d'une part et ceux du ^{13}C et du ^{31}P d'autre part, sont différents et sont présentés avec leurs applications dans deux parties séparées. Auparavant, nous rappelons brièvement quelques aspects théoriques généraux de la relaxation longitudinale.

B.III.1. Equation d'évolution de l'aimantation longitudinale, effet Overhauser et temps de relaxation.

Considérons deux noyaux i et j de spin 1/2 d'une molécule en solution et soit $\vec{r}_{ij}$ le vecteur internucléaire. Le système d'équations qui décrit l'évolution des aimantations longitudinales I_{zi} et I_{zj} des deux noyaux a pour expression [18] :

$$\frac{d}{dt} I_{zi} = -\rho_{ij}(I_{zi} - I_{oi}) - \sigma_{ij}(I_{zj} - I_{oj}) \qquad (6)$$

I_{oi} et I_{oj} sont les valeurs à l'équilibre des aimantations,

$$\rho_{ij} = K^2 r_{ij}^{-6}[J(\omega_i - \omega_j) + 3J(\omega_i) + 6J(\omega_i + \omega_j)] \qquad (7)$$

$$\sigma_{ij} = K^2 r_{ij}^{-6}[(6J(\omega_i + \omega_j) - J(\omega_i - \omega_j)] \qquad (8)$$

avec

$$K^2 = (\gamma_i \gamma_j \hbar)^2/10 \qquad (9)$$

γ_i, γ_j et ω_i, ω_j sont respectivement les rapports gyromagnétiques et les fréquences de Larmor des deux spins. La densité spectrale $J(\omega)$ est définie par :

$$J(\omega) = (1/2) \int_{-\infty}^{+\infty} G(\tau) e^{-i\omega\tau} \, d\tau \qquad (10)$$

où $G(\tau)$ est la fonction d'auto-corrélation associée au mouvement de réorientation du vecteur $\vec{r}_{ij}$. Dans le modèle le plus simple d'un mouvement de diffusion rotationnel isotrope :

$$G(\tau) = \exp(-|\tau|/\tau_c) \tag{11}$$

et

$$J(\omega) = \tau_c/(1 + \omega^2\tau_c^2) \tag{12}$$

τ_c, le temps de corrélation, caractérise le mouvement moléculaire.

En régime permanent, la relaxation longitudinale se manifeste dans une expérience dite de l'effet Overhauser [19]. Si on applique un fort champ de radiofréquence au spin j, I_{zj} prend la valeur $I_{zj}(rp)$ et la valeur de I_{zi} en régime permanent est donnée d'après (6) par :

$$I_{zi}(rp) - I_{oi} = -(\sigma_{ij}/\rho_{ij})(I_{zj}(rp) - I_{oj}) \tag{13}$$

pour une saturation complète du spin j, c'est-à-dire $I_{zj}(rp) = 0$, $I_{zi}(rp)$ est augmentée par rapport à sa valeur d'équilibre de la quantité :

$$\eta_{ij} = (I_{zi} - I_{oi})/I_{oi} = (I_{oj}/I_{oi})(\sigma_{ij}/\rho_{ij}) \tag{14}$$

soit :

$$\eta_{ij} = (\gamma_j/\gamma_i)(\sigma_{ij}/\rho_{ij}) \tag{15}$$

Autrement dit, si on sature le signal du noyau j, l'intégrale du signal du noyau i augmente d'un facteur η_{ij}.

Par ailleurs si, à $t = o$, on bascule les spins i et j de 180° (par rapport à la direction Oz du champ magnétique) on peut suivre l'évolution dans le temps des aimantations I_{zi} et I_{zj} (par exemple avec une séquence d'impulsions de type inversion-récupération). La courbe de retour à l'équilibre des aimantations est donnée en résolvant le système (6) avec $I_{zi}(0) = -I_{oi}$ et $I_{zj}(0) = -I_{oj}$. La solution est une combinaison linéaire de deux exponentielles. Si on fait le même type d'expérience en saturant sélectivement en permanence un des noyaux (j par exemple) $I_{zj} = 0$ et d'après (6) le retour à l'équilibre de I_{zi} suit une simple exponentielle :

$$(I_{oi} - I_{zi})/2I_{oi} = \exp(-t/T_{1i}) \qquad (16)$$

le temps de relaxation T_{1i} a pour expression :

$$1/T_{1i} = \rho_{ij} \qquad (17)$$

Les coefficients σ_{ij} et ρ_{ij} des équations (6) dépendent d'une part de la distance entre les noyaux à la puissance 6 et d'autre part du temps de corrélation qui caractérise le mouvement moléculaire. Par conséquent, l'étude de la relaxation apporte des renseignements à la fois sur la conformation et sur la mobilité.

B.III.2. Relaxation longitudinale des protons

Dans le cas des acides nucléiques, les protons (de la base et du sucre) sont, en général, magnétiquement non équivalents : les différences de déplacement chimique sont grandes par rapport aux couplages scalaires. Ces différences sont toutefois négligeables devant la fréquence de Larmor : avec $\gamma_i = \gamma_j = \gamma_H$, on a $\omega_i \sim \omega_j = \omega$.

a) Application de l'effet Overhauser à l'étude de la conformation de la base par rapport au sucre

L'effet Overhauser observé sur le proton i en saturant le proton j a pour expression d'après (15) en explicitant σ_{ij} et ρ_{ij} :

$$\eta_{ij} = h(\omega) = (6J(2\omega) - J(o))/(J(o) + 3J(\omega) + 6J(2\omega)) \qquad (18)$$

Si le proton i est couplé dipolairement à plusieurs protons j et si la relaxation croisée entre les protons (voir ci-dessous) est négligeable, l'irradiation d'un proton j provoque une augmentation de l'aimantation du proton i donnée par :

$$\eta_{ij} = \sigma_{ij}/\sum_j \rho_{ij} = (r_{ij}^{-6}/\sum_j r_{ij}^{-6})h(\omega) \qquad (19)$$

La somme des effets Overhauser observés en saturant successivement tous les protons couplés au proton i est égale à :

$$\sum_j \eta_{ij} = h(\omega) \qquad (20)$$

et le rapport des effets Overhauser observés en saturant le proton j et le proton k vaut :

$$\eta_{ij}/\eta_{ik} = (r_{ij}/r_{ik})^{-6} \qquad (21)$$

La variation de l'effet Overhauser d'un proton à l'autre permet de déterminer précisément grâce à l'exposant 6 les valeurs relatives des distances entre protons.

L'application au cas des nucléotides consiste à mesurer l'effet Overhauser observé sur le proton de la base H_6 ou H_8 (voir la section A) en saturant successivement les protons du sucre pour étudier le mouvement et la conformation de la base par rapport au sucre. La mesure d'effets Overhauser non-négligeables quels que soient les protons H_1', , H_2', , H_3', ou H_5', et H_5'' irradiés a mis en évidence la flexibilité de la base par rapport au sucre [4, 5]. L'effet important souvent mesuré en saturant H_1', dont la distance minimum à H_6 ou H_8 est obtenue quand l'orientation de la base est *syn* ($T = 0°$, $\chi = 240°$) et est, à la puissance -6, trois fois plus faible que $[H_2',-H_6(H_8)]_{min}$ et $[H_3',-H_6(H_8)]_{min}$ (qui sont réalisées lorsque la base est orientée en *anti* ; voir la section A) montre qu'il existe un équilibre *syn/anti* des orientations de la base des nucléotides en solution. Suivant l'importance de l'effet Overhauser dû à H_1', comparé à celui de l'ensemble des autres protons, on peut en déduire la prédominance de l'une ou l'autre des orientations *syn* et *anti*. Cette méthode s'applique aussi bien aux ribo- qu'aux déoxyribonucléotides.

L'effet Overhauser dépend, via $h(\omega)$, de la fonction $J(\omega)$ et dans un modèle de mouvement isotrope, caractérisé par un temps de corrélation τ_c, $J(\omega)$ a l'expression (12) et l'intensité de l'effet Overhauser et donc l'efficacité de la méthode présentée est fonction du produit $\omega\tau_c$, autrement dit du rapport entre la fréquence de Larmor et la fréquence du mouvement (Fig. 1) :

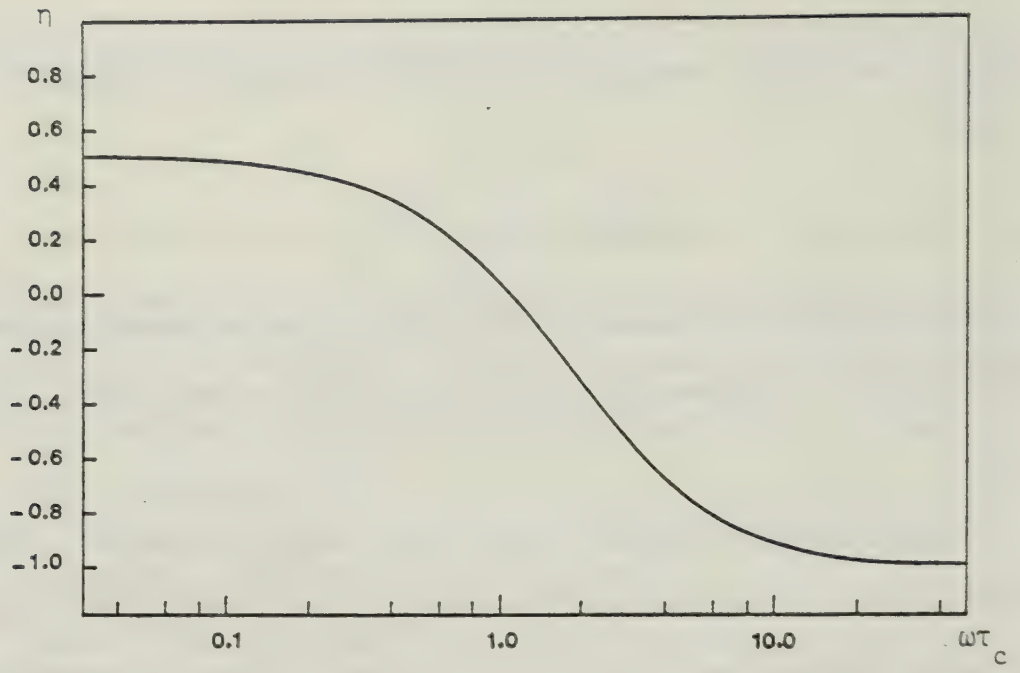

Fig. 1 - Courbe semi-logarithmique de l'effet Overhauser proton-proton η (équation (18) dans le texte) en fonction du produit $\omega\tau_c$. La fréquence de Larmor $\omega/2\pi$ est de 250 MHz.

i) $\omega\tau_c \ll 1$: c'est la condition de "rétrécissement extrême" ; $J(\omega) = \tau c$ et $h(\omega) = 0,5$ l'effet Overhauser est maximum. Cette condition est réalisée pour les nucléotides et dinucléotides aux fréquences usuelles ($\tau_c \sim 10^{-10}$ s) (voir chapitre II).

ii) $\omega\tau_c \sim 1$: quand le produit $\omega\tau_c$ est voisin de l'unité, l'effet Overhauser devient négligeable ($\eta = 0$ quand $\omega\tau_c = 1,12$). Cette condition tend à se réaliser dans les oligonucléotides comportant quatre résidus et plus à température ambiante, et à fréquence moyenne (250 MHz) (voir les sections B et C du chapitre III) : les méthodes basées sur l'effet Overhauser deviennent inefficaces.

iii) $\omega\tau_c \gg 1$: c'est la région dite des mouvements lents ; l'effet Overhauser est négatif et tend vers -1. Quand le produit $\omega\tau_c$ est supérieur à 1, les effets de relaxation croisée sont très importants (voir ci-dessous) et les raies deviennent très larges de sorte que les mesures et leur inter-

prétation sont difficiles. C'est le cas rencontré dans les complexes polynucléotides multibrins et les acides nucléiques naturels à température ambiante. Toutefois on peut s'affranchir des effets de relaxation croisée en utilisant des séquences d'impulsions appropriées [20].

Hormis le fait que l'effet Overhauser est négligeable quand $\omega\tau_c \sim 1$, l'étude de la conformation de la base par la mesure de l'effet Overhauser proton-proton présente un autre inconvénient : lorsqu'il existe plusieurs protons non-échangeables sur la base, suffisamment proches pour se relaxer mutuellement de manière efficace (cas de l'uracile et de la cytosine dans lesquelles le proton H_6 est couplé aux protons du groupe CH_3 et au proton H_5 respectivement) la contribution des protons du sucre à la relaxation des protons de la base est considérablement réduite et rend l'effet Overhauser peu efficace pour étudier la conformation de la base par rapport au sucre. La deutération sélective des protons de la base est une solution à ce problème et a été appliquée dans ce travail à l'uridine et ses dérivés dans lesquels le proton H_5 est remplacé par un deutérium (voir la section A du chapitre II).

b) Application des mesures de temps de relaxation à l'étude de la conformation de la base et à l'étude des mouvements moléculaires.

Nous nous plaçons dans le cas le plus courant des expériences de relaxation où l'ensemble des spins des protons est basculé de 180° et où le retour à l'équilibre des composantes longitudinales sont suivis simultanément. Pour un ensemble de N protons, le système d'équations d'évolution généralisé s'écrit d'après (6) :

$$\frac{d}{dt} I_{zi} = -\sum_j \rho_{ij} (I_{zi} - I_o) - \sum_j \sigma_{ij} (I_{zj} - I_o) \qquad (22)$$

qu'on peut réécrire [21] :

$$\frac{d}{dt} I_{zi} = -R_{1i} (I_{zi} - I_o) - \sum_j \sigma_{ij} (I_{zj} - I_{zi}) \qquad (23)$$

et :

$$R_{1i} = 1/T_{1i} = \sum_j (\rho_{ij} + \sigma_{ij}) \tag{24}$$

$$= 3\,K^2 \sum_j r_{ij}^{-6}[J(\omega) + 4J(2\omega)] \tag{25}$$

$$\sigma_{ij} = K^2\, r_{ij}^{-6}[6J(2\omega) - J(o)] \tag{26}$$

Le terme $R_{1i}(T_{1i})$ est appelé vitesse (temps) de relaxation initiale du proton i et correspond à la pente de la tangente à l'origine (t = o) de la courbe $\mathrm{Log}(I_{zi} - I_o) = f(t)$. Le terme σ_{ij} gouverne la relaxation croisée entre les spins. Lorsque celle-ci est négligeable c'est-à-dire $\sigma_{ij} \ll R_{1i}$, la courbe $\mathrm{Log}(I_{zi} - I_o)$ est pratiquement linéaire en fonction du temps et coïncide avec la tangente de pente R_{1i}. Dans l'autre cas limite où $\sigma_{ij} \gg R_{1i}$, la vitesse de relaxation longitudinale de l'ensemble des N protons tend vers la même valeur R_1 donnée par :

$$R_1 = (1/N) \sum_i R_{1i} \tag{27}$$

Dans les cas intermédiaires, l'allure de la courbe $\mathrm{Log}(I_{zi} - I_o)$ du proton i dépend de la valeur de R_{1i} comparée à R_1 : elle présente (quand σ_{ij} est négatif) une concavité si R_{1i} est plus grand que R_1 et une convexité dans le cas inverse. Les valeurs relatives de σ_{ij} et R_{1i} dépendent des distances r_{ij} entre protons et, dans un modèle de diffusion isotrope, de la valeur du produit $\omega\tau_c$.

Dans les résidus nucléotides, les vitesses de relaxation initiales diffèrent suivant les protons en particulier entre les protons du sucre et varient considérablement suivant que le sucre est le ribose ou le déoxyribose. Avec le ribose, en l'absence de toute influence des protons de la base, on peut distinguer trois classes de protons :

i) ceux du groupe exocyclique $H_{5'}$ et $H_{5''}$, très près l'un de l'autre (1,8 Å) se relaxent mutuellement et ont les vitesses de relaxation les plus élevées ;

ii) les protons $H_{2'}$, $H_{3'}$, $H_{4'}$ relaxés essentiellement chacun par deux protons voisins ;

ii) le proton $H_{1'}$ qui n'est relaxé que par un seul proton ($H_{2'}$) et dont la vitesse de relaxation est plus de deux fois inférieure à celles des autres protons du cycle. Avec le déoxyribose il ne subsiste plus que deux classes : d'une part les deux groupes ($H_{5'}$, $H_{5''}$) et ($H_{2'}$, $H_{2''}$) et d'autre part les protons $H_{1'}$, $H_{3'}$, $H_{4'}$ tous trois proches de l'un des deux groupes CH_2 et dont les vitesses de relaxation sont plus importantes que dans le cas du ribose.

Dans les nucléotides et oligonucléotides, en général, la pente de la tangente à l'origine (R_{1i}) des courbes de retour à l'équilibre de l'aimantation des protons est mesurable bien que dans le cas du déoxyribose, les R_{1i} des quatre protons H_2,$H_{2''}$ et H_5,$H_{5''}$ représentant 80% de la valeur moyenne R_1, les effets de relaxation croisée sont plus prononcés.

L'application de la mesure des $T_{1i}(R_{1i})$ à l'étude de l'orientation de la base consiste à analyser l'influence du proton de la base H_6 (ou H_8) sur la relaxation des protons du sucre. Cette analyse n'est possible qu'avec les ribonucléotides : la relaxation des protons du déoxyribose induite par les deux groupes CH_2 en 2' et 5' rend négligeable toute contribution des protons de la base.

Plusieurs méthodes d'analyse des T_{1i} sont utilisées pour étudier la conformation de la base par rapport au sucre. Premièrement, la simple évaluation du rapport $T_1(H_{1'})/T_1(H_{2'})$ ou $T_1(H_{1'})/T_1(H_{3'})$ indique s'il y a prépondérance de l'une ou l'autre des orientations *syn* ou *anti*. En effet, comme on l'a vu précédemment, en l'absence d'influence du proton de la base, ce rapport est supérieur à deux et correspond au cas d'une orientation en

anti de la base dans laquelle H_6 (ou H_8) est loin de H_1, alors qu'il tend vers l'unité pour une orientation en *syn* prépondérante dans laquelle H_6 (ou H_8) est en regard de H_1,.

La deuxième méthode tire son origine de la connaissance précise que l'on possède de la géométrie des résidus nucléotides grâce aux données cristallographiques. Par la mesure des constantes de couplage proton-proton, on connaît la conformation moyenne du sucre (voir la partie II) c'est-à-dire les proportions des conformations en équilibre (N, S et gg, tg, gt) et à partir des données cristallographiques on peut évaluer les sommes moyennes $\sum_j \langle r_{ij}^{-6} \rangle$ entre les protons du sucre. Pour chaque valeur de l'angle de torsion T entre la base et le sucre (voir la section A) on peut estimer les distances entre les protons du sucre et de la base et connaître la totalité du terme $\sum_j \langle r_{ij}^{-6} \rangle$ pour chaque proton. En supposant le temps de corrélation τ_c unique pour le résidu nucléotide à une fréquence ω donnée, la fonction $(J(\omega) + 4J(2\omega))$ de l'expression (25) ne dépend que de τ_c et cette fonction, $f(\tau_c)$, peut être calculée pour chaque proton et chaque valeur de T (de 0 à 2π) à partir des T_{1i} expérimentaux et des sommes $\sum_j \langle r_{ij}^{-6} \rangle$. L'examen préalable des empêchements stériques entre la base et le sucre ayant montré qu'à l'intérieur de chacun des domaines *syn* et *anti*, il n'existe qu'une région limitée la plus probable [22], si l'une des deux prédomine les $f(\tau_c)$ de l'ensemble des protons sont identiques pour une certaine valeur de T. La méthode consiste à calculer la courbe $\Delta f^{-1}(\tau_c)/\overline{f^{-1}(\tau_c)}$ (statistique sur l'ensemble des protons du résidu) en fonction de T : le (ou les) minimum(s) de la courbe donne alors une valeur de l'angle T de l'orientation prédominante et la valeur du temps de corrélation τ_c. Cette dernière peut être vérifiée en la comparant à celles déduites du T_1 des protons dont la relaxation est insensible à l'orientation de la base (H_4', , H_5', , H_5'' du sucre, H_5 de la base par exemple).

La troisième méthode a pour objet l'évaluation des proportions des conformations *syn* et *anti* en équilibre et est basée sur l'estimation de la distance moyenne entre le proton $H_{1'}$ du sucre et le proton H_6 (ou H_8) de la base. Dans chacune des régions les plus probables *syn* et *anti*, il existe une valeur de T pour laquelle la distance $H_{1'}$-$H_{6(8)}$ est minimum, c'est-à-dire pour laquelle la relaxation entre les deux protons est la plus efficace (à cause de l'exposant 6 de r_{ij}). La valeur $\langle r_{1'6(8)}^{-6} \rangle$ contenue dans l'expression (25) représente une moyenne entre les distances minimums $(r_{1'6(8)}^{-6})_{syn}$ et $(r_{1'6(8)}^{-6})_{anti}$ de chacune des deux régions :

$$\langle r_{1'6(8)}^{-6} \rangle = p_{syn}(r_{1'6(8)}^{-6})_{syn} + p_{anti}(r_{1'6(8)}^{-6})_{anti} \qquad (28)$$

avec $p_{syn} + p_{anti} = 1$; p_{syn} et p_{anti} sont les proportions respectives des orientations *syn* et *anti*. Pour connaître la valeur de $\langle r_{1'6(8)}^{-6} \rangle$ il faut d'abord connaître le temps de corrélation τ_c (en le supposant unique) ce qui peut être réalisé par les différentes méthodes présentées ci-dessus ou directement par la mesure des T_1 à deux fréquences (si la condition $\omega\tau_c << 1$ n'est plus vérifiée ; voir ci-dessous). Ensuite, dans le cas des purines pour lesquelles la deutération en position 8 est très facile (par chauffage dans D_2O à 80°C), la différence $R_1(H_{1'}) - R_1^{\ddot{}}(H_{1'})$ des vitesses de relaxation de $H_{1'}$ en présence et en l'absence de H_8 donne alors la valeur de $\langle r_{1'8}^{-6} \rangle$ et donc les proportions relatives des orientations *syn* et *anti* à partir de l'équation (28) (les détails de la méthode sont rapportés dans la section C du chapitre II). On peut, par ailleurs, sans deutérier évaluer $R_1^{\ddot{}}(H_{1'})$ en calculant la somme $\sum_{j \neq 6(8)} \langle r_{1'j}^{-6} \rangle$ à partir des données cristallographiques et de la connaissance de la conformation moyenne du sucre. C'est ce qui a été effectué dans le cas des pyrimidines pour lesquels la deutération en position 6 est très difficile à réaliser.

L'intérêt des méthodes basées sur les T_1 par rapport à celles basées sur l'effet Overhauser est qu'elles restent efficaces même quand $\omega\tau_c$ devient voisin de l'unité (quand $\omega\tau_c = 1,12$ les termes σ_{ij} sont nuls donc l'effet Overhauser est nul (voir ci-dessus) alors que les effets de relaxation croisée disparaissent complètement). Leur inconvénient est qu'elles sont peu sensibles dans le cas des déoxyribonucléotides.

Ces méthodes d'analyse de l'orientation de la base ont été exploitées ensemble ou séparément pour les différents composés étudiés dans ce travail.

Jusqu'à présent on n'a considéré que le cas où le temps de corrélation est unique. Si cette hypothèse a été vérifiée pour les mono et dinucléotides par l'étude de la relaxation du ^{13}C et du ^{1}H ([23, 24] et parties B et C du chapitre II) par contre pour les oligonucléotides, il est possible a priori que les temps de corrélation apparents soient différents d'un résidu à l'autre ou même qu'ils diffèrent entre la base et le sucre, suivant la structure de la molécule. Une variation du temps de relaxation (voir l'expression (25)) peut alors être interprétée soit comme un changement de conformation, soit comme un changement de mobilité. L'étude de la relaxation des protons à plusieurs fréquences nous permet de lever cette ambiguïté et apporte des informations sur la structure dynamique des oligo et polynucléotides.

c) Applications de la mesure des temps de relaxation à l'étude de la structure dynamique

En effet lorsque la condition de rétrécissement extrême ($\omega\tau_c << 1$) n'est plus vérifiée, ce qui est le cas pour les oligo- et polynucléotides comme l'indique l'allure des courbes de T_1 en fonction de la température (voir chapitres III et IV), le temps de relaxation dépend de la fréquence. Le rapport des T_1 mesurés à deux fréquences différentes ω et ω' est égal d'après l'expression (25) à :

$$T_{1i}(\omega)/T_{1i}(\omega') = (J(\omega') + 4J(2\omega'))/(J(\omega) + 4J(2\omega)). \qquad (29)$$

et est indépendant des termes r_{ij}^{-6} c'est-à-dire de la conformation. Si ce rapport est le même quel que soit le proton considéré, alors un modèle de diffusion isotrope à un seul temps de corrélation τ_c suffit à décrire le mouvement moléculaire et on peut remplacer dans (29) $J(\omega)$ par son expression (12). Le rapport des T_1 mesurés à deux fréquences donne alors directement la valeur de τ_c (la courbe du rapport des T_1 en fonction de τ_c est présentée dans la section A du chapitre IV). Ainsi, la mesure du temps de relaxation des protons en fonction de la fréquence et de la température permet d'étudier la mobilité (temps de corrélation, énergie d'activation) de l'unité base-sucre des résidus dans les oligonucléotides (sections B et C du chapitre III) et les polynucléotides (chapitre IV).

Par ailleurs, il faut considérer les cas où un modèle a un seul temps de corrélation n'est plus compatible avec les résultats des mesures de relaxation. La propriété bien connue qu'ont les nucléotides de former des agrégats en solution quand la concentration devient élevée (voir la partie I de cette section et réf. [3]), l'existence d'équilibre rapide entre des formes plus ou moins ordonnées de polynucléotide en solution rendent nécessaire l'introduction de modèle à plusieurs temps de corrélation pour interpréter les résultats des mesures de relaxation. De telles études ont été effectuées dans ce travail, dont les détails sont rapportés dans les sections B et C du chapitre III et dans la section B du chapitre IV.

B.III.3. Relaxation longitudinale ^{13}C et ^{31}P

Dans les équations précédentes, on remplace i par ^{13}C ou ^{31}P et j par ^{1}H et pour toutes les expériences de relaxation (effet Overhauser et T_1) les aimantations des protons sont saturées ($I_{zj} = 0$).

a) Relaxation du ^{13}C

La relaxation du ^{13}C est due essentiellement à l'interaction dipolaire avec les protons qui lui sont directement liés et du fait que les distances r_{CH} sont fixes, son étude ne renseigne que sur la mobilité locale : les mesures de η_{CH} et de T_1 donnent directement la valeur du temps de corrélation τ_c (dans un modèle isotrope) (expressions (15) et (17)). Chacun des deux paramètres, effet Overhauser et temps de relaxation, est plus ou moins efficace selon la valeur du produit $\omega\tau_c$ (voir le début de la partie III) :

i) $\omega\tau_c << 1$. $J(\omega) = \tau_c$ et $\rho_{CH} = (K^2/r_{CH}^6)\,\tau_c = 2\sigma_{CH}$ (d'après (7) et (8)). L'effet Overhauser est maximum : $\eta_{CH} = (1/2)(\gamma_H/\gamma_C) = 1{,}99$ mais est indépendant de τ_c. Par contre $1/T_1 (=\rho_{CH})$ est proportionnel à τ_c.

ii) $\omega\tau_c \sim 1$. La fonction $J(\omega)$ est maximum. Les variations de η_{CH} sont très sensibles aux variations en τ_c alors que T_1 est autour de son minimum, lequel est trop plat pour en déduire une valeur de τ_c précise.

iii) $\omega\tau_c >> 1$. L'effet Overhauser est négligeable, seul le T_1 est significatif. Cependant, dans ces conditions, la largeur de raie des signaux est très importante et les mesures sont difficiles.

Par ailleurs, les mesures de η et de T_1 effectuées sur des carbones appartenant à différentes parties d'une même molécule permettent de détecter des différences de mobilité entre ces différentes parties et de tester la validité d'un modèle isotrope.

Dans les acides nucléiques et leurs constituants, cette étude s'applique à la mobilité de l'unité base-sucre par l'intermédiaire des carbones protonés de la base, des quatre carbones du cycle du sucre et du carbone du groupe exocyclique. Ainsi, il a été montré que, dans les nucléotides [23, 24], le mouvement de réorientation global de la molécule est plus rapide que les mouvements locaux (base/sucre, N/S ...) et est isotrope ; la condition $\omega\tau_c << 1$ est réalisée aux fréquences usuelles, le τ_c des nucléotides est

de l'ordre de 10^{-10} s. Dans les polynucléotides de poids moléculaire élevé, c'est la situation inverse : le mouvement de l'ensemble de la molécule est très lent comparé aux mouvements locaux (dans la section A du chapitre IV, la relaxation du ^{13}C dans poly I est étudiée).

L'inconvénient de l'étude de la relaxation du ^{13}C réside principalement dans la faible abondance isotopique du ^{13}C (voir le début de la section, tableau I) : les temps d'accumulation sont très longs.

b) Relaxation du ^{31}P

L'étude de la relaxation du ^{31}P est par contre plus facile (l'abondance isotopique du ^{31}P est de 100%).

Si η_{PH} reste indépendant des distances r_{PH} par définition (éq. (15)) par contre, T_1 dépend de ces distances qui en général varient avec la conformation. L'efficacité des mesures de η et T_1 est soumise aux mêmes conditions qu'au a) suivant la valeur de $\omega\tau_c$. Lorsque η_{PH} n'est ni maximum ($\eta_{max} = 1{,}23$) ni négligeable, on peut en principe en déduire (dans un modèle isotrope) une valeur de τ_c et tirer de la valeur de T_1 la distance r_{PH} (ou la somme $\sum_H r_{PH}^{-6}$ dans le cas où plusieurs protons sont couplés au phosphore). L'intérêt de l'étude de la relaxation du ^{31}P dans les acides nucléiques est d'apporter des informations sur la conformation autour du groupe phosphate qui relie deux résidus entre eux et sur sa mobilité, c'est-à-dire la mobilité de la chaîne principale. La contribution dipolaire à la relaxation est due essentiellement aux protons H_3', , H_5' et H_5''.

Cependant, l'interaction dipolaire avec les protons n'est pas la seule contribution à la relaxation du phosphore. Il existe un autre mécanisme responsable de la relaxation : l'anisotropie de déplacement chimique (CSA) [18]. Le terme ρ_{PH} doit être remplacé par $\rho_P = \rho_{PH} + \rho_{CSA}$ dans les expressions de η_{PH} et de T_1. Le terme ρ_{CSA} est proportionnel au carré du champ magnétique (quand $\omega\tau_c \ll 1$) et son influence peut être prédominante à fréquence élevée ; par ailleurs, le terme d'anisotropie de déplacement chimique n'est en général

pas connu. Il est donc nécessaire, pour exploiter les résultats des mesures de relaxation du ^{31}P de pouvoir séparer la contribution de l'interaction dipolaire de celle de l'anisotropie de déplacement chimique. Nous montrons au chapitre IV (section A) que la mesure de l'effet Overhauser $^{31}P-^{1}H$ et du T_1 à deux fréquences permet de réaliser cette opération.

REFERENCES

1. CHACHATY, C., ZEMB, T., LANGLET, G., TRAN-DINH, S., BUC, H. and MORANGE, M. (1976) Eur. J. Biochem. 62, 45.

2. SUNDARALINGAM, M. (1969) Biopolymers 7, 821.

3. SUNDARALINGAM, M. (1975) Ann. N.Y. Acad. Sci. 255, 3.

4. TRAN-DINH, S., GUSCHLBAUER, W. and GUERON, M. (1972) J. Am. Chem. Soc. 94, 7903.

5. GUERON, M., CHACHATY, C. and TRAN-DINH, S. (1973) Ann. N.Y. Acad. Sci. 222, 307.

6. ALTONA, C. and SUNDARALINGAM, M. (1973) J. Am. Chem. Soc. 95, 2333.

7. WATSON, J.D. and CRICK, F.H.C. (1953) Nature 171, 737 and 964.

8. ARNOTT, S., DOVER, S.D. and WONACOTT, A.J. (1969) Acta Cryst. 25, 2192.

9. ARNOTT, S., HUKINS, D.W.L., DOVER, S.D., FULLER, W. and HODGSON, A.R. (1973) J. Mol. Biol. 81, 107.

10. WANG, A.H.J., QUIGLEY, G.J., KOLPAK, F.J., CRAWFORD, J.L., VAN BOOM, J.H., VAN DER MAREL, G. and RICH, A. (1979) Nature, 282, 680.

11. VISWAMITRA, M.W., KENNARD, O., JONES, P.G., SHELDRICK, G.M., SALISBURY, S., FAVELLO, L. and SHAKKED, Z. (1978) Nature 273, 687.

12. SCHEVITZ, R.W., PODJARNY, A.D., KRISHNAMACHARI, N., HUGHES, J.J., SIGLER, P.B. and SUSSMAN, J.L. (1979) Nature 278, 188.

13. GIESSNER-PRETTRE, C. and PULLMAN, B. (1977) J. Theor. Biol. 65, 171 and 189.

14. SCHWEIZER, M.P., BROOM, A.D., TS'O, P.O.P. and HOLLIS, D.P. (1968) J. Am. Chem. Soc. 90, 1043.

15. GREY, A.A., SMITH, I.C.P., HRUSKA, F.E. (1971) J. Am. Chem. Soc. 93, 1765.

16. SCHWEIZER, M.P., BANTA, E.B., WITKOWSKI, J.T. and ROGINS, R.K. (1973) J. Am. Chem. Soc. 95, 3770.

17. KARPLUS, M. (1959) J. Chem. Phys. 30, 11.

18. ABRAGAM, A. (1966) Principles of Nuclear Magnetism, Clarendon Press, Oxford.

19. NOGGLE, J.H. and SCHIRMER, R.E. (1971). The Nuclear Overhauser Effect : Chemical Applications Academic Press, New York, N.Y.

20. WAGNER, G. and WÜTHRICH, K. (1979) J. Mag. Res. 33, 675.

21. KALK, A. and BERENDSEN, H.J.C. (1976) J. Mag. Res. 24, 343.

22. NEUMANN, J.M., BORREL, J., THIERY, J.M., GUSCHLBAUER, W. and TRAN-DINH, S. (1977) Biochim. Biophys. Acta 479, 427.

23. LÜDEMANN, H.D., WESTHOF, E. and RÖDER, O. (1974) Eur. J. Biochem. 49, 143.

24. IMOTO, T., AKASAKA, K. and HATANO, H. (1975) Chem. Phys. Lett. 32, 86.

CHAPITRE II

ÉTUDE DE LA CONFORMATION ET DE LA FLEXIBILITÉ DES MONO- ET DINUCLÉOSIDES MONOPHOSPHATES EN SOLUTION

Ce chapitre regroupe trois articles consacrés à l'étude de la conformation et de la flexibilité des mono- et dinucléosides monophosphates en solution.

Le premier "Comparative conformation of Uridine and Pseudouridine and their derivatives, Neumann, J.M. Bernassau, J.M. Guéron, M. and Tran-Dinh, S. (1980) Eur. J. Biochem. 108, 457" relate l'étude comparée de la conformation et de la flexibilité de l'uridine et de la pseudouridine et de leurs dérivés par RMN-^{1}H. Ce travail a été effectué en collaboration avec MM. M. Guéron et J.M. Bernassau (Ecole Polytechnique). La conformation de la base par rapport au sucre a été soigneusement étudiée par la mesure des effets Overhauser et des temps de relaxation. Pour faciliter l'étude de la conformation de la base de l'uridine et de ses dérivés, il a fallu deutérier ceux-ci en position 5 ; la substitution ^{1}H-^{2}H a été réalisée par MM. Bernassau et Tran-Dinh.

Les deux autres articles "Conformation and flexibility of GpC and CpG in neutral aqueous solution using ^{1}H-NMR and relaxation times measurements, Neumann, J.M., Guschlbauer, W. and Tran-Dinh, S. (1979) Eur. J. Biochem. 100, 141" et "^{1}H-NMR comparative studies of dinucleoside monophosphates. Influence of different factors on the conformational equilibria of nucleoside and dinucleoside monophosphates in aqueous solution Tran-Dinh, S., Neumann, J.M. and Borrel, J. (1981) Biochim. Biophys. Acta 655, 167" sont

consacrés à l'étude des conformations des six diribonucléosides monophosphates GpC, CpG, ApC, CpA, ApU et UpA par RMN-^{1}H. A partir des résultats obtenus et de ceux relatifs à des travaux antérieurs, l'influence, sur l'équilibre conformationnel des mono- et dinucléotides, des différents facteurs liés aussi bien à la structure chimique des résidus qu'aux conditions physico-chimiques, est analysée et discutée.

A. COMPARATIVE CONFORMATIONS OF URIDINE AND PSEUDOURIDINE AND THEIR DERIVATIVES

NEUMANN, J.M., BERNASSAU, J.M., GUERON, M. and TRAN-DINH, S.

(1980) Eur. J. Biochem. 108, 457.

Based on the chemical shift of the imino proton of hydrogen-bonded pseudouridine (ψrd)39 in yeast $tRNA^{Phe}$, Hurd and Reid [1] proposed that the proton involved in the hydrogen-bond to A31 is the N_1 rather than the N_3 proton of ψrd. This requires ψrd to be in a *syn* conformation, a proposition on which the crystal structure of tRNA is presently mute. Hurd and Reid pointed out that the substitution of Urd for ψrd does not inhibit the tRNA from functioning in protein synthesis, but blocks the control by certain tRNAs of the operon for biosynthesis of the corresponding aminoacid. They suggested that if (ψrd)39 were indeed *syn*, whereas Urd were *anti* in the same position, the regulatory effect of this otherwise rather minor modification could be better understood (Fig. 1).

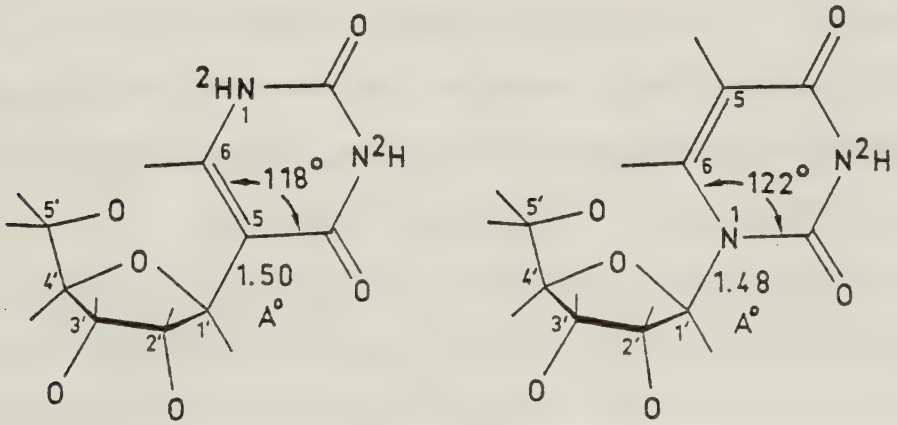

Fig. 1 - Schematic representation of uridine and pseudouridine.

The *syn/anti* question is thus raised within a context of biological function (regulation), regarding the nucleic acid, tRNA, whose structure is by far the best known of all. It therefore seemed worthwhile collecting more information, so we decided to examine the conformation of Urd and ψrd derivatives in solution. We chose the method of nuclear Overhauser enhancement, which enables one to compare the distances of the base proton H_6 (Fig. 1) to the various sugar protons, and is thus a method of choice for the study of the orientation of the glycosidic bond [2-7] : for *syn* orientations, H_6 is closest to $H_{1'}$ and the NOE to H_6 will be mainly from $H_{1'}$. For *anti* orientations, the NOEs will be mainly from other sugar protons than $H_{1'}$.

The measurements are straightforward for ψrd in which H_6 is the only non exchangeable proton on the base moiety. For Urd, prior deuteration on the 5 position is required in order to avoid a contribution of H_5 to the relaxation of H_6. This is specially nefarious since the chemical shifts of $H_{1'}$ and H_5 are so close that separate saturation of each of them is not possible.

A.I. EXPERIMENTAL SECTION

Urd, 3'UMP and 5'UMP were deuterium-labelled in position 5 according to the method of Wataya et al. [8]. The exchange was followed by ^{1}H-NMR. Figure 2 shows the 250 MHz proton spectrum of uridine labelled in the 5 position. The H_5 resonance has disappeared together with the H_5-H_6 coupling. The proton-deuterium exchange times are of the order of hours for Urd, a few days for 3'UMP and a week for 5'UMP, all at 80°C.

The compounds were lyophilized and dissolved in ^2H_2O 10^{-4} M EDTA, pD ≃ 7 at a final concentration between 5 and 10 mM. The sample tubes (12 and 5 mm diameter for the Varian XL-100 and CAMECA spectrometers respectively) were sealed after either degassing on the vacuum line or bubbling with nitrogen gas. In order to avoid overlapping between the water peak and

the sugar resonances, the experiments on the Varian XL-100 were performed at 10°C. At high field (250 MHz) the separation between the water and the sugar proton resonances is satisfactory at room temperature.

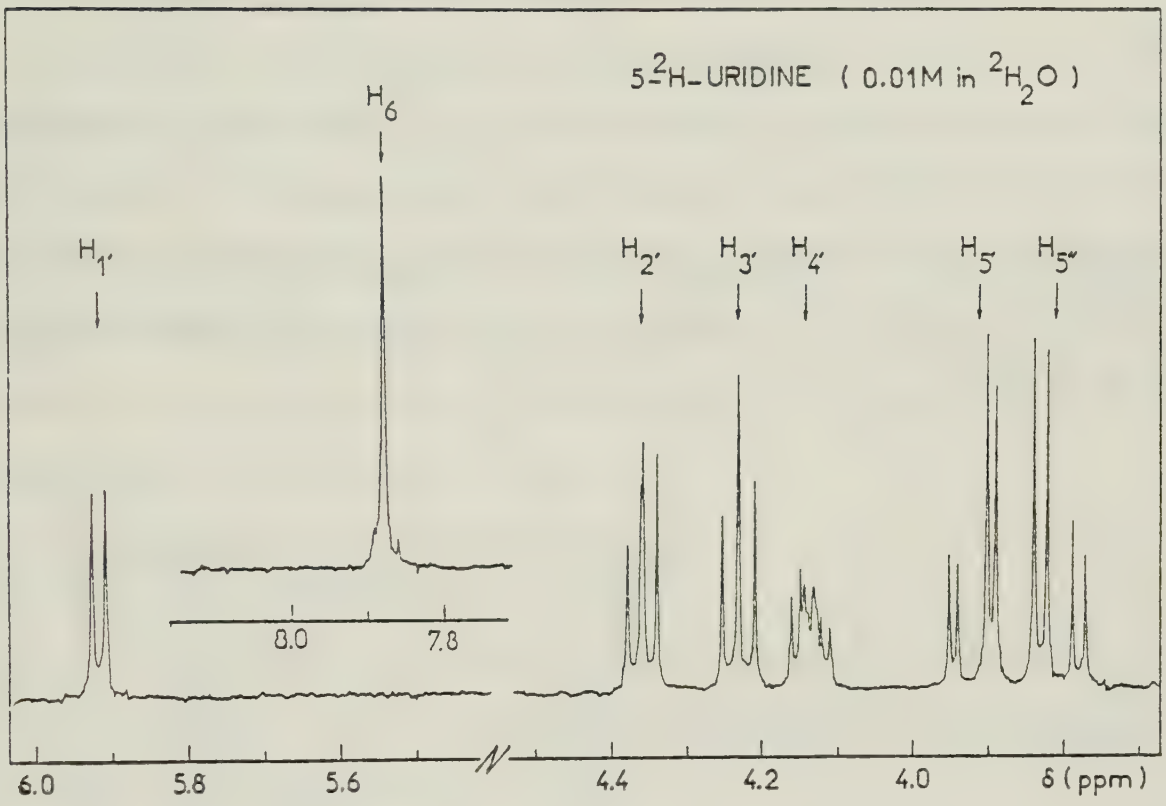

Fig. 2 - 250 MHz proton spectrum of uridine labelled in the 5 position. The H_6 peak of d-5 uridine is flanked by a weak doublet due to nondeuterated molecules.

NMR measurements

Proton spectra were measured on a Varian XL-100 (100 MHz) in the FT mode, or on a Cameca TSN 250 (250 MHz) in CW or FT. Relaxation was studied by inversion-recovery. Because recovery is non-exponential [9, 10] the significant relaxation parameter was obtained from the initial recovery rate (see below).

The NOEs at 250 MHz were measured in the CW mode, using a large radiofrequency observation field and sweeping slowly (1 min) through the enhanced line observed in the dispersion mode. The peak-to-peak signal is then proportional to the integrated intensity of the unsaturated absorption [5].

At 100 MHz the NOE was obtained in the FT mode. Saturation by "homodecoupling" was interrupted immediately before the 90° observation pulse. Instead of trying to saturate any one line exclusively, we measured the degree of saturation of each line of the spectrum and the different contributions to the NOE were all taken into account. For example, in the case of pseudouridine (Fig. 3), irradiation of $H_{2'}$ causes a 20% saturation of $H_{3'}$ and the NOE on H_6 is 11%.

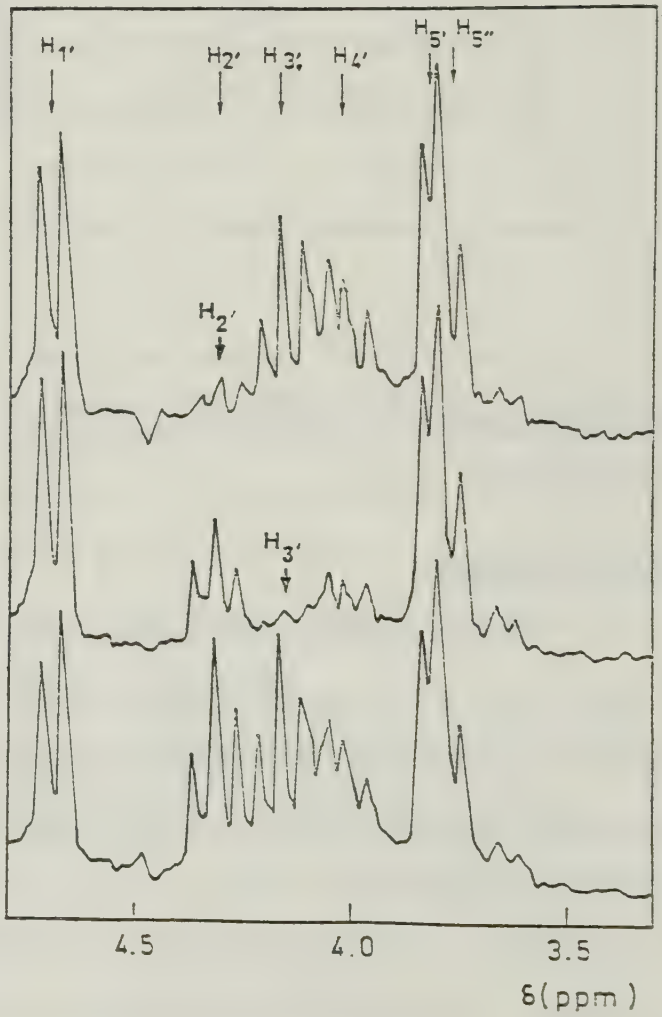

Figure 3

100 MHz proton spectra of pseudouridine with and without saturation of $H_{2'}$ or $H_{3'}$. Note the partial saturation of $H_{3'}$ upon saturation of $H_{2'}$, and vice versa.

Conversely, irradiation of H_3, causes 50% saturation of H_2, and the NOE is 14%. The observed enhancements can then be expressed as a function of the individual enhancements $\eta_{2'-6}$ and $\eta_{3'-6}$ as follows :

$$0.9\ \eta_{2'-6} + 0.2\ \eta_{3'-6} = 0.11$$

$$0.5\ \eta_{2'-6} + \eta_{3'-6} = 0.14$$

leading to

$$\eta_{2'-6} = 0.10 \quad \text{and} \quad \eta_{3'-6} = 0.090$$

On both spectrometers, the NOE was measured by comparing signal intensity with the irradiating field on or away from the proton resonance to be saturated. Statistical error was 2% at 250 MHz, 5% at 100 MHz. In the latter case, data were accumulated for 15 min.

A.II. THEORY OF THE NUCLEAR OVERHAUSER EFFECT

In a system of two protons I and S, separated by a distance r_{IS}, the coupled equations for the longitudinal magnetizations M_I and M_S are, in the absence of a radiofrequency field :

$$\frac{d}{dt} M_I = -\rho_{IS}(M_I - M_o) - \sigma_{IS}(M_S - M_o) \tag{1}$$

$$\frac{d}{dt} M_S = -\sigma_{IS}(M_I - M_o) - \rho_{IS}(M_S - M_o) \tag{2}$$

where

$$\rho_{IS} = \frac{1}{10}\left(\frac{\gamma^2\hbar}{4\pi\varepsilon_o c^2 r_{IS}^3}\right)\tau_c\left(1 + \frac{3}{1+\omega^2\tau_c^2} + \frac{6}{1+4\omega^2\tau_c^2}\right) \tag{3}$$

$$\sigma_{IS} = \frac{1}{10}\left(\frac{\gamma^2\hbar}{4\pi\varepsilon_o c^2 r_{IS}^3}\right)\tau_c\left(-1 + \frac{6}{1+4\omega^2\tau_c^2}\right) \tag{4}$$

and where γ is the magnetogyric ratio and ω the Larmor frequency of protons, τ_c is the dipolar correlation time and M_o is the equilibrium magnetization of either species. The units are SI and $4\pi\varepsilon_o c^2 = 10^7$. If M_S is reduced to

zero (saturation) the steady-state value of M_I is given by :

$$M_I/M_o = 1 + \eta_{IS} \tag{5}$$

where $\eta_{IS} \equiv \sigma_{IS}/\rho_{IS}$.

In the extreme narrowing limit, $\eta_{IS} = 0.5$ and $M_I = 1.5\ M_o$, a well known result.

A more realistic model for a nucleotide is a system of more than two nuclei, whose distances vary due to internal motions. These are taken into account (5) by using the average value $\langle r^{-6} \rangle$ instead of r^{-6} in eqs (3) and (4). The value of η_{IS} is now

$$\eta_{IS} = \sigma_{IS}/(\sum_{s'} \rho_{IS'}) \tag{6}$$

where the summation is over all protons except I, and where only proton S is saturated.

By eqs (6) and (4), one sees that η_{IS} is proportional to $\langle r_{IS}^{-6} \rangle$. The strong dependence on distance means that in a rigid system, the closest proton S will give by far the largest NOE. It is only if the molecule is flexible, so that proton I comes close to various protons S, S', S" ... in turn, that NOEs will be obtained upon saturation of more than one proton. This is indeed the situation found in nucleotides where NOEs to a base proton are found upon saturation of a number of sugar protons and this is direct evidence for rotation around the glycosidic bond, as discussed in detail earlier (5).

An interesting consequence of the theory is that in the extreme narrowing limit, the sum of all enhancements (or the enhancement when all protons S are saturated) is equal to 0.5.

A.III. RESULTS

A.III.1. Sugar conformations

The spectra of all the compounds examined here have been published and assigned previously, and the values of the chemical shifts and J couplings determined [11-13]. The populations of the ribose conformers N, S are quite similar for the two classes of compounds, the proportion of N conformer being between 0.44 and 0.56 in every case [14, 15]. Our observations agree with those just quoted. In view of the results on the glycosidic orientation discussed below, this indicates that there is no strong correlation between base orientation and sugar conformation in the compounds studied here, despite suggestions that such a correlation generally holds [16, 18].

A.III.2. NOEs

In table I, we give the NOEs observed on the H_6 proton of the base for all the compounds studied. In general, the NOE measurements at the two frequencies (100 MHz and 250 MHz) are in good agreement. For all compounds, NOEs are obtained from $H_{1'}$, $H_{2'}$ and $H_{3'}$ of the ribose ring, and there is also a small contribution from the exocyclic protons $H_{5'}$,$H_{5''}$. The fact that enhancements are obtained from different sugar protons shows that H_6 comes at times close to each of them. Assuming that the observed NOEs are intramolecular, as indicated by the invariance of the NOEs versus concentration (5 to 10 mM), the multiple NOEs demonstrate rotation around the glycosidic bond, as found earlier for other nucleotides [5, 6, 20].

The distributions of NOEs are quite different for the ψ and U families. In the former case, the NOE from $H_{1'}$ is larger than the sum of all others and hence the molecule is *syn* a large proportion of the time. In the latter, the NOEs are mainly from $H_{2'}$ and $H_{3'}$, and the NOE from $H_{1'}$ is small (less than 20% of the total). Therefore the contribution of the *anti* conformation is much larger. The interpretation is qualitative but clearcut : ψrd and its nucleotides are mainly *syn*, the Urd family mainly *anti*.

Table I - NOE values (in percentage) observed on proton H_6 (*)

Compounds \ Irradiated proton		1'	2'	3'	5' and 5"	Total
ψrd	a	26	10	9	6	51
	b	26	12	7	4	45
ψrd-3'-P	a	22	15[c]		5	42
	b	26	21[c]		4	51
Urd	a	8	23	8	4	43
	b	10	23	11	6	50
3'UMP	a	≃5	37[c]		≃5	47
5'UMP	a	≃5	28[c]		≃5	38

a) Measured at 100 MHz in FT mode. Probe temperature = 10°C

b) Measured at 250 MHz in CW mode. Probe temperature = 25°C

c) Lines were not resolved

(*) NOE from H_4, was always compatible with zero (< 2%).

A quantitative estimate of the *syn-anti* distribution can be obtained, using for instance the formulation of ref 5, but it is somewhat hazardous since there is at the present time no good model for the detailed geometry (or geometries) of the *syn* and *anti* conformers. Therefore it seems best to stay at the level of the strong qualitative interpretation given above. Note that the clear difference found between the two families does not mean that either has a rigid conformation. On the contrary NOEs from numerous protons demonstrate rotation around the glycosidic bond in each case. This is clear for ψrd and its monophosphates, as well as for Urd. For 3'UMP and 5'UMP which (like Urd) are mainly *anti*, the case for a *syn*

contribution rests on the 5% NOE from $H_{1'}$, so the evidence for rotation is not as good. The analysis of the sugar proton relaxation times suggests that there is indeed a *syn* contribution for 3'UMP but hardly for 5'UMP.

A.III.3. Relaxation measurements

The relaxation of a system of dipolar-coupled spins after a non-selective 180° pulse is not exponential [9, 10], as should be clear from equations (1) and (2). We have measured the initial rate of recovery after the 180° pulse, which is given by $T^{-1} = \Sigma_{s'}(\rho_{IS'} + \sigma_{IS'})$. The results are shown in Table II which also includes values for pyrazomycin [19], a nucleotide whose base contains no non-exchangeable proton.

Table II - Initial recovery time T after a non selective 180° pulse.

		$T(H_{1'})/T(H_{2'})$	$H_{1'}$	$H_{2'}$	$H_{3'}$	$H_{4'}$	$H_{5'5''}$	H_6
ψrd	a	1.5	2.0	1.3	1.1	1.1	0.37	1.6
	b	1.3	2.6	2.0	1.7	2.2	0.50	3.1
ψrd-3'-P	c	1.4	2.0	1.4	1.3	1.5	0.37	2.4
Urd	a	2.2	2.6	1.2	1.6	1.6	0.37	1.6
3'-UMP	d	2.0	2.4	1.2	1.3	1.7	0.35	1.0
5'-UMP	d	2.7	3.2	1.2	1.3	1.2	0.34	0.9
Pyrazomycin	b	2.7	5.1	1.9	1.7	1.9	0.50	

(a) 10°C, 100 MHz ; (b) Ref. 19 ; (c) 25°C, 250 MHz ;
(d) 25°C, 250 MHz. For these experiments, non deuterated compounds were used ; this only affects the relaxation time of H_6.

For pyrazomycin, we can divide the sugar protons in three classes. $H_{5'}$ and $H_{5''}$ are close together and relax each other efficiently. $H_{3'}$ and $H_{2'}$ are each relaxed by two neighbouring protons, and $H_{4'}$ though connected to

three protons is in a similar situation, given the orientations of the exocyclic group. Lastly $H_{1'}$ is relaxed by one proton ($H_{2'}$) only, and its relaxation time should therefore be about twice as long as that of $H_{2'}$ and $H_{3'}$. The experimental results are in reasonable agreement with this analysis.

If we now return to the ψ and U families we expect the sugar proton relaxation times to be reduced compared to pyrazomycin because of the dipolar coupling to the base proton H_6. For *syn* conformations, the effect on $H_{1'}$ will be important, and the ratio of the relaxation time of $H_{1'}$ to that of $H_{2'}$ or $H_{3'}$ will come closer to one. Using this ratio as a qualitative criterion, it appears that the ψ compounds are more *syn* than the U compounds, among which 5'UMP would be the most *anti*. This is in agreement with the NOE results.

A.IV. DISCUSSION

A.IV.1. The *syn-anti* problem

The problem of nucleoside and nucleotide conformations is the subject of a detailed and recent review [21]. The orientation around the glycosidic bond has been extensively studied. In crystals, the structures are mostly *anti* but *syn* conformations are also found [22]. For example, crystals of 3'-5'cyclic AMP contain two molecules in the asymetric unit cell, one *syn*, the other *anti* [23]. Guanosine and other puric nucleosides are also *syn* in the crystal [24], as well as 4-thiouridine [25]. In 6-methyluridine [26], the bulky substituent forces the *syn* orientation.

As for oligomers, a spectacular case is that of crystalline $(dGpdC)_6$ which forms a double-stranded helix, left-handed, and in which G is *syn* [27] in striking contrast to the standard right-handed DNA helix with bases in *anti* orientation.

The solution conformations (and flexibility) have been studied by various methods, including ultrasonic absorption [28, 29] and NMR. The NMR methods are varied : chemical shift of the sugar protons [30-32], J (C-H)

couplings [33, 34], rare-earth effects [35-37], proton-proton NOE [2-6, 17, 18] and proton relaxation studies involving selective deuteration [38-40]. The problem has also been analyzed theoretically [41, 42]. Except for NOE and relaxation measurements, these methods measure effects indirectly related to geometry, and their interpretation is therefore delicate.

Early work using indirect methods generally concluded that the glycosidic bond is *anti*. For example a change in the chemical shift of the base proton upon titration of the phosphate group was considered evidence for an *anti* conformation [30]. Or, in the pionnering rare-earth study of 5'AMP [35], the observations were analyzed in terms of a single structure, and it was concluded that the glycosidic bond is *anti*. Similarly, early theoretical studies stressed the *anti* conformation, even while noting the possibility of *syn* conformations [41].

These early conclusions were however not entirely justified by the data. For instance, lacking a quantitative interpretation, the shift of the base proton upon phosphate titration means only that *anti* conformations occur a finite proportion of the time ; it does not exclude the occurence of *syn* conformations. Similarly, the "*anti*" conclusion from the rare-earth study [35] is dependent on the assumption that the conformation is unique.

On the other hand, rotation around the glycosidic bond was strongly suggested by ultrasonic absorption, which demonstrated in adenosine an intramolecular motion around 10^9 Hz [28], and NOE experiments gave direct evidence for *syn-anti* equilibria [4, 5]. These results appear to have had discrete but significant impact : more recently experiments, or computations using the same methods which were discussed above are nowadays interpreted in terms of *syn-anti* equilibria [32, 37, 43, 44]. The consensus has become that there is a *syn-anti* equilibrium, whose proportions depend on the nucleotide species with the population of the *anti* conformation often higher in 5'-nucleotides.

How does one reconcile this view with the prevalence of "*anti*" structures found in many, though not all, crystals of mononucleotides and oligomers, and which have lead to the proposition of a "rigid nucleotide" [22] ? It would seem that the determining factor in such cases is not a preferred conformation of the isolated nucleotide but rather the internucleotide constraints induced by stacking and hydrogen bonding, together with their consequences on the shape of the sugar phosphate-backbone. Indeed, it has been shown that the *anti* contribution is larger for aggregates of 5'-GMP than in the isolated molecule [5].

A.IV.2. Conformation of the Urd and ψrd compounds

The present work shows that these compounds exhibit rotation around the glycosidic bond and that the ψ compounds are mainly *syn*, the U's mainly *anti*. This characterization is derived directly from measurements which are fairly simple in concept, execution and interpretation. It makes no use of modeled molecular properties. It should therefore in our opinion be considered highly trustworthy, although it disagrees with earlier descriptions, which were obtained on the basis of less direct methods [13].

Fuller use of the data could be considered ; for example the absolute value of the relaxation time of H_6 can be combined with the NOEs and an estimate of the rotational correlation time to give the average distance (i.e. $\langle r^{-6} \rangle^{1/6}$) of H_6 to each of the sugar protons [19]. This can be completed by the analysis of the relaxation of the sugar protons, coupled to the introduction of structural data (Van der Waals radii). One can then try to delimit more closely the base orientations [19]. This will however not be attempted here. We feel that the motion of nucleotides is potentially too complex and the analysis too elaborate to be reliable unless carried out by careful comparison between a large series of nucleotides. Here we shall be content to consider rapidly the origin of the difference between Urd and ψrd with respect to *syn/anti* geometry. Since this difference is found both in

nucleosides and nucleotides, it cannot be determined by the phosphate group. A possibility is that the range of *syn* angles available is restricted by steric hindrance between the base oxygen and the sugar. This could be less severe in ψrd due mainly to the differences in angles of the base at N_1 and C_5 (122° and 118° respectively) (Fig. 1) and also, secondarily, to the difference in length of the glycosidic bond : r_{C-N} = 0.148 nm, r_{C-C} = 0.150 nm [45, 46].

There have been no previous NOE measurements on the ψ nucleotides but the NOE of ψrd was studied by Nanda et al. [7] who concluded that *syn* and *anti* conformations are present in roughly equal proportions. The NOE enhancements of H_6 due to H_1', , H_2', and H_3', were 0.22, 0.19 and 0.12. These values disagree somewhat with ours due may be to the large concentration (0.1 M) used by Nanda et al. which could give rise to intermolecular interactions and increase the *anti* contribution. It is also possible that partial saturation of the 2' proton occured together with 3' saturation in these experiments which were carried out at 100 MHz. The method used here to circumvent this problem is presented above in the experimental section.

Although NOE experiments have been carried out on various U derivatives [3], we do not know of any on uridine and its monophosphates. The early work was usually performed at high concentration (> 0.1 M) where aggregation may occur.

A.IV.3. Significance for tRNA

A last point to be examined is the significance of the present work for the conformation of ψrd in tRNA. Our results indicate that ψ compounds, though mostly *syn*, can take both *syn* and *anti* conformations. Therefore we cannot conclude that ψrd must be *syn* in tRNA. A fortiori, we cannot argue that the substitution of Urd by ψrd in tRNA amounts to replacing an *anti* by a *syn* nucleotide. However, it could be that the constraints of the structure of the anticodon loop and stem, including the hydrogen-bonds of

the A31-39 basepair stabilize different orientations viz. *anti* for Urd and *syn* for ψrd. The differences found here between the U and ψ compounds reinforce the proposition for a *syn* conformation of ψrd in position 39. Conversely, if this proposition is confirmed, the solution study would give elements for its explanation in terms of nucleotide properties. At the same time it would raise the question of the conformation of the other ψrds found in tRNA, notably in the universal TψC sequence.

REFERENCES

1. HURD, R.E. and REID, B.R. (1977) Nucleic Acid Res. 4, 2747.

2. NOGGLE, J.H. and SCHIRMER, R.E. (1971) The Nuclear Overhauser Effect : Chemical Applications Academic Press. N.Y.

3. SCHIRMER, R.E., DAVIS, J.P., NOGGLE, J.H. and HART P.A. (1972) J. Am. Chem. Soc. 94, 2561.

4. HART, P.A. and DAVIS, J.P. (1971) J. Am. Chem. Soc. 93, 753.

5. TRAN-DINH, S., GUSCHLBAUER, W. and GUERON, M. (1972) J. Am. Chem. Soc. 94, 7903.

6. GUERON, M., CHACHATY, C. and TRAN-DINH, S. (1973) Ann. N.Y. Acad. of Sci. 222, 307.

7. NANDA, R.K., TEWARI, R., GOVIL, G. and SMITH, I.C.P. (1974) Can. J. Chem. 52, 371.

8. WATAYA, Y., HAYATSU, H. and KAWAZO, Y. (1972) J. Am. Chem. Soc. 94, 8927.

9. AKASAKA, K., IMOTO, T., SHIBATA, S. and HATANO, H. (1975) J. Magnet. Res. 18, 328.

10. KALK, A. and BERENDSEN, H.J.C. (1976) J. Magnet. Res. 24, 343.

11. FUJIWARA, S. and VETSUKI, M. (1968) in "Recent Developments of Magnetic Resonances in Biological Systems" S. Fujiwara and L.H. Piette, Ed., Hirokawa Publishing Co., Inc., Tokyo.

12. HRUSKA, F.E., GREY, A.A. and SMITH, I.C.P. (1970) J. Am. Chem. Soc. 92, 4088.

13. SCHLEICH, T., BLACKBURN, B.J. and LAPPER, R.D. and SMITH, I.C.P. (1972) Biochemistry 11, 137.

14. DAVIES, D.B. and DANYLUK, S.S. (1974) Biochemistry 13, 4417.

15. DAVIES, D.B. and DANYLUK, S.S. (1975) Biochemistry 14, 543.

16. SUNDARALINGAM, M. (1969) Biopolymers 7, 821.

17. LUDEMANN, H.D., WESTHOF, E. and RODER, O. (1974) Eur. J. Biochem. 49, 143.

18. LUDEMANN, H.D., RODER, O., WESTHOF, E., GOLDAMMER, E.V. and MULLER, A. (1975) Biophys. Struct. Mechanism 1, 121.

19. NEUMANN, J.M., BORREL, J., THIERY, J.M., GUSCHLBAUER W. and TRAN-DINH, S. (1977) Biochim. Biophys. Acta 479, 427.

20. TRAN-DINH, S. and CHACHATY, C. (1973) Biochim. Biophys. Acta 335, 1.

21. DAVIES, D.B., Progress in NMR Spectroscopy (1978) Pergamon Press 12, 135.

22. SUNDARALINGAM, M. Conformation of Biological Molecules and Polymers. The Jerusalem Symposia on Quantum Chemistry and Biochemistry, V. The Israel Academy of Sciences and Humanities, Jerusalem 1973.

23. WATENPAUGH, K., DON, J., JENSEN, L.H. and FURBERG, S. (1968) Science 159, 206.

24. RAO, S.T. and SUNDARALINGAM, M. (1970) J. Am. Chem. Soc. 92, 4963.

25. SAENGER, W. and SCHEIT, K.H. (1970) J. Mol. Biol. 50, 153.

26. SUCK, D., SAENGER, W. and VORBRUGGEN, H. (1972) Nature 235, 333.

27. WANG, A.H., QUIGLEY, G.J., KOLPAK, F.J., CROWFORD, J.L., Van BOOM, J.H., Van der MAREL, G. and RICH, A. (1979) Nature 282, 680.

28. RHODES, L.M. and SCHIMMEL, P.R. (1971) Biochemistry 10, 4426.

29. HEMMES, P., OPPENHEIMER, L. and JORDAN, F. (1974) J. Am. Chem. Soc. 96, 6023.

30. DANYLUK, S.S. and HRUSKA, F.E. (1968) Biochemistry 7, 1038.

31. SCHWEIZER, M.P., BROOM, A.D., TS'O, P.O.P. and HOLLIS, D.P. (1968) J. Am. Chem. Soc. 90, 1042.

32. JORDAN, F. and NIV, H. (1977) Biochim. Biophys. Acta 476, 265.

33. LEMIEUX, R.U., NAGABHUSHAN, T.L. and PAUL, B. (1972) Can. J. Chem. 50, 773.

34. DELBAERE, L.T.J., JAMES, M.N.G. and LEMIEUX, R.U. (1973) J. Amer. Chem. Soc. 95, 7866.

35. BARRY, C.D., NORTH, A.C.T., GLASEL, J.A., WILLIAMS, R.J.P. and XAVIER, A.V. (1971) Nature 232, 236.

36. FAZAKERLEY, G.V., RUSSELL, J.C. and WOLFE, M.A. (1977) Eur. J. Biochem. 76, 601.

37. DOBSON, C.M., GERALDES, C.F.G.C., RATCLIFFE, G. and WILLIAMS, R.J.P. (1978) Eur. J. Biochem. 88, 259.

38. CHACHATY, C., ZEMB, T., LANGLET, G., TRAN-DINH, S., BUC, H. and MORANGE M. (1976) Eur. J. Biochem. 62, 45.

39. CHACHATY, C., YOKONO, T., TRAN-DINH, S. and GUSCHLBAUER, W. (1977) Biophys. Chem. 6, 151.

40. NEUMANN, J.M., GUSCHLBAUER, W. and TRAN-DINH, S. (1979) Eur. J. Biochem. 100, 141.

41. BERTHOD, H. and PULLMAN, B. (1971) Biochim. Biophys. Acta 232, 595.

42. BERTHOD, H. and PULLMAN, B. (1973) FEBS Letters 30, 231.

43. LEE, C.H. and SARMA, R.H. (1976) J. Am. Chem. Soc. 98, 3541.

44. GIESSNER-PRETTE, C. and PULLMAN, B. (1977) J. Theor. Biol. 65, 189.

45. SUNDARALINGAM, M. (1975) Ann. N.Y. Acad. Sci. 225, 3.

46. ROHRER, D.C. and SUNDARALINGAM, M. (1970) J. Am. Chem. Soc. 92, 4950.

B. CONFORMATION AND FLEXIBILITY OF GpC AND CpG IN NEUTRAL AQUEOUS SOLUTION USING ^{1}H-NMR AND RELAXATION TIMES MEASUREMENTS

NEUMANN, J.M., GUSCHLBAUER, W. and TRAN-DINH, S.

(1979) Eur. J. Biochem. 100, 141.

The continuing interest in the conformation of dinucleoside phosphates can be divided into three main areas : (a) solid-state studies of self-complementary dinucleoside phosphates, highlighted by the recent mini-helices ApU [1] and GpC [2] ; (b) solution studies on all 16 dinucleoside phosphates [3-5] which quite clearly indicated that even at ambient temperature only small parts of these compounds are stacked, in equilibrium with several other extended conformations ; (c) studies on the interaction of self-complementary dinucleotides and oligonucleotides [6-12] with intercalating drugs in order to obtain precise details of their interactions with nucleic acids.

It has been found from all these studies that dinucleoside phosphates in dilute solutions will probably be poor models for the study of nucleic acids, but they may be relevant for the conformation of single-stranded nucleic acids. Only at very high concentrations or in crystals will self-complementary dinucleotides and oligonucleotides self-associate to mimic double-stranded nucleic acids [13, 14].

The development of the nuclear Overhauser effect [15-18] and in particular relaxation techniques [6, 19-24] has allowed the detailed conformation of nucleic acid components to be studied and has furnished interesting results concerning the rotational flexibility of the glycosidic linkage. It has thus been observed that purine nucleosides, and in particular

guanosine, show a large contribution of the *syn* conformation even in mononucleoside and dinucleoside phosphates [5, 16-18, 23]. This has been confirmed recently by Dobson et al. using the lanthanide probe method [25]. Previous theoretical computations [26] had already envisaged this possibility in dinucleoside phosphates. These findings open new aspects for the conformation of nucleic acid components and show that these components are highly flexible in dilute solution. The purpose of this paper is to show the similarities and the differences in conformation and in flexibility between the self-complementary dinucleoside monophosphates GpC and CpG. The data obtained by using ^{1}H NMR at 250 MHz and proton relaxation measurements will be discussed in comparison with those of GpU and UpG.

B.I. MATERIALS AND METHODS

GpC and CpG were purchased from P.L. Biochemicals. They were dissolved in $^{2}H_2O$ and were freed of possible divalent ions by shaking with Chelex 100 or by addition of EDTA. The pH was adjusted to 7-8. The samples were lyophilized twice in $^{2}H_2O$ and redissolved in $^{2}H_2O$ at a final concentration of 0.01 mol/l. These solutions were introduced into NMR tubes, degassed in a vacuum line and sealed. Deuteration of H-8 guanine was obtained by heating the sealed sample tubes at 80°C for 3 h.

The ^{1}H NMR spectra were recorded on a Cameca-TSN 250 spectrometer. The apparatus operated in the pulsed Fourier-transform mode, was associated with a 24 K Nicolet computer. The chemical shifts were measured at various temperatures between 22°C and 65°C with an accuracy better than 0.005 ppm from 3-(trimethylsilyl)-($^{2}H_4$)propionic acid. Some experiments were performed with phosphorus noise-decoupling at 101.2 MHz to clarify the fine structure of H-4', H-5' and H-5" resonances.

The T_1 relaxation time of protons was obtained by the inversion recovery method (180°-τ-90° sequences) at 45°C to avoid the overlapping of the residual ^{2}HHO signal with the resonances of the ribose ring protons.

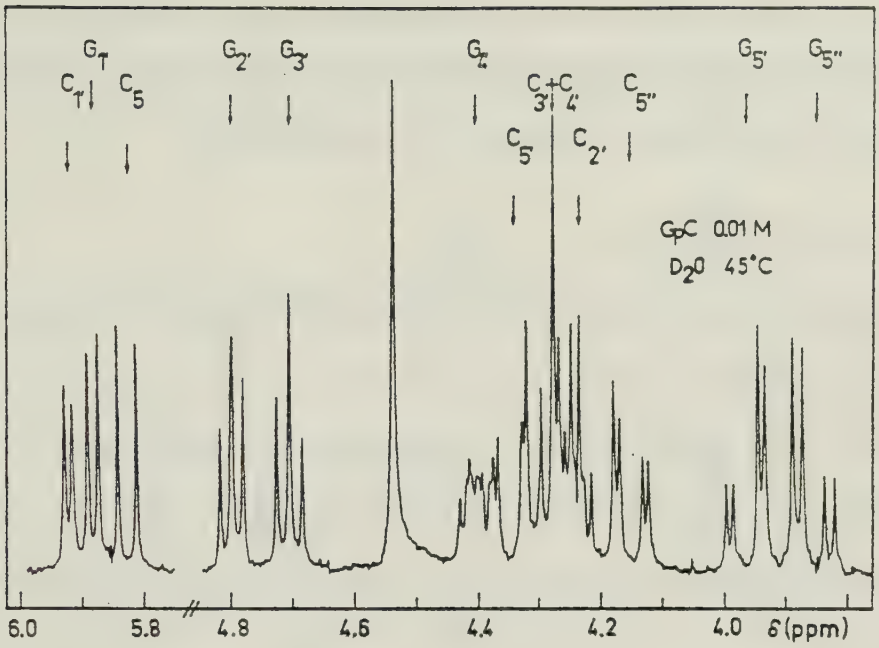

Fig. 1 - 250 MHz ^{1}H-NMR spectrum with ^{31}P noise decoupling of GpC in neutral aqueous solution at 45°C.

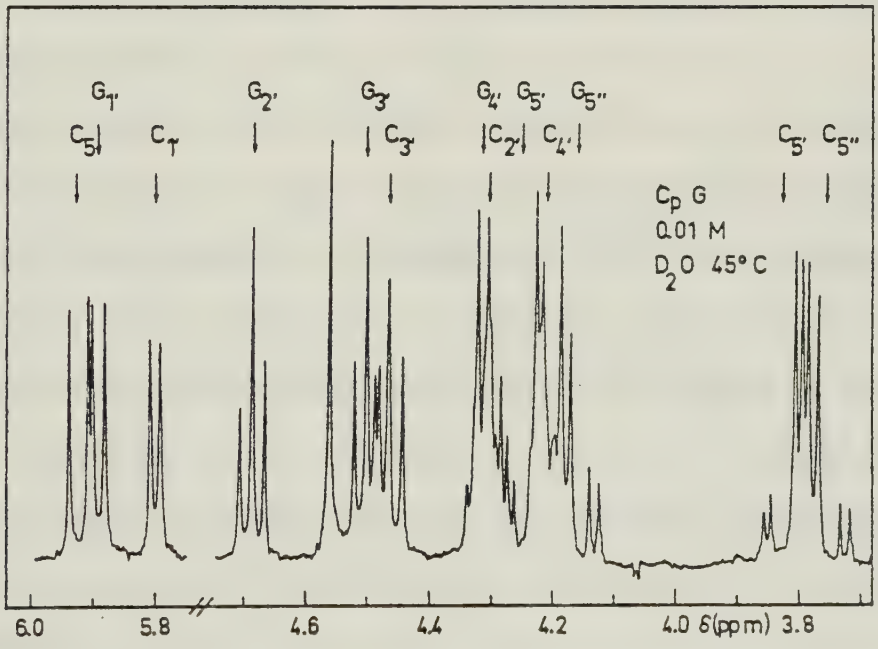

Fig. 2 - 250 MHz ^{1}H-NMR spectrum with ^{31}P noise decoupling of CpG in neutral aqueous solution at 45°C.

The $\pi/2$ pulse width is only 3.5 µs. The delay between the sequences was 22 s, i.e. about seven times the longest relaxation time of observed protons. At 45°C chemical shifts and coupling constants are similar to those at 65°C indicating that association phenomena are negligible.

B.II. RESULTS AND DISCUSSION

Figures 1 and 2 show the ^{1}H-NMR spectra with ^{31}P noise decoupling of GpC and CpG in $^{2}H_2O$ at 45°C. Identification of the protons was achieved by comparison with the spectra of the corresponding monomers and by decoupling. The assignments are in agreement with those of Ezra et al. [4]. The determination of certain coupling constants between ribose protons was sometimes difficult because of the overlapping of the signals from the two ribose moieties. In particular, the coupling constants of the 5'-bound residue's exocyclic methylene protons were virtually inaccessible due to the overlapping with those of the 3' residue (Figs 1 and 2) even at high frequencies [3, 4]. Without using very elaborate methods, like selective deuteration of one of the residues [3, 4], we have determined the coupling constants involving the 5', 5" protons of the exocyclic group by using the relaxation measurement method ; since the difference between the relaxation rates of the ribose ring protons (less than 1 s^{-1}) and those of the exocyclic methylene protons (2.5-3.0 s^{-1}) is very important, one can observe only the 5', 5" proton signals as shown in figure 3 with the sequence 180°-τ-90° and with τ values sufficiently small.

The change of chemical shifts and coupling constants as a function of temperatures was followed for GpC and CpG in 5°C steps from 25°C to 65°C. Except for the H-5 of the pC residue in GpC which shifts 0.176 ppm downfield between 25°C and 65°C, no very dramatic changes in chemical shift have been noted (Table I). On the other hand, the coupling constants J_{HH} and J_{PH} (Table II) changed quite noticeably with temperature ; this variation has not been observed for the mononucleotides [27, 28]. In the case of GpC, $J_{1'2'}$

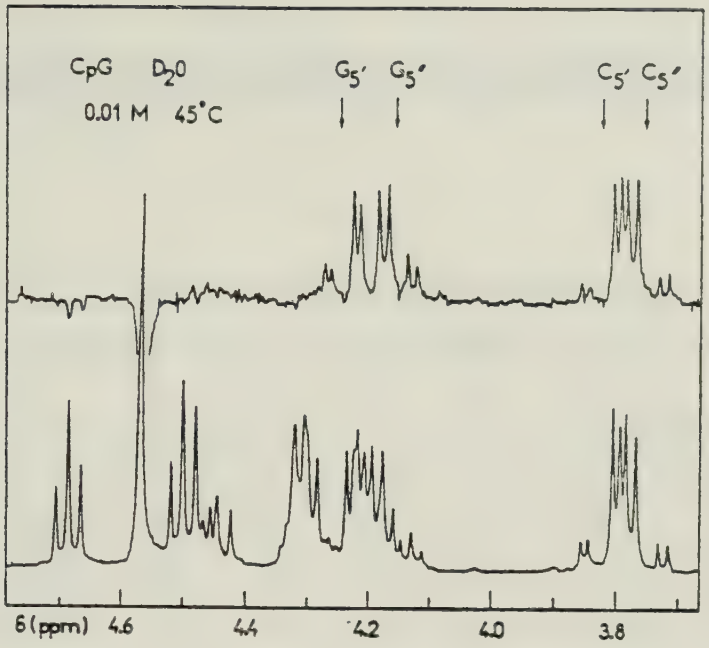

Fig. 3 - Determination of $J_{4'5'}$ and $J_{4'5''}$ of the two exocyclic groups of CpG with the use of the inversion recovery method (see text). (A) Normal spectrum with ^{31}P noise decoupling of CpG ; (B) spectrum with ^{31}P noise decoupling of the same compound obtained by using the (180°-τ-90°) sequences with τ = 0.7 s.

was small both for Gp ($J_{1'2'}$: 3.5 Hz) and for pC ($J_{1'2'}$: 2.8 Hz) at 25°C while they increased at 65°C (4.7 Hz and 3.4 Hz respectively) approaching those of the monomers (Table II). In the same temperature interval, $J_{3'4'}$ decreased from 6.2 Hz to 4.9 Hz for Gp and from 7.0 Hz to 6.4 Hz for pC. These results show that the effect of temperature on the mean sugar conformation is more important for Gp than for pC. In the case of CpG, only the coupling constants of the Cp residue showed important changes : $J_{1'2'}$ (Cp) = 3.4 Hz, $J_{3'4'}$ (Cp) = 6.5 Hz at 25°C, and $J_{1'2'}$ (Cp) = 4.2 Hz, $J_{3'4'}$ (Cp) = 5.8 Hz at 65°C.

When the temperature varied from 25°C to 65°C, $J_{4'5'}$ and $J_{4'5''}$ of the 3'-residue exocyclic group of both GpC and CpG remained unchanged, while $J_{4'5'}$, $J_{4'5''}$ and $J_{5''P}$ of the 5' residue increases notably (see Table II). This indicates that the conformation around the phosphodiester

Table I - Proton chemical shifts of GpC and CpG in ^2H_2O at 25°C and 65°C. Shifts were measured relative to 3-(trimethylsilyl)-($^2H_4$)propionic acid.

Compound	Temp.	Shifts of guanyl protons						
		8	1'	2'	3'	4'	5'	5''
	°C	ppm						
GpC	25	8.016	5.856	4.798	4.655	4.408	4.004	3.873
GpC	65	7.988	5.890	4.798	4.731	4.398	3.949	3.848
3'GMP	25	8.006	5.940	4.826	4.788	4.408	3.898	3.842
Monomer-dimer		-0.010	0.084	0.028	0.133	0.000	-0.106	-0.031
CpG	25	8.026	5.899	4.658	4.508	4.313	4.269	4.155
CpG	65	8.013	5.897	4.705	4.491	4.311	4.227	4.150
5'GMP	25	8.117	5.941	4.752	4.480	4.344	4.101	4.101
Monomer-dimer		0.091	0.042	0.094	-0.028	0.031	-0.168	-0.054

Compound	Temp.	Shifts of cytidyl protons							
		6	5	1'	2'	3'	4'	5'	5''
	°C	ppm							
GpC	25	7.816	5.708	5.898	4.209	4.273	4.273	4.399	4.144
GpC	65	7.822	5.884	5.931	4.250	4.278	4.278	4.324	4.156
5'CMP	25	8.044	6.150	5.977	4.32±0.01		4.285	4.191	4.080
Monomer-dimer		0.228	0.442	0.079	0.111	0.047	0.012	-0.208	-0.064
CpG	25	7.750	5.893	5.768	4.310	4.437	4.215	3.830	3.759
CpG	65	7.715	5.958	5.825	4.300	4.481	4.204	3.822	3.743
3'CMP	25	7.915	6.094	5.941	4.552	4.424	4.287	3.943	3.841
Monomer-dimer		0.165	0.201	0.173	0.242	-0.013	0.072	0.113	0.082

Table II - Proton-proton and proton-phosphorus coupling constants of GpC and CpG in ^2H_2O at 25° and 65°. Spin-spin coupling constants were determined to better than 0.2 Hz.

Compound	Temp.	Coupling constants, J, for guanyl residue									
		$J_{1'2'}$	$J_{2'3'}$	$J_{3'4'}$	$J_{4'5'}$	$J_{4'5''}$	$J_{5'5''}$	$J_{3'P}$	$J_{5'P} \approx J_{5''P}$	N	f_{gg}
	°C	Hz								%	
GpC	25	3.5	4.8	6.2	2.7	4.2	13.1	8.2		64	70
GpC	65	4.7	5.1	4.9	3.0	4.2	12.9	10.0		51	67
3'GMP	25	5.8	5.2	3.4	3.0	4.1	12.9	8.5		37	67
Monomer-dimer		2.3	0.4	-2.8	0.3	-0.1	-0.2	0.3			
CpG	25	4.8	5.0	5.2	2.3	3.5	11.7		4.0	52	81
CpG	65	5.2	5.3	4.7	3.0	4.2	11.8		4.7	47	67
5'GMP	25	6.0	5.2	3.5	3.4	3.4			4.8	37	71
Monomer-dimer		1.2	0.2	-1.7	1.1	-0.1			0.8		

Compound	Temp.	Coupling constants, J, for cytidyl residue										
		J_{56}	$J_{1'2'}$	$J_{2'3'}$	$J_{3'4'}$	$J_{4'5'}$	$J_{4'5''}$	$J_{5'5''}$	$J_{3'P}$	$J_{5'P} \approx J_{5''P}$	N	f_{gg}
	°C	Hz									%	
GpC	25	7.6	2.8	4.6	≈7.0	1.5	2.0	11.8		3.5	71	100
GpC	65	7.6	3.4	4.9	≈6.4	2.0	2.7	11.4		4.6	65	93
5'GMP	25	7.6	3.4	4.6	6.4	2.3	2.7	11.8		4.7	65	90
Monomer-dimer		0.0	0.6	0.0	-0.6	0.8	0.7	0.0		1.2		
CpG	25	7.6	3.4	5.0	6.5	3.0	4.0	13.2	8.5		66	67
CpG	65	7.6	4.2	5.3	5.8	3.0	4.2	13.0	8.5		58	67
3'CMP	25	7.6	4.2	5.3	6.4	2.7	4.2	12.9	9.0		60	70
Monomer-dimer		0.0	0.8	0.3	-0.1	-0.3	0.2	-0.3	0.5			

linkage was strongly affected by the change in temperature. The effect still appears to be larger in the case of GpC than CpG : for the same temperature interval the four coupling constants mentioned changed more than 30% in the case of the pC residue.

In general, the coupling constants of GpC and CpG at 65°C were very similar to those of the corresponding monomers (see Table II).

B.II.1. Ribose and Backbone Conformation

The mole fractions of the N conformation [29] and of the gg rotamer [30] were computed from the proton-proton coupling constants and are included in Table II. The proportion of N conformer is more important for the C than for the G residue in both dinucleoside monophosphates studied. In the case of GpC at 25°C, the N form predominates for both residues ; the proportion of gg rotamer, f_{gg}, is about 70% in Gp, while it is almost equal to 100% in pC. These results suggest that the rotation about the phosphodiester linkage is very reduced for GpC. In the case of CpG, we noted that at the same condition of temperature, the N proportion of both residues is less important than that in GpC. Although the gg rotamer is always favoured for CpG, f_{gg} of Cp residue is only 67%, much lower than that of pC in GpC. In addition, the small values of $J_{5'P}$, $J_{5''P}$ and $J_{3'P}$ indicate that the conformers gg (around the $C_{5'}$-$O_{5'}$ bond) and g- or g+ (around the $C_{3'}$-$O_{3'}$ bond) are favoured in both dinucleoside monophosphates studied.

The largest change in the N/S equilibrium as a function of temperature is observed in the Gp moiety of GpC between 25°C and 65°C, χ_N (the fraction of N conformer) decreases from 0.64 to 0.51, while under the same experimental conditions, the pG residue in CpG is virtually unchanged (χ_N decreases from 0.52 to 0.47). For the cytidine residues of both GpC and CpG, a decrease of the N form is observed, although it remains predominant even at 65°C.

The results obtained for the Gp residue in GpC are completely different from those of the corresponding Gp residue in GpU [5] ; here the predominant sugar conformation is the S form (χ_S = 0.60), as in the monomers, while the N form dominates in Gp of GpC under similar conditions of temperature and concentration. On the other hand, the residue pG behaves very similarly in CpG (Table II) and in UpG [5] with $\chi_N/\chi_S \approx 1$.

B.II.2. Conformation around the Glycosidic Bond

The conformation of the base around the glycosidic bond of the G and C residues was studied by measuring the longitudinal relaxation rates of the protons before and after deuteration of H-8 of guanine. The initial relaxation rate of a proton i can be obtained from the plot of $\log[M_o - M_z(t)] = f(t)$ over a time range such that cross-relaxation effects are negligible [21-23]. Under the narrowing conditions mentioned in previous papers [5, 19-14], the relaxation rate is expressed as :

$$\frac{1}{T_{1i}} = \frac{3}{10}\gamma_H^4 \cdot \hbar^2 \cdot f(\tau_c) \cdot \sum_j \langle r_{ij}^{-6} \rangle \qquad (1)$$

$$f(\tau_c) = \tau_c/(1+\omega^2\tau_c^2) + 4\tau_c/(1+4\omega^2\tau_c^2) \qquad (2)$$

where r_{ij} is the distance between protons i and j, ω the Larmor frequency, τ_c the correlation time.

In Table III, the experimental relaxation times T_1 of the protons of GpC and CpG, measured at 45°C, are summarized. It is noteworthy from these results that the relaxation times T_1 of proton H-1' of both G residues increased considerably after deuteration of H-8. This shows unequivocally that the *syn* conformation exists in the G residues of both GpC and CpG.

Table III - Proton longitudinal relaxation times (in sec) of GpC and CpG in ^2H_2O at 45°C.

Compound	T_1 for guanyl protons						T_1 for cytidyl protons						
	8	1'	2'	3'	5'5''	$f(\tau_c)$ $\times 10^{-10}$	6	5	1'	2'	3'	5'5''	$f(\tau_c)$ $\times 10^{-10}$
GpC	2.47	2.46	0.98	1.00	0.38	4.45	0.97	2.50	3.04	1.31		0.37	4.60
[8-^{2}H]GpC		3.25	1.26	0.97	0.37		1.04	2.57	3.00	1.26		0.39	
$(Z_{i8})^b$		(24%)	(56%)										
CpG	1.58[a]	2.22	1.23	0.94	0.37	3.90	0.92	3.00	2.46		0.84	0.35	3.70
Cp[8-^{2}H]G		3.60	1.58	1.03	0.36		0.87	3.20	2.42		0.97	0.35	
$(Z_{i8})^b$		(36%)	(38%)	(20%)									

[a] If we do not take into account the contribution of H-3' of Cp to relaxation of H-8 of pG, this value of T_1 would be 2.10 s.

[b] Calculated from eq. (3) (see text).

After deuteration of H-8 of guanine, the T_1 of the cytidine protons of GpC remained the same within the experimental error. In the case of CpG, however, deuteration of H-8 changed the T_1 of H-3' of the Cp residue from 0.84 s to 0.97 s, while the relaxation times of the other protons remained unchanged. The proton H-8 of guanine contributes therefore to the relaxation of H-3' of the C of CpG. Similar results have been observed for UpG [5], thus in both cases the H-8 of the G residue must be very close to the H-3' of the other residue, at least part of the time. This will only be the case, if (a) the base orientation of the G residue is *anti*, (b) the exocyclic group of the 5' residue is in the gg conformation, and (c) the phosphate group is oriented in such a way that the conformers g'g' ($\phi_2 = 180°$) and g- ($\phi_1, = 180°$) are adopted. These conditions are entirely compatible with experimental results from the coupling constants (see above and Table II).

Deuteration of H-8 of G also permits the influence of H-6 of C on the relaxation of the sugar protons of the cytidyl residue to be evaluated. It will be shown later that in both dimers the correlation time τ_c compu-

ted from T_1 values of the guanyl protons is comparable with that obtained from the cytidyl residue. Furthermore, the relaxation rates of the sugar protons are not very sensitive to conformational changes of the ribose ring as had been shown previously [31]. Thus the comparison between the two sets of ribose proton T_1 values of [8-^{2}H]G and the cytidyl moiety in both dimers should give information about the orientation of the base.

In [8-^{2}H]GpC the T_1 of H-1' and H-2' of pC are very similar to those of [8-^{2}H]Gp (Table III) which indicates that in pC of GpC, neither H-1' nor H-2' contribute to the relaxation of H-6 of C. In other words, the *syn* conformation in the case of pC is highly improbable and the *anti* conformation predominates.

In contrast, in Cp[8-^{2}H]G, the T_1 values of H-1' and H-3' of Cp are lower than those in the [8-^{2}H]pG residue. The *anti* and *syn* conformation appear therefore equally probable.

In order to evaluate the contribution of each ribose proton of the G residue to the relaxation of H-8 of the base, we have computed the ratio

$$Z_{i8} = \frac{1/T_{1i} - 1/T^*_{1i}}{1/T_{18}} \qquad i = 1',\ 2',\ \text{or}\ 3' \qquad (3)$$

where $1/T^*_{1i}$ is the relaxation rate of proton i after deuteration of H-8. According to equation (1) this ratio is equal to :

$$Z_{i8} = \frac{\langle r_{i8}^{-6} \rangle}{\sum_{j \neq 8} \langle r_{j8}^{-6} \rangle}$$

The sum $\sum_j \langle r_{ij}^{-6} \rangle$ have been computed taking into account the N/S equilibrium and the exocyclic rotamer distributions f_{gg}, g_{gt}, and f_{tg} as a function of the glycosidic torsion angle T. In figure 3 the values of $\Delta f^{-1}(\tau_c)/\langle f^{-1}(\tau_c)\rangle$ for the four nucleoside residues are plotted as a function of the torsion angle T, where $f^{-1}(\tau_c) = 0.3\ T_{1i}.\gamma^4.\hbar^2 \sum_j \langle r_{ij}^{-6} \rangle$, and

taking into account all the protons which are sensitive to base orientation, i.e. H-8, H-6, H-1', H-2' and H-3'. This is the method used in previous publications [5, 20, 22, 23, 31]. The value of $f(\tau_c)$ in normally computed from the minima of the curve $\Delta f^{-1}(\tau_c)/\langle f^{-1}(\tau_c)\rangle F(T)$, but it can also be determined independently by other ways : (a) from the T_1 of sugar protons 1', 2' and 3' [31] of [8-^{2}H]G, which do not depend on the base orientation, or (b) from the T_1 of H-5 of the residues, the relaxation of which depends solely on H-6, the distance r_{56} being constant (Table III). We have observed that the values of $f(\tau_c)$ of the two residues of a given dimer are very similar. Thus, this confirms the approximation of isotropic orientation of the whole molecule [5] as in the case for nucleosides [19, 22, 24, 31] and mononucleotides [20, 21, 23].

The values of Z_{i8} (equation (3)) are included in table III ; these results show that for the Gp moiety of GpC, dipolar coupling between protons H-8 and H-2' is very important : more than 50% of the relaxation of H-8 is due to H-2'. H-1' also contributes to the relaxation of H-8 while the influence of H-3' on H-8 is negligible. Quite clearly, the *syn* conformation of the G moiety is predominant. This is confirmed by the results in figure 4A, where a minimum is observed for T = 70°, corresponding to the *syn* range.

Lastly, figure 4B shows that the cytidine residue in GpC adopts the *anti* conformation while for CpG both *anti* and *syn* are equally probable, as had been already suggested by the T_1 measurements.

From the data presented we can conclude that there is a very large difference in behaviour between GpC and CpG. None of the conformations we have observed preferentially corresponds to those observed in single-crystal studies. The crystal structure of GpC [32], very similar to that encountered in RNA [33], is characterized by two stacked bases in the *anti* conformation, with both sugars in the N form and the gg rotamer of the exocyclic group. Part of these features are retained in the solution conformation of GpC :

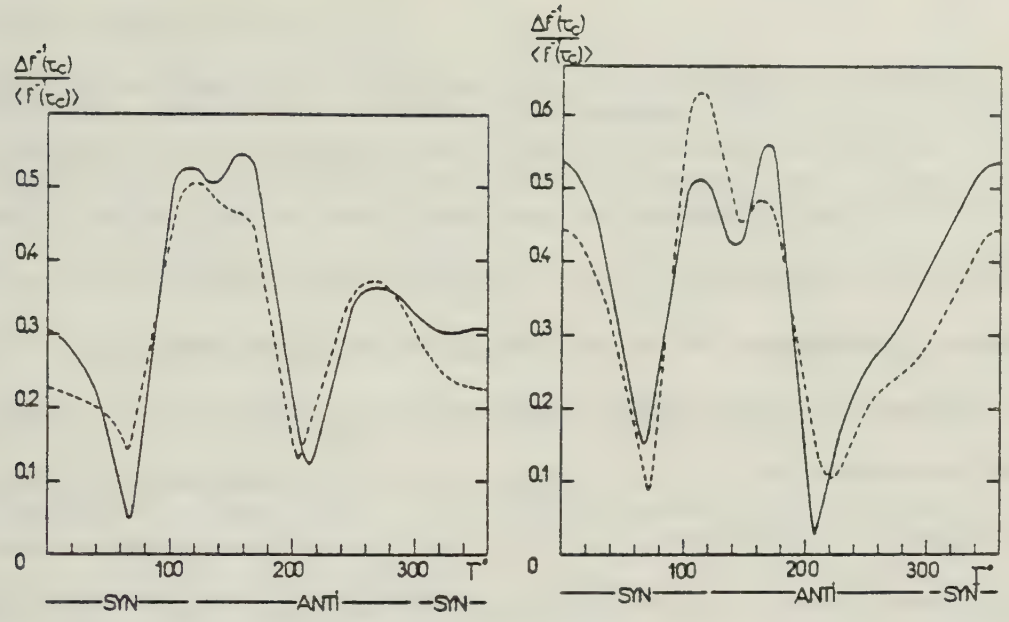

Fig. 4 - Plots of $\Delta f^{-1}(\tau_c)/\langle f^{-1}(\tau_c)\rangle$ vs T for the two residues of GpC and CpG. (A) (——) Gp of GpC ; (....) pG of CpG. (B) (——) pC of GpC ; (....) Cp of CpG.

the pC part of GpC with a preferential *anti* conformation of the glycosidic linkage, the pure gg orientation of the 4'-5' bond and a larger predominance of the N form approaches the conformation encountered in the crystal. This is quite clearly not the case for the Gp moiety, which is predominantly oriented in the *syn* conformation, the percentage of the N form is lower and the exocyclic group is only 2/3 in the gg conformation. Furthermore, GpC is quite sensitive to temperature changes, as far as the sugar conformation, the glycosidic linkage and the exocyclic and phosphate bonds are concerned. These results are qualitatively in agreement with those of Ezra et al. [4] who conclude that "GpC displays a maximum of 45% stacked population".

In the case of CpG, both the Cp and the pG residue behave very much like the mononucleotides, in particular, as far as the flexibility of the base around the glycosidic linkage is concerned [16-18]. The temperature effect is therefore relatively small and less important than in GpC, since CpG is very little stacked. This again agrees with the data of Ezra et al.[4],

who concluded that about 25% of the GpC molecules are stacked at room temperature.

We wish to emphasize also the important difference which exists between GpC and GpU concerning the sugar conformation of the Gp moiety. At 45°C only 40% of the Gp residues assume the N form in GpU, while in the case of GpC the N form predominates in Gp ; on the other hand, both pC and pU show a large predominance of the N form in their sugar moieties.

CpG and UpG show similar conformational properties : in both cases the pG residues shows an N/S ≈ 1, while the N form predominates in both pyrimidine moieties. Furthermore, in both cases the guanine base is quite close to the ribose ring of the pyrimidine moiety at least part of the time. In all four dinucleoside phosphates the *syn* conformation exists in the guanine moiety.

Finally, it should be noted that there is no apparent correlation between the sugar conformation (N/S equilibrium) and the glycosidic base-sugar orientation (*syn-anti* distribution) as had already been observed in the nucleosides [22] and nucleotides [23]. In GpC and CpG the N form always predominates, although the base-sugar orientations differ completely.

REFERENCES

1. SEEMAN, N.C., ROSENBERG, J.M., SUDDATH, F.L., KIM, J.J.P. and RICH, A. (1976) J. Mol. Biol. 104, 109.

2. ROSENBERG, J.M., SEEMAN, J.M., DAY, R.O. and RICH, A. (1976) J. Mol. Biol. 104, 145.

3. LEE, C.H., EZRA, F.S., KONDO, N.S., SARMA, R.H. and DANYLUK, S.S. (1976) Biochemistry, 15, 3627.

4. EZRA, F.S., LEE, C.H., KONDO, N.S., DANYLUK, S.S. and SARMA, R.H. (1977) Biochemistry, 16, 1977.

5. CHACHATY, C., YOKONO, T., TRAN-DINH, S. and GUSCHLBAUER, W. (1977) Biophys. Chem. 6, 151.

6. NEIDLE, S., ACHARI, A., TAYLOR, G.L., BERMAN, H.M., CARRELL, H.L., GLUSKER, J.P. and STALLINGS, W.C. (1977) Nature (Lond.) 269, 304.

7. TSAI, C.C., JAIN, S.C. and SOBELL, H.M. (1977) J. Mol. Biol. 114, 301.

8. JAIN, S.C., TSAI, C.C. and SOBELL, H.M. (1977) J . Mol. Biol. 114, 317.

9. KRUGH, T.R. and REINHARDT, C.G. (1975) J. Mol. Biol. 97, 133.

10. REINHARDT, C.G. and KRUGH, T.R. (1977) Biochemistry 16, 2890.

11. PATEL, D.J. (1974) Biochemistry, 13, 2388.

12. PATEL, D.J. (1974) Biochemistry, 13, 2396.

13. BORER, P.N., KAN, L.S. and TS'O, P.O.P. (1975) Biochemistry, 14, 4847.

14. KAN, L.S., BORER, P.N. and TS'O, P.O.P. (1975) Biochemistry, 14, 4864.

15. SCHIRMER, R.E., NOGGLE, J.H., DAVIS, J.P. and HART, P.A. (1970) J. Am. Chem. Soc. 92, 3266.

16. TRAN-DINH, S., GUSCHLBAUER, W. and GUERON, M. (1972) J. Am. Chem. Soc. 94, 7903.

17. TRAN-DINH, S. and CHACHATY, C. (1973) Biochim. Biophys. Acta. 335, 1.

18. GUERON, M., CHACHATY, C. and TRAN-DINH, S. (1973) Ann. N.Y. Acad. Sci. 222, 307.

19. LÜDEMANN, H.D., WESTHOF, E. and RÖDER, O. (1974) Eur. J. Biochem. 49, 143.

20. CHACHATY, C., ZEMB, T., LANGLET, G., TRAN-DINH, S., BUC, H. and MORANGE, M. (1976) Eur. J. Biochem. 62, 45.

21. AKASAKA, K., IMOTO, T., SHIBATA, S. and HATANO, H. (1975) J. Magnet. Res. 18, 328.

22. NEUMANN, J.M., BORREL, J., THIERY, J.M., GUSCHLBAUER, W. and TRAN-DINH, S. (1977) Biochim. Biophys. Acta 479, 427.

23. TRAN-DINH, S. and CHACHATY, C. (1977) Biochim. Biophys. Acta 500, 405.

24. PLACH, H., WESTHOF, E., LÜDEMANN, H.D. and MANGEL, R. (1977) Eur. J. Biochem. 80, 295.

25. DOBSON, C.M., GERALDES, C.F.G.C., RATCLIFFE, G. and WILLIAMS, R.J.P. (1978) Eur. J. Biochem. 88, 259.

26. STELLMAN, S.D., HINGERTY, B., BROYDE, S.B., SUBRAMANIAN, E., SATO, T. and LANGRIDGE, R. (1973) Biopolymers, 12, 2731.

27. TRAN-DINH, S., THIERY, J., GUSCHLBAUER, W. and DUNAND, J.J. (1972) Biochim. Biophys. Acta 281, 289.

28. TRAN-DINH, S., and GUSCHLBAUER, W. (1975) Nucleic. Acids Res. 2, 873.

29. ALTONA, C. and SUNDARALINGAM, M. (1972) J. Am. Chem. Soc. 94, 8205 and (1973) J. Am. Chem. Soc. 95, 2333.

30. HRUSKA, F.E. (1973) Jerus. Symp. Quantum Chem. Biochem. 5, 345.

31. TRAN-DINH, S., NEUMANN, J.M., THIERY, J.M., HUYNH-DINH, T., IGOLEN, J. and GUSCHLBAUER, W. (1977) J. Am. Chem. Soc. 99, 3267.

32. DAY, R.O., SEEMAN, N.C. ROSENBERG, J.M. and RICH, A. (1973) Proc. Natl Acad. Sci. U.S.A. 70, 849.

33. ARNETT, S., HUKINS, D.W., DOVER, S.D., FULLER, W. and HODGSON, A.R. (1973) J. Mol. Biol. 81, 107.

C. ^{1}H-NMR COMPARATIVE STUDIES OF DINUCLEOSIDE MONOPHOSPHATES. INFLUENCE OF DIFFERENT FACTORS ON THE CONFORMATIONAL EQUILIBRIA OF NUCLEOSIDE AND DINUCLEOSIDE MONOPHOSPHATES IN AQUEOUS SOLUTION

TRAN-DINH, S., NEUMANN, J.M. and BORREL, J.

(1981) Biochim. Biophys. Acta 655, 167.

It is well known that nucleic acids exist in various forms depending on the hydratation degree, the nature of the sugar (ribose or deoxyribose), the salt concentration, the temperature, etc ... X-ray diffraction studies have demonstrated that in fibers of DNA or RNA, the sugar and base conformations vary considerably for different nucleic acid forms. For example, the N conformation is exclusively present in the A-form of nucleic acids and the S conformation in the B-form of DNA [1-2]. Similar properties have been found in oligo- [3-7] and polynucleotides [8-9]. It is therefore interesting to study not only the conformation and the motion of each residue in oligonucleotides but also the influence of different factors which can monitor the change in the conformational equilibrium of these molecules.

Among the analytical techniques available, there is no doubt that NMR is now one of the most powerful tools for investigating relatively small molecules in solution. The sugar conformation of mono- and oligonucleotides can be satisfactorily determined from the J_{H-H} and J_{P-H} coupling constants using the Karplus equation. Numerous results are already available for mono- [10-16], di- [17-26] and trinucleotides [27-29] ; however most of them have been obtained from the analysis of NMR spectra recorded under given experimental conditions. Only a few papers [30-35] have been devoted to investigations of the influence of for example, pH, temperature, salt concentration etc ... These studies yield undoubtebly important information about the

structural properties of molecules but also require much NMR instrument time and a considerable effort in the preparation of NMR samples especially when dealing with the pH effect.

Concerning the base orientation about the glycosidic bond, owing to the lack of a coupling between the base and the sugar protons, the determination of the base conformation cannot be obtained by a simple analysis of ^{1}H-NMR spectra as has been done for the sugar conformation. Among the NMR methods that have been used up to now to study the base conformation : chemical shift of sugar protons [36-38], J(C-H) coupling [39, 40], rare-earth effects [41-43], proton-proton NOE [44-52] and proton relaxation studies [25, 26, 53-56] involving selective deuteration, except for nuclear Overhauser enhancement (NOE) and relaxation measurements, these methods measure effects indirectly related to the geometry and their interpretation is therefore delicate.

In the present work, we have investigated the conformation of four dinucleoside monophosphates ApC, CpA, ApU and UpA, by ^{1}H-NMR at 250 MHz, under various experimental conditions (temperatures and concentrations) and then compared them with our previous work on GpC, CpG, GpU and UpG [25, 26]. We use the proton relaxation measurements and the effects of selective deuteration on proton T_1's as methods for studying the base conformation. The effects, due to the intra- and the intermolecular interactions between residues in dinucleosides monophosphates, on the proton chemical shifts and coupling constants have been carefully analyzed by varying the experimental conditions (temperature and concentration).

In the last section, we have presented a discussion about the influence of structural and physico-chemical factors on the conformational equilibria of nucleoside and dinucleoside monophosphates in aqueous solution.

C.I. EXPERIMENTAL PROCEDURE

ApC, CpA, ApU and UpA were purchased from P-L Biochemicals. They were dissolved in ^2H_2O and were freed of possible divalent ions by shaking with Chelex 100 or by addition of EDTA. The pH was adjusted to 7-8. The samples were lyophilized twice in ^2H_2O and redissolved in ^2H_2O at a final concentration of 10 mM. The NMR samples tubes were sealed after degassing on the vacuum line. Deuteration of H^8 of adenine was obtained by heating the sealed sample tubes at 80°C for 3 h.

The ^1H-NMR spectra were recorded on a CAMECA TSN 250 spectrometer. The apparatus, operated in the pulsed Fourier-transform mode, was associated with a 24K Nicolet computer. The chemical shifts were measured at various temperature between 22°C and 65°C with an accuracy better than 0.005 ppm from 3-(trimethylsilyl)-($^2H_4$) propionic acid. Some experiments were performed with phosphorus noise-decoupling at 101.2 MHz to clarify the fine structure of H_4' , H_5' and H_5'' resonances.

The T_1 relaxation time of protons was obtained by the inversion recovery method (180°-τ-90° sequences) at about 45°C to avoid the overlapping between the residual ^2HHO signal and the resonances of the ribose ring protons. The π/2 pulse width is only 3.5 μs. The delay between the sequences was 22 sec., i.e. about seven times the longest relaxation time of observed protons. At 45°C, chemical shifts and coupling constant are similar to those at 65°C indicating that association phenomena are negligeable.

C.II. RESULTS AND DISCUSSION

C.II.1. Ribose conformation

a) Temperature and concentration effects on the average conformation of the ribose ring

The chemical shifts and the coupling constants J_{H-H} , J_{P-H} of ApC, CpA, ApU and UpA were measured as a function of temperature between 25° and 65°C. The data obtained at these two extreme temperatures are reported in tables I and II. Proton resonances were identified from comparisons with the spectra of the corresponding monomers and by proton-proton, phosphorus-proton decoupling. The assignments are in agreement with those of Ezra et al. [21]. The determination of the coupling constants involving the 5', 5" protons of the exocyclic group was carried out using the ^{31}P noise decoupling and the sequence 180°-τ-90° method described in a previous paper [26].

The results in table I show that, in general, the resonances of the ribose ring and the base protons are somewhat shifted towards lower fields when the temperature increases. As far as ApC is concerned, on going from 25° to 65°C, the H^2 and H_3, chemical shifts for Ap residue manifest large variations (0.10 and 0.13 ppm) and similarly H^5 and H_1, chemical shifts of pC residue varied by about 0.19 and 0.12 ppm respectively. Significant shift variations have also been observed for the same protons of ApU but their magnitudes are reduced by about 30% for Ap and 20% for pU (with respect to those of ApC). The changes in chemical shifts are smaller for CpA and UpA. In the case of CpA, the chemical shifts for H^2 and H_2, of pA change by 0.05 ppm and 0.07 ppm respectively. The variations in the chemical shift of UpA protons are much smaller less than 0.04 ppm for the same temperature interval.

Table I - Proton chemical shifts of dinucleoside monophosphates in neutral aqueous solution at 25 and 65°C (in ppm from TMP).

	T°	purine residue								pyrimidine residue							
		H_8	H_2	$H_{1'}$	$H_{2'}$	$H_{3'}$	$H_{4'}$	$H_{5'}$	$H_{5''}$	H_6	H_5	$H_{1'}$	$H_{2'}$	$H_{3'}$	$H_{4'}$	$H_{5'}$	$H_{5''}$
ApC (10 mM)	25	8.337	8.135	6.037	4.846	4.668	4.473	4.033	3.902	7.729	5.711	5.760	4.167	4.258		4.372	4.141
	65	8.375	8.236	6.074	4.858	4.801	4.461	3.972	3.873	7.790	5.903	5.877	4.230	4.264		4.321	4.157
		0.038	0.101	0.037	0.012	0.133	-0.012	-0.061	-0.029	0.061	0.192	0.117	0.063	0.006		-0.051	0.016
ApC (1.5 mM)	25	8.373	8.167	6.059	4.861	4.653	4.465	4.024	3.900	7.715	5.668	5.730	4.141	4.237		4.361	4.141
	65	8.334	8.234	6.075	4.858	4.737	4.468	3.975	3.874	7.780	5.879	5.859	4.218	4.254		4.312	4.148
		-0.039	0.067	0.016	-0.003	0.084	0.003	-0.049	-0.026	0.065	0.211	0.129	0.077	0.017		-0.049	0.007
CpA	25	8.410	8.216	6.099	4.619	4.522	4.357	4.314	4.153	7.706	5.826	5.723	4.309	4.437	4.173	3.883	3.785
(20 mM)	65	8.407	8.264	6.111	4.692	4.513	4.364	4.259	4.159	7.694	5.917	5.793	4.288	4.482	4.211	3.851	3.760
		-0.003	0.048	0.012	0.073	-0.009	0.007	-0.055	0.006	-0.012	0.091	0.070	-0.021	0.045	0.038	-0.032	-0.025
ApU	25	8.331	8.155	6.046	4.864	4.651	4.479	4.027	3.896	7.756	5.609	5.745		4.261		4.336	4.136
(20 mM)	65	8.331	8.228	6.076	4.874	4.731	4.482	3.979	3.876	7.791	5.752	5.838		4.291		4.293	4.151
		0.000	0.073	0.030	0.010	0.080	0.003	-0.048	-0.020	0.035	0.143	0.093		0.030		-0.043	0.015
UpA	25	8.408	8.222	6.108	4.722	4.540	4.373	4.265	4.148	7.750	5.785	5.741	4.246	4.476	4.189	3.799	3.730
(20 mM)	65	8.409	8.258	6.116	4.749	4.525	4.367	4.246	4.155	7.731	5.824	5.779	4.273	4.506	4.204	3.793	3.721
		0.001	0.036	0.008	0.027	-0.015	-0.006	-0.019	0.007	-0.019	0.039	0.038	0.027	0.030	0.015	-0.006	-0.009

Table II - Proton-proton and proton-phosphorus coupling constants (in Hz) of dinucleoside monophosphates in neutral aqueous solution at 25 and 65°C.

		purine residue								pyrimidine residue								
	T°C	$J_{1'2'}$	$J_{2'3'}$	$J_{3'4'}$	$J_{4'5'}$	$J_{4'5''}$	$J_{5'5''}$	$J_{3'P}$	$J_{5'5''P}$	J_{56}	$J_{1'2'}$	$J_{2'3}$	$J_{3'4'}$	$J_{4'5'}$	$J_{4'5''}$	$J_{5'5''}$	$J_{3'P}$	$J_{5'5''P}$
ApC	25	3.8	4.9	5.5	2.6	3.4	13.1	9.0		7.6	2.7	5.0	6.7	~1.5	~1.5	11.4		4.5
	65	4.9	5.1	4.4	2.7	3.8	12.9	8.0		7.6	3.5	5.0	6.0	2.0	2.7	11.7		4.5
CpA	25	4.2	5.0	5.5	~2.	3.0	11.4		4.0	7.6	3.3	5.2	6.3	2.3	3.8	13.1	8.5	
	65	4.6	5.2	5.2	2.3	3.8	12.0		5.0	7.6	4.3	5.2	5.4	2.3	4.2	13.1	8.5	
ApU	25	3.8	4.9	5.2	2.3	3.0	13.0	8.5		8.0	3.0	5.2	6.5	~1.5	~1.8	12.0		4.5
	65	5.2	4.9	4.6	2.3	3.8	12.9	8.2		8.0	3.8	5.1	6.0	2.0	3.1	11.0		4.0
UpA	25	4.8	5.2	5.0	2.5	3.5	12.0		4.2	8.0	4.6	4.9	5.3	3.0	3.8	12.9	8.0	
		5.2	5.0	4.5	3.1	3.8	11.4		5.0	8.0	5.0	5.1	4.7	3.0	3.8	12.7	9.0	

For all dinucleoside monophosphates studied, $J_{1',2'}$ increases while $J_{3',4'}$ decreases with increasing temperature ; this indicates that the N conformer, which is predominant at room temperature, is less favoured at higher temperature (Table III). Thus the temperature effect consists of reducing the difference between the N and S proportions in dinucleoside monophosphates : when the temperature increases, the ratio N/S tends to unity, the equilibrium value for a large number of ribonucleosides and ribonucleotides in aqueous solutions.

In order to distinguish between effects due to intra- and intermolecular interactions on the chemical shifts and coupling constants, the variation of these two NMR parameters was also monitored by varying the ApC concentration between 5.10^{-2} M and 10^{-3} M, since among the heterodimers, this compound exhibits the largest temperature effect. No significant spectral modification has been observed (δ and J) for the pC residue. On the other hand, for the Ap residue, the proton chemical shifts varied substantially while the proton-proton coupling constants remained unchanged with dilution : the H^2, H^8, $H_{1'}$ protons exhibited shifts to lower fields of about 0.10 ppm, 0.07 ppm and 0.06 ppm respectively when the ApC concentrations decrease from 5.10^{-2} M to $1.5.10^{-3}$ M (Fig. 1). This concentration effect on proton chemical shifts in Ap residue is quite similar to that observed for AMP's [49]. Therefore, the shifts observed for H^2, H^8 and $H_{1'}$ for the Ap residue in ApC (or ApU) is essentially due to the base-base stacking between two neighbouring dimers (intermolecular association). In contrast, the H_5 , $H_{1'}$, H^6, $H_{2'}$ shifts or pC and the $H_{3'}$ shift of Ap occuring when the temperature is varied (table I) are probably due to the intramolecular interaction between the two residues of the same dimer. This hypothesis was confirmed from studies of the temperature effect on the chemical shift of the ApC protons at low concentrations. We found that for the same temperature interval, the chemical shift variations of H^2, H^8 and $H_{1'}$ of Ap are much smaller at

Table III - N conformer proportion, gg rotamer proportion and difference in chemical shifts (in ppm) between the two protons $H_{5'}$, $H_{5''}$ of dinucleoside monophosphates at 25 and 65°C

		purine residue			pyrimidine residue		
	T°C	% N	% gg	Δδ(5'-5")	% N	% gg	Δδ(5'-5")
ApC	25	59	75	0.131	71	100	0.231
	65	47	69	0.099	63	91	0.164
				0.032			0.067
CpA	25	57	88	0.161	66	74	0.098
	65	53	74	0.100	56	69	0.091
				0.061			0.007
ApU	25	58	84	0.131	68	100	0.200
	65	47	74	0.103	61	86	0.142
				0.028			0.058
UpA	25	51	75	0.117	54	65	0.069
	65	46	64	0.091	48	65	0.072
				0.026			-0.003
GpC[a)]	25	64	70	0.131	71	100	0.255
	65	51	67	0.101	65	93	0.168
				0.030			0.087
CpG[a]	25	52	81	0.114	66	67	0.071
	65	47	67	0.077	58	67	0.079
				0.037			-0.008

low concentrations ($\simeq 10^{-3}$ M) than at higher concentrations, while the shift variations for H_5 , $H_{1'}$, H^6, $H_{2'}$ of pC and $H_{3'}$ of Ap are practically the same under both experimental conditions (Table I). The fact that the proton-proton coupling constants are temperature dependent but insensitive to dilution leads us to the conclusion that intermolecular base-base stacking does not modify the average conformation of dinucleoside monophosphates while intramolecular interaction excerces a great influence on the conformation equilibrium of the ribose ring by favouring the N conformer. It is worth noting that at room temperature, the intermolecular base-base stacking of ApC and ApU at concentrations around 0.01 M is not at all negligeable.

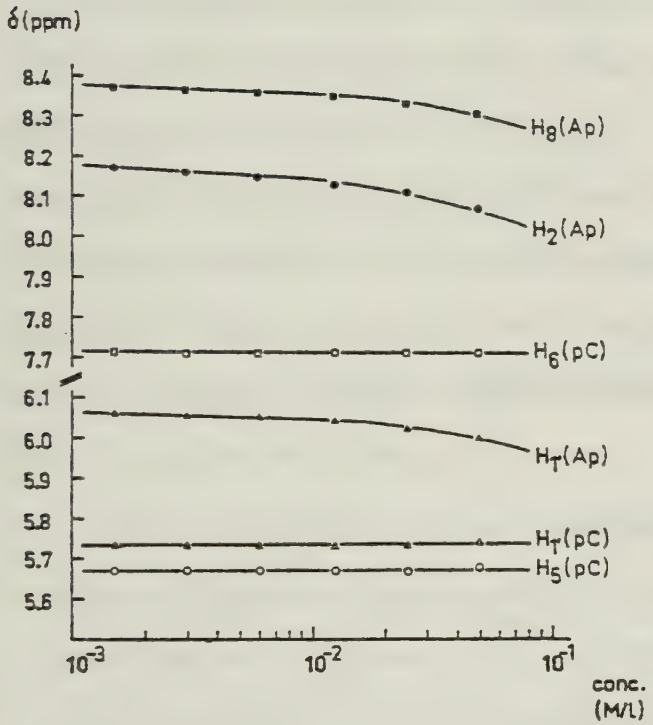

Figure 1

Effect of concentration on the proton chemical shifts of ApC in neutral aqueous solution at 25°C.

The data in tables I and II also indicate that : i) the dimers (ApC, ApU) which exhibit the largest chemical shift variations manifest at the same time, the largest variations in the N/S ratio ; ii) intermolecular base-base stacking occurs to a much lesser extent with CpA, UpA than with ApC and ApU ; iii) for these last two compounds, the intramolecular inter-

action between both residues of the same molecule is very pronounced (greatest variation in the N/S ratio). It seems likely that intramolecular interaction also favours aggregation. On the basis of proton chemical shift and proton-proton coupling variations, the degree of association of the dinucleoside phosphates studied can be classified in the following order : ApC > ApU > CpA > UpA. This degree of association is therefore greater : i) in pu-py than in py-pu compounds ; ii) with C than with U residue. These conclusions are in agreement with those of Ezra et al. [21] based on the difference in the chemical shifts and coupling constant between monomers and dimers.

b) Temperature effects on the exocyclic group conformation

The mole fractions of the gg rotamer (and N conformer) computed from the proton-proton coupling constants and the difference in chemical shifts between the two protons $H_{5'}$, $H_{5''}$, $\Delta\delta(5'-5'')$, of the exocyclic group are summarized in table III. In the case of ApC and ApU at 25°C, the proportion of gg rotamer, f_{gg}, is about 80% in Ap, while it is almost equal to 100% in pC and pU. These results suggest that the rotation about the phosphodiester linkage of ApC and ApU is highly reduced, similar to the case of GpC [26].

The gg rotamer is always favoured in CpA and UpA, although f_{gg} is only 74% in Cp and 65% in Up, much lower than that of pC and pU (in ApC, ApU). In addition the small values of $J_{5'P}$, $J_{5''P}$ and $J_{3'P}$ indicate that the conformers g'g' (around the $C_{5'}$-$O_{5'}$ bond) and g^- or g^+ (around the $C_{3'}$-$O_{3'}$ bond) are favoured for all the dinucleoside monophosphates studied.

When going from 25° to 65°C, the $H_{5'}$ and $H_{5''}$ resonances are shifted to higher fields in contrast to the other protons of the base and the ribose ring, and at the same time $J_{4'5'}$, $J_{4'5''}$ increase (Table II). In the same temperature interval, the variation of $\Delta\delta(5'-5'')$ depends on the position of the observed residue with respect to the phosphate group.

The $\Delta\delta(5'-5'')$ variation is larger for 5'- than for 3'-residue ; in particular, in the case of CpA and UpA, this variation is quite small for the 3' residue (Cp and Up). This is probably due to the weak association character of these compounds.

It follows from the results in table III that decreasing the temperature has the effect of increasing the N and the gg proportions and the difference in chemical shifts between the 5' and 5" protons, $\Delta\delta(5'-5'')$. This correlation between N%, f_{gg} % and $\Delta\delta(5'-5'')$ has already been observed [57, 31] in nucleosides and nucleotides. In fact, when the N proportion increases, $H_{3'}$ is statistically more axial, this in turn reduces the rotation freedom of the exocyclic group and consequently reinforces the magnetic non-equivalence between $H_{5'}$ and $H_{5''}$. On the other hand, in the 2,2'-anhydro-pyrimidine derivatives [58], a cyclic nucleoside family, in which the gg rotamer is unfavoured (f_{gg} = 0.18 in 2,2'-O-anhydro-uridine), f_{gg} increases and $\Delta\delta(5'-5'')$ decreases with increasing temperature. This is not surprising, since the temperature effect consists of reducing the difference in population between the three rotamers, gg, gt, tg and the magnetic non-equivalence between the 5' and 5" protons. From the above discussion, the temperature effect on f_{gg}%, $\Delta\delta(5'-5'')$ can be expressed as follows :

i) If $f_{gg} > 0.33$, when $t^{\circ}\nearrow \Longrightarrow f_{gg}\searrow$, $\Delta\delta(5'-5'')\searrow$

ii) If $f_{gg} < 0.33$, when $t^{\circ}\nearrow \Longrightarrow f_{gg}\nearrow$, $\Delta\delta(5'-5'')\searrow$

0.33 is the equilibrium value of $f_{gg} = f_{gt} = f_{tg}$ when the rotation of the exocyclic is completely free (for $t^{\circ} \to \infty$).

In addition, the large upfield shift of $H_{5'}$ compared with $H_{5''}$ (Table I) and the large variation of the N proportion with increasing temperature (Table III) tend to confirm our previous suggestion that $H_{3'}$ is statistically more close to $H_{5'}$ than $H_{5''}$ [31].

C.II.2. Base conformation around the glycosidic bond

The base conformation around the glycosidic bond of purine and pyrimidine residues has been investigated by measuring the longitudinal relaxation rates of protons. In order to better evaluate the average distance between H^8 and the ribose protons of the adenyl residue, the T_1 measurement was also performed after deuterating the C-8 position. The procedure and the method of interpretation have been described in detail in previous papers [25, 26, 53-56].

The initial recovery rate after the 180° pulse has been obtained from the slope of the $\mathrm{Log}[M_o - M_z(t)] = f(t)$ plot.

The difference between the relaxation rates before and after deuteration is given by the following relation :

$$\frac{1}{T_{1i}} - \frac{1}{T^*_{1i}} = \frac{3}{10}\gamma_H^4 h^2 < r_{i8}^{-6} > f(\tau_c) \qquad (1)$$

where $1/T^*_{1i}$ is the relaxation rate of proton i after deuteration,

$$f(\tau_c) = \frac{\tau_c}{1 + \omega^2\tau_c^2} + \frac{4\tau_c}{1 + 4\omega^2\tau_c^2}$$

ω, γ, h have the usual meanings,

$<r_{i-8}>$ is the average distance between the i proton and H^8.

For all the dinucleoside monophosphates studied, the T_1 experiments have been performed at 45°C to avoid the overlapping between the residual H^2HO signal and the resonances of the ribose ring protons. The data are reported in table IV. Although the chemical shift of a large number of protons can be measured with precision, the longitudinal relaxation times T_1 of $H_{2'}$, $H_{3'}$, $H_{4'}$ of the pyrimidine residues has not been determined due to the poor separation between the corresponding resonance lines.

Table IV - Initial recovery time T_1 (in second after a non-selective 180° pulse) of dinucleoside monophosphates in neutral aqueous solution at 45°C.

	purine residue							pyrimidine residue			
	H_8	$H_{1'}$	$H_{2'}$	$H_{3'}$	$H_{4'}$	$H_{5'}$, 5''	τ_c ($\times 10^{10}$ s)	H_5	H_6	$H_{1'}$	$H_{5'}$, 5''
ApC	2.74 (3.37)	2.77 (3.41)	1.23	0.97	1.53	0.3	0.96	2.64	1.12 (1.38)	2.64 (3.26)	0.35
$A(D_8)pC$		3.05	1.21	1.07	1.55	0.3		2.60	1.01	2.82	0.4
CpA	1.61	2.63	1.30	1.06	1.22	0.4	0.78	2.63	0.99	2.49	0.4
$CpA(D_8)$		3.30	1.69	1.28	1.19	0.4		2.46	0.92	2.52	0.4
ApU	2.22 (2.65)	2.51 (3.00)	1.19	1.00	1.25	0.3	0.93	2.90	1.00 (1.19)	3.11 (3.71)	0.3
$A(D_8)pU$		2.92	1.30	1.10	1.37	0.3		2.82	0.95	3.12	0.3
UpA	1.63	2.66	1.13	1.26	1.25	0.4	0.80	2.77	0.98	2.81	0.35
$UpA(D_8)$		3.33	1.63	1.22	1.23	0.3		2.74	0.97	2.66	0.4

- The values in brackets are the initial recovery times, normalized for a τ_c value of $0.8.10^{-10}$ seconds found in CpA and UpA.

a) Conformation of the adenyl bases

Examination of the data in table IV reveals that the T_1 value of H^8 (of the adenyl residue) depends on the position of the phosphate group, 3' or 5'. The $T_1(H^8)$ value for ApC (2.7 sec.) and for ApU (2.2 sec.) is much higher than that of CpA and UpA (1.6 sec). In addition, if all the T_1 relaxation times are normalized for the same value of $f(\tau_c)$ (= $3.7.10^{-10}$ corresponding to a $\tau_c = 0.8.10^{-10}$ sec.), the difference in $T_1(H^8)$ between the 3' and 5' residues is found to be more pronounced (Table IV). Similarly, it was stated on the basis of the T_1 normalized values in table IV that the T_1 relaxation time for $H_{1'}$ in the 3'-adenyl residue is always longer than that in the 5'-adenyl one. The same situation has been observed for GpC and CpG [26]. From these results we concluded that : H^8 is statistically

located further from the ribose protons in the 3'-phosphate than in the 5'-phosphate residue. The *anti* conformation is more favoured in the former than in the latter residue. These conclusions were strongly supported by measurements on the T_1 relaxation times of the same compounds after deuteration at the C-8 position : the relaxation rate variations for $H_{1'}$ before and after deuteration are found to be quite different for the two kinds of residue (3' or 5'), about 9% to 14% for the Ap residue in ApC and ApU and 20% for the pA residue in CpA and UpA indicating the highly *anti* character of the former two compounds.

b) Conformation of the pyrimidine bases

It also follows from the results in table IV that the T_1 values of $H_{1'}$ are longer for 5'- than for 3'-pyrimidine residues : for example the $T_1(H_{1'})$ of pC is about 3.4 sec. (normalized value) while the $T_1(H_{1'})$ of Cp is only 2.5 sec. A similar remark can be made for the T_1 value of H^6 even though the difference in T_1 between the 5'- and the 3'- residues is not as substantial as for $H_{1'}$, since the H^6 relaxation is mainly governed by the dipolar interaction with H^5. By using the above mentioned arguments we may conclude that for the pyrimidine moieties, the *anti* character is more pronounced in the 5'- than in the 3'- phosphate residue, in contrast to the purine residues in heterodinucleoside monophosphates.

c) Evaluation of *syn* and *anti* proportions

Owing to the lack of T_1 values for some ribose ring protons, in particular for the case of pyrimidine residues, the information about the *syn-anti* equilibrium obtained from the plot of $\Delta f(\tau_c)^{-1}/\overline{f(\tau_c)^{-1}}$ vs the glycosidic torsion angle T [25, 26, 53-56] is only qualitative. These curves (Fig. 2) indicate an equilibrium between two privileged conformations for the base : the one, *anti*, with T of about 200° ± 20° and the other, *syn*, with T of about 60° ± 20° similar to the case for a large number of

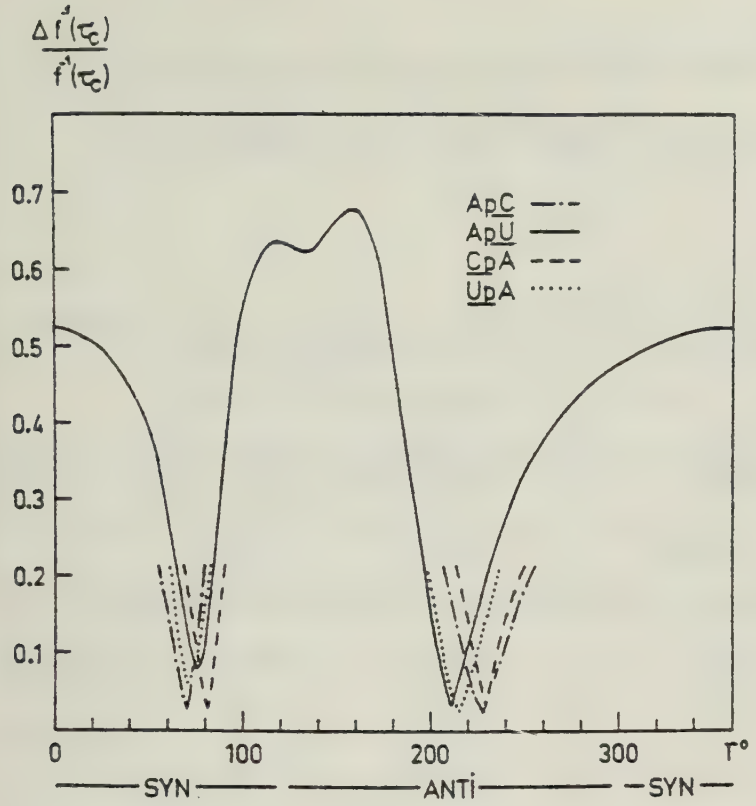

Figure 2

Plots of $\Delta f^{-1}(\tau_c)/\overline{f^{-1}(\tau_c)}$ versus the glycosidic torsion angle Γ for pyrimidine residues of ApC, ApU, CpA and UpA.

nucleotides [53, 55] and dinucleoside monophosphates [25, 26, 56] in aqueous solution. As it has been shown previously, the T_1 relaxation time for $H_{1'}$ is very sensitive to the conformational change around the glycosidic bond and its value can be determined with precision. Therefore, information about the *syn-anti* character of the base may be obtained by calculating the average distance $\langle r_{1'-8} \rangle$ or $\langle r_{1'-6} \rangle$. In fact, we showed in earlier work [59] that from a knowledge of the N, S proportions, the interatomic distances and the correlation time, one can calculate the relaxation time T_1^* for all the ribose protons, in particular for $T_1^*(H_{1'})$ in the case where the base proton (H^8 or H^6) is absent. Furthermore, in the case of purine residues, $T_1^*(H_{1'})$ can also be obtained directly from $^1H^8 \rightarrow {}^2H^8$ substitution. We have found that the calculated value agrees well with the one measured after deuteration. As far as the correlation time τ_c is concerned, this parameter can be determined in different ways : i) from the plot $\Delta f^{-1}(\tau_c)/\overline{f^{-1}(\tau_c)}$; ii) from the T_1 values of the ribose protons in the absence of H^8 (after deuteration) or iii) from the T_1 relaxation time of $H_{5'}$, $H_{5''}$ or $H_{4'}$, the T_1 value of

these protons does not depend on the base orientation. The calculated values for τ_c and the average distances $\langle r_{1'-8} \rangle$, and $\langle r_{1'-6} \rangle$ are summarized in tables IV and V respectively.

Table V - Mean distance (in Å) between the ribose proton $H_{1'}$ and the base proton H^8 (or H^6) and *anti* proportion of dinucleoside monophosphates.

	purine residue		pyrimidine residue	
	$\langle r_{1'8} \rangle$	% *anti*	$\langle r_{1'6} \rangle$	% *anti*
ApC	3.65	96	3.2	87
CpA	3.1	65	2.8	56
ApU	3.3	80	3.55	99
UpA	3.1	65	2.9	66

The average distance in table V are found to be intermediate between two extreme values $r_{1'-8(6)}(syn)$ and $r_{1'-8(6)}(anti)$ corresponding to the two privileged *syn* and *anti* conformations mentioned above. If the distances $r_{1'-8(6)}(syn)$ and $r_{1'-8(6)}(anti)$ are known with precision, one can calculate the *syn* and *anti* proportions from the average distance $\langle r_{1'-8} \rangle$ or $\langle r_{1'-6} \rangle$:

$$\frac{1}{\langle r_{1'-8} \rangle^6} = \frac{P(anti)}{[r_{1'-8}(anti)]^6} + \frac{P(syn)}{[r_{1'-8}(syn)]^6} \qquad (2)$$

In practice, the *syn* and the *anti* conformations are note unique within each region and the probability for the neighbouring conformation is not zero. On the other hand, it is well known that the relaxation between two protons is more efficient when they are the shortest distance apart. For this reason, the values of r(*syn*) and r(*anti*) in eq. (2) have been assumed to be equal to the shortest distance in each region, corresponding to T = 40° and T = 220° respectively

$$r_{1'-8}(syn) = 2.7 \text{ Å}$$

$$r_{1'-8}(anti) = 3.8 \text{ Å}$$

$$r_{1'-6}(syn) = 2.5 \text{ Å}$$

$$r_{1'-6}(anti) = 3.6 \text{ Å}$$

The *anti* proportions calculated by this method for different residues in the dinucleoside monophosphates studied are summarized in table V. The results clearly show that ApC, ApU are more *anti* than CpA and UpA. Since the first two dimers are also those which exhibit the largest degree of association, the *anti* conformation is thus highly favoured in the stacked forms.

C.III. INFLUENCE OF DIFFERENT FACTORS ON THE CONFORMATIONAL EQUILIBRIA OF NUCLEOSIDE AND DINUCLEOSIDE MONOPHOSPHATES

The results on the deoxyribose nucleotides and their dimers are far from complete especially for the base conformation. In addition, as far as the sugar conformation is concerned, it has been observed that there is no striking difference between monomers and dimers : in both cases, the S proportion is always preponderant (> 65%) and varies only a little with temperature [23]. In contrast, the N conformer is generally predominant in the ribonucleosides and ribodinucleoside monophosphates [60] and their proportions depend very much on experimental conditions. For these reasons, in this section, we would like to limit the discussion on the naturally occurring ribonucleoside derivatives in aqueous solution. A part from the influence of the above mentioned sugar structure, the base structure, the position of the phosphate group, the temperature and pH are among the most important structural and physico-chemical factors, which can modify the conformational equilibria of ribonucleosides and their dimers.

C.III.1. Influence of the base structure

It is well known that the steric hindrance is much larger with pyrimidine than with purine bases. The average conformation of the ribose ring and the base around the glycosidic bond are therefore expected to be different for the two families of compounds. The N conformer is generally less favoured in purine than in pyrimidine compounds (Table VI). This is also true for deoxynucleoside derivatives [23,60]. The dimerization effect resides in increasing the N proportion in both residues. However within a given heterodimer, the N conformer is always less favoured in the purine than in the pyrimidine moiety (Table VII).

Concerning the base conformation, it has been shown by nuclear Overhauser enhancement [47-50] and proton relaxation [25, 26, 53-56] studies that the purine nucleotides are more flexible than the pyrimidine compounds and that the *anti* proportion is smaller in the first than in the second family (Table VIII), in particular 5'UMP is mostly *anti* [50]. In general, the rotation of the base in dimers is much more reduced than in monomers due to the intra- and intermolecular base-base interactions in the dimers. On the other hand, the base conformation around the glycosidic bond of both residues in a dimer depends strongly on the degree of association as has been shown in section C.II. Therefore, the influence of the base structure on the *syn-anti* equilibrium is found to be more or less reduced. We have noted however that all the 5'-pyrimidine residues in dinucleoside monophosphates are highly *anti* (Table VIII).

C.III.2. Influence of the phosphate group

Although the phosphate group is voluminous, its presence does not change the average conformation of the ribose very much : there is no great difference between nucleosides and the corresponding mononucleotides [14, 15, 30, 31, 49] or when the relative position of the phosphate group (2', 3' or 5') is modified (Table VI). The origin of the influence of the phosphate

Table VI - N conformer proportion of nucleosides and nucleotides : influence of the position of the phosphate group, the base structure and pH on the N/S equilibria.

	pH	% N	Ref.
Adenosine	7.0 1.4	34 45	[35]
Inosine	~7.0	44	[52]
2'AMP	~7.5	38 33	[49] [15]
3'AMP	~7.5	38 33	[49] [15]
5'AMP	~7.5	38	[49], [14]
2'AMP	7.5 1.2	45 56	[30]
3'GMP	8.2 1.3	37 50	[31]
5'GMP	8.2 1.2	40 62	[31]
Uridine	6.8	53	[16]
Cytidine	8.0 1.0	60 62	[32]
2'UMP	~7.0	45	[15]
3'UMP	~7.0	56	[15]
5'UMP	~7.0	45	[14]
2'CMP	~7.0	50	[15]
3'CMP	~7.0	59	[15]
5'CMP	~7.0	51	[14]

Table VII - N proportion of dinucleoside monophosphates : influence of the temperature and the relative position of the two residues (with respect to the phosphate group) on the N/S equilibria.

	T°C	3' residue % N	5' residue % N	Ref.
ApA	20	60	59	[20]
	72	48	50	
ApG	20	51	52	[20]
	80	41	48	
ApC	20	63	74	[21]
	80	44	63	
	25	59	71	a)
	65	47	63	
ApU	25	58	68	a)
	65	47	61	
GpC	25	64	71	[26]
	65	51	65	
CpA	25	66	57	a)
	65	56	53	
CpG	20	68	56	[21]
	80	52	47	
	25	66	52	[26]
	65	58	47	
UpA	25	54	51	a)
	65	48	46	
UpC	20	60	63	[20]
	80	52	67	
UpU	20	56	56	[20]
	89	51	53	

a) this work

group on the conformation of mononucleotides resides in the steric interaction between this group and the base. We can easily find with a molecular model that the rotation freedom of the base does not change when the phosphate group is in the 2' or 3' position. The results obtained from nuclear Overhauser enhancement studies on GMP's [47] and AMP's [48, 49] have shown that the *anti* conformation is more favoured in 5'- than in 2'- and 3'-nucleotides (Table VIII). For the last two compounds, the *syn* conformation is highly predominant.

Table VIII - *anti* proportion of mono- and dinucleoside monophosphates. Influence of the base structure and the position of the phosphate group (for mononucleotides) or the relative position of the two residues with respect to the phosphate group (for dinucleosides monophosphates) on the *syn-anti* equilibria.

Nucleotides	% *anti*	Ref.	Dinucleoside monophosphates	Purine residues % *anti*	Pyrimidine residues % *anti*	Ref.
2'AMP	33	a)	ApC	96	87	e)
3'AMP	28	a)	CpA	65	56	e)
5'AMP	54	c)	ApU	80	99	e)
2'GMP	37	b)	UpA	65	66	e)
3'GMP	28	b)	GpC	54	98	[26]
5'GMP	54	c)	CpG	10	49	[26]
5'IMP	63	c)	GpU	22	91	[25]
3'UMP	70	d)	UpG	54	49	[25]
5'UMP	80	c)				
5'CMP	75	c)				

a) evaluated from NOE measurements in ref. [48] ; b) evaluated from NOE measurements in ref. [47] ; c) evaluated from T_1 measurements in ref. [53] ; d) evaluated from T_1 measurements in ref. [50] ; e) this work.

Concerning dinucleoside monophosphates, the influence of the phosphate group position on the ribose conformation does not seem to be determinant : the N proportions are practically equivalent in both residues of ApA, UpU and CpC [20] (Table VII). If the N proportion is higher for each residue

of ApC and ApU than that of the corresponding residue in CpA and UpA, this is probably due to the fact that in heterodimers, the relative position of both residues (pu-py or py-pu) monitors the N-S equilibrium. In addition, the *anti* proportion of any residue in ApC and ApU is always higher than that in the corresponding residue of CpA and UpA (Table VIII). This is not surprising, since the base orientation of a residue depends not only on the relative position of the phosphate group but also on the presence of another residue especially when intramolecular interaction between both residues of the same dimer is large. In pu-py dimers, the influence of the last factor is very efficient.

C.III.3. Temperature effect

In aqueous or ammonia solutions, the N-S equilibrium of nucleosides [51, 52] and nucleotides [30, 31] is practically unchanged with temperature. In contrast, the temperature effect is much more noticeable in the case of dinucleoside monophosphates : it consists of reducing the difference in population between the N and S proprotions. When temperature increases, the N proportion which is generally preponderant in dinucleoside monophosphates at room temperature, decreases to the value observed in the corresponding mononucleotides (section C.II).

As far as the base conformation around the glycosidic bond is concerned, owing to overlapping between the residual $^{1}H^{2}HO$ signal and the resonances of some ribose protons, the temperature dependence of the *syn-anti* equilibrium has not been studied so far. However, the fact that the proportion of N conformer and gauche-gauche rotamer decreases with increasing temperature suggests that higher temperatures cause a decrease in the *anti* conformation which is predominant in the pu-py dimers at room temperature.

C.III.4. pH effect

The pH effect on the conformational equilibrium of the ribose and the base has been studied for the first time with GMP's in our laboratory [30, 31, 47]. The protonation of the base at N^7 (but not the phosphate group) has a strong effect on the ribose conformation in the pH interval between 8 and 0.5 : the S conformation is favoured at neutral pH while the N form is predominant at acidic pH (Table VI). Similar results have been obtained for adenosine [35] and cytidine derivatives [32] (Table VI). In the case of dinucleoside monophosphates, the pH effect on the ribose conformation of the G residue in GpC and CpG [61] is found to be almost the same : decreasing pH from 8 to 1 increases the N proportion from 55% to 63% for GpC and from 52% to 64% forCpG. On the other hand, nuclear Overhauser enhancement (NOE) experiments on GMP's have shown that tne *syn-anti* equilibrium of those compounds is also affected when the pH varies : lowering pH favours the *syn* conformation which is already predominant in 2'GMP and 3'GMP at neutral pH.

A part from the main factors mentioned above, the important role of salt is well known for the formation of secondary and tertiary structures of nucleic acids and polynucleotides. However, the salt effect on the molecular conformation does not seem be very determinant for nucleoside - and dinucleoside monophosphates.

REFERENCES

1. ARNOTT, S. (1970) Progr. Biophys. Mol. Biol. 21, 265.

2. ARNOTT, S. and HUKINS, D.W.L. (1972) Biochem. Biophys. Res. Comm. 47, 1504.

3. WANG, A.H., QUIGLEY, G.J., KOLPAK, F.J., CROWFORD, J.L., Van BOOM, J.H., Van Der MAREL, G. and RICH, A. (1979) Nature (Lond) 282, 680.

4. PATEL, D.J. (1977) Biopolymers 16, 1635.

5. PATEL, D.J. and HILBERS, C.W. (1975) Biochemistry 14, 2651.

6. HAASNOOT, C.A.G., Den HARTOG, J.H.J., De ROOIJ, J.F.M., Van BOOM, J.H. and ALTONA, C. (1980) Nucleic Acids Res. 8, 169.

7. BORER, P.N., KAN, L.S. and TS'O, P.O.P. (1975) Biochemistry 14, 4847.

8. MICHELSON, A.M., MASSOULIE, J. and GUSCHLBAUER, W. (1967) Progress in Nucleic Acid Res., DAVIDSON, T.N. and COHN, W.E., Eds, Academic, New-York, p. 83.

9. PATEL, D.J. (1978) J. Polymer Sym. 62, 117, John Wiley and Sons, Inc.

10. HRUSKA, F.E., GREY, A.A. and SMITH, I.C.P. (1970) J. Am. Chem. Soc. 92, 4088.

11. WOOD, D.J., HRUSKA, F.E., MYNOTT, R.J. and SARMA, R.H. (1973) Can. J. Chem. 51, 2571.

12. ALTONA, C. and SUNDARALINGAM, M. (1972) J. Am. Chem. Soc. 94, 8205.

13. ALTONA, C. and SUNDARALINGAM, M. (1973) J. Am. Chem. Soc. 95, 2333.

14. DAVIES, D.B. and DANYLUK, S.S. (1974) Biochemistry 13, 4417.

15. DAVIES, D.B. and DANYLUK, S.S. (1975) Biochemistry 14, 543.

16. SCHLEICH, T., BLACKBURN, B.J., LAPPER, R.D. and SMITH, I.C.P. (1972) Biochemistry 14, 543.

17. TS'O, P.O.P., KONDO, N.S., SCHWEIZER, M.P. and HOLLIS, D.P. (1969) Biochemistry 8, 997.

18. BANGERTER, B.W. and CHAN, S.I. (1969) J. Am. Chem. Soc. 91, 3910.

19. KONDO, N.S., FANG, K.N., MILLER, P.S. and TS'O, P.O.P. (1972) Biochemistry 11, 1991.

20. LEE, C.H., EZRA, F.S., KONDO, N.S., SARMA, R.H. and DANYLUK, S.S. (1976) Biochemistry 15, 3627.

21. EZRA, F.S., LEE, C.H., KONDO, N.S., DANYLUK, S.S. and SARMA, R.H. (1977) Biochemistry 16, 1977.

22. ALTONA, C. (1975) in Structure and Conformation of Nucleic Acids and Protein-Nucleic Acid Interactions. Ed. by SUNDARALINGAM, M. and RAO, S.T. University Park Press, Baltimore, p. 613.

23. CHENG, D.M. and SARMA, R.H. (1977) J. Am. Chem. Soc. 99, 7333.

24. KAN, L.S., CHENG, D.M., MILLER, P.S., YANO, J. and TS'O, P.O.P. (1980) Biochemistry 19, 2122.

25. CHACHATY, C., YOKONO, T., TRAN-DINH, S. and GUSCHLBAUER, W. (1977) Biophys. Chem. 6, 151.

26. NEUMANN, J.M., GUSCHLBAUER, W. and TRAN-DINH, S. (1979) Eur. J. Biochem. 100, 141.

27. KONDO, N.S., EZRA, F. and DANYLUK, S.S. (1975) FEBS Lett. 53, 213.

28. ALTONA, C., Van BOOM, J.H. and HAASNOOT, C.A.G. (1976) Eur. J. Biochem. 71, 557.

29. CHENG, D.M., DANYLUK, S.S., DHINGRA, M.M., EZRA, F.S., MacCOSS, M., MITRA, C.K. and SARMA, R.H. (1980) Biochemistry 19, 2491.

30. TRAN-DINH, S., THIERY, J., GUSCHLBAUER, W. and DUNAND, J.J. (1972) Biochim. Biophys. Acta 281, 289.

31. TRAN-DINH, S. and GUSCHLBAUER, W. (1975) Nucleic Acids Res. 2, 873.

32. REMIN, M. and SHUGAR, D. (1973) J. Am. Chem. Soc. 95, 8146.

33. REMIN, M., DARZYNKIEWICZ, E., DWORAK, A. and SHUGAR, D. (1976) J. Am. Chem. Soc. 98, 367.

34. SARMA, R.H., LEE, C.H., EVANS, F.E., YATHINDRA, N. and SUNDARALINGAM, M., (1974) J. Am. Chem. Soc. 96, 7337.

35. HRUSKA, F.E., WOOD, D.J. and SINGH, H. (1977) Biochim. Biophys. Acta 474, 129.

36. DANYLUK, S.S. and HRUSKA, F.E. (1968) Biochemistry 7, 1038.

37. SCHWEIZER, M.P., BROOM, A.D., TS'O, P.O.P. and HOLLIS, D.P. (1968) J. Am. Chem. Soc. 90, 1042.

38. JORDAN, F. and NIV, H. (1977) Biochim. Biophys. Acta 476, 265.

39. LEMIEUX, R.U., NAGABHUSHAN, T.L. and PAUL, B. (1972) Can. J. Chem. 50, 773.

40. DELBAERE, L.T.J., JAMES, M.N.G. and LEMIEUX, R.U. (1973) J. Am. Chem. Soc. 95, 7866.

41. BARRY, C.D., NORTH, A.C.T., GLASEL, J.A., WILLIAMS, R.J.P. and XAVIER, A.V. (1971) Nature (Lond) 232, 236.

42. DOBSON, C.M., GERALDES, C.F.G.C., RATCLIFFE, G. and WILLIAMS, R.J.P. (1978) Eur. J. Biochem. 88, 259.

43. INAGAKI, F., TASUMI, M. and MIYAZAWA (1978) Biopolymers 17, 267.

44. NOGGLE, J.H. and SCHIRMER, R.E. (1971) The Nuclear Overhauser Effect : Chemical Applications, Academic Press, New-York.

45. SCHIRMER, R.E., DAVIS, J.P., NOGGLE, J.H. and HART, P.A. (1972) J. Am. Chem. Soc. 94, 2561.

46. HART, P.A. and DAVIS, J.P. (1971) J. Am. Chem. Soc. 93, 753.

47. TRAN-DINH, S., GUSCHLBAUER, W. and GUERON, M. (1972) J. Am. Chem. Soc. 94, 7903.

48. GUERON, M., CHACHATY, C. and TRAN-DINH, S. (1973) Ann. N.Y. Acad. Sci. 222, 307.

49. TRAN-DINH, S. and CHACHATY, C. (1973) Biochim. Biophys. Acta 335, 1.

50. NEUMANN, J.M., BERNASSAU, J.M., GUERON, M. and TRAN-DINH, S. (1980) Eur. J. Biochem. 108, 457.

51. LÜDEMANN, H.D., WESTHOF, E., and RÖDER, O. (1974) Eur. J. Biochem. 49, 143.

52. LÜDEMANN, H.D., RÖDER, O., WESTHOF, E., GOLDAMMER, E.V. and MÜLLZE, A. (1975) Biophys. Struct. Mech. 1, 121.

53. CHACHATY, C., ZEMB, T., LANGLET, G., TRAN-DINH, S., BUC, H. and MORANGE, M. (1976) Eur. J. Biochem. 62, 45.

54. NEUMANN, J.M., BORREL, J., THIERY, J.M., GUSCHLBAUER, W. and TRAN-DINH, S. (1977) Biochim. Biophys. Acta 479, 427.

55. TRAN-DINH, S. and CHACHATY, C. (1977) Biochim. Biophys. Acta 500, 405.

56. CHACHATY, C., PERLY, B., FORCHIONI, A. and LANGLET, G. (1980) Biopolymers 19, 1211.

57. HRUSKA, F.E., WOOD, D.J., McCAIG, T.N., SMITH, A. and HOLY, A., (1974) Can. J. Chem. 52, 497.

58. GUSCHLBAUER, W., TRAN-DINH, S., BLANDIN, M. and CATLIN, J.C. (1974) Nucleic Acids Res. 1, 855.

59. TRAN-DINH, S., NEUMANN, J.M., THIERY, J.M., HUYNH-DINH, T., IGOLEN, J. and GUSCHLBAUER, W. (1977) J. Am. Chem. Soc. 99, 3267.

60. DAVIES, D.B. (1978) Progress in NMR Spectroscopy 12, 135, Pergamon Press, Oxford.

61. NEUMANN, J.M. and TRAN-DINH, S. Unpublished results.

CHAPITRE III

ÉTUDE DE LA CONFORMATION ET DE LA STRUCTURE DYNAMIQUE DES OLIGONUCLÉOTIDES EN SOLUTION

Ce chapitre est consacré à l'étude de la conformation et de la structure dynamique de deux oligodéoxynucléotides, le tetramère dApTpGpT et l'hexamère à séquence auto-complémentaire dApCpApTpGpT, par RMN-^{1}H à différentes fréquences (400, 276, 250 et 90 MHz). Ces molécules ont été synthétisées au laboratoire de chimie organique de l'Institut Pasteur sous la direction de MM. J. Igolen et T. Huynh-Dinh. MM. S.K. Kan et G. Simmonot de l'Institut d'Electronique Fondamentale (Orsay) nous ont aidé dans l'enregistrement des spectres à 400 MHz.

Le chapitre contient trois articles. Le premier "Methods for the assignment of DNA fragment proton resonances. ^{1}H-NMR spectra of dApTpGpT and dApCpApTpGpT, Tran-Dinh, S., Neumann, J.M., Huynh-Dinh, T., Igolen, J. and Kan, S.K. (1982) Org. Mag. Res. 18, 148" présente à partir de l'analyse spectrale de dApTpGpT et de dApCpApTpGpT une méthode générale pour l'attribution des signaux des spectres en proton des oligodéoxynucléotides.

Les deux suivants "^{1}H-NMR and relaxation studies of dApTpGpT in neutral aqueous solution, Neumann, J.M., Huynh-Dinh, T., Kan, S.K., Genissel, B., Igolen, J. and Tran-Dinh, S. (1982) Eur. J. Biochem. 121, 317" et "^{1}H-NMR studies of helix-coil transition, conformation and dynamic structure of the self-complementary deoxyhexanucleotide dApCpApTpGpT in aqueous solution, Tran-Dinh, S., Neumann, J.M., Huynh-Dinh, T., Genissel, B., Igolen, J. and Simmonot, G. (1982) Eur. J. Biochem. (sous presse) traitent

respectivement de la conformation et de la structure dynamique du tetramère et de l'hexamère. Pour ce dernier, qui, grâce à sa séquence auto-complémentaire forme un complexe bicaténaire, la transition hélice-pelote statistique est soigneusement étudiée.

A. METHODS FOR THE ASSIGNMENT OF DNA FRAGMENT PROTON RESONANCES. ^{1}H-NMR SPECTRA OF dApTpGpT AND dApCpApTpGpT

TRAN-DINH, S., NEUMANN, J.M., HUYNH-DINH, T., IGOLEN, J. and KAN, S.K.

Org. Mag. Res. 18, 148.

The thermodynamics and kinetics of the helix coil transition of short self-complementary deoxyribo oligonucleotides have been studied extensively by ^{1}H- and ^{31}P- NMR spectroscopy during the last few years [1-7]. Most of this work was carried out by monitoring the chemical shifts and line width change of the NH and base proton resonances.

Information on the conformation and dynamic structure of DNA fragments can also be obtained from measurements of the sugar and base proton chemical shifts, ^{1}H-^{1}H coupling constants, nuclear Overhauser enhancement (NOE) and relaxation times. The double helix structure (A-, B-, Z-DNA forms) can be deduced from the sugar conformation [8-10] ; the $H_{1'}$ and $H_{2'}$ chemical shifts should be sensitive to the base conformation change while the $H_{2''}$ chemical shift may reflect the modification of the phosphate group environment and hence give information about the change in the helicity of the strand, the helix-coil transition, interactions with ions etc ...

Unfortunately analysis of the sugar proton resonances spectra is complicated in the case of deoxyribonucleotides : no ^{1}H-NMR spectrum with complete assignment of DNA fragments containing more than three residues has yet been published to our knowledge ; for the hexamers, the $H_{1'}$ proton resonances are fairely well separated at high frequences (> 360 MHz), however their assignment is still unresolved. This is probably one of the reasons why the ^{1}H-NMR investigations of short DNA fragments in aqueous solution have not progressed as quickly as expected.

In the present communication we present a general method to assign the non-exchangeable proton resonances, especially for the sugar protons, of two DNA fragments : dApTpGpT (dATGT) and dApCpApTpGpT (dACATGT) (scheme) in neutral aqueous solution. We believe that once the proton resonances of each nucleotide unit are assigned the determination of the proton-proton coupling constants will cause little difficulty since the sugar conformations of the different residues of a DNA fragment in aqueous solution are generally found to be similar.

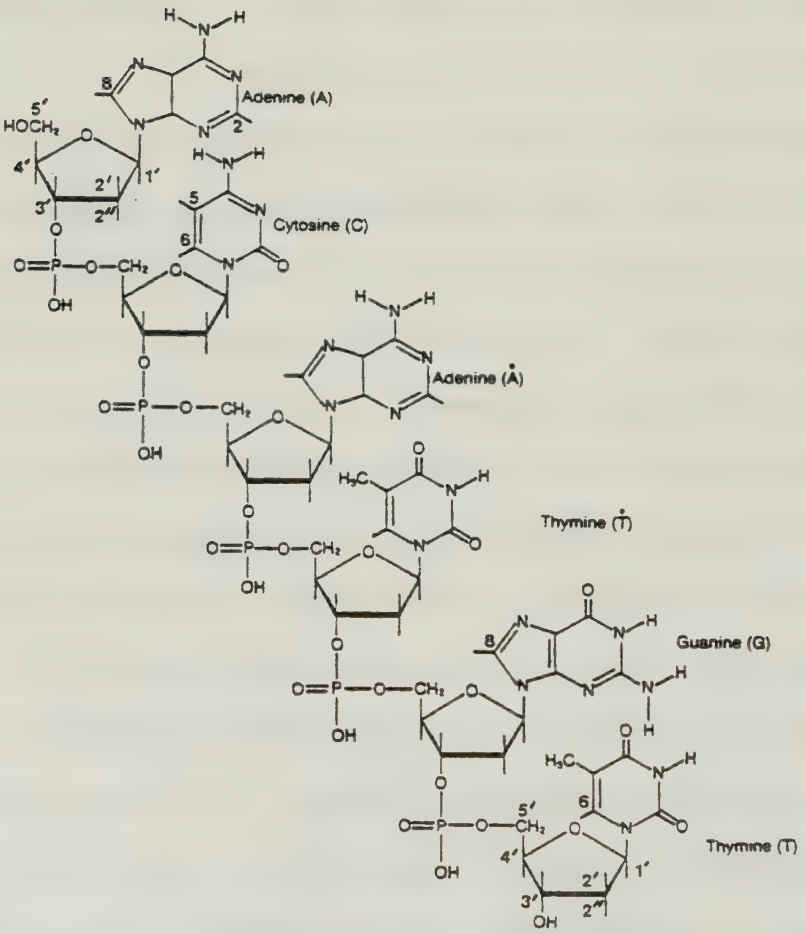

Schematic representation of dApCpApTpGpT.

A.I. EXPERIMENTAL

dApTpGpT and dApCpApTpGpT are synthetized from the dimers DMT GpT_{Bz}, DMT ApTp and DMT ApCp prepared according to published literature [11]

$$\text{DMT ApTp} + {}^{HO}\text{GpT}_{Bz} \rightarrow \text{DMT ApTpGpT}_{Bz}$$
$$5'\text{HO}_{\text{ApTpGpT}_{OH3'}}$$

$$\text{DMT ApCp} + {}^{HO}\text{ApTpGpT}_{Bz} \rightarrow \text{DMT ApCpApTpGpT}_{Bz}$$
$$5'\text{HO}_{\text{ApCpApTpGpT}_{OH3'}}$$

The compounds were dissolved in ^2H_2O containing 0.1 M NaCl and were freed of possible divalent ions by addition of EDTA (0.1 mM). The pH were adjusted to 7-8 by addition of a small amount of NaOH. The samples were lyophilized twice in ^2H_2O and redissolved in ^2H_2O at final concentrations of 5-8 mM. The solutions were introduced into NMR tubes, degassed in a vacuum line and sealed.

The ^{1}H-NMR spectra were recorded on a laboratory-built 400 MHz ^1H high resolution spectrometer (I.E.F. 400). This spectrometer operates in Fourier transform mode associated with a 24K Texas Instruments 980 A computer (8K program, 16K data). The chemical shifts were measured from 3-(trimethylsilyl-$^2H_4$) propionic acid.

A.II. RESULTS AND DISCUSSION

In general the oligonucleotide proton resonance lines are broad at low temperature due to a restricted molecular motion or an exchange between different forms. By contrast, the proton spectra of these compounds are generally well resolved at high temperature, i.e. above that of the helix-coil transition (> 60°C). The ideal temperature for recording the ^1H-NMR spectra and comparing the chemical shifts of their components is in the range from 60° to 70°C. Above 70°C the H_8 proton of A and G residues will exchange efficiently with ^2H_2O.

Figures 1 and 2 show the 400 MHz proton spectra of dATGT and dACATGT in neutral aqueous solution at 65°C and 68°C respectively.

A.II.1. Sugar proton assignments

The identification of the deoxyribose proton resonances was carried out in two stages : in the first stage the proton signals of the same residue were found, then the nature and sequential position were determined for each residue.

a) Proton resonances of the same residue

The most reliable method to identify the resonance lines of the same residue is of course proton-proton decoupling, which should be used to check the assignment validity whenever a large temperature variation is applied to the sample. The distinction between the resonances of the H_2' and H_2'' protons (above and below the sugar plane respectively) may be obtained from the coupling measurements. In fact, the molecular model shows

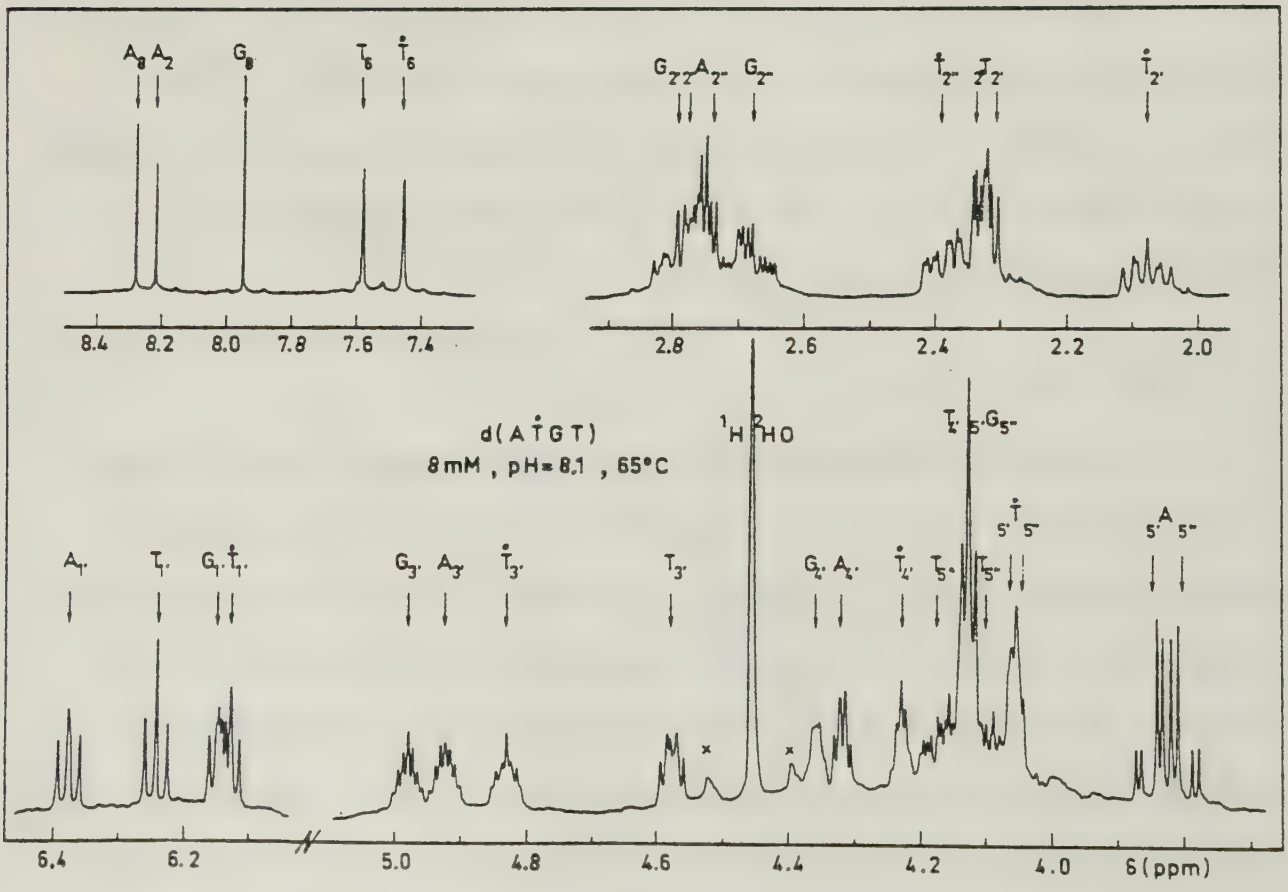

Fig. 1 - 400 MHz ^{1}H-NMR spectrum of dApTpGpT in neutral aqueous solution

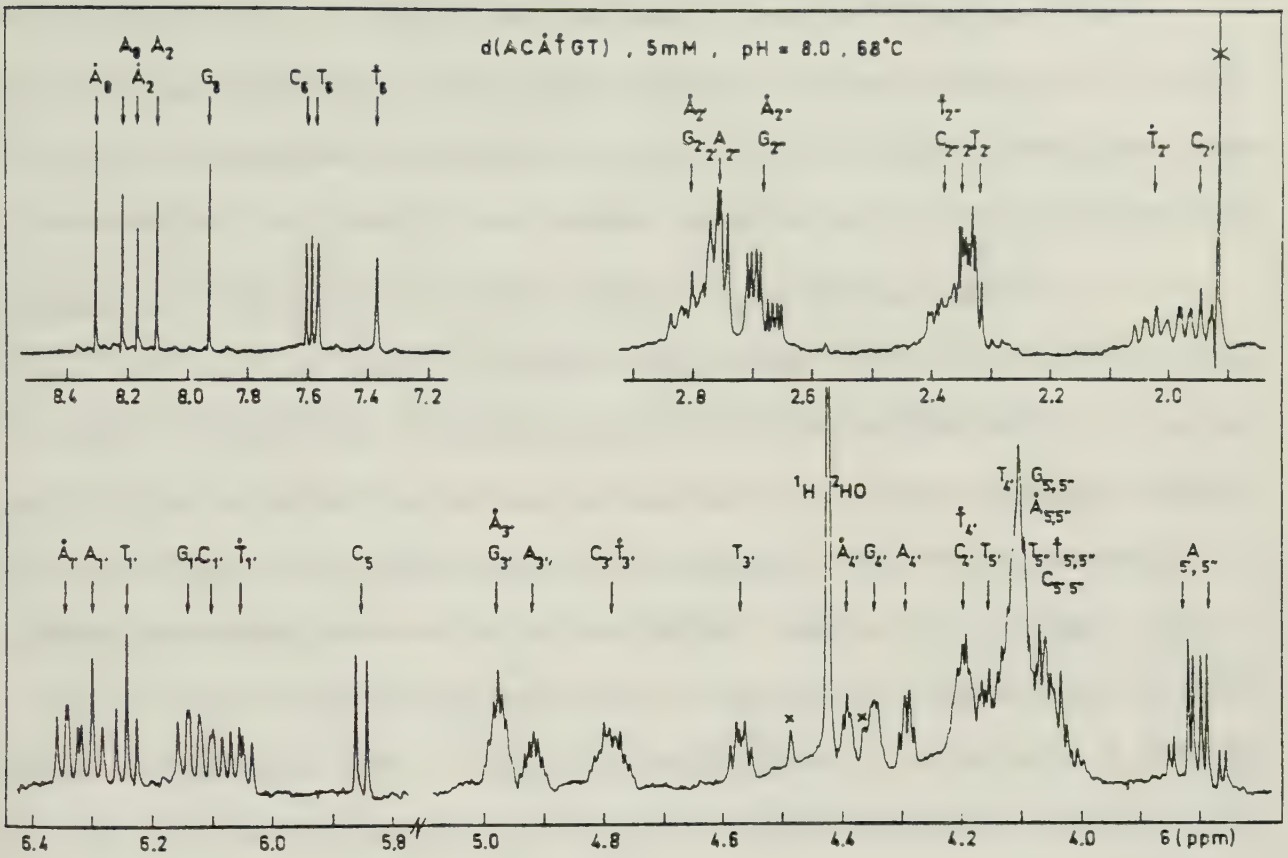

Fig. 2 - 400 MHz ^{1}H-NMR spectrum of dApCpApTpGpT in neutral aqueous solution.

that the dihedral angle $\phi_{3'4'}$ is practically equal to $\phi_{2''3'}$ whatever the position (endo or exo) of $H_{3'}$ and $H_{2'}$ while the $C_{1'}OC_{4'}$ plane remains fixed. The $J_{2''3'}$ value is therefore expected to be of the same order as $J_{3'4'}$ and similarly $J_{2'3'}$ should not be very different from $J_{1'2''}$. In the case of the naturally occuring deoxyribonucleosides dA, dG, dC, dT and their derivatives [12-15] the S conformation ($J_{1'2'}$ > 7 Hz) is much more probable than the N conformation ($J_{3'4'}$ < 3.5 Hz). Consequently $J_{2''3'} \approx J_{3'4'} < 3.5$ Hz and $J_{2'3'} \approx J_{1'2''} > 5.5$ Hz. This situation remains practically unchanged for the deoxyoligomers. The $H_{2'}$ and $H_{2''}$ multiplets have quite different aspects : the fine splittings of about 3 Hz are only observed in the $H_{2''}$ resonances (Figs. 1 and 2) ; the total splitting of the $H_{2'}$ multiplet lies around 29 Hz whereas that for $H_{2''}$ is clearly narrower, only 22-23 Hz. These criteria allow the $H_{2'}$ and $H_{2''}$ resonance lines to be quickly identified even when partially overlapped by the signals form the other residues.

b) Nature and sequential position of each residue

The chemical shift comparison between the oligonucleotide studied and its components does not always give an unambiguous assignment even at high temperature, and other criteria should thus be used for this purpose.

i) Initial and terminal residues : Once the resonances are grouped into nucleotide units, the initial and terminal residues can easily be recognized [14] : the initial residue is characterized by the exocyclic proton CH_2OH resonances which are observed in the vicinity of 3.85 ppm, upfield from the resonances of the other CH_2OP groups (4.0-4.2 ppm), and appear in general for high magnetic field as two quadruplets as in the case of mononucleosides. Owing to the absence of the phosphate group in the 3' position on the other hand the $H_{3'}$ multiplet of the terminal residue ($\simeq$ 14 Hz) has a smaller total splitting than the other residues (18-19 Hz) and is located upfield ($\simeq$ 4.60 ppm) from the other $H_{3'}$ resonances (4.8-5.0 ppm). In the case of dATGT and dACATGT, the $H_{2'}$ and $H_{2''}$ protons of the initial residue, dA, and of the terminal residue, dT, are almost magnetically equivalent in contrast to the case of the internal residues (Figs 1 and 2) and their chemical shifts are not very affected by the temperature effect.

ii) Purine and pyrimidine residues : In most cases the S conformation is strongly predominant in naturally occuring deoxyriboses, i.e. the $C_{2'}$ carbon is situated in the endo position most part of the time and thus very close to the base. The ring current of the purine bases in therefore found to exert a strong effect on the $H_{2'}$ and $H_{2''}$ chemical shifts : the $H_{2'}$ and $H_{2''}$ resonances of dA and dG residues are generally located between 2.65 and 2.80 ppm while those of dC and dT are observed at higher field between 1.95 and 2.40 ppm. Moreover at high temperature the $H_{2'}$ and $H_{2''}$ resonances of the internal purine residues are very close, with $\delta H_{2'}$ slightly greater than $\delta H_{2''}$, while those of the internal pyrimidine residues are generally

well separated with $\delta H_2'$ much smaller than $\delta H_2''$. These important facts allow the purine and pyrimidine proton resonances to be distinguished. For example the H_1' and H_3' signals of the purine and pyrimidine families were identified by saturating the H_2' and H_2'' resonances of dA and dG simultaneously with a high decoupling power. In general except for the terminal residue, the H_3' resonances of the purine residues are observed at lower fields than those of the pyrimidine residues. The same is true for the H_4' resonances.

iii) Distinction between dA and dG or dC and dT residues : Owing to the difference in the ring current between the A and G bases, the dA_1' , resonances are located downfield from the dG_1' resonances (i.e. $\delta A_1' > \delta G_1'$).

At low temperature, intra-and intermolecular interactions occur and affect the conformations of each residue differently. As a result, the magnetic non-equivalence between H_2' and H_2'' of a given residue on the one hand and between the same proton (H_2' or H_2'') of different residues on the other hand is often more accentuated at low temperatures. Thus the dC_1' and dC_2' resonances in dACATGT have been assigned on the basis of the hydrogen bond number and configuration difference between the GC and AT base pairs ; the chemical shift variations of the H_1' and H_2' protons versus temperature are much larger for the dC than for the dT residue. Details on the dACATGT melting behaviour will be described elsewhere.

iv) H_5' and H_5'' resonances : Apart from the initial residue, the H_5' and H_5'' resonances of the other residues spread over a spectral region of about 0.2 ppm, between 4.0 ppm and 4.2 ppm, and are hence very close to or overlap the pyrimidine H_4' signals. This makes the resonance assignment for this spectral region difficult without a phosphorus decoupling unit and a really high magnetic field (> 600 MHz). With a high-frequency spectrometer equipped with a phosphorus decoupling unit, the H_5' and H_5'' resonances can be assigned by the relaxation method [16]. In fact the relaxation rates of the sugar ring protons ($\simeq 1\ sec^{-1}$) are quite different from those of the

exocyclic methylen protons (2.5-3.0 sec^{-1}) and we can only observe the $H_{5'}$, $H_{5''}$ signals by using the sequence 180°-τ-90° for the T_1 measurements with an appropriate τ value [16].

A.II.2. Base proton assignments

The base proton resonance assignments for dATGT and dACATGT were accomplished by a set of interlocking procedures : longitudinal relaxation time and NOE measurements, comparison with the corresponding component spectra, ^1H-^2H chemical exchange and temperature-dependent chemical shift studies.

The A_2 and A_8 (or G_8) proton signals were distinguished from their longitudinal relaxation times, T_1 , [17-18], $T_1(A_2)$ being much greater than $T_1(A_8$ or $G_8)$. The A_8 and G_8 assignment was achieved independently with the ^1H-^2H exchange method by heating the neutral ^2H_2O solution at about 80°C for 3 hours.

The A_8 resonances are observed in the region of 8.2-8.3 ppm whereas the G_8 resonances are located upfield in the vicinity of 8.0 ppm at 70°C. For short DNA fragments the purine base proton assignment can be verified on the basis of the NOE measurement by irradiating the sugar protons.

The C_6 and C_5 doublets, with J_{5-6} about 7.5 Hz, exhibit quite different chemical shifts : $\delta(C_6) \simeq 7.60$ ppm and $\delta(C_5) \simeq 5.85$ ppm at 68°C. The thymine H_6 resonance is characterized by a small splitting of about 2 Hz due to coupling with the methyl group. In the case of dATGT and dACATGT, the H_6 resonance of the internal thymidylyl residue is located about 0.2 ppm upfield from that of the terminal residue.

Lastly, when several residues of the same nature are present in a self-complementary duplex or in a long chain, the base proton resonances of the external, internal and central residues can also be distinguished by following the chemical shift variations versus temperature, especially in the temperature range where the helix-coil transition takes place [1-3].

REFERENCES

1. PATEL, D.J. (1975) Biochemistry 14, 3984.

2. PATEL, D.J. and HILBERS, C.W. (1975) Biochemistry 14, 2651.

3. HILBERS, C.W. and PATEL, D.J. (1975) Biochemistry 14, 2656.

4. MILLER, P.S., CHENG, D.M., DREON, N., JAYARAMAN, K., KAN, L.S., LEUTZINGER, E.E., PULFORD, S.M. and TS'O, P.O.P. (1980) Biochemistry 19, 4688.

5. PHILLIPS, D.R. and ROBERTS, G.C.K. (1980) Biochemistry 19, 4795.

6. DAVANLOO, P., ARMITAGE, I.M. and CROTHERS (1979) Biopolymers 18, 663.

7. EARLY, T.A. and KEARNS, D.R. (1980) Nucl. Acids Res. 8, 5795.

8. ARNOTT, S. and HUKINS, D.W.L. (1973) J. Mol. Biol. 81, 93.

9. ARNOTT, S., HUKINS, D.W.L., DOVER, S.D., FULLER, W. and HODGSON, A.R. (1973) J. Mol. Biol. 81, 107.

10. ARNOTT, S., CHANDRASEKASAN, R., HUKINS, D.W.L., SMITH, P.J.C. and WATTS, L. (1974) J. Mol. Biol. 88, 523.

11. Van BOOM, J.H., BURGERG, P.M.J., Van Der MAREL, VERDEGAAL, C.H.M. and WHILE, G. (1977) Nucl. Acids Res. 4, 1047.

12. DAVIES, D.B. and DANYLUK, S.S. (1974) Biochemistry 13, 4417.

13. CHENG, D.M. and SARMA, R.H. (1977) J. Am. Chem. Soc. 99, 7333.

14. CHENG, D.M., DHINGRA, M.M. and SARMA, R.H. (1978) Nucl. Acids Res. 5, 4399.

15. ALTONA, C., Van BOOM, J.H. and HAASNOTT, C.A. (1976) Eur. J. Biochem. 71, 557.

16. NEUMANN, J.M., GUSCHLBAUER, W. and TRAN-DINH, S. (1979) Eur. J. Biochem. 100, 141.

17. GUERON, M., CHACHATY, C. and TRAN-DINH, S. (1973) Ann. N.Y. Acad. Sci. 222, 397.

18. TS'O, P.O.P., BARRETT, J.C., KAN, L.S. and MILLER, P.S. (1973) Ann. N.Y. Acad. Sci. 222, 290.

B. ^{1}H-NMR AND RELAXATION STUDIES OF dApTpGpT IN NEUTRAL AQUEOUS SOLUTION

NEUMANN, J.M., HUYNH-DINH, T., KAN, S.K., GENISSEL, G., IGOLEN, J.
and TRAN-DINH, S.

(1982) Eur. J. Biochem. 121, 317.

The structures of DNA fragments in aqueous solution, in particular self-complementary duplexes have been widely investigated by ^{1}H- and ^{31}P-NMR during the last few years [1-9]. Many studies have been carried out on the helix-coil transition or the exchange phenomena of protons involved in hydrogen bonds by observing the NH and base proton resonances for which the assignments are now relatively well known [1-3].

Information on the sugar-base conformations and mobilities in single- and double-stranded forms can also be obtained from measurements of ^{1}H-^{1}H coupling constants, nuclear Overhauser enhancements (NOE) and relaxation times. This first requires a thorough analysis of the proton spectra of DNA fragments. Unfortunately apart from di- [10-11] and some trideoxyribonucleotides [11-12], no ^{1}H-NMR spectrum with complete assignment of DNA fragments containing more than three residues has yet been published to our knowledge.

Furthermore, little is known about the dynamic structure of single- and double-stranded forms in aqueous solution [6-9]. In small molecules such as mononucleotides, the overall molecular motion is much faster than the local motion of different groups, while in polynucleotides the reverse is true. In a molecule of intermediate size, the contribution of both overall and local motions to the relaxation times may be of the same order and should therefore be taken into consideration in some cases.

In the present paper the conformation and dynamic structure of a tetradeoxyribonucleoside triphosphate dApTpGpT (dATGT) in aqueous solution are investigated by ^{1}H-NMR at various frequencies, temperatures and concentrations. The dATGT conformations were determined simultaneously from analysis of the 400 MHz proton spectra and from NOE measurements and the dynamic structure from ^{1}H relaxation times measured at 90 and 250 MHz. The similarities and differences in conformation and mobility between residues of dATGT were also examined.

In view of the considerable effort being spent on the detailed NMR analysis of short sequences of nucleic acids we think that a knowledge of the NMR parameters, conformations and dynamic structures of deoxyoligonucleotides such dATGT is an important stage in the study of longer DNA fragments.

B.I. MATERIALS AND METHODS

dApTpGpT and the dinucleoside monophosphates (dApT and dGpT) used to identify the dATGT proton resonances were prepared in our laboratory according to the following scheme :

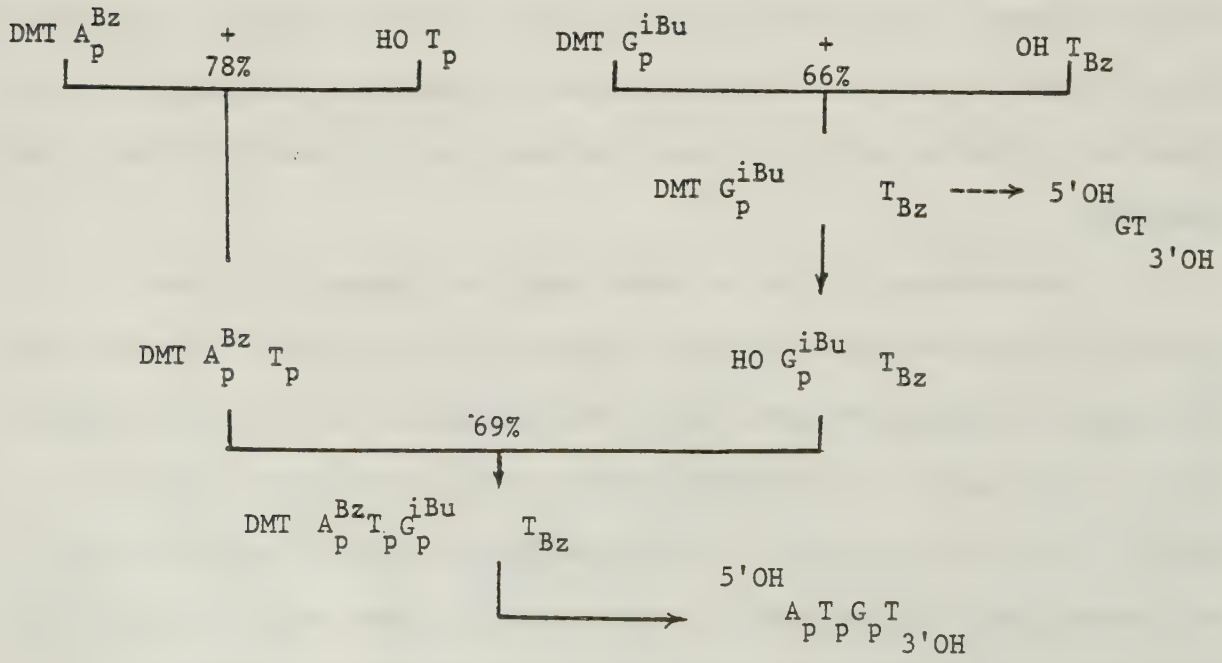

The key intermediates in this synthesis were the o.chlorophenyl trichloroethyl phosphotriesters prepared from protected nucleosides with a monofunctional reagent as described by Van Boom [13] and Köster [14].

The fully protected nucleotides were purified by silicagel column chromatography with a mixture of dichloromethane and methanol (1-5%) and precipitated as white amorphous solids with petroleum ether.

The dimethoxy trityl groups were removed with 2% benzene sulfonic acid in methylene chloride-methanol [3-1] at 0°C for 10 mn and the resulting 5'-OH nucleotide separated from dimethoxy trityl alcohol on silicagel column chromatography.

The 2.2.2-trichloroethyl group was quantitatively removed by treatment with activated zinc dust in anhydrous pyridine with triisopropyl benzene sulfonic acid. The reaction was complete in 3 mn.

The condensation procedure was used on 5 mmole scale, with a 1.2 molar excess of the charged phosphate and coupling agent (triisopropyl benzene sulfonyl nitro triazole). The reaction was complete after 2 h at room temperature and the oligo nucleotides chromatographied on silicagel column.

The protecting groups were removed with the following procedure :

1. Tetra-n-butyl ammonium fluoride in tetrahydrofuran-pyridine-water (8:1:1) (v/v) for 18 h at room temperature.
2. Concentrated ammonium hydroxide for 18 h at 50°C.
3. HCl 0.01 N for 2 h at room temperature.

The dinucleotide and tetranucleotide are purified on Sephadex G-10 and G-25 gel column chromatography with 0.05 M Et_3NH^+, HCO_3^- and their purity checked with high pressure liquid chromatography on Permaphase AAX and reserve phase Lichrosorb RP-18 (5 µg).

dATGT was dissolved in ^2H_2O containing 0.1 mM EDTA, pH ≃ 8.0. The samples were lyophilized twice in ^2H_2O and dissolved in ^2H_2O at final concentrations of 1-8 mM. These solutions were introduced into NMR tubes, degassed in a vacuum line and sealed.

Proton chemical shifts and coupling constants were obtained from 400 MHz ^{1}H-NMR spectra recorded on a laboratory-built 400 MHz ^{1}H high resolution spectrometer (I.E.F. 400). This spectrometer operates in Fourier transform mode associated with a 24 K Texas Instruments 980 A computer (8 K program, 16 K data).

NOE's were measured at 250 MHz on a CAMECA-TSN 250 in the continuous-wave mode, using a large radiofrequency observation field and sweeping slowly (1 min) through the enhanced line observed in the dispersion mode [15].

^{1}H longitudinal relaxation time experiments were performed at 90 MHz (on a Bruker WH 90) and 250 MHz (on a CAMECA-TSN 250) using the inversion recovery method (180°-τ-90°).

B.II. RESULTS AND DISCUSSION

B.II.1. Temperature and concentration effects on proton chemical shifts. Inter- and intramolecular interactions

Figures 1 and 2 show the 400 MHz ^{1}H-NMR spectra of dATGT in neutral aqueous solution. Identification of the sugar proton resonances was obtained by comparison with the dAT and dGT spectra [10] and by proton-proton decoupling. The initial residue is characterized by the exocyclic proton CH_3OD resonances in the vicinity of 3.85 ppm and the terminal residue by the $H_{3'}$ multiplet which has a smaller total splitting (≃ 14 Hz instead of 18-19 Hz) and is located upfield from the other $H_{3'}$ resonances (Fig. 1). It is worth noting that only fine splittings of about 3 Hz are observed in the $H_{2''}$ resonances and the total splitting is larger for the $H_{2'}$ (29 Hz) than for the $H_{2''}$ (22-23 Hz) multiplets. The purine and pyrimidine resonances can be

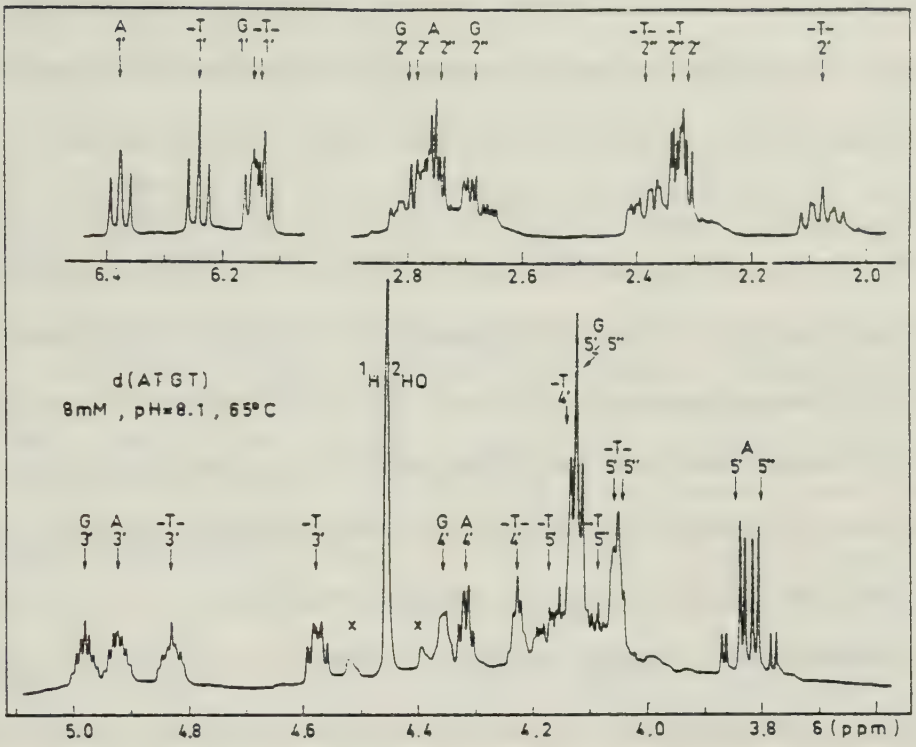

Fig. 1 - 400 MHz proton spectrum of dATGT in neutral aqueous solution

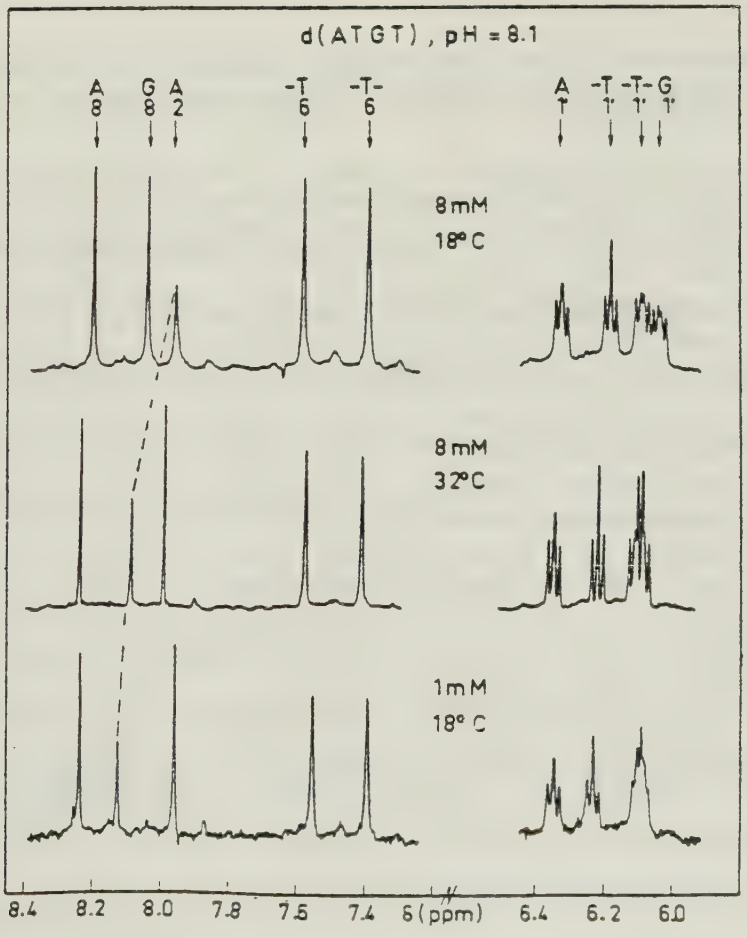

Fig. 2 - Temperature and concentration effects on the base and $H_{1'}$ proton chemical shifts of dATGT.

distinguished on the basis of the $H_{2'}$ and $H_{2''}$ chemical shifts. The $H_{2'}$ and $H_{2''}$ resonances of dA and dG exhibit chemical shifts of 2.6-2.8 ppm while those of dC and dT residues are located at higher fields between 1.9 and 2.4 ppm.

The base protons were assigned not only by comparison with the mono- and dimer spectra but also by means of Overhauser enhancement, T_1 relaxation time measurements (see below) and ^1H-^2H chemical exchange. Details on the interpretation of ^1H-NMR spectra (in particular the assignments of the sugar protons) obtained from DNA fragments containing more than three residues will be published elsewhere [16].

In order to distinguish between effects due to inter- and intramolecular interactions, the proton chemical shifts of dATGT were followed versus temperature and concentration. Table I gives the results obtained from an 8 mM sample at 18° and 65°C.

Table I - Temperature effect on proton chemical shifts (in ppm from TMP) of 8 mM d(ATGT) measured at 400 MHz in ^2H_2O at neutral pH.

Residue	T°	H_8/H_6	H_2/CH_3	$H_{1'}$	$H_{2'}$	$H_{2''}$	$H_{3'}$	$H_{4'}$	$H_{5'}$	$H_{5''}$
	18°C	8.191	7.952	6.318	2.623	2.731	4.900	4.336	3.860	3.825
Ap	65°C	8.275	8.210	6.378	2.784	2.735	4.919	4.314	3.850	3.806
	Δ	0.084	0.258	0.060	0.161	0.004	0.019	- 0.022	- 0.010	- 0.019
	18°C	7.388	1.713	6.087	1.953	2.313	4.852	4.259	4.09	4.08
pTp	65°C	7.451	1.748	6.137	2.079	2.390	4.828	4.224	4.05	4.04
	Δ	0.063	0.035	0.050	0.126	0.083	- 0.024	- 0.035	- 0.04	- 0.04
	18°C	8.035		6.036	2.833	2.651	5.028	4.415	4.14	4.14
pGp	65°C	7.948		6.149	2.800	2.683	4.977	4.356	4.12	4.12
	Δ	- 0.087		0.113	- 0.033	0.032	- 0.051	- 0.059	- 0.02	- 0.02
	18°C	7.579	1.764	6.177	2.273	2.316	4.558	4.14	4.18	4.08
pT	65°C	7.577	1.792	6.246	2.318	2.336	4.567	4.13	4.17	4.07
	Δ	- 0.002	0.028	0.069	0.045	0.020	0.009	- 0.01	- 0.01	- 0.01

The proton chemical shifts of 1 mM dATGT and their variations compared with the 8 mM sample at 18°C are reported in table II.

Table II - Concentration effect on proton chemical shifts (in ppm from TMP) of d(ATGT) measured at 400 MHz in ^2H_2O at neutral pH and at 18°C (the data for 8 mM dATGT are reported in table I).

Residue		H_8/H_6	H_2/CH_3	$H_{1'}$	$H_{2'}$	$H_{2''}$	$H_{3'}$	$H_{4'}$	$H_{5'}$	$H_{5''}$
Ap	δ(1mM)	8.234	8.121	6.345	2.761	2.730	4.905	4.339	3.863	3.830
	δ(1mM)-δ(8mM)	0.043	0.169	0.027	0.138	- 0.001	0.005	0.003	0.003	0.005
pTp	δ(1mM)	7.393	1.672	6.098	1.987	2.339	4.835	4.216	4.067	4.052
	δ(1mM)-δ(8mM)	0.005	- 0.041	0.011	0.034	0.026	- 0.017	- 0.043	- 0.026	- 0.031
pGp	δ(1mM)	7.958		6.090	2.802	2.672	4.975	4.364	4.12	4.12
	δ(1mM)-δ(8mM)	- 0.077		0.054	- 0.031	0.021	- 0.053	- 0.051	- 0.02	- 0.02
pT	δ(1mM)	7.552	1.752	6.232	2.298	2.318	4.586	4.12	4.18	4.08
	δ(1mM)-δ(8mM)	- 0.027	- 0.012	0.055	0.025	0.002	0.028	0.02	0.00	0.00

Except for G_8, which shows a shift to higher fields, the signals of the other protons shift more or less to lower fields either with increasing temperature or with dilution.

In the case of the A and G residues, these temperature and dilution effects, which are stronger for the A than for the G residue, are very similar. The protons most sensitive to temperature and concentration effects can be classified in the following order :

$$A_2 > A_{2'} > A_8 > A_{1'}$$

and

$$G_{1'} > G_8$$

Figure 2 illustrates this situation and also shows that the largest proton chemical shift variations occur between 18 and 32°C. The ^1H-NMR spectrum of dATGT at 8 mM and at 32°C is comparable to that obtained from a 1 mM sample at 18°C and in general not very different from the 8 mM dATGT spectrum at 65°C. These results suggest that the temperature effect on the chemical

shifts on the A and G protons in an 8 mM solution of DATGT is mainly due to intermolecular base-base stacking (whose effect is likely weak for concentrations lower than 1 mM).

Among the four residues of dATGT, only the pT terminal residue protons are insensitive to temperature and concentration changes. In the case of pTp the temperature effect is clearly stronger than that of dilution : a change from 18 to 65°C causes δ ($H_{2'}$) and δ ($H_{2''}$) to vary by about 0.13 ppm and 0.08 ppm respectively whereas a drop in the dATGT concentration from 8 mM to 1 mM leads to a chemical shift variation of only 0.03 ppm. This particular behaviour of pTp protons seems to be due to intramolecular interactions between the pTp residue and the others.

It is worth noting that in most cases the temperature and concentration strongly affect the $H_{2'}$ chemical shift but have little or no effect on δ ($H_{2''}$). We attribute this large δ ($H_{2'}$) variation to the modification of the base conformation.

B.II.2. Sugar conformations

The 400 MHz ^{1}H-NMR spectra of dATGT are well resolved at 65°C, allowing most of the coupling constants between the sugar protons to be determined. The accuracy in the determination of the coupling constants between the sugar ring protons $J_{1'2'}$, $J_{1'2''}$, $J_{2'3'}$, $J_{2''3'}$ and $J_{3'4'}$ is better than ±0.1 -0.2 Hz. Apart from $J_{4'5'}$ and $J_{4'5''}$ of the Ap residue, measured with an accuracy better than ±0.1 Hz, the error in the determination of these coupling constants for the other residues is about ±0.2 -0.3 Hz due to poor separation of the $H_{4'}$, $H_{5'}$ and $H_{5''}$ resonance signals even at 400 MHz. At 32°C the proton resonance lines are relatively broad and the proton spectra of dATGT are poorly resolved in some regions. Only the coupling constants between the sugar ring protons $H_{1'}$, $H_{2'}$, $H_{3'}$ and $H_{4'}$ can therefore be determined.

Table III - Temperature effect on coupling constants (in Hz) J_{H-H} and J_{P-H} of 8 mM d(ATGT) measured at 400 MHz in ^2H_2O at neutral pH.

Residue	T°	%S	J_{6-CH_3}	$J_{1'2'}$	$J_{1'2''}$	$J_{2'3'}$	$J_{2''3'}$	$J_{2'2''}$	$J_{3'4'}$	$J_{3'-P}$	$J_{4'5'}$	$J_{4'5''}$	$J_{5'5''}$	$J_{5',5''-P}$
Ap	18°C	78		8.0	5.8	5.6	2.4	a)	2.3	6.0	3.1	4.2	12.5	
	65°C	71		7.7	6.1	5.5	3.2	14.0	3.1	5.8	3.0	4.2	12.5	
pTp	18°C	80	1.0	9.0	5.6	6.2	2.6	14.2	2.3	a)	a)	a)	a)	a)
	65°C	74	1.0	8.7	5.7	6.4	2.2	14.1	3.1	5.7	2.8	4.3	11.5	
pGp	18°C	77		9.0	5.4	6.1	2.5	13.9	2.7	a)	a)	a)	a)	a)
	65°C	73		8.0	6.0	6.1	3.0	14.0	3.0	6.0	~ 4	~ 4	a)	a)
pT	18°C	64	1.3	7.0	6.5	6.0	3.9	a)	3.9		a)	a)	a)	a)
	65°C	66	1.0	6.8	6.9	6.4	4.3	13.9	3.5		2.2	3.2	11.0	4.9

a) unresolved signals

In table III are reported the coupling constants J_{HH} , J_{PH} of dATGT obtained at 18 and 65°C. It should be noted that no concentration effect on the coupling constants has been observed similar to the case of mono and dinucleoside monophosphates [17]. These results confirm the above conclusion obtained from the proton chemical shift study indicating a pronounced intermolecular stacking in the 8 mM dATGT sample at 18°C.

The $J_{1'2'}$ values of the extreme residues Ap and pT are practically identical with those of the corresponding monomers [18-19] while those of the two central residues, pTp and pGp, are slightly higher. A similar situation has also been observed in the case of dTTA [12]. The sugar conformation was deduced from the proton-proton coupling constants using the Altona and Sundaralingam model [20, 21] ; the proportions of the S conformation (2'endo-3'exo) are summarized in table III for the different residues. Although the S conformation is highly favoured for all dATGT residues, the data in table III indicate a slight difference in the average conformation between the extreme and central residues. In particular the two thymidylyl residues pT and pTp exhibit different sugar conformations (64 and 80% of S

conformation respectively at 18°C). This seems to correlate with the temperature and concentration effect differences mentioned above.

The S/N equilibria are modified slightly (Table III) when the temperature varies from 18 to 65°C. The S proportion in the first three residues Ap, pTp, pGp decreases at high temperature but remains unchanged in the case of the terminal residue pT.

Lastly the small $J_{4'5'}$ and $J_{4'5''}$ values indicate a clear predominance of the gg rotamer for the exocyclic group, as in the majority of nucleosides and nucleotides in aqueous solution.

B.II.3. Base conformation around the glycosidic bond and dynamic structure of dATGT

In the case of ribonucleotides and their derivatives, the relaxation of the sugar protons $H_{1'}$, $H_{2'}$ and $H_{3'}$ is sensitive to the base orientation due to dipole interaction with the base proton, H_8 or H_6 [22]. As a result, the T_1 proton relaxation time measurement constitutes an efficient method of investigation of the base conformation around the glycosidic bond. For the 2'-deoxyribonucleotides and their analogues on the other hand the influence of the base proton (H_8 , H_6) on the relaxation rate of $H_{1'}$, $H_{2'}$ and $H_{3'}$ is slight because of the presence of $H_{2''}$ and its proximity to the other sugar ring protons. Proton relaxation data thus provide a large amount of interesting information on the dynamic structure or molecular mobility but little about the base orientation. NOE measurement of the base proton (H_8 or H_6) with successive saturation of $H_{1'}$, $H_{2'}$ and $H_{3'}$ appears to be a good method of studying the base conformation. However in the case of large oligonucleotides of more than six residues, $\omega\tau_c$ tends towards unity when ω is large ($> 2\pi \times 250 \times 10^6$) and hence the sum of NOE (from all other protons) is much smaller than 50%. It should be noted that the NOE measurements also allow the base protons to be identified, especially when two or more residues of the same nature are present.

a) Nuclear Overhauser enhancements

Table IV reports the NOE data obtained at 250 MHz and at 35°C, temperature for which intermolecular stacking is found, by chemical shift measurement versus t°C, to be slight in dATGT. In general, the enhancements are obtained from different sugar protons, indicating the flexibility of each residue. Among the sugar ring protons the NOE value from $H_{2'}$ is large and is practically the same for all residues. This is not surprising since the S conformation is strongly predominant whatever the residue ; $H_{2'}$ is thus in the endo position most of the time and the minimum distance $r_{2'-8(6)}$ is shorter than the other minimum distances between the deoxyribose protons and H_8 or H_6.

Table IV - Nuclear Overhauser enhancements of base proton signals of d(ATGT) measured at 250 MHz and at 35°C.

Irradiated proton	A_8	$-T_6-$	G_8	$-T_6$
CH_3		11		14
$H_{1'}$	11	a)	5	a)
$H_{2'}$, $H_{2''}$	11	10	10	11
$H_{3'}$	a)	a)	5	a)
$H_{5'}$, $H_{5''}$	a)			
Total	22	21	20	25

a) Enhancement smaller than 3%.

The NOE distributions of the Ap residue at 35°C are quite different from that of the others. In the former case, the NOE from $H_{1'}$, $\eta_{1'}$, is a large as $\eta_{2'}$ from $H_{2'}$, while for the other residues the sum of NOE from all other sugar protons is equal to or smaller than $\eta_{2'}$. Since the minimum

distance $r_{1'-8}$ is longer than $r_{2'-8}$, these results clearly show that the *syn* conformation is favoured in the first residue, dAp, as in the case of 3'AMP [23].

Concerning the G residue, the *syn* and *anti* conformations can be considered as equiprobable since no difference in NOE from $H_{1'}$ and $H_{3'}$ was observed. In the case of the pT and pTp residues, the data in table IV indicate that the relaxation of the base proton, H_6 , is essentially governed by the dipolar interaction arising from the CH_3 group and $H_{2'}$; the NOE measurement can therefore lead to no clear conclusion about the *syn/anti* equilibrium.

It is worth noting that the sum of the NOE values is about 22 ± 2% for all residues corresponding to a correlation time of 0.4 nsec, in good agreement with the τ_c value deduced from the relaxation data (see below).

b) Relaxation time measurements

The longitudinal relaxation times of dATGT protons were determined versus temperature at two frequencies (90 and 250 MHz).

It is important to note that for ribonucleotides and their derivatives, the cross-relaxation effect (for $\omega\tau_c << 1$) is only detectable in the case of H_4, due to its proximity to the exocyclic protons CH_5,$H_{5''}$OH or CH_5,$H_{5''}$-OP [24]. In the case of deoxyribonucleotides on the contrary we observed for all protons a more or less strong cross-relaxation effect characterized by a slight deviation from the tangent at the origin of the magnetization decay curves. This is due to the fact that the CH_5,$H_{5''}$ and CH_2,$H_{2''}$ groups, which relax very quickly, contribute 80% to the average relaxation rate of all the protons in a given residue.

Figure 3 shows the initial relaxation time T_1 measured at 90 and 250 MHz versus temperature. At t > 65°C no clear difference was found between T_1 (90 MHz) and T_1 (250 MHz) whereas the frequency effect on the T_1

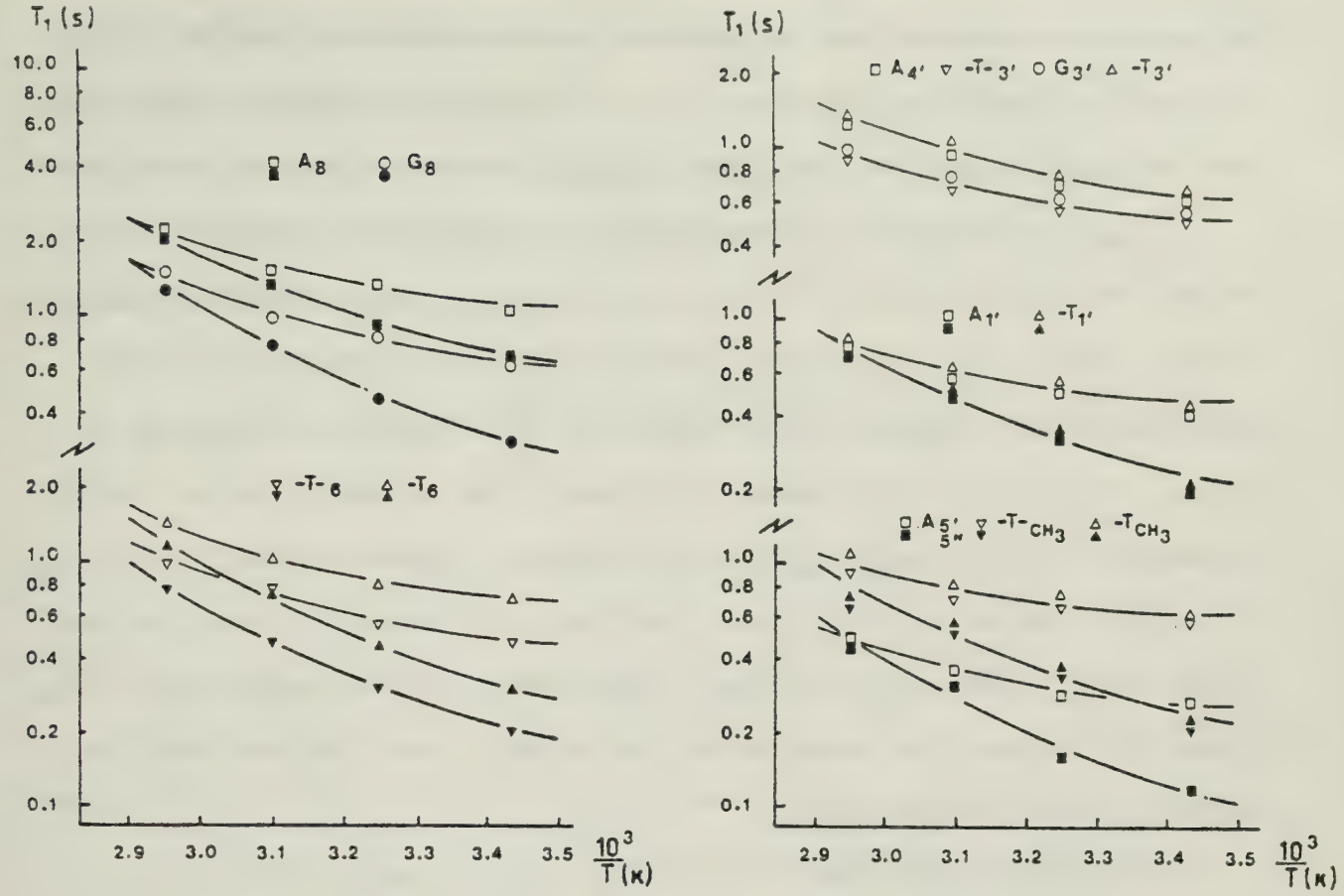

Fig. 3 - Semi-Log plot of proton initial relaxation times T_1 versus reciprocal absolute temperature at 90 and 250 MHz.

Table V - Ratios of proton longitudinal relaxation times measured at 90 250 MHz between 18 and 65°C.

T°	A_8	pTp_6	$pTpCH_3$	G_8	pT_6	$pTCH_3$	$\overline{T_1(90)/T_1(250)}$ a)
18°C	0.60	0.43	0.43	0.50	0.44	0.40	0.43 ± 0.04
35°C	0.67	0.56	0.56	0.55	0.58	0.60	0.57 ± 0.02
50°C	0.86	0.62	0.78	0.72	0.72	0.69	0.71 ± 0.06
65°C	0.98	0.77	0.76	0.87	0.82	0.78	0.80 ± 0.05

a) average value over the proton T_1 ratios of three terminal residues T,G,T.

values becomes more and more substantial as the temperature decreases from 65 to 18°C. The shape of the Log $T_1 = f(1/T°)$ curves in figure 3 indicates that $\omega\tau_c$ is still smaller than unity in the temperature interval considered.

The striking fact to emerge from figure 3 is that the initial relaxation rate of the pT and pTp base proton H_6 on the one hand and that of the A and G residue H_8 on the other hand differ respectively by about 50% whatever the frequency. This difference in $1/T_1$ can be interpreted as due to a mobility or conformation difference. This ambiguity can be removed by taking the ratio $T_1(90)/T_1(250)$ for different protons (Table V) [25]. It is seen from the data in figure 3 and table V that the T_1 ratios of the pT and pTp H_6 proton are practically identical at a given temperature. The pT and pTp residues can therefore be considered to have the same mobility but not the same conformation.

The results in table V also show that the ratio $T_1(90)/T_1(250)$ is much the same for the three terminal residues of dATGT while the T_1 ratio of the first residue, Ap, is clearly larger, corresponding obviously to a shorter correlation time. Thus, on the basis of the above NOE data and the T_1 relaxation time measurements, the discrepancy in T_1 (H_8) between the A and G residues can be attributed to a difference in the mobility and conformation of the bases.

Another interesting remark is that the ratios $T_1(90)/T_1(250)$ for the two methyl groups are virtually identical with that obtained from the base protons in the three terminal residues of dATGT. This is somewhat surprising since the internal rotational motion of the methyl group is very fast and hence the ratio $T_1(90)/T_1(250)$ for this group is expected to be much larger, corresponding to a short correlation time.

In fact if the molecule is assumed to undergo an isotropic motion with an apparent correlation time τ_c , and the internal rotational motion of CH_3 is characterized by a correlation time $\tau_r \ll \tau_c$ (with a three-position random jump mechanism), the relaxation rate $1/T_1$ of the methyl group may be expressed as follows [26] :

$$\frac{1}{T_1} = 0.6 \frac{\gamma^4 \hbar^2}{r^6} \left[\frac{1}{4} f(\omega,\tau_c) + \frac{3}{4} f(\omega,\tau_c') \right] \qquad (1)$$

where

$$f(\omega,\tau_c) = \frac{\tau_c}{1 + \omega^2\tau_c^2} + \frac{4\tau_c}{1 + 4\omega^2\tau_c^2} \qquad (2)$$

and

$$\tau_c'^{-1} = \tau_c^{-1} + \tau_r^{-1} \qquad (3)$$

Since $\tau_r \ll \tau_c$, $f(\tau_c') \simeq f(\tau_r)$. In the present case $\tau_c \simeq 0.4\ 10^{-9}$ sec, and for $\tau_r \simeq 10^{-11}$ sec $f(\omega,\tau_c)$ ($\gtrsim 10^{-9}$ sec at 90 and 250 MHz) is much larger than $f(\tau_r)$ ($= 5.10^{-11}$ sec). Consequently, the relaxation rate, $1/T_1$, becomes proportional to $f(\omega,\tau_c)$ and the ratio $T_1(\omega)/T_1(\omega')$ of the methyl protons should have the same value as the other protons. Therefore, when $\omega\tau_c \simeq 1$, the T_1 ratio of the methyl group, obtained from two different frequencies, reflects not its internal rotational motion but the motion of the molecule or of the fragment carrying this methyl group. Since CH_3 groups always have a better S/N ratio than other proton groups in a molecule, their relaxation times, $T_1(CH_3)$, are easy to determine accurately even at low concentrations of compound ($\lesssim 10^{-3}$ M).

Figure 4 gives the Log τ_c values deduced from the T_1 ratio [25] versus $1/T°$ for the Ap and the other residues separately. Two straight lines with similar slopes are obtained, corresponding to an activation energy of 4-6 kcal/mole.

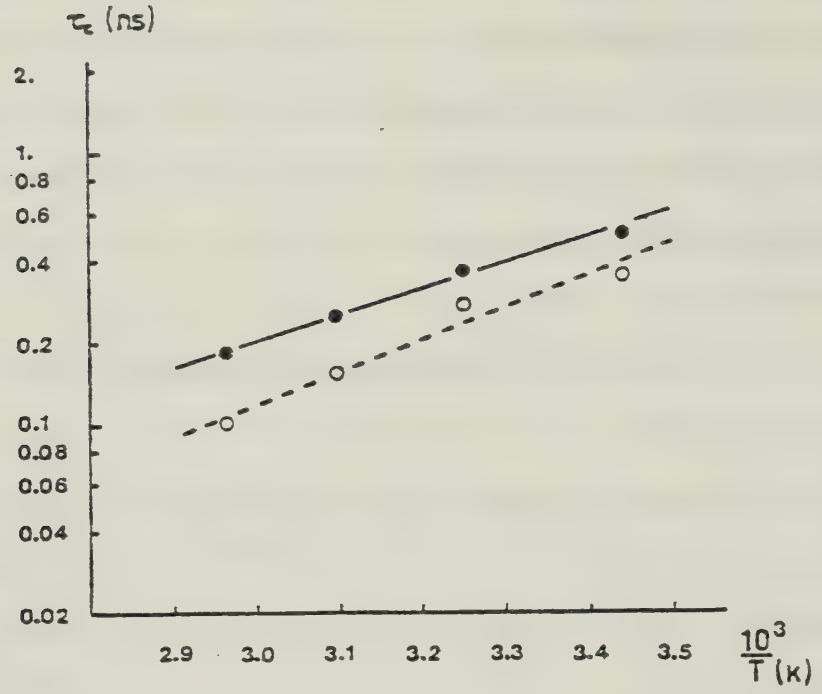

Fig. 4 - Semi-Log plot of correlation times versus reciprocal absolute temperature. ——•—— three terminal residues of dATGT, --- o --- Ap residue.

As the temperature increases from 18 to 65°C, the mean correlation time value for all the dATGT residues varies from 0.5 to 0.2 nsec, as in the case of poly I (0.7-0.4 nsec) [25] and poly U (0.7-0.3 nsec) [27] for the same temperature interval. The small difference between the mean τ_c value of dATGT and that of single-stranded poly I and poly U is probably due to the fact that in the former case the overall motion of the whole molecule is not too slow with respect to the local motion as it is the case with polynucleotides. In fact, the correlation time obtained from the ^{31}P relaxation time data for the three phosphate groups in dATGT [$T_1(^{31}P)$ = 2.5 sec] and from the $^{31}P-\{^1H\}$ NOE (= 1.7) measurement (both results obtained at 36.4 MHz) is about 1.5 nsec at 18°C. If we assume that the bulky phosphate groups undergo the same overall motion as the whole molecule, with a correlation time τ_g of 1.5 nsec, and that the local motion of the sugar-base unit is independent of the former motion in a first

approximation, the correlation time of the local motion τ_l can be calculated from the apparent correlation time τ_c (0.5 nsec at 18°C)

$$\frac{1}{\tau_g} + \frac{1}{\tau_l} = \frac{1}{\tau_c} \quad \text{with} \quad \tau_g = 1.5 \text{ nsec}, \quad \tau_c = 0.5 \text{ nsec}$$

At 18°C, the local correlation time τ_l (= 0.75 nsec) is found to be practically the same as in poly I and poly U.

REFERENCES

1. PATEL, D.J. and HILBERS, C.W. (1975) Biochemistry 14, 2651.
2. PATEL, D.J. and TONELLI, A.E. (1975) Biochemistry 14, 3990.
3. PATEL, D.J. (1975) Biopolymers 16, 1635.
4. MILLER, P.S., CHENG, D.M. DREON, N., JAYARAMAN, K., KAN, L.S., LEUTZINGER, E.E., PULFORD, S.M. and TS'O, P.O.P. (1980) Biochemistry 19, 4688.
5. PHILLIPS, D.R. and ROBERTS, G.C.K. (1980) Biochemistry 19, 4795.
6. DAVANLOO, P., ARMITAGE, I.M. and CROTHERS, D.M. (1979) Biopolymers 18, 663.
7. EARLY, T.A. and KEARNS, D.R. (1980) Nuc. Acids Res. 8, 5795.
8. HOGAN, M.E. and JARDETZKY, O. (1979) Proc. Natl. Acad. Sci. 76, 6341.
9. BOLTON, P.H. and JAMES, T.L. (1980) Biochemistry 19, 1388.
10. CHENG, D.M. and SARMA, R.H. (1977) J. Am. Chem. Soc. 99, 7333.
11. DHINGRA, M.M. and SARMA, R.H. (1979) Stereodynamics of Molecular Systems (SARMA, R.H. ed.), pp. 3-38, Pergamon Press, New-York.
12. ALTONA, C., Van BOOM, J.H., HAASNOOT, C.A.G. (1976) Eur. J. Biochem. 71, 557.

13. Van BOOM, J.H., BURGERG, P.M.J., Van Der MAREL, G., VERDEGAAL, C.H.M. and WILLE, G. (1977) Nuc. Acids Res. 4, 1047.

14. KOHLI, V., BLÖCKER, H. and KÖSTER, H. (1980) Tetrahedron Lett. 21, 501.

15. TRAN-DINH, S., GUSCHLBAUER, W. and GUERON, M. (1972) J. Am. Chem. Soc. 94, 7903.

16. TRAN-DINH, S., NEUMANN, J.M., HUYNH-DINH, T., IGOLEN, J. and KAN, S.K. (1982) Org. Mag. Res. 18, 148.

17. TRAN-DINH, S., NEUMANN, J.M. and BORREL, J. (1981) Biochim. Biophys. Acta 655, 167.

18. LEE, C.H., EVANS, F.E. and SARMA, R.H. (1975) FEBS Lett. 51, 73.

19. WOOD, D.J., HRUSKA, F.E. and OGILVIE, K.K. (1974) Can. J. Chem. 52, 3353.

20. ALTONA, C. and SUNDARALINGAM, M. (1972) J. Am. Chem. Soc. 94, 8205.

21. ALTONA, C. and SUNDARALINGAM, M. (1973) J. Am. Chem. Soc. 95, 2333.

22. NEUMANN, J.M. BERNASSAU, J.M., GUERON, M. and TRAN-DINH, S. (1980) Eur. J. Biochem. 108, 457.

23. GUERON, M., CHACHATY, C. and TRAN-DINH, S. (1973) Ann. N.Y. Acad. Sci. 222, 307.

24. TRAN-DINH, S., NEUMANN, J.M., THIERY, J.M., HUYNH-DINH, T., IGOLEN, J. and GUSCHLBAUER, W. (1977) J. Am. Chem. Soc. 99, 3267.

25. NEUMANN, J.M. and TRAN-DINH, S. (1981) Biopolymers 20, 89.

26. KALK, A. and BERENDSEN, H.J.C. (1976) J. Mag. Res. 24, 343.

27. NEUMANN, J.M. and TRAN-DINH, S. (1982) Biopolymers 21, 383.

C. ^{1}H-NMR STUDIES OF HELIX-COIL TRANSITION, CONFORMATION AND DYNAMIC STRUCTURE OF THE SELF-COMPLEMENTARY DEOXYHEXANUCLEOTIDE dApCpApTpGpT IN AQUEOUS SOLUTION

TRAN-DINH, S., NEUMANN, J.M., HUYNH-DINH, T., GENISSEL, B.
IGOLEN, J. and SIMMONOT, G.

(1982) Eur. J. Biochem. (sous presse)

In recent years, short self complementary oligonucleotides of defined sequence, used as nucleic acid models, have been investigated extensively by ^{1}H-NMR spectroscopy [1-12]. Most of this work has been carried out by monitoring the NH and base protons and has provided important information about the thermodynamics and kinetics of the helix-coil transition.

In principle, the conformations and dynamic structures of single and double stranded oligonucleotides can also be obtained from the analysis of sugar proton spectra and proton T_1 measurements. The chemical shifts of $H_{1'}$ and $H_{2'}$ should be sensitive to the base orientation and in the case of DNA fragments, the chemical shifts of the $H_{2''}$ protons are expected to be influenced by the change in the phosphate group conformation (or environment). Unfortunately, though synthesis is easier for DNA than for RNA fragments, the sugar proton spectra of the former are more complicated to interpret due to the overlapping of the $H_{2'}$ and $H_{2''}$ resonances at low and medium frequencies (< 300 MHz).

Among various self complementary deoxyoligomers studied, particular attention has been given to investigation of dApTpGpCpApT (dATGCAT) by ^{1}H-NMR [3, 4, 7-9], however the resonance assignment for the sugar protons and some of the base protons is still unresolved. This is due not only to the fact that the dATGCAT spectra have been recorded at medium frequencies (< 300 MHz), but also to the lack of proton spectra for dATGCAT derivatives,

from which resonance assignment by chemical shift comparisons could be realized. Furthermore it was demonstrated that the double helices of hexamers such as dATGCAT [3, 7, 9] and rAAGCUU [2] with GC base pairs in the center of the duplex, open in a sequential order from the end of the duplex with increasing temperature. It is therefore important to know if this rule is still valid in the case of similar sequences like dApCpApTpGpT (dACATGT) where the AT base pairs are located at the central positions.

In the present paper, the helix-coil transition, conformations and dynamic structures of single and double stranded dACATGT in H_2O and D_2O solutions were investigated at various temperatures by ^1H-NMR spectroscopy. The chemical shifts and coupling constants of the non exchangeable protons were determined at 400 MHz ; the chemical shifts and linewidths of the imino exchangeable protons at 276 MHz and the proton longitudinal relaxation times were measured at two frequencies, 90 and 250 MHz. The results are compared with those obtained for dATGCAT and other oligomers.

C.I. EXPERIMENTAL SECTION

dApCpApTpGpT was prepared according to published literature [13]. The purification was performed using Sephadex G-25 gel column chromatography and checked with HPLC on Permaphase AAX and on reverse phase Li chrosorb RP-18 (5 μ).

In the case of the non-exchangeable proton observation, dACATGT was dissolved in ^2H_2O containing 0.1 M NaCl + 5 mM $PO_4^{=}$ and was freed of possible divalent ions by shaking with Chelex 100 and then by adding EDTA (0.1 mM). The pH was adjusted to 7-8 by the addition of a small amount of NaOH. The samples were lyophilized twice in ^2H_2O and redissolved in ^2H_2O at a final concentration of 5 mM. These solutions were introduced into NMR tubes, degassed on a vacuum line and sealed. Proton chemical shifts and

coupling constants were obtained from 400 MHz ^{1}H-NMR spectra recorded on a laboratory-built high resolution spectrometer (I.E.F. 400). This spectrometer operates in the Fourier transform mode associated with a 24K Texas Instruments 980A computer (8 K program, 16 K data). The proton chemical shifts were measured from 3-(trimethylsilyl-$^2H_4$) propionic acid. ^{1}H longitudinal relaxation time experiments were performed at 90 MHz (on a Bruker WH 90) and 250 MHz (on a CAMECA-TSN 250) using the inversion recovery method (180°-τ-90°).

In the exchangeable proton observations, dACATGT was dissolved in ^1H_2O containing 0.2 M NaCl + 4 mM $PO_4^{=}$, pH = 8.0. ^{1}H-NMR spectra were recorded on a laboratory-built 276 MHz high resolution spectrometer, using a special sequence to eliminate the water peak.

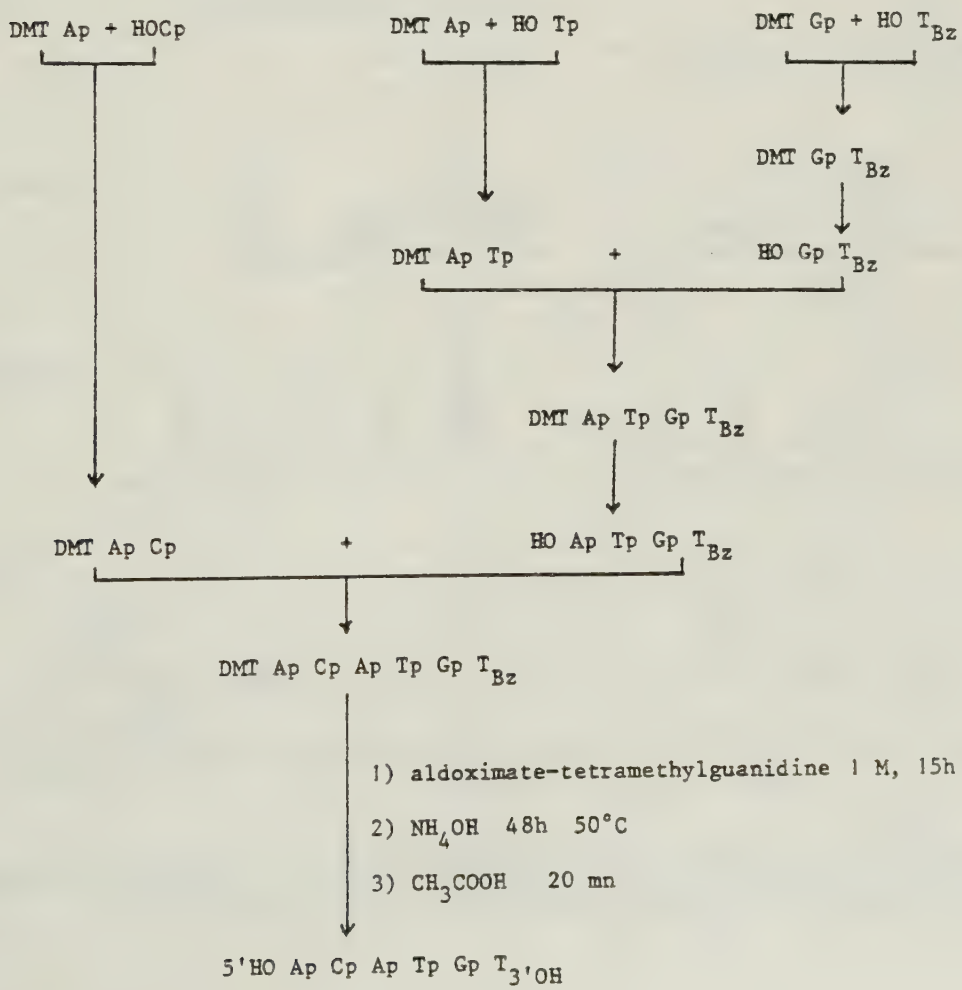

C.II. RESULTS

C.II.1. Non-exchangeable protons

a) Sugar and base proton assignments

In general, an oligonucleotide molecule in aqueous solution tends to associate at room temperature with other molecules by intermolecular base-base stacking, hydrogen bond formation, helix-coil transition, etc ... Consequently oligonucleotide proton spectra strongly depend on temperature and exhibit broad resonance lines at low temperatures due to a restricted molecular motion or an exchange between different forms. This situation is illustrated in figures 1a, b, c, which show the 400 MHz proton spectra of dACATGT (5 mM + 0.1 M NaCl + 5 mM $PO_4^{=}$, pH = 8.0) obtained at various temperatures.

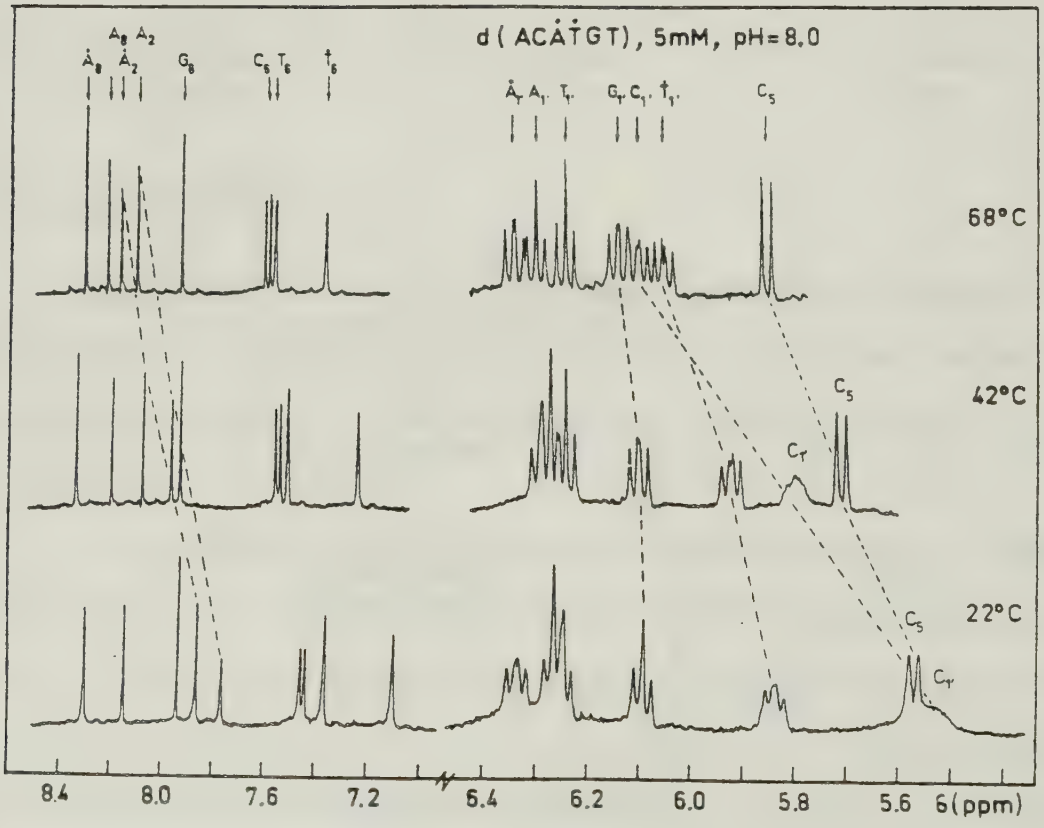

Fig. 1 - 400 MHz proton spectra of dACATGT in D_2O at different temperatures (22°C, 42°C and 68°C). a) Base protons and H_1' sugar protons.

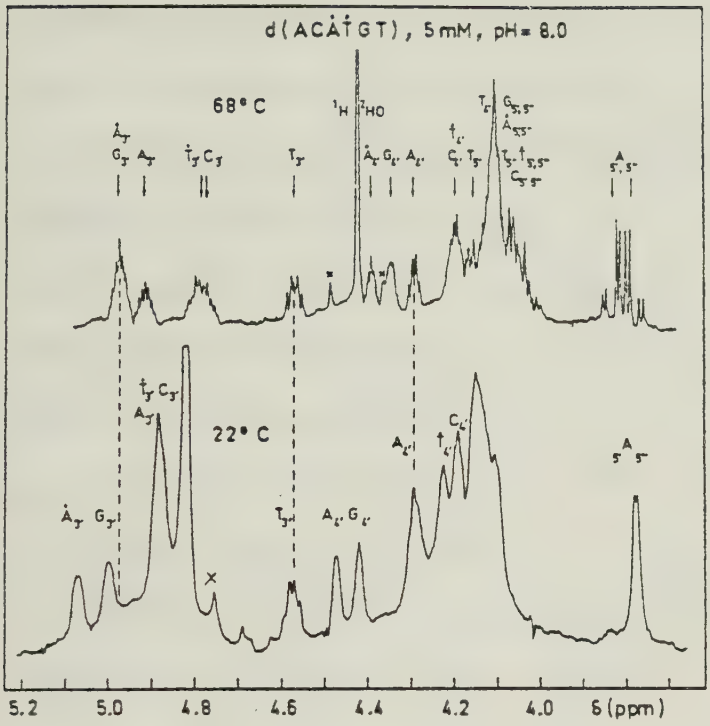

Figure 1b

$H_{3'}$, $H_{4'}$, $H_{5'}$ and $H_{5''}$ sugar protons of dACÀṪGT.

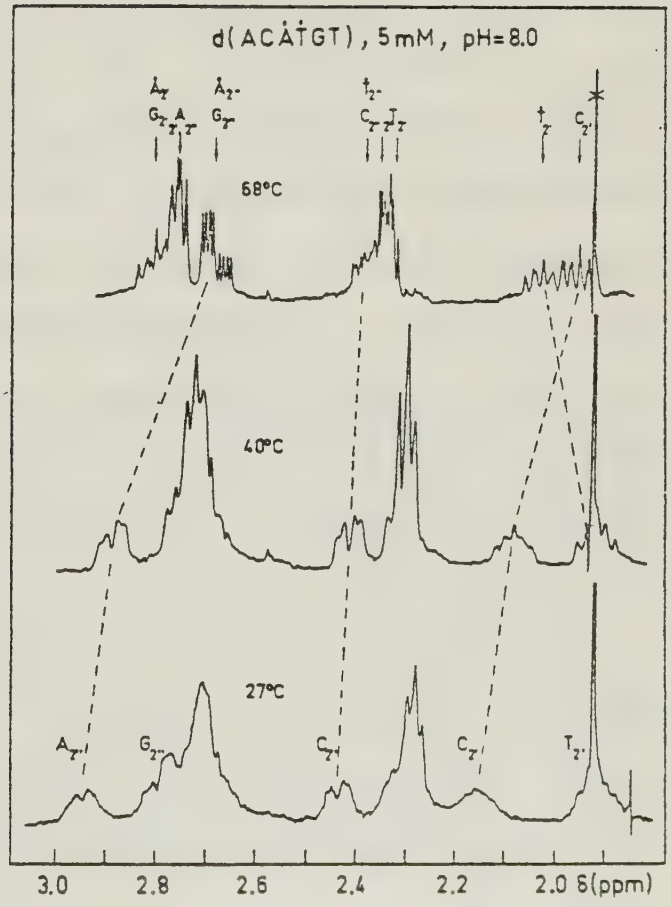

Figure 1c

$H_{2'}$, $H_{2''}$ sugar protons of dACÀṪGT.

A general method for the assignment of DNA fragments proton resonances has already been presented [14] and used to interpret the 400 MHz proton spectra of $\dot{d}\dot{A}CATGT$ in neutral aqueous solution. We resume here only some essential points. Apart from the comparisons with dGT and $d\dot{A}TGT$ spectra obtained at high temperature ($t° > 60°C$), the identification of $\dot{d}\dot{A}CATGT$ proton resonances was performed in two stages : in the first stage, proton signals of the same residue were determined from proton-proton decoupling, which was applied systematically to all proton resonances, especially those for which chemical shift crossovers occur as the temperature is varied ; the nature and sequential position was then determined for each residue. The initial residue is characterized by exocyclic proton CH_2OD resonances in the vicinity of 3.85 ppm and the terminal residue by the $H_{3'}$ multiplet, which has a smaller total splitting ($\simeq$ 14 Hz instead of 18-19 Hz), and is located upfield from the other $H_{3'}$ resonances (Fig. 1b). The resonance signals of the $H_{2'}$ and $H_{2''}$ protons (above and below the sugar plane respectively) can be distinguished by the fact that the total splitting is larger for $H_{2'}$ ($\simeq$ 29 Hz) than for $H_{2''}$ (22-23 Hz), and only fine splittings of about 3 Hz are observed in the $H_{2''}$ resonances. The $H_{2'}$ and $H_{2''}$ resonances of the purine residues exhibit chemical shifts of 2.6-2.8 ppm, while those of the pyrimidine residues are located at higher fields between 1.9 and 2.4 ppm (Fig. 1c). Except for the terminal residue, the $H_{3'}$ resonances of dA and dG are located at lower fields compared with those of dC and dT residues. The same is true for the $H_{4'}$ resonances. Owing to the difference in the ring current effect between the A and G bases, the $A_{1'}$ resonances are located downfield from the $G_{1'}$ resonances, i.e. $\delta A_{1'} > \delta G_{1'}$.

The base proton resonance assignments for $\dot{d}\dot{A}CATGT$ were determined from a set of interlocking procedures : longitudinal relaxation time measurements, comparisons with dGT and $d\dot{A}TGT$ spectra and ^1H-^2H chemical exchange. The A_8 and $\dot{A}_8$ signals were distinguished on the basis of the T_1 measurement ;

the $T_1(H_8)$ value for the initial residue is about twice as long as the $T_1(H_8)$ value for the internal residues (see below), similar to the case of dATGT [15]. The same assignments for the A_8 , A_2 , $\dot{A}_8$ and $\dot{A}_2$ signals, based on the fact that the presence of a 5'-phosphate results in a ≃ 0.1 ppm downfield shift in the H_8 purine resonance [16], have already been established for dATGCAT [4]. The difference in chemical shift between the T_6 and $\dot{T}_6$ protons of dACATGT is substantial, thus allowing comparisons to be made for the dGT and dATGT proton spectra. The distinction between the T_6 and $\dot{T}_6$ resonances was also based on T_1 relaxation time measurements : the H_6 relaxation time is longer for the terminal than for the internal residue (see below). In the case of dATGCAT, the assignments of the T_6 and $\dot{T}_6$ resonances are difficult, due to the small difference in chemical shift between these protons at low temperatures. However at $t° > 70°C$, the two thymine H_6 resonances of dATGCAT were found to be well separated [4] ; one is situated at 7.55 ppm very close to the T_6 signal (7.57 ppm) of dACATGT and the other at 7.42 ppm very close to the dACATGT T_6 signal (7.38 ppm at 70°C). Therefore we suggest that the signal located at lower-field is assigned to the H_6 proton of the terminal thymidylyl residue as in the case of dACATGT.

b) Temperature effects on proton chemical shifts

The chemical shifts of the dACATGT non-exchangeable protons were studied as a function of temperature between 20 and 72°C. In all cases, the proton linewidths decrease with increasing temperature in contrast with the case of dATGCAT, where the proton linewidths were found to be larger at 41-46°C (≃ 7.5 Hz) than at 2°C (≃ 6.4 Hz) [4]. The striking fact to emerge from figure 1a is that for $t° \leqslant 42°C$, the resonance lines of the $C_{1'}$ proton are particularly broad compared with the other $H_{1'}$ protons, while at high temperatures, the $C_{1'}$ linewidth is found to be the same as with the other

H_1, protons. The C_2, resonance also exhibits the same behaviour but in a less pronounced way.

It follows from figures 1a, b, c, that for increasing temperatures, the H_1, and base protons exhibit downfield shifts while some of the H_2, and $H_{2''}$ protons shift in the opposite direction. This is also true for the H_3, and H_4, protons with the exception of the extreme residue. At high temperatures ($t° > 60°C$) $\delta H_{2'} > \delta H_{2''}$ for purine, while $\delta H_{2'} << \delta H_{2''}$ for the pyrimidine families, but at low temperatures $\delta H_{2''} > \delta H_{2'}$ in the case of the internal purine residues (Fig. 1c).

In figure 2, the chemical shifts of the base, H_1, and some H_2, and $H_{2''}$ protons are plotted against temperature between 20 and 72°C.

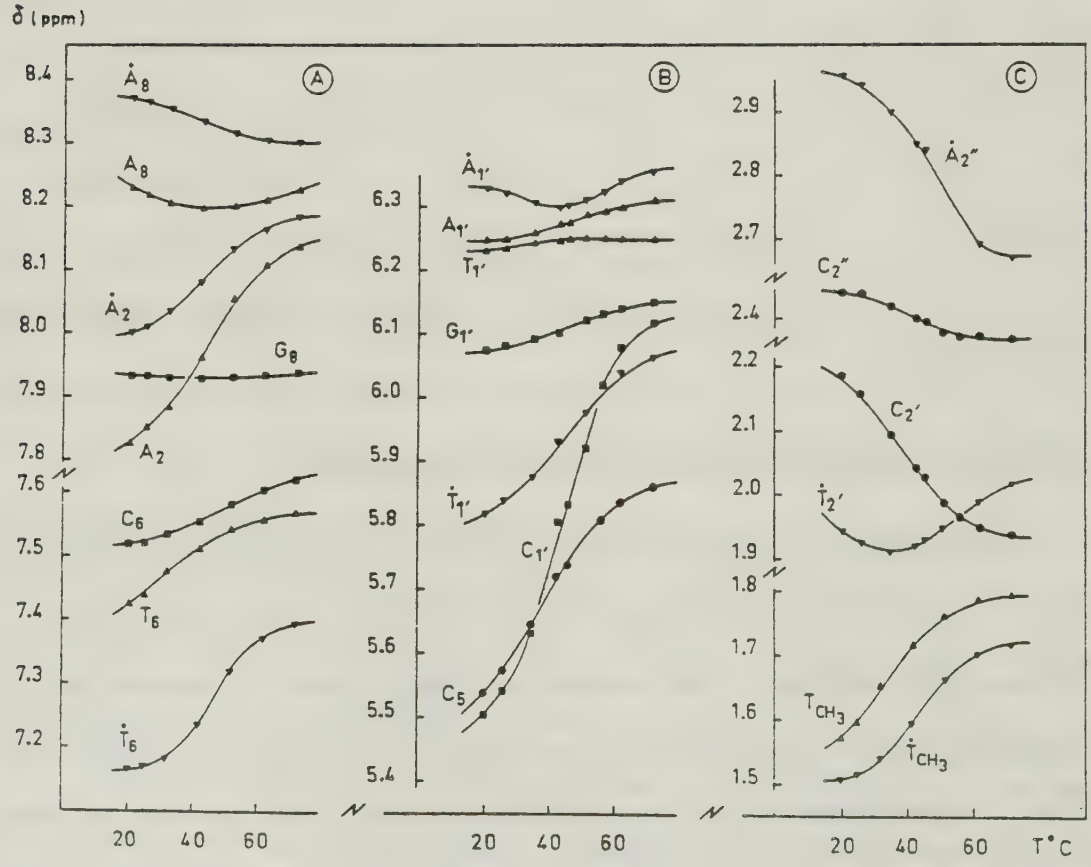

Fig. 2 - Temperature dependence of the proton chemical shifts of dACATGT (5 mM in D_2O + 0.1 M NaCl + 5 mM $PO_4^{=}$, pH = 8).

The chemical shifts of all dACATGT protons measured at two extreme temperatures are reported in table I. The results in figure 2a show that the temperature dependent behaviour of purine base protons is very similar for dACATGT and dATGCAT, in particular the G_8 chemical shift is insensitive to temperature effects. In contrast, the pyrimidine H_6 protons of these two hexamers behave differently : the T_6 and $\dot{T}_6$ signals of dACATGT are separated by about 0.25 ppm whatever the temperature while those of dATGCAT practically coincide at 20°C as mentioned above.

Table I - Temperature effect on proton chemical shifts (in ppm from TMP) of 5 mM d(ACATGT) in neutral aqueous solution (0.1 N NaCl + 5 mM PO_4HNa_2, pH = 8.0).

	t°C	H_8/H_6	H_2/H_5 CH_3	H_1'	H_2'	H_2''	H_3'	H_4'	H_5'	H_5''
A	72°C	8.219	8.108	6.306	2.76	2.76	4.915	4.290	3.829	3.784
	20°C	8.218	7.822	6.248	2.71	2.71	4.930	4.283	3.771	3.763
	Δδ	0.001	0.286	0.058	0.05	0.05	-0.015	0.007	0.058	0.021
C	72°C	7.603	5.862	6.139	1.944	2.372	4.775	4.20		
	20°C	7.515	5.534	5.500	2.191	2.443	4.879	4.18	a)	a)
	Δδ	0.088	0.328	0.639	-0.247	-0.071	-0.104	0.02		
$\dot{A}$	72°C	8.303	8.170	6.348	2.79	2.680	4.976	4.391		
	20°C	8.369	7.999	6.319	2.68	2.961	5.063	4.465	a)	a)
	Δδ	-0.066	0.171	0.029	0.11	-0.281	-0.087	-0.074		
$\dot{T}$	72°C	7.380	1.708	6.061	2.025	2.351	4.797	4.20		
	20°C	7.167	1.508	5.812	1.940	2.324	4.879	4.21	a)	a)
	Δδ	0.213	0.200	0.249	0.085	0.027	-0.082	-0.01		
G	72°C	7.932		6.147	2.79	2.680	4.976	4.343		
	20°C	7.935		6.069	2.69	2.815	4.992	4.413	a)	a)
	Δδ	-0.003		0.078	0.10	-0.135	-0.016	0.070		
T	72°C	7.572	1.791	6.245	2.32	2.33	4.568	~4.13		
	20°C	7.424	1.588	6.229	2.28	2.28	4.569	~4.14	a)	a)
	Δδ	0.148	0.203	0.016	0.04	0.05	-0.001	0.01		

a) between 4.17 and 4.09 ppm

The important remark that can be made from an examination of the data in figure 2 and table I is that in the 20-72°C temperature interval several sugar protons exhibit chemical shift variations which are as large as, or even larger than those of the base protons. The sugar protons which are most sensitive to the temperature effect are $C_{1'}$, $C_{2'}$, $A_{2''}$, $\dot{T}_{1'}$ and $G_{2''}$ (Table I) ; particular attention is drawn to the $C_{1'}$ chemical shift variation ($\Delta\delta C_{1'}$ = 0.64 ppm between 20°C and 72°C) which is much larger than with other protons. It is worth noting that all the above mentioned protons belong to internal and central residues.

It is difficult to make at this time comparisons between the temperature effects on $H_{1'}$ proton chemical shifts between $\ddot{d}ACATGT$ and $\dot{d}\dot{A}TCGAT$, since the $\dot{d}\dot{A}TGCAT$ proton spectra have not been well resolved at 270 MHz and the $H_{1'}$ resonance assignment has only been a tentative [4]. Nevertheless, due to the similarity between chemical shift and temperature dependent behaviours for the $H_{1'}$ protons of these two compounds, we suggest that resonances n° 5, 6 [4] are assigned to the $A_{1'}$ and $\dot{A}_{1'}$ protons, the resonance n° 4 to the terminal thymidylyl $H_{1'}$ and the resonance n° 1 (or 2) to the $C_{1'}$ proton.

c) Proton-proton coupling constants

The 400 MHz ^{1}H-NMR spectra of $\ddot{d}ACATGT$ are well resolved at t > 62°C allowing most of the coupling constants between the sugar protons to be determined. The accuracy in the determination of the coupling constants was better that ±0.1 - 0.2 Hz for $J_{1'2'}$, $J_{1'2''}$, $J_{2'3'}$, $J_{2''3'}$ and ±0.2 - 0.3 Hz for $J_{3'4'}$. The $J_{4'5'}$ and $J_{4'5''}$ coupling constants of the initial residue, dAp, were measured with an accuracy better then ±0.1 Hz. The coupling constants involving the exocyclic protons, $J_{4'5'}$, $J_{4'5''}$, of the other residues were not determined specifically due to the poor separation between the $H_{4'}$, $H_{5'}$ and $H_{5''}$ resonances at 400 MHz. However, their magni-

tudes are estimated in the range of 2.2 - 3.5 Hz from the ^1H spectra at high temperatures ($t° > 65°C$).

Other than for the $C_{1'}$ proton, the $H_{1'}$ resonances are well resolved between 20°C and 72°C (Fig. 1) ; this allows the $J_{1'2'}$ and $J_{1'2''}$ coupling constants to be determined even at low temperatures. Figure 1a shows that apart from the $G_{1'}$ proton, which displays a triplet with $J_{1'2'} \approx J_{1'2''} \approx 7$ Hz at 22°C and a quadruplet with $J_{1'2'} = 7.9$ Hz, $J_{1'2''} = 6.2$ Hz at $t° > 42°C$, the coupling constants $J_{1'2'}$ and $J_{1'2''}$ of the other residues are practically insensitive to temperature effects. In table II, the proton-proton coupling constants of dACATGT at 62-68°C are reported.

The $J_{1'2'}$ values of the extreme residues Ap and pT are slightly smaller than those of the internal residues. Similar results have also been obtained for dATGT [15].

Table II - Coupling constants (in Hz) for d(ACATGT) in neutral aqueous solution at 62-68°C.

	S %	$J_{1'2'}$	$J_{1'2''}$	$J_{2'2''}$	$J_{2'3'}$	$J_{2''3'}$	$J_{3'4'}$	$J_{3'-P}$	$J_{4'5'}$	$J_{4'5''}$	$J_{5'5''}$	J_{5-6} J_{6-CH_3}
A	70	7.2	6.9	13.8	5.7	3.3	3.1	6.1	3.4	4.1	12.7	
C	76	8.1	5.7	13.9	6.2	2.8	2.5	5.8	a)	a)	b)	7.6
Ȧ	72	7.8	6.2	13.8	5.6	3.0	3.0	6.1	a)	a)	b)	
Ṫ	75	8.2	5.7	14.0	6.4	2.9	2.7	5.8	a)	a)	b)	1.3
G	72	7.9	6.2	13.8	5.9	3.0	3.0	6.0	a)	a)	b)	
T	64	7.0	7.0	13.9	6.4	4.2	4.0		a)	a)	b)	1.5

a) between 2.2 and 3.5 Hz

b) about 11.5 Hz

d) T_1 relaxation times

The longitudinal relaxation times of the dACATGT protons were determined versus temperature at two frequencies (90 and 250 MHz). Since the sugar proton resonances are not well resolved at these frequencies, only the T_1 relaxation times of the base protons can be measured with an accuracy better than ±5%.

We have observed for all dACATGT protons, a more or less strong cross-relaxation effects characterized by a slight deviation from the tangent at the origin of the magnetization decay curves as in the case of dATGT [15]. This is due to the fact that in the case of deoxynucleotides, CH_5,H_5" and CH_2,H_2" groups, which relax very quickly, contribute 80% of the average relaxation rate of all the protons in a given residue.

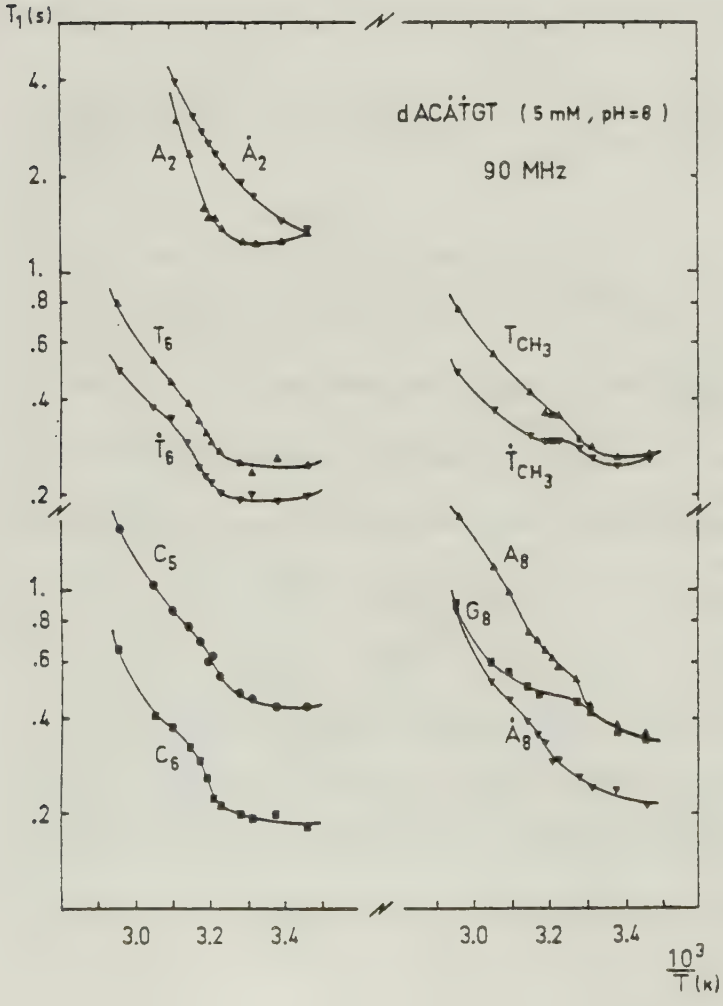

Figure 3

Temperature dependence of longitudinal relaxation times T_1 of dACATGT base protons measured at 90 MHz.

In figures 3 and 4, the initial relaxation times, T_1, measured at 90 and 250 MHz respectively are plotted versus temperature. At 90 MHz (Fig. 3), the T_1 values vary slightly between 16 and 37° and then increase quickly with the temperature for $t° > 37°C$. Most of the Log $T_1 = f(1/T°)$ curves (T_6 , $\dot{T}_6$, C_5 , C_6 , A_8 , $\dot{A}_8$) present a break point around $t° = 43°C$. At 250 MHz, the T_1 values vary slightly with temperature in the 22-65°C interval and most of the Log $T_1 = f(1/T°)$ curves show a minimum around 40°C indicating that $\omega\tau_c$ (apparent) is equal to unity. It is worth noting that for a given frequency, the Log $T_1 = f(1/T°)$ curves corresponding to the pyrimidine base protons, T_6 , $\dot{T}_6$, C_5 and C_6 very similar, while those of the purine base protons are different. The curve of the G_8 proton presents a particular aspect : the $T_1(G_8)$ and $T_1(\dot{A}_8)$ values are practically the same at high temperatures ($t° > 60°C$), while at low temperature, $T_1(G_8)$ is close to $T_1(A_8)$, the H_8 relaxation time of the initial residue ; this is true whatever the frequency (90 or 250 MHz).

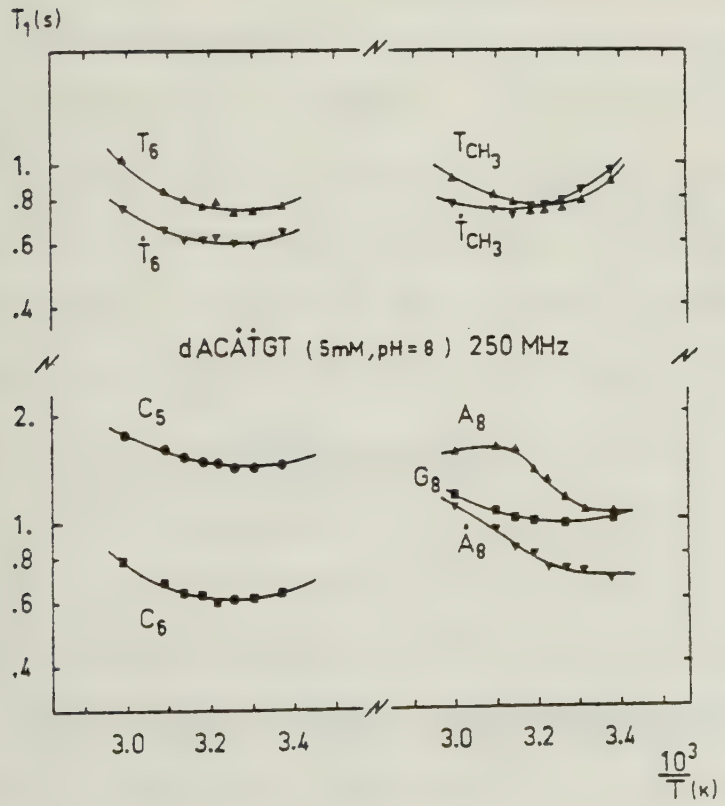

Figure 4

Temperature dependence of longitudinal relaxation times T_1 of dACȦTGT base protons measured at 250 MHz.

As far as the A_2 and $\dot{A}_2$ protons are concerned, their longitudinal relaxation times are much longer than those of the other protons and are complicated to interpret since they are essentially relaxed by the protons of the neighbouring residues. Therefore only the T_1 values at 90 MHz were obtained (Fig. 3).

C.II.2. Exchangeable protons

The imino exchangeable protons of dAC$\ddot{A}$TGT (4 mM dAC$\ddot{A}$TGT in H_2O + 0.2 M NaCl + 4 mM $PO_4^{=}$, pH = 8.0) were observed at 276 MHz (Fig. 5a). Three well separated NH resonances were observed at 5°C ; this demonstrates that dAC$\ddot{A}$TGT forms stable duplexes at low temperature. Resonances situated at 12.41 and 13.44 ppm were assigned to the NH protons of the GC and $\ddot{A}$T base pairs respectively, while the resonance at 13.03 ppm, much larger than other two and unobservable when t° > 15°C, was attributed to the extreme AT base pair, similar to the case of dA$\dot{T}$GC$\dot{A}$T [3, 7]. In figures 5b and 5c, the

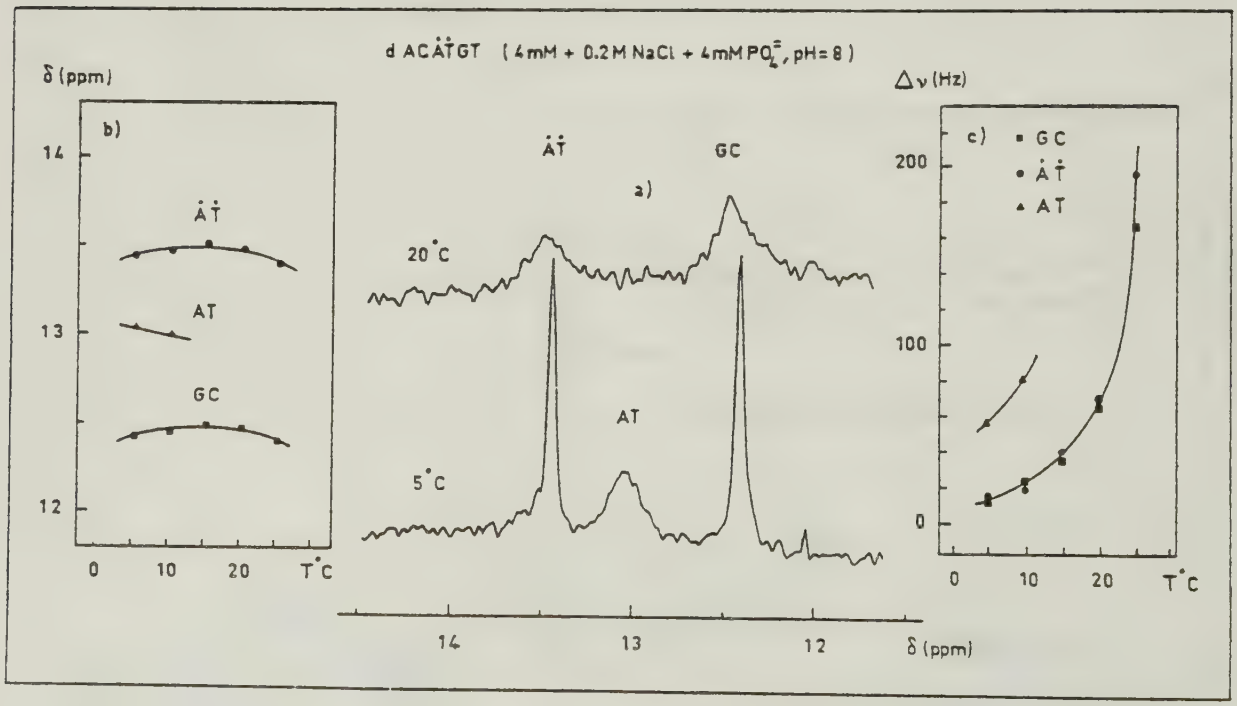

Fig. 5 - a) 276 MHz spectra of the imino-protons of dAC$\ddot{A}$TGT in H_2O at 5°C and 20°C. Temperature dependence of the imino-proton chemical shifts b) and linewidths c).

chemical shift and the line width of the imino protons are plotted versus temperatures between 5°C and 25°C. An important remark is that in this temperature interval the imino proton chemical shifts corresponding to the GC and $\dot{A}\dot{T}$ base pairs exhibit a small variation and the same temperature dependent behaviour. Similarly, the line broadenings of these protons are practically identical when the temperature is varied.

C.III. DISCUSSION

C.III.1. Fraying

Since the NH resonance of the extreme AT base pair broadens and disappears at $t° > 15°C$, while the NH resonances of the GC internal and $\dot{A}\dot{T}$ central base pairs shift slightly and broaden in a strictly similar way with increasing temperature and finally disappear for $t° > 25°C$ (Fig. 5), one can reasonably conclude that the fraying process consists of only two stages ; the two extreme AT base pairs open at first ; the GC internal and $\dot{A}\dot{T}$ central base pairs then open simultaneously at higher temperatures. This situation differs from that of dATGCAT where the chemical shift variations corresponding to the NH protons of the AT extreme and $\dot{A}\dot{T}$ internal base pairs are substantial ; the chemical shifts and linewidths of the individual base pairs change in a sequential order on raising the temperature [3, 7]. These results suggest that the GC base pair, involving three hydrogen bonds, constitutes the strongest fixation point in the above sequences and thus monitors the helix-coil opening process.

C.III.2. Transition midpoints

In principle, the midpoint transition temperature, $t°_{1/2}$, for each base pair can be determined from the $\delta = f(t°)$ curves since the magnetic environment of each proton is usually different for the coil and helix ; the observed chemical shifts depend therefore on the population of each form. This is valid only when there is no other process, such as the change in the

base conformation around the glycosidic bond which occurs independently with the helix-coil transition and induces additional proton shifts. In the case of purine nucleotides, it is well known that 2'- , 3'-GMP and 2'- , 3'-AMP exhibit a high proportion of the *syn* conformation [17, 18] while the conformations of the 5'-pyrimidine nucleotides are mostly *anti* and are not sensitive to the temperature effect. As a result, the $t^{\circ}_{1/2}$ value of the extreme AT residues was calculated from the $\delta = f(t^{\circ})$ curves of the T_6 and T_{CH_3} protons : $t^{\circ}_{1/2}(AT) = 32 \pm 2^{\circ}C$. The transition temperatures determined from the base and sugar protons ($\dot{A}_2$, $\dot{A}_8$, T_{CH_3} , $\dot{T}_6$, $\dot{A}_{2''}$ for $\dot{\dot{A}}\dot{T}$ and C_5 , C_6 , $C_{1'}$, $C_{2'}$, $C_{2''}$ for GC) were found to be practically the same for the $\dot{\dot{A}}\dot{T}$ and GC base pairs : $t^{\circ}_{1/2}$ ($\dot{\dot{A}}\dot{T}$ and GC) = 43 ± 3°C. This result confirms the conclusion concerning the fraying process of $dA\dot{\dot{C}}\dot{\dot{A}}TGT$ deduced from the temperature dependence of the NH linewidths according to which the GC and $\dot{\dot{A}}\dot{T}$ base pairs open simultaneously. In the case of $d\dot{A}T\dot{G}C\dot{A}T$ [4], the average $t^{\circ}_{1/2}$ value determined from the proton chemical shift vs temperature plots if about 34°C for the AT extreme residues and between 40°C and 45°C for the internal and central base pairs in good agreement with the above values.

C.III.3. Helix-coil dissociation constant and enthalpy

The dissociation constant, K_d , can also be determined from the $\delta = f(t^{\circ})$ curves relative to the base and sugar protons of the internal residues ($\dot{\dot{A}}\dot{T}$ and GC) which monitor the helix-coil dissociation. The fact that the proton line widths constantly decrease with increasing temperatures from 20°C to 72°C (Figs 1a, b, c) and all the resonances display an average signal indicates a rapid exchange between the helix and coil forms. The observed chemical shift, δ_{obs} , reflects therefore the relative variation of the helix and coil populations and is given by :

$$\delta_{obs} = \alpha\delta_c + \left[\frac{1 - \alpha}{2}\right] 2\delta_H \qquad (1)$$

where α is the coil proportion, δ_c and δ_H are the chemical shifts corresponding to the coil and helix forms respectively ; δ_c can be obtained at $t° > 70°C$ and δ_H at $t° \simeq 20°C$.

The coil proportion, α, was calculated as a function of temperature from the $\delta = f(t°)$ curve of the $\dot{T}_{1'}$ and $C_{1'}$ protons. The calculations were based on the following assumptions : i) The GC and $\dot{\dot{A}}\dot{\dot{T}}$ base pairs open simultaneously and hence both monitor the helix-coil dissociation ; ii) The *anti* conformation is favoured for the 5'-phosphate pyrimidine nucleotides and the base rotation around the glycosidic bond is difficult for the case of pyrimidine nucleotides ; iii) Both the $\dot{T}_{1'}$ and $C_{1'}$ protons are located far from the phosphate groups, their chemical shifts not therefore being sensitive to the change in conformation around the phosphodiester bonds. Table III summarizes the coil proportion, α, calculated from the $\delta(C_{1'})$ and $\delta(\dot{T}_{1'}) = f(t°)$ curves for various temperatures between 20°C and 72°C. It is worth noting that the same average α values were also found from the $\delta = f(t°)$ curves relative to the C_5 , $C_{1'}$, $\dot{T}_6$, $\dot{T}_{1'}$ and $\dot{T}_{CH_3}$ protons.

Table III - α proportion of the coil form of dAC$\dot{\dot{A}}\dot{\dot{T}}$GT at different temperatures calculated from the $C_{1'}$ and $\dot{T}_{1'}$ proton chemical shift variations versus temperature.

T°	26°C	35°C	42°C	45°C	51°C	56°C	62°C
α	0.10	0.27	0.52	0.55	0.69	0.82	0.93

Figure 6 shows the semi-Log plot of the dissociation constant, K_d , versus temperature ($K_d = (2\alpha^2 C)/(1-\alpha)$ with C = 5 mM of dACATGT). A straight line was obtained for the Log $K_d = f(1/T°)$ curve indicating that apart from the helix-coil dissociation, no other mechanism occurs having an influence on the chemical shift variations of the above protons. A dissociation enthalpy of 36 kcal/mole was found for dACATGT in good agreement with the values obtained for dATGCAT (34 kcal/mole, ref. 4) and for rCCGC (33 kcal/mole, ref. 1).

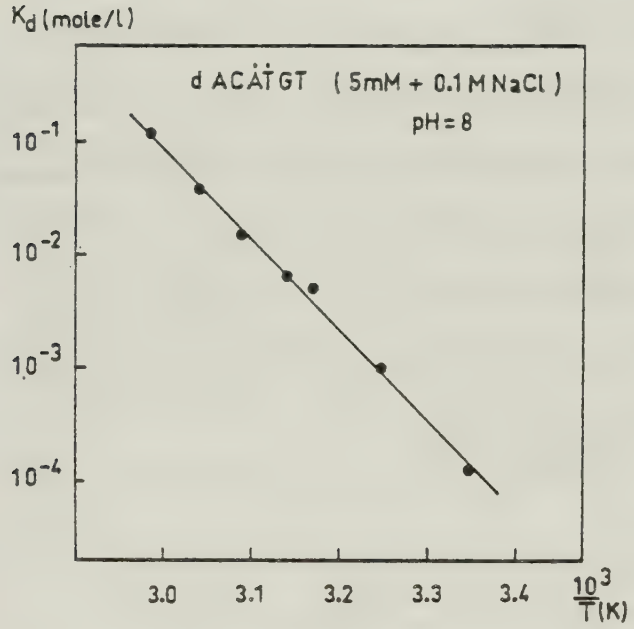

Figure 6

Semi-Log plot of the dissociation constant K_d versus reciprocal absolute temperature as derived from the proton chemical shift data.

In our opinion, the present method based on the temperature dependence of the observed chemical shifts is very simple and convenient to determine the dissociation enthalpy. It also permits us to know from the linearity of the Log $K_d = f(1/T°)$ plot if any other mechanism is occuring independently of the helix-coil dissociation. On the other hand, the method, using the expression of Gralla and Crothers [19] :

$$\Delta H = \frac{-4.37}{(1/T_{1/2} - 1/T_{3/4})}$$

where $T_{1/2}$ and $T_{3/4}$ are the maximum and the upper half height of the melting curve, $\partial\alpha/\partial T = f(T°K)$, and the other method, based on the variation of the midpoint temperature versus oligonucleotide strand concentration [1], seem to be a little more complicated.

C.III.4. Conformation of dACATGT

The insignificant temperature effect on proton-proton coupling constants involving sugar ring protons shows that the average sugar conformation of the dACATGT residues remains practically unchanged when this hexamer changes from the coil to the helix form on lowering the temperature. The high value of $J_{1'2'}$ compared to that of $J_{3'4'}$ (Table II) indicates a strong predominance of the S (2' endo, 3' exo) conformation for the sugar ring. Examination of the data in table II also reveals a slight difference in the average conformation between the extreme and internal residues : the S proportion is smaller for the AT extreme residues than for the other residues similar to the case of dATGT [15].

As far as the helical conformation is concerned, it has been shown in the case of rAAGCUU, a ribonucleotide [2], that the $J_{1'2'}$ values of all six residues are small (< 1.5 Hz) at low temperatures indicating a clear preference for the N conformation ($C_{3'}$ endo, $C_{2'}$ exo). The G_8 proton chemical shift depends strongly on temperature ; its variation, $\Delta\delta G_8$, is about 0.6 ppm on going from 10 to 80°C. These characteristics have been ascribed to the A family of conformations. In contrast to ribonucleotide duplexes, all the six residues of dACATGT adopt the S conformation most of the time and the chemical shift changes only slightly with temperatures between 20°C and 72°C (Fig. 2). These results suggest that dACATGT duplexes adopt the B helical conformation as in the case of other deoxyoligonucleotides such as dATGCAT [8], $dCG(CG)_n$ [5], dCCGG and dGGCC [6].

An important question to be considered is why the C_1, proton resonance is particularly broad between 20°C and 42°C but becomes as narrow as the other H_1, resonances at higher temperatures (Fig. 1a). The hypothesis for a possible presence of paramagnetic ions can be excluded since special precautions (EDTA, Chelex 100) were taken to eliminate these ions in the sample solution. In addition, di- or trivalent ions usually bind to the phosphate groups and bases but not to the carbon 1' of the sugar ring. The additional line width of the C_1, proton observed only at temperatures lower that $t^{\circ}_{1/2}$ (≈ 43°C) strongly suggests that this phenomena is directly connected to the helix formation. In fact, it can be seen from the molecular model for the right handed Watson-Crick B-DNA helices with the *anti* orientation for the bases that : i) the carbonyl group $C_2 = O$ of the cytidine base is located above the H_1, proton of the same residue ; ii) only in the case of the GC base pair, which involves three hydrogen bonds instead of two for the AT base pair, the H_1, proton is close to the hydrogen bond involving the oxygen atom of the cytidine $C = O$ and the hydrogen atom of the guanine NH_2 group. Therefore, the observed chemical shift of the C_1, proton was found to be strongly influenced by the helix-coil dissociation and to reflect the relative proportion of both forms. In principle, the helix-coil exchange rate can be calculated from the C_1, linewidths measured at two frequencies. Unfortunately, for frequencies lower than 400 MHz, the overlapping between the C_5 and C_1, resonances does not enable the C_1, linewidth to be accurately determined.

In the case of dATGT, temperature and concentration greatly influence the chemical shift for the H_2, but not for the H_2,, protons [15]. For example the H_2, protons of dA and dT residues exhibit a chemical shift variation of 0.16 ppm and 0.13 ppm respectively on going from 18 to 65°C. This large δ variation relative to the H_2, protons of single stranded dATGT has been attributed to the modification of the base conformation around the glycosidic bond. In the case of dACATGT, the H_2,, protons of the internal purine residues

($\dot{A}_{2"}$ and $G_{2"}$) also exhibit large variations in chemical shift between 20°C and 72°C. At low temperature, the $\dot{A}_{2"}$ resonance is located at lower fields and is well separated from the other $H_{2"}$ and $H_{2'}$ purine protons ; the same is true for the $A_{3'}$ resonance (Figs 1b, c). However, above 65°C, $\dot{A}_{2"}$ and $G_{2"}$ on the one hand and $\dot{A}_{3'}$ and $G_{3'}$ on the other hand are found to be magnetically equivalent indicating the same environment for these protons in the coil state. In general, the chemical shift variation observed for the $H_{2"}$, $H_{3'}$ and $H_{4'}$ protons of the purine residues in dA$\dot{C}\dot{A}$TGT between 20°C and 72°C decreases from the central to the extreme residues, i.e. $\Delta\delta\dot{A}_2 > \Delta\delta_{G2"} > \Delta\delta G_{2"}$ etc ... (Table I). This behaviour suggests that : i) The chemical shift variations of these protons reflect the changes in the phosphodiester angles and hence in the relative position between the sugar of the 3'-phosphate purine residue and the pyrimidine base of the 5'-phosphate adjacent residue ; ii) The distorsion is maximum for the central and minimum for the extreme residues.

C.III.5 Dynamic structure of dA$\dot{C}\dot{A}$TGT

In the case of ribonucleotides and their derivatives, T_1 proton relaxation time measurement is an efficient method to investigate the base conformation around the glycosidic bond since the relaxation of the sugar protons, $H_{1'}$, $H_{2'}$, $H_{3'}$, is sensitive to the base orientation [20, 21]. In contrast, for 2'-deoxyribonucleotides, the influence of the base proton (H_8 or H_6) on the sugar proton relaxation rate is slight because of the presence of $H_{2"}$ and its proximity to the other sugar ring protons. Nevertheless, comparisons of the base proton T_1 for the residues of the same family can reveal differences in conformation and mobility.

It follows from the results in figures 3 and 4 that whatever the frequency and temperature, the T_1 values of the A_8 and T_6 protons are always longer for the extreme than for the internal residues, in particular $T_1(A_8)$ is about twice $T_1(\dot{A}_8)$. This difference in T_1 may be due to a difference in

conformation (via the $\sum_j r_{ij}^{-6}$ term) or mobility. This ambiguity can be removed using the T_1 ratio, $T_1(90)/T_1(250)$ versus temperature for different protons (Table IV). The results in Table IV show that the T_1 ratio of the T_6 and $\dot{T}_6$ protons is practically the same at any given temperatures between 22°C and 60°C indicating the same mobility for both thymine bases. For the adenine bases, the mobility of the initial and internal bases is found to be the same for t < 45°C but above this temperature, the initial base, dAp, appears to undergo a more rapid local motion than the internal base as the T_1 ratio of the A_8 proton tends to unity more quickly than the other protons for t° > 45°.

Table IV - Ratios of base proton longitudinal relaxation times measured at 90 and 250 MHz between 22°C and 60°C.

T°	A_8	C_5	C_6	$\dot{A}_8$	$\dot{T}_6$	$\dot{T}_{CH_3}$	G_8	T_6	T_{CH_3}	$\overline{T_1(90)/T_1(250)}$ [a]
22°C	0.34	0.29	0.29	0.33	0.26	0.26	0.35	0.30	0.27	0.30 ± 0.03
29°C	0.39	0.32	0.31	0.33	0.33	0.32	0.30	0.31	0.39	0.34 ± 0.03
37°C	0.43	0.36	0.35	0.40	0.31	0.41	b)	0.34	0.54	0.37 ± 0.04
40°C	0.46	0.41	0.41	0.41	0.37	0.41	0.44	0.40	0.50	0.41 ± 0.03
45°C	0.44	0.49	0.49	0.47	0.48	0.43	0.47	0.46	0.54	0.47 ± 0.03
50°C	0.62	0.52	0.53	0.47	0.52	0.47	0.53	0.49	0.57	0.51 ± 0.05
60°C	0.78	0.67	0.63	0.67	0.57	0.57	0.61	0.57	0.71	0.64 ± 0.05

a) Mean value over all the base protons except for T_{CH_3} above 37°C and A_8 shows 50°C
b) At this temperature, the G_8 signal collapses with the A_2 signal.

From the above discussion we can assign the difference in the longitudinal relaxation times of the base protons between extreme and internal residues to the difference in conformation (or environment). This is not surprising since the base protons of the internal residues can also be

relaxed by the neighbouring residue protons as it has been shown for the case of dinucleoside monophosphates [21-23]. Therefore the difference in T_1 values of the base protons for the residues of the same family can be considered as a good criterion for proton resonance assignement. The small T_1 ratio between the thymine H_6 protons, $T_1(T_6)/T_1(\dot{T}_6)$ compared with $T_1(A_8)/T_1(\dot{A}_8)$ can be explained by the fact that the thymine H_6 proton which is relaxed by sugar protons and essentially by the CH_3 group of the same base is less sensitive to dipolar interactions from the protons of the neighbouring residues.

In general, the T_1 ratios, $T_1(90)/T_1(250)$, of the dAC$\ddot{A}$TGT base protons are practically the same (within 10%) at a given temperature (Table IV) showing that the base mobility does not vary very much between residues. It is to be noted, however, that the T_1 ratios are slightly higher for the purine than for the pyrimidine protons except for the methyl group of the terminal thymidylyl residue, whose T_1 ratio is also slightly higher than the average value at $t° > 37°C$.

It has already been shown that for intermediate temperatures an equilibrium exists between the coil and helix forms of dAC$\ddot{A}$TGT with a $t°_{1/2}$ of about 43°C. Therefore the T_1 value versus temperature is expected to reflect this situation. At 250 MHz, owing to the fact that $\omega\tau_c$ (apparent) is close to unity (Fig. 4), the T_1 values measured at this frequency were found to change slightly with temperature. However at 90 MHz, most of the Log T_1 = f(1/T°) curves (Fig. 3) present a break point at 43°C, i.e. equal to the $t°_{1/2}$ value for the helix-coil transition and exhibit shapes very different to those obtained with single species in solution. For example, in the case of dA$\dot{T}$GT [15], poly I [24] and poly U [25], the Log T_1 = f(1/T°) curves manifest a regular decrease with decreasing temperature.

Under fast exchange conditions, the observed T_1 can be expressed as follows :

$$\frac{1}{T_{1obs}} = \frac{\alpha}{T_{1C}} + \frac{1 - \alpha}{T_{1H}} \qquad (2)$$

where α is the coil proportion, T_{1C} and T_{1H} are the longitudinal relaxation times of the coil and helix forms respectively.

Assuming in the case of the coil state that : i) the base conformation ($\sum_j r_{ij}^{-6}$) remains unchanged with temperature ; ii) the motions of the internuclear vectors depend on a single correlation time, the proton T_1 relaxation time is given by :

$$\frac{1}{T_{1C}} = \frac{3}{10} \gamma^4 . \hbar^2 . \sum_j r_{ij}^{-6} f(\tau_c) \qquad (3)$$

where

$$f(\tau_c) = \frac{\tau_c}{1 + \omega^2 \tau_c^2} + \frac{4\tau_c}{1 + 4\omega^2 \tau_c^2}$$

The above assumptions were found to be verified in the case of single stranded oligo- [15] and polynucleotides [24, 25].

At high temperatures ($t° > 65°C$), since only the coil form exists, its average correlation time τ_c can thus be determined from the T_1 ratios, $T_1(90)/T_1(250)$ of the base protons (τ_c = 0.2 nsec at 65°C), this in turn allows the sum $\sum_j r_{ij}^{-6}$ to be calculated for each proton. For intermediate temperatures, the T_{1C} value of each base proton can be calculated by assuming an activation energy of about 4 kcal/mole for the local motion of the coil.

Using the coil proportions, α, in table III and the T_{1obs} values given in figure 4, the T_1 relaxation times, T_{1H}, and the correlation times $\tau_c(H)$ corresponding to the helix form at various temperatures can be determined by assuming to a first approximation that assumptions i) and ii) remain valid for the helix state. Data processing was carried out on relaxation time data for the internal residue proton (Fig. 4) with an exception

for G_8 , whose Log $T_1 = f(1/T°)$ curve seems to indicate a change in environment (or in conformation) independent of the helix-coil transition.

In figure 7, Log $\tau_c(H)$ versus the reciprocal absolute temperature data are represented. The points obtained are grouped in two straight lines : the first one with a slope corresponding to ΔE = 7 kcal/mole and the second corresponding to ΔE = 9 kcal/mole were obtained for the purine and pyrimidine base protons respectively. The discrepancy between the ΔE values seems to be due to the fact that the model involving a single correlation time for all residues is not well suited for the helix form. The mobilities appear to be different for the purine and pyrimidine base as revealed by a systematical slight difference in the T_1 ratios in Table IV. The greater base-sugar flexibility of the purine (higher T_1 ratios and smaller ΔE) compared with pyrimidine compounds is well known for steric considerations.

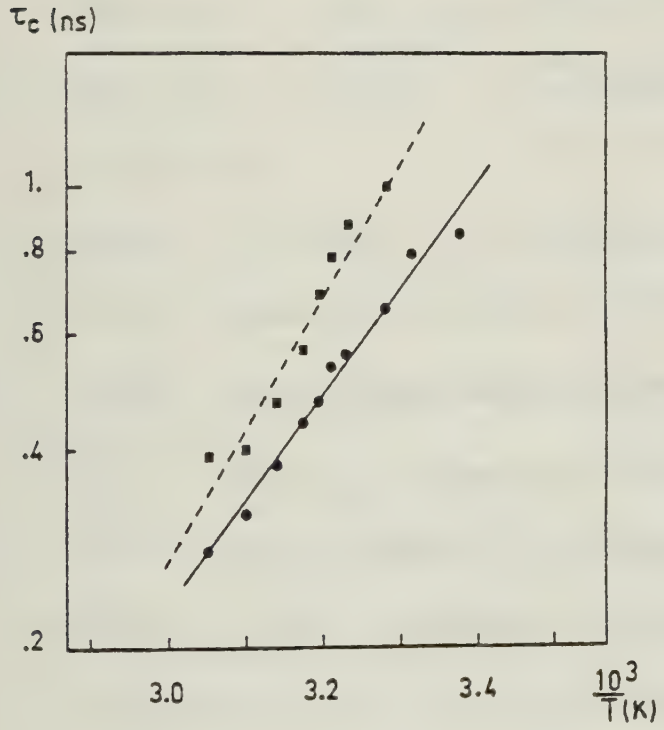

Figure 7

Semi-Log plot of the correlation times τ_c versus reciprocal absolute temperature as derived from the T_1 proton relaxation data : purine base proton $\dot{A}_8$ (——) ; pyrimidine base protons C_5 , C_6 , $\dot{T}_6$ (---).

The τ_c value of the helix form can also be evaluated directly from the T_1 ratio at 22°C since the coil proportion is negligible at this temperature. A $\tau_c(H)$ value of about 1 nsec was obtained, in agreement with that deduced for the purine protons but smaller than that deduced for the

pyrimidine protons (1.4 nsec) (Fig. 7). This appears to indicate that the anisotropic character is more dominant for the pyrimidine family.

ACKNOWLEDGMENT

We wish to thank Prof. Guéron (Ecole Polytechnique, Palaiseau, France) for the use of his 276 MHz high resolution spectrometer and Drs Plateau and Sigueroa for their help in obtaining the exchangeable proton spectra.

REFERENCES

1. ARTER, D.B., WALKER, G.C., UHLENBECK, O.C. and SCHMIDT, P.G. (1974) Biochem. Biophys. Res. Commun. 61, 1089.
2. BORER, P.N., KAN, L.S. and TS'O, P.O.P. (1975) Biochemistry 14, 4847.
3. PATEL, D.J. (1974) Biochemistry 13, 2396.
4. PATEL, D.J. (1975) Biochemistry 14, 3984.
5. PATEL, D.J. (1976) Biochemistry 15, 533.
6. PATEL, D.J. (1977) Biopolymers 16, 1635.
7. PATEL, D.J. and HILBERS, C.W. (1975) Biochemistry 14, 2651.
8. PATEL, D.J. and TONELLI, A.E. (1975) Biochemistry 14, 3990.
9. HILBERS, C.W. and PATEL, D.J. (1975) Biochemistry 14, 2656.
10. EARLY, T.A. and KEARNS, D.R. (1980) Nucl. Acids Res. 8, 5795.
11. MILLER, P.S., CHENG, D.M., DREON, N., JAYARAMAN, K., KAN, L.S., LEUTZINGER, E.E., PULFORD, S.M. and TS'O, P.O.P. (1980) Biochemistry 19, 4688.
12. PHILLIPS, D.R. and ROBERTS, G.C.K. (1980) Biochemistry 19, 4795.
13. Van BOOM, J.H., BURGERS, P.M.J., Van der MAREL, G., VERDEGAAL, C.H.M. and WILLE, G. (1977) Nucl. Acids Res. 4, 1047.

14. TRAN-DINH, S., NEUMANN, J.M., HUYNH-DINH, T., IGOLEN, J. and KAN, S.K. (1982) Org. Mag. Res. 18, 148.

15. NEUMANN, J.M., HUYNH-DINH, T., KAN, S.K., GENISSEL, B., IGOLEN, J. and TRAN-DINH, S. (1982) Eur. J. Biochem. 121, 317.

16. MILLER, P.S., FANG, K.N., KONDO, N.S. and TS'O, P.O.P. (1971) J. Am. Chem. Soc. 93, 6657.

17. TRAN-DINH, S., GUSCHLBAUER, W. and GUERON, M. (1972) J. Am. Chem. Soc. 94, 7903.

18. GUERON, M., CHACHATY, C. and TRAN-DINH, S. (1973) Ann. N.Y. Acad. Sci. 222, 297.

19. GRALLA, J. and CROTHERS, D.M. (1973) J. Mol. Biol. 78, 301.

20. NEUMANN, J.M., BORREL, J., THIERY, J.M., GUSCHLBAUER, W. and TRAN-DINH, S. (1977) Biochem. Biophys. Acta 479, 427.

21. TRAN-DINH, S., NEUMANN, J.M. and BORREL, J. (1981) Biochem. Biophys. Acta 655, 167.

22. CHACHATY, C., YOKONO, T., TRAN-DINH, S. and GUSCHLBAUER, W. (1977) Biophys. Chem. 6, 151.

23. NEUMANN, J.M., GUSCHLBAUER, W. and TRAN-DINH, S. (1979) Eur. J. Biochem. 100, 141.

24. NEUMANN, J.M. and TRAN-DINH, S. (1981) Biopolymers 20, 89.

25. NEUMANN, J.M. and TRAN-DINH, S. (1982) Biopolymers 21, 383.

CHAPITRE IV

ÉTUDE DE LA CONFORMATION ET DE LA STRUCTURE DYNAMIQUE DES POLYNUCLÉOTIDES EN SOLUTION

Ce chapitre regroupe deux articles consacrés à l'étude de la conformation et de la structure dynamique des homopolynucléotides.

Le premier "Conformation and dynamic structure of Poly I in neutral aqueous solution by ^{1}H, ^{2}H, ^{13}C and ^{31}P NMR spectroscopy, Neumann, J.M. and Tran-Dinh, S. (1981) Biopolymers 20, 89" relate l'étude de Poly I par résonance et relaxation des protons à deux fréquences (250 et 90 MHz) et celles du ^{31}P (111,6 et 36,4 MHz), du ^{13}C (75,4 MHz) et du ^{2}H (13,8 MHz).

Le second article "^{1}H-NMR comparative studies of polynucleotides : conformation and dynamic structure of Poly U and Poly C in neutral solution, Neumann, J.M. and Tran-Dinh, S. (1982) Biopolymers 21, 383" est consacré à l'étude comparée de Poly U et Poly C par RMN-^{1}H à 250 et 90 MHz. La conformation et la mobilité des résidus dans les polynucléotides font l'objet d'une discussion à la fin de cet article.

A. CONFORMATION AND DYNAMIC STRUCTURE OF POLY I IN NEUTRAL AQUEOUS SOLUTION BY ^{1}H, ^{2}H, ^{13}C AND ^{31}P NMR SPECTROSCOPY

NEUMANN, J.M. and TRAN-DINH, S.

Biopolymers 20, 89.

It is well known that polynucleotide structures depend closely on experimental conditions : pH, salt concentration, temperature [1-5] and these polymers therefore provide interesting models for the structure study of nucleic acids. Among the homopolynucleotides containing a single naturally occurring purine or pyrimidine base, poly inosinic acid (poly I) behaves in a particular way. In neutral saline solution it can associate not only with poly C but also with poly A to form a two-stranded or three-stranded complex : poly I.poly C, poly A.poly I, polyA.2 poly I [2-4]. Depending on the case therefore poly I behaves as poly G or poly U. At room temperature and in neutral solution with a low salt concentration, poly I shows hydrodynamic properties characteristic of a random coil.

Although some polynucleotides in solution have been the subject of recent NMR studies [6-14] the conformation and dynamic structure of poly I are still unknown. Moreover most of this work was carried out by ^{1}H- and ^{31}P-NMR [8-12] and little use has been made of ^{13}C-NMR spectroscopy [6, 7].

There is no doubt that ^{1}H-NMR is a popular method for the study of biological systems nor that ^{31}P-NMR can provide direct information about the phosphodiester linkage. In the case of polynucleotides, interesting dynamic information has been obtained from ^{1}H and ^{31}P relaxation measurements at given frequency [8-10]. However owing to the difficulty of inter-

pretation of ^{1}H and ^{31}P data (see sections A.I and A.II) some hypotheses must be advanced : for example with ^{1}H relaxation data at a fixed frequency it is impossible to know whether or not the segmental motions of the sugar and of the base are different ; for greater ease of interpretation it must be assumed that the molecular motion is isotropic, i.e. the correlation time τ_c is common for all protons, and that the sums $\sum r_{H-H}^{-6}$ and $\sum r_{P-H}^{-6}$ are constant and hence the molecular conformation does not change with temperature [3-10]. These hypotheses have not been verified experimentally. It is therefore very useful not only to study other nuclei but also to determine relaxation parameters at different frequencies and temperatures in order to give a more quantitative interpretation.

In the present work the conformation and dynamic structure of poly I were investigated by ^{1}H, ^{2}H, ^{13}C and ^{31}P relaxation measurements carried out as a function of temperature. The ^{1}H relaxation experiments were performed at 90 MHz and 250 MHz, and the ^{31}P experiments at 36.4 and 111.6 MHz. A brief discussion on different methods of analysis of ^{1}H, ^{13}C- and ^{31}P- relaxation data and their applications to the study of the poly I structure is given in section A.II.

A.I. THEORETICAL BACKGROUND

To facilitate the discussion on the data presented here we would like to recall some fundamental results relative to the relaxation theory given in numerous papers, books and reviews [15-21]. This section will concerned spin 1/2 and spin 1 systems.

A.I.1. Spins 1/2 relaxation

Consider a system of two dipolar-coupled spins I and S, separated by a constant distance r_{IS}. The equation for the longitudinal magnetization $\langle I_z \rangle$ is :

$$\frac{d}{dt}\langle I_z\rangle = -\rho_{IS}\,(\langle I_z\rangle - I_o) - \sigma_{IS}\,(\langle S_z\rangle - S_o) \tag{1}$$

$$\rho_{IS} = K^2\,[J_o(\omega_I - \omega_S) + 3J_1(\omega_I) + 6J_2(\omega_I - \omega_S)]r_{IS}^{-6} \tag{1a}$$

$$\sigma_{IS} = K^2\,[6J_2(\omega_I + \omega_S) - J_o(\omega_I - \omega_S)]r_{IS}^{-6} \tag{1b}$$

$$K^2 = \frac{(\gamma_I\gamma_S\hbar)^2}{10} \tag{1c}$$

$J_m(\omega)$ refers to the spectral density functions. In the simplest case where the rotational reorientation of the internuclear IS vector is isotropic, characterized by a correlation time τ_c , $J_m(\omega)$ is given by

$$J_m(\omega) = \frac{\tau_c}{1 + \omega^2\tau_c^2} \tag{2}$$

A similar equation may be written for $\langle S_z\rangle$ by permuting I and S in equation (1).

In the presence of other relaxation mechanisms than the dipolar interaction and assuming the absence of cross-correlation between these processes, ρ_{IS} is replaced by :

$$\rho_I = \rho_{IS} + \rho_I^o \tag{3}$$

where ρ_{IS} is the dipolar relaxation term given by equation (1a) and ρ_I^o the contribution from other mechanisms.

If we now introduce a strong rf field at the resonance frequency ω_S so that $\langle S_z\rangle = 0$, at the steady state the magnetization of I is enhanced by :

$$\eta = \frac{\langle I_z\rangle - I_o}{I_o} = \frac{\gamma_S}{\gamma_I}\cdot\frac{\sigma_{IS}}{\rho_{IS}} \tag{4a}$$

In the present paper this is the case for ^{13}C and ^{31}P observation under proton noise decoupling (I = ^{13}C, ^{31}P ; S = ^{1}H).

If the relaxation is not purely dipolar

$$\eta = \frac{\gamma_S}{\gamma_I} \frac{\sigma_{IS}}{\rho_{IS} + \rho_I^o} \tag{4b}$$

The return to equilibrium of longitudinal magnetization $\langle I_z(t) \rangle$, after a 180° pulse (inversion recovery method) with $\langle S_z \rangle = 0$, is a single exponential function with a time constant $1/T_1$ given by

$$\frac{1}{T_1} = \rho_{IS} \tag{5a}$$

in the case of pure dipolar relaxation. On the other hand if I is relaxed by other mechanisms such as chemical shift anisotropy, for instance I = ^{31}P :

$$\frac{1}{T_1} = \rho_{IS} + \rho_I^o \tag{5b}$$

If the spins I and S are of the same species but non-equivalent (case of ^1H) : $I_o = S_o$, $\omega_I = \omega_S = \omega$, the initial recovery rate $1/T_1$ can be obtained from the slope at the origin of the $\log(\langle I_z(t) \rangle - I_o) = f(t)$ curve after a 180° pulse

$$\frac{1}{T_1} = \rho_{IS} + \sigma_{IS} \tag{6a}$$

$$\frac{1}{T_1} = 3\ K^2\ [J_1(\omega) + 4J_2(2\omega)] \tag{6b}$$

In the case where the molecular motion is anisotropic equations (1), (1a), (1b) are still valid but the spectral densities $J_m(\omega)$ depend on the dynamic model ; some have been given elsewhere [16, 19-25].

A.I.2. Spin 1 relaxation

For the relaxation mechanism of spin > 1/2, the most important factor is the interaction between electric fields and the quadrupole moment of nuclei. For S = 1 (case of ^2H in the present work) assuming that the asymmetry parameter is zero the relaxation rates $1/T_1$ and $1/T_2$ can be expressed by :

$$\frac{1}{T_1} = \frac{3}{80} \left(\frac{e^2qQ}{\hbar}\right)^2 [J_1(\omega) + 4J_2(2\omega)] \qquad (7)$$

$$\frac{1}{T_2} = \frac{3}{160} \left(\frac{e^2qQ}{\hbar}\right)^2 [3J_o(o) + 5J_1(\omega) + 2J_2(2\omega)] \qquad (8)$$

where $e^2qQ/\hbar$ is the deuterium quadrupolar coupling constant. Under extreme narrowing conditions

$$\Delta\nu_{1/2} = \frac{1}{\pi T_2} = \frac{1}{\pi T_1} \qquad (9)$$

where $\Delta\nu_{1/2}$ is the width at half height of the deuterium peak.

A.II. APPLICATIONS TO THE DYNAMIC STRUCTURAL STUDY OF POLY I

Each poly I residue contains eight non-exchangeable protons directly bonded with seven carbon atoms : two on the base (C_2, C_8) and five on the ribose ($C_{1'}$, $C_{2'}$, $C_{3'}$, $C_{4'}$, C_5). It is therefore useful to study the relaxation of these two nuclei simultaneously. The results obtained will yield important information about the molecular motion of the ribose and the base. For the phosphodiester backbone a ^{31}P relaxation study is certainly necessary Some particular applications for each nucleus ^{13}C, ^1H, ^{31}P, ^2H together with their respective advantages and disadvantages are presented briefly here.

A.II.1. ^{13}C relaxation

The ^{13}C spin-lattice relaxation time measurements have been considered as a standard method to study molecular motion in liquid solution. In many cases the relaxation of protonated carbons is governed by dipolar interaction with protons directly bonded to the carbon observed ; the chemical shift anisotropy and spin rotation contributions are negligible in macromolecules at present field strengths. However with the concentrations normally used (< 0.1 M in monomer unit) a T_1 experiment takes too much instrument time. In addition, even in the case of an isotropic motion, one T_1 measurement is certainly not enough to determine the correlation time of macromolecules because of the non unequivocal correspondence between T_1 and τ_c. An alternative practice is to measure the $^{13}C-\{^1H\}$NOE by the gate decoupling method.

The expression for $^{13}C-\{^1H\}$NOE can be obtained by replacing $\omega_I = \omega_C$, $\omega_S = \omega_H$ and $\gamma_H/\gamma_C = 3.98$ in equations (1a), (1b) and (4a). As in the case of T_1 , the ^{13}C-NOE measurements show whether the molecular motion is isotropic : in this case all the NOE values for protonated carbons are the same as it has been observed for poly I in aqueous solution at neutral pH (see below). Thus the reorientation motion of the C-H vectors as a whole can be described by mean of a single correlation time τ_c. The corresponding spectral densities $J_m(\omega)$ are now represented by equation (2). Figure 1 shows the plot of $^{13}C-\{^1H\}$NOE values vs τ_c at 75.4 MHz. At this frequency

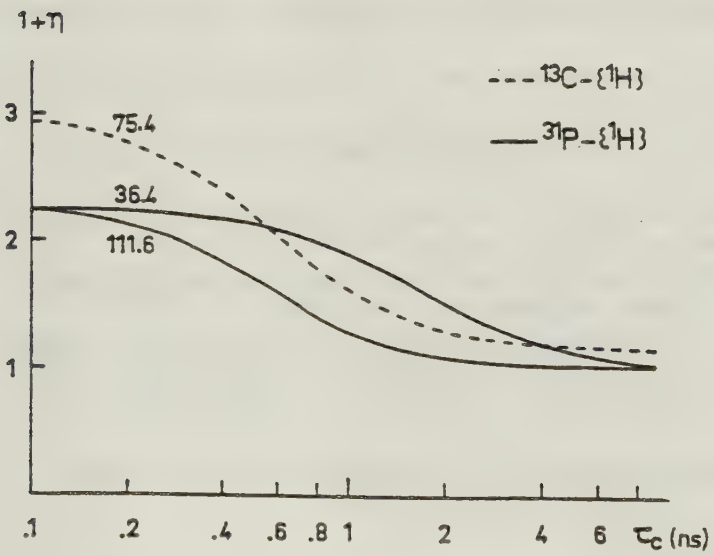

Fig. 1 - Semi-log plot of ^{31}P (36.4 and 111.6 MHz) and ^{13}C (75.4 MHz) NOE upon non-selective proton saturation versus correlation time τ_c (solid and dashed curves respectively).

the ^{13}C-NOE is sensitive to τ_c variations in the time interval between 0.2 and 2 nsec.

A.II.2. ^{1}H relaxation

In the absence of paramagnetic ions the proton relaxation mechanism is essentially governed by dipolar interaction. Unlike ^{13}C, the proton relaxation depends on others neighbouring protons and owing to the r^{-6} dependence is very sensitive to conformational changes. Consequently data processing is difficult and often needs a preliminary hypothesis on the nature of the molecular motions. In the case of nucleosides and nucleotides, ^{13}C-, ^{1}H-NMR studies have shown that the reorientation of the whole molecule is very much faster than intramolecular motions and that the relaxation of any proton depends on a single correlation time τ_c [26-29]. For polynucleotides the molecular motions are not well known. A preliminary ^{13}C relaxation study is therefore necessary for the interpretation of ^{1}H-NMR results.

In the case of a molecule undergoing an isotropic motion, $1/r_{IS}^6$ in equation (1) is replaced by $\sum_S 1/r_{IS}^6$ and $J_m(\omega)$ by equation (2) :

$$\frac{1}{T_1} = \frac{3}{10} \gamma_H^4 \hbar^2 \sum_S 1/r_{IS}^6 \left[\frac{1}{1 + \omega^2 \tau_c^2} + \frac{4}{1 + 4\omega^2 \tau_c^2} \right] \tau_c \qquad (10)$$

Thus for a given proton the ratio of T_1 measured at two different frequencies is independent of the internuclear distances between protons and consequently is the same for all. This constitutes a criterion to verify the isotropic nature of the molecular motion.

Figure 2 plots T_1(90 MHz)/T_1(250 MHz) versus τ_c. It is interesting to note that the variation of this ratio becomes significant for τ_c values between 0.1 and 2 nsec.

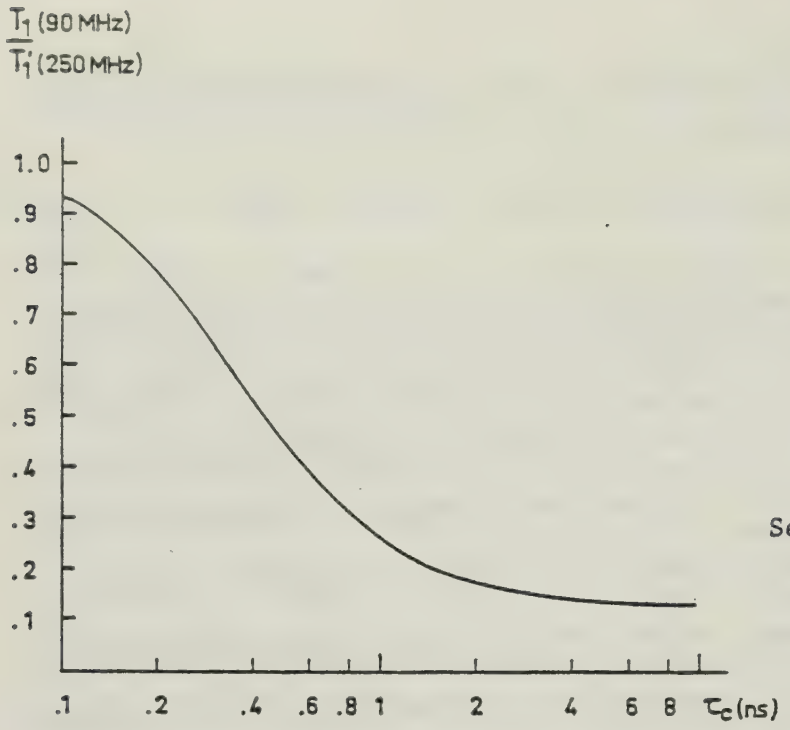

Figure 2

Semi-log plot of $T_1(^1H)$ ratio at 90 and 250 MHz versus correlation time τ_c.

In the case of poly A, Akasaka [8] observed a minimum on the $T_1 = f(1/T)$ curve for H_8 and H_1, protons and evaluated the correlation time τ_c and the sum $\sum r_{IS}^{-6}$ at the corresponding temperature from the T_1 minimum value taking $\omega\tau_c \approx 1$.

A.II.3. ^{31}P relaxation

^{31}P-NMR has been widely used to study the conformation and dynamic structure of polynucleotides and nucleic acids [8-12, 30-34]. Owing to the relative sensitivity of phosphorus, ^{31}P-NMR experiments require much less instrument time but the interpretation of ^{31}P relaxation data is more complicated than for ^{13}C ; this is because on the one hand the CSA contribution, which depends on the square of the laboratory magnetic field, is usually unknown and on the other hand, in the case of polynucleotides, the phosphorus is relaxed by several protons of which the distances from the phosphorus atom are not known precisely and depend on the molecular conformation. In general it is assumed that the CSA contribution is negligible at low frequency (< 40 MHz) and that the ^{31}P relaxation in oligo and polynucleotides is due to 3 protons 5', 5'', 3', their average distance from the phosphorus atom being about 2.7 to 3.0 Å.

From T_1/T_2 ratio, the correlation time τ_c may be evaluated by assuming isotropic molecular motion [10]. In view of numerous possibilities for error in the spin echo measurements of T_2 [35] and the difficulty of evaluating the CSA contributions in T_1 and T_2 we prefer not to use this method. In the present work, T_1 and $^{31}P-\{^1H\}$NOE experiments are performed at two frequencies (36.4 MHz and 111.6 MHz).

In the case of a molecule undergoing an isotropic motion the relation between relaxation time T_1 and NOE, T_1, η and T_1', η', at two frequencies ω and ω' respectively, can be deduced from equations (1b), (4b), (5b) :

$$\frac{\eta'}{\eta} \cdot \frac{T_1}{T_1'} = \frac{\sigma_I'}{\sigma_I} \qquad (11)$$

where σ_I is given by eq. (1b).

This equation is valid whatever the importance of the CSA contribution and is a function of a single parameter τ_c. In figure 3 the ration $\eta' T_1/\eta T_1'$ is plotted vs τ_c for two frequencies 36.4 and 111.6 MHz. It follows from this figure that the ratio $\eta' T_1/\eta T_1'$ is sensitive to τ_c variations in the time interval between 0.1 and 2 nsec.

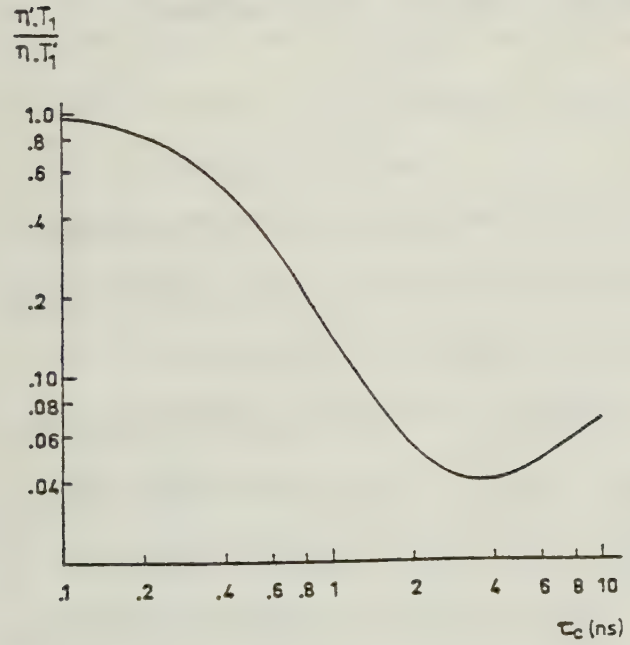

Figure 3

Log-log plot of $\eta' T_1/\eta T_1'$ vs τ_c ; η, T_1 and η', T_1' are $^{31}P-\{^1H\}$NOE and $T_1(^{31}P)$ at 36.4 and 111.6 MHz respectively.

In figure 1, $^{31}P-\{^{1}H\}NOE$ is plotted vs τ_c at 36.4 and 111.6 MHz for the case where the molecular motion is isotropic and the ^{31}P relaxation assumed to be solely due to the dipolar interaction. From the experimental value of $\eta' T_1 / \eta T_1'$ the correlation time τ_c (Fig. 3) then the ^{31}P-NOE value for the case of purely dipolar relaxation can be calculated. Comparison between the computed and experimental ^{31}P-NOE values allows the CSA contribution to be evaluated from the following equations :

$$\frac{\eta_{obs}}{\eta_{cal}} = \frac{\rho_{IS}}{\rho_{IS} + \rho_{CSA}} \tag{12}$$

$$\rho_{IS} = \frac{1}{T_{1DD}} = \frac{\eta_{obs}}{\eta_{cal}} \cdot \frac{1}{T_{1obs}}$$

$$\rho_{CSA} = \frac{1}{T_{1CSA}} = \frac{\eta_{cal} - \eta_{obs}}{\eta_{cal}} \cdot \frac{1}{T_{1obs}} \tag{13b}$$

$$\frac{1}{T_{1obs}} = \frac{1}{T_{1DD}} + \frac{1}{T_{1CSA}} \tag{14}$$

$$\frac{1}{T_{1CSA}} = \frac{1}{15} \gamma^2 H^2 \, (\sigma_{/\!/} - \sigma_{\perp})^2 \, \frac{2\tau_c}{1 + \omega^2 \tau_c^2} \tag{15}$$

The limiting factor in this method is mainly the experimental error when ^{31}P-NOE values become small.

A.II.4. ^{2}H relaxation

Deuterium substitution at the 8 position of poly I can be obtained by heating the heavy water solution of poly I at 85°C for about 3 hours. For a given laboratory magnetic field the Larmor frequency of ^{2}H is about 6 times smaller than that of the proton and therefore the extreme narrowing conditions are usually satisfied, i.e. $\omega\tau_c << 1$ and $T_1 = T_2$. Consequently only a measurement of the width at half-height, $\Delta\nu_{1/2}$, of the deuterium line is required. For correlation times $\tau_c \approx 10^{-9}$ sec., $\Delta\nu_{1/2}$ is about a few tenths

of Hz. The value of 1.1 10^6 rad s^{-1} has been taken for the quadrupole coupling constant.

Another advantage of ^{2}H-NMR is that the deuterium relaxation times T_1 and T_2 are relatively short, involving considerably less instrument time, and are not sensitive to the presence of paramagnetic ions in the sample solution.

A.III. EXPERIMENTAL SECTION

Poly I containing no free salt was purchased from GIPEP (France). According to the supplier, its average molecular weight, estimated from the sedimentation velocity measurement, is about 300,000. The product was either dialysed extensively against a solution of 5.10^{-4} % EDTA, 5.10^{-3} M NaCl, pH ≃ 7 by the flow dialysis method or dissolved directly in water containing ≃ 10^{-3} M EDTA and the pH was adjusted to 7-8 by addition of a small amount of NaOH. The NMR results obtained are practically independent of the sample preparation method.

The sample were freeze-dried twice in ^2H_2O at final concentrations of 0.06-0.10 M in monomer unit. For ^{1}H and ^{31}P relaxation studies, these solutions were introduced into 5 mm NMR tubes, degassed in a vacuum line and sealed. It is worth noting that appreciable diminutions of the phosphorus relaxation time T_1 and NOE were observed with non-degassed samples. In the case of deuterium observation, the overlapping of the residual ^{2}HHO signal from normal H_2O was avoided by dissolving poly I ($^2H_8$) in deuterium-depleted water (C.E.A.-Saclay).

^{1}H-NMR spectra were recorded at 250 MHz on a CAMECA-TSN 250 and at 90 MHz on a Bruker WH90. ^{2}H-NMR experiments were performed at 13.8 MHz on a Bruker WH90. Phosphorus relaxation times T_1 and ^{31}P-{^{1}H}NOE were determined at 36.4 MHz (on WH90) and at 111.6 MHz on the FT spectrometer built in the laboratory of Prof. M. Guéron (Ecole Polytechnique, Palaiseau, France).

^{1}H and ^{31}P relaxation times T_1 were obtained by the inversion recovery method (180°-τ-90°).

^{13}C-NMR experiments were performed at 75.4 MHz on a Bruker CXP-300 at Karlsruhe (RFA). With the good sensitivity of this spectrometer (S/N = 700 for 1% ethyl benzen) a few hundred scans were enough to obtain a ^{13}C-NMR spectrum with an acceptable signal-to-noise ratio (poly I, 0.1 M). For ^{13}C-{^{1}H}NOE, the FID recordings were performed with and without NOE alternately : in the former (with NOE), the ^{1}H decoupler is set on continuously while in the second (without NOE), the ^{1}H decoupler is gated on during the acquisition time. This method eliminates in the NOE measurement any error due to field homogeneity variation.

A.IV RESULTS

A.IV.1. ^{1}H-NMR

The chemical shifts and coupling constants J_{H-H} , J_{P-H} were measured vs temperature at 250 MHz. Table I sums up the proton chemical shifts of poly I at two extreme temperature values, 22°C and 62°C, as well as those of 5'IMP [36] and 3'IMP at neutral pH and at room temperature. The results in this table show that at 22°C the chemical shift of $H_{2'}$ is practically the same for monomers and polymer while the $H_{3'}$, $H_{4'}$, $H_{5'}$, $H_{5''}$ signals of poly I are shifted more or less to the low field with respect to the corresponding monomers. This effect is certainly due to the phosphate groups at 3' and 5' positions in polynucleotides. By contrast, the poly I resonances H_2, H_8 and $H_{1'}$ are shifted to higher field about 0.2 to 0.3 ppm (compared with the corresponding monomers). This extra shift probably reflects a change in the base orientation around the glycosidic linkage [37]. It follows from the data in table I that the temperature variation scarcely affects the proton chemical shifts of poly I, indicating that the base-base stacking and formation of multistranded complex occuring in aqueous solution are negligible.

Table I - ^{1}H chemical shifts (in ppm from TMP) of poly I, 3'IMP and 5'IMP in $^{2}H_2O$ at neutral pH.

Compounds	H_8	H_2	$H_{1'}$	$H_{2'}$	$H_{3'}$	$H_{4'}$	$H_{5'}$	$H_{5''}$
Poly I 22°C	8.252	8.055	5.918	4.731	4.807	4.479	4.218	4.156
Poly I 62°C	8.267	8.094	5.956	4.749	4.816	4.470	4.213	4.151
Δδ	0.015	0.039	0.038	0.018	0.009	-0.009	-0.005	-0.005
5'IMP 22°C a)	8.566	8.216	6.136	4.796	4.506	4.356	4.016	
3'IMP 22°C	8.390	8.234	6.141	4.808	4.725	4.422	3.908	3.908

a) Evans et al. [36].

In harmony with the proton chemical shifts, the results concerning the coupling constant J_{H-H} , J_{P-H} in table II show that no great difference exists between monomers and polymer and that the temperature has little effect on the coupling constants.

Table II - ^{1}H-^{1}H and ^{31}P-^{1}H coupling constants (in Hz) of poly I, 3'IMP and 5'IMP in $^{2}H_2O$ at neutral pH.

Compounds	$J_{1'2'}$	$J_{2'3'}$	$J_{3'4'}$	$J_{4'5'}$	$J_{4'5''}$	$J_{5'5''}$	$J_{3'P}$	$J_{5'5''-P}$	% S	% gg
Poly I 22°C	5.3	5.2	3.0	3.0	4.0	12.2	7.0	~4	54	63
Poly I 62°C	6.0	4.6	3.9	2.7	4.2	11.8	7.5	~4	61	64
5'IMP 22°C a)	5.8	5.2	3.6	2.9	3.8	12.0		4.8	59	67
3'IMP 22°C	5.7	5.3	3.2	3.4	3.4		8.4		58	65

a) Evans et al. [36].

Proton spin lattice relaxation times T_1 measured at two frequencies, 90 and 250 MHz, are plotted as a function of the reciprocal absolute temperature in figure 4.

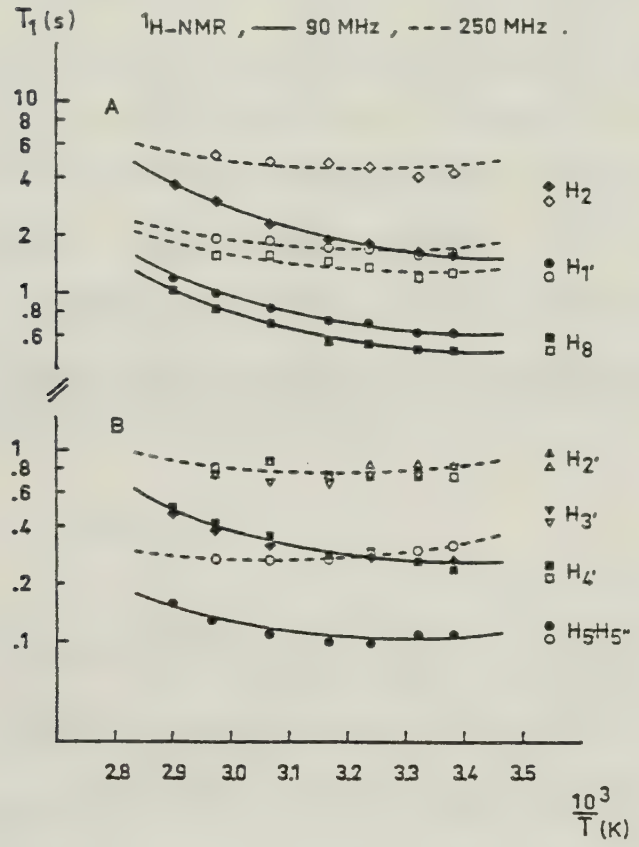

Figure 4

Temperature dependence of proton longitudinal relaxation times T_1 measured at 90 MHz and 250 MHz (solid and dashed curves respectively).

As expected, the proton relaxation time T_1 is frequency-dependent : $T_1(250) > T_1(90)$ whatever the temperature. Inspection of the data in figure 4 reveals three important points :

a) the ratio $T_1(90)/T_1(250)$ at a given temperature is practically the same for all protons and increases by about 40% as the temperature rises from 22°C to 62°C :

$$T_1(90)/T_1(250) = 0.36 \pm 0.03 \text{ at } 22°C$$

$$T_1(90)/T_1(250) = 0.52 \pm 0.03 \text{ at } 62°C$$

b) the variation of T_1 with temperature is less pronounced at 250 MHz than at 90 MHz ;

c) the extreme narrowing conditions are far from being satisfied.

A.IV.2. ^{13}C-NMR

Figure 5 shows the ^{13}C-NMR spectrum of poly I in neutral aqueous solution at 75.4 MHz. Assignments of the different ^{13}C have been made either by comparison with the 5'-IMP spectrum [38], by measuring ^{13}C-NOE to distinguish protonated and non-protonated carbons of the base or by deuterium substitution at the 8 position.

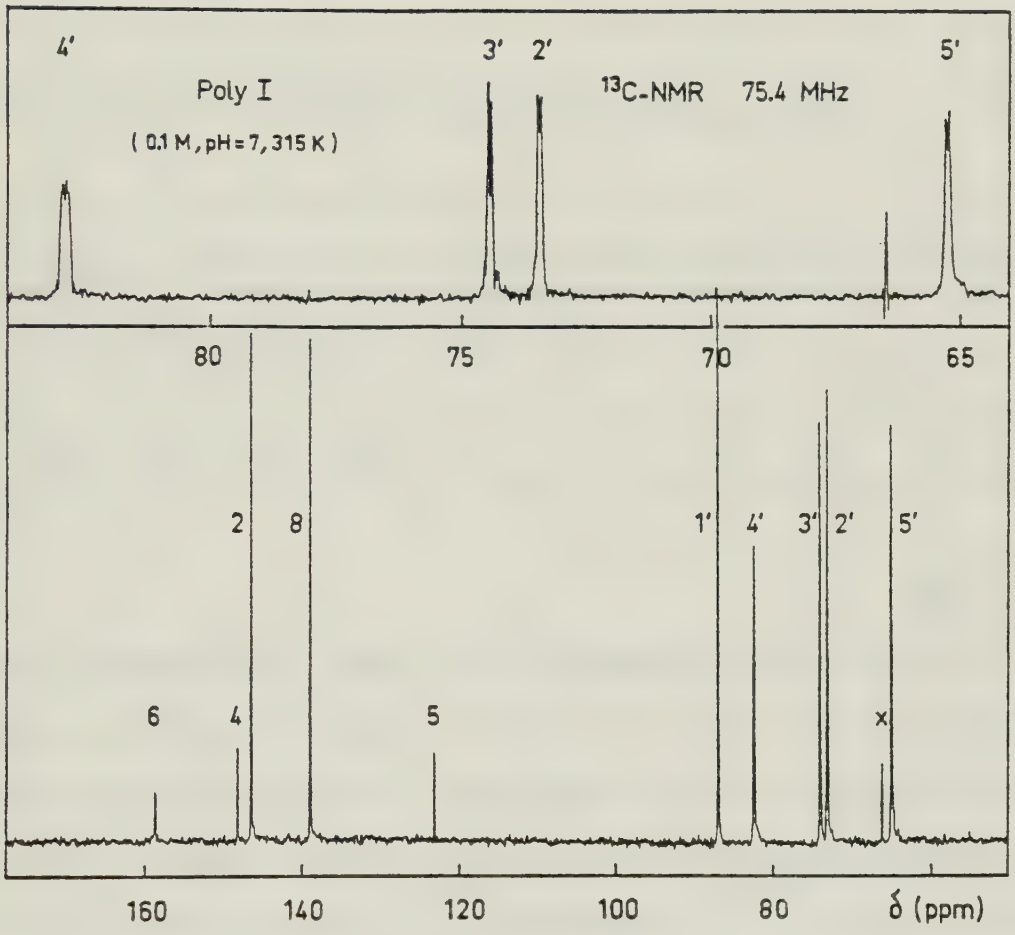

Fig. 5 - ^{13}C-NMR spectrum of poly I (0.1 M, pH ≃ 7, in $^{2}H_2O$ at 315°K) recorded at 75.4 MHz under proton noise decoupling (5000 scans, with an acquisition time = 0.5 sec.).

Table III sums up the chemical shifts of all carbons and the NOE of protonated carbons at 27°C and 62°C. The temperature effect on the ^{13}C chemical shift is not very great ($\Delta\delta < 0.15$ ppm). The same behaviour was noticed for poly U [39]. It should be emphasized that ^{13}C-{^{1}H}NOE is inde-

pendent of the carbon position (on the sugar, the exocyclic group or the base) and is practically the same at given temperature. In contrast to the chemical shifts and coupling constants, ^{13}C-NOE is sensitive to temperature : NOE increases by about 20% as the temperature rises from 22°C to 62°C.

Table III - ^{13}C chemical shifts (in ppm from external TMS) and NOE of protonated carbons (upon non selective proton saturation) of poly I in $^{2}H_2O$ at 75.4 MHz.

		C_4	C_5	C_6	C_2	C_8	$C_{1'}$	$C_{2'}$	$C_{3'}$	$C_{4'}$	$C_{5'}$
22°C	δ	148.471	123.526	158.840	146.756	139.299	87.371	73.394	74.381	82.277	65.241
	NOE				1.80	~1.9	2.03	1.90	2.19	2.05	1.80
		$\overline{NOE}$ = 1.95 ± 0.14									
62°C	δ	148.616	123.656	158.937	146.805	139.428	87.420	73.394	74.413	82.842	65.322
	NOE				2.36	~2.3	2.22	2.36	2.45	2.44	2.39
		$\overline{NOE}$ = 2.36 ± 0.08									
Δδ		0.145	0.130	0.097	0.049	0.129	0.049	0.000	0.032	0.065	0.081

A.IV.3. ^{31}P-NMR

The spin lattice relaxation time T_1 and ^{31}P-{^{1}H}NOE were measured vs temperature at 36.4 MHz and 111.6 MHz. In figure 6, Log T_1 is plotted against the reciprocal absolute temperature. Two straight lines of different slope were obtained for both frequencies. Unlike proton T_1 (Fig. 4) the relaxation time T_1(^{31}P) decreases as the laboratory magnetic field increases, clearly indicating large CSA contributions to the ^{31}P relaxation at high frequencies.

Figure 7 shows the ^{31}P-{^{1}H}NOE variation observed at 36.4 MHz and 111.6 MHz vs 1/T. As expected, the NOE values are larger at low frequency than at high frequency. At 72°C the NOE value (≃ 2.0) measured at 36.4 MHz is close to the maximum (2.23), showing that the ^{31}P relaxation at this frequency is mainly due to the dipole-dipole interaction with protons.

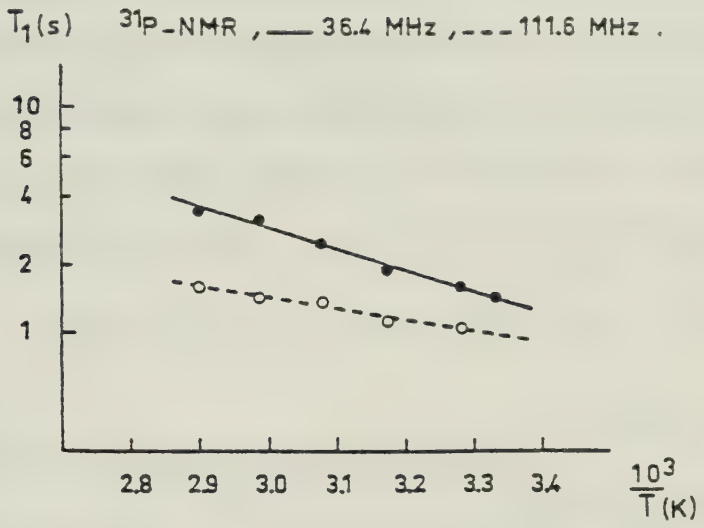

Fig. 6 - Temperature dependence of ^{31}P longitudinal relaxation time T_1 upon non-selective proton saturation at 36.4 MHz and 111.6 MHz (solid and dashed curves respectively).

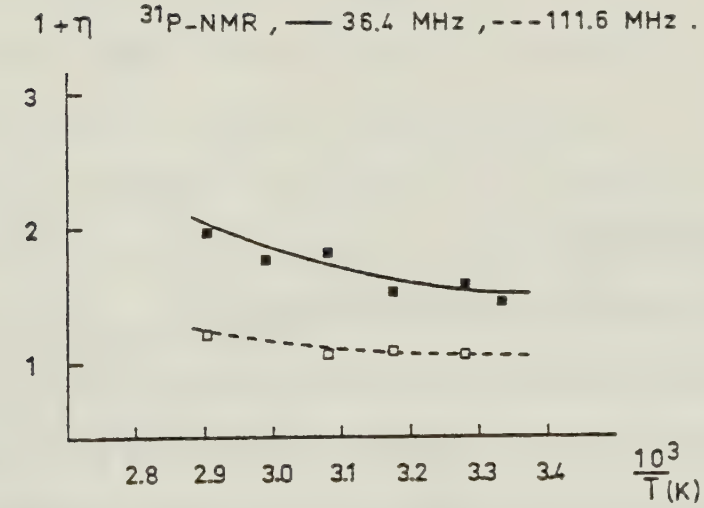

Fig. 7 - Temperature dependence of $^{31}P-\{^{1}H\}$NOE at 36.4 MHz and 111.6 MHz (solid and dashed lines respectively).

A.IV.4. ^{2}H-NMR

The width at half height of the $^{2}H_8$ peak was measured at various temperatures (Fig. 8). As the temperature increases the linewidth at half-height decreases from about 120 Hz to 40 Hz. It is important to note that a continued heating of the sample over several hours at t > 65°C induces the exchange reaction between $^{2}H_8$ and $^{1}H_8$, causing the disappearance of the $^{2}H_8$ signal.

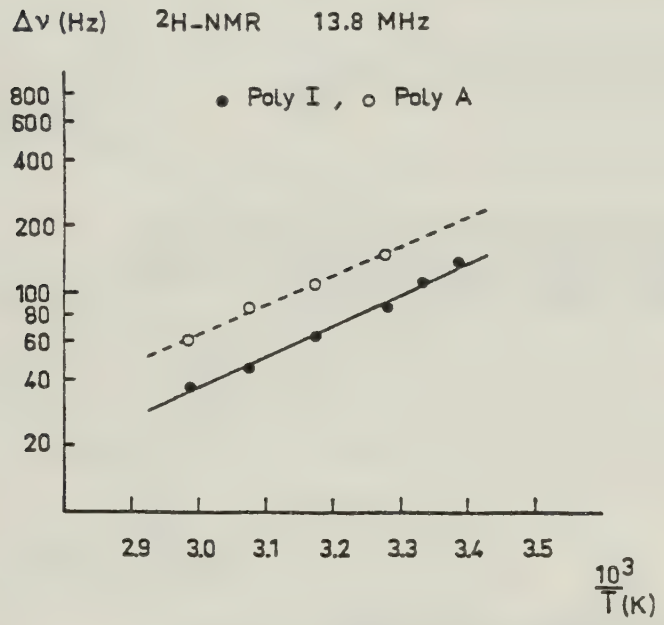

Figure 8
Temperature dependence of $^{2}H_8$ linewidth at half height at 13.8 MHz (—— poly I, ... poly A).

A.V. DISCUSSION

A.V.1 Conformation of poly I

a) Ribose and phosphate backbone conformation

The proportion of the S conformer and that of the gg rotamer were computed from the proton-proton coupling constants and are included in table II. The results in this table show that the ribose ring is flexible and exists in equilibrium between two conformers N and S as in the case of mononucleotides. At room temperature the proportion of the S conformer is prepon-

derant and is favoured at higher temperature, as observed for some dinucleoside monophosphates [40, 41]. Surprisingly the gg proportion of poly I (≃ 60%) is distinctly smaller than that of the 5' residue in the majority of the dimers (~ 90%), indicating that the rotation around the phosphodiester linkage is not greatly reduced in poly I.

The small values of $J_{5'-P}$, $J_{5''-P}$ and $J_{3'-P}$ show a clear preference for the g'g' (around the $C_{5'}-O_{5'}$ bond) ang g^- or g^+ (around the $C_{3'}-O_{3'}$ bond) conformers.

b) Conformation around the glycosidic bond

From examination of the proton relaxation data in figure 4, the ratio $T_1(H_{1'})/T_1(H_{3'})$ is found to be about 2.3 and independent of temperature. The value of this ratio is smaller than that (> 2.5) obtained from purine nucleosides [29, 42] with no exchangeable proton on the base or when H_8 is substitued by a deuterium [27, 41]. These results suggest that the *syn* and *anti* conformations are in equilibrium in aqueous solution. On the other hand by using the τ_c value calculated from the ratio $T_1(90)/T_1(250)$ (see below) the computed average distance $\langle r_{1'-8} \rangle$ is found to be about 3.4 Å. This value, larger than that (3.0 Å) obtained for 5'IMP, 5'GMP and 5'AMP [27], indicates that the *anti* character in poly I is more pronounced than in the case of 5'-purine nucleotides. This conclusion is corroborated by the upfield shift of H_2 , H_8 and $H_{1'}$ observed in poly I (Table I).

A.V.2. Dynamic structure of poly I

a) Ribose-base unit

The same NOE value observed for all the protonated carbons on the ribose as well as on the base (Table IV) shows clearly that the correlation time τ_c distribution is uniform within the ribose-base unit. We may therefore consider that this unit undergoes an isotropic motion and the reorienta-

tion of C-H vectors may be characterized by a single correlation time τ_c. This conclusion is supported by the proton relaxation study. In fact it is shown in figure 4 that for a given temperature the ratio of T_1 measured at 90 MHz and 250 MHz is practically the same for all non-exchangeable protons, so the necessary conditions for an isotropic motion model is well satisfied (see section A.II.2.).

Table IV - Correlation times τ_c (in nanosecond) of poly I and poly A in ^2H_2O deduced from ^{13}C, ^1H, ^2H and ^{31}P NMR relaxation data.

Nucleus	τ_c at 22°C			τ_c at 62°C		
	Poly I	Poly A		Poly I	Poly A	
^{13}C	0.7	3.0 (H_8) 1.5 (H_1')	a)	0.4	0.5 (H_8) 0.5 (H_1')	a)
^1H	0.7			0.4		
^2H	0.9	1.5	b)	0.3	0.4	b)
^{31}P	2.0	5.0	a	0.9	0.9	a)

a) τ_c values were estimated from the semi-log plot of τ_c vs reciprocal temperature in figure 2 of ref. 8

b) Neumann and Tran-Dinh, unpublished results.

The τ_c values deduced from ^{13}C-{^1H}NOE, the ratio $T_1(90)/T_1(250)$ and the width at half-height of $^2H_8$ (see section A.II, Fig. 1 and Fig. 2) are plotted vs the reciprocal absolute temperature in figure 9, and those at 22°C and 62°C are reported in table IV for the purpose of comparison As seen from the results in this table, the τ_c values obtained from ^{13}C-NOE on the one hand and from proton relaxation measurements on the other hand are exactly the same, and close to that calculated from the linewidth of $^2H_8$. In all cases (^{13}C, ^1H, ^2H) a straight line is obtained for the plot

$\tau_c = f(1/T)$ (Fig. 9), suggesting that in the temperature interval between 22°C and 62°C the motion of the ribose-base unit is governed by a single process in accordance with the isotropic model. A similar conclusion has been reached for the case of oligo- [43] and polynucleotides [8].

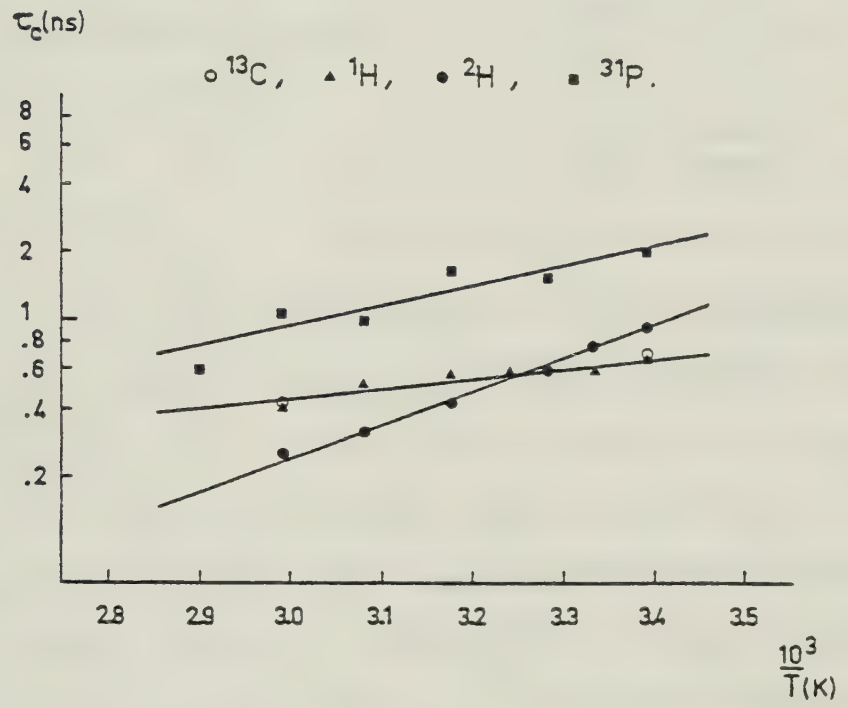

Fig. 9 - Temperature dependence of correlation times for poly I obtained from ^{13}C(o), ^{1}H(▲), ^{2}H(•) and ^{31}P(■) - NMR studies.

Activation energies of 2 kcal/mole from ^{13}C or ^{1}H relaxation studies and of 6 kcal/mole from the deuterium linewidth have been evaluated (Fig. 9). A value of 6 to 8 kcal/mole has been found for poly A [8].

b) Phosphate backbone

The information obtained from ^{31}P-NMR relaxation is certainly not enough to propose a motion model for the phosphate backbone. However if we assume that the motion of the phosphate group is isotropic, the correlation time τ_c and the CSA contribution may be calculated from experimental values of $\eta' T_1/\eta T_1'$ measured at 36.4 and 111.6 MHz (see section A.III.3). For example at 36.4 MHz, T_1 = 3.45 sec, η_{obs} = 0.98 at 72°C. The τ_c and η_{cal} values

are 0.5 ± 0.16 10^{-9} sec and 1.12 ± 0.06 respectively. The small uncertainty on η_{cal} (0.06) compared to that on τ_c is due to the slight variation of η when $\tau_c < 10^{-9}$ sec (Fig. 1).

From equations (13a) and (15) the dipole-dipole and CSA contributions as well as the chemical shift anisotropy $\sigma = |\sigma_{//} - \sigma_{\perp}|$ can be deduced :

$$\frac{1}{T_{1DD}} = \frac{0.88}{T_{1obs}} \qquad (T_{1DD} = 3.9 \text{ sec})$$

$$\frac{1}{T_{1CSA}} = \frac{0.12}{T_{1obs}}$$

$$\sigma = |\sigma_{//} - \sigma_{\perp}| = 112 \text{ ppm.}$$

A 12% CSA contribution to the ^{31}P relaxation at 36.4 MHz and a value of 112 ± 11 ppm for the chemical shift anisotropy are obtained. Similarly the CSA contribution of 72% is calculated at 111.6 MHz, corresponding to a σ value : 124 ± 12 ppm. Thus the average value of the chemical shift anisotropy $\sigma = \sigma_{//} - \sigma_{\perp}$ is about 118 ± 18 ppm, in good agreement with that calculated by Akasaka et al. [9] (120 - 130 ppm) or estimated by Guéron and Shulman (136 ppm) [30]. It is worth noting that while the extreme narrowing conditions are satisfied for the CSA term at 36.4 MHz, the same is not true at 111.6 MHz. The ratio of CSA contributions (12/72) is therefore not equal to the square of the ratio of laboratory magnetic fields (see equation (15)).

The sum of the sixth power of phosphorus-proton distance, $\sum_H r_{PH}^{-6}$ may be evaluated from the τ_c and T_{1DD} values. Assuming that the ^{31}P relaxation is only due to three protons 5', 5" and 3', equidistant from the phosphorus atom, the average distance $\langle r_{P-H} \rangle$ is found to be 2.8 Å in very satisfactory agreement with the values estimated by other authors [8, 33, 43].

In view of the small CSA contribution (12%) and the relatively high values of η_{obs} at 36.4 MHz, we may now calculate τ_c from η_{obs}, taking into account the CSA contribution. Figure 9 shows the plot of $\tau_c(^{31}P)$ vs reciprocal absolute temperature. The activation energy of about 4 kcal/mole

deduced from the slope of this curve is lower than the value given by Akasaka for poly A (8 kcal/mole) [8] but in close agreement with that obtained by Davanloo et al. for oligonucleotides (4-6 kcal/mole) [43].

c) Mobility in polynucleotides and nucleic acids

In order to compare the dynamic structure of poly I and poly A, the τ_c values of the latter, deduced from ^1H and ^{31}P [8] as well as from ^2H [44] relaxation measurements at 22°C and 62°C, are included in table IV. The results indicate that the mobility of the sugar base unit and that of the phosphate group at high temperature are respectively the same in both polymers, whereas at room temperature they are slower in poly A than in poly I. This can be explained by the considerable base-base stacking in poly A at low temperature. In general the τ_c values observed in poly I as well as in other polynucleotides (poly A, poly C, poly U) [8, 9] are relatively short, in the nanosecond region. These correlation times should represent local motion [9] while the overall tumbling of such a large molecule ($M \simeq 300,000$) should be much slower ($\sim 10^{-6}$ sec) and therefore have no detectable influence on the relaxation parameters. Thus the isotropic motion of the sugar-base unit can be explained in the following way : although the reorientation of the whole molecule is slow, the motion resulting from different internal reorientations in the sugar-base unit (rotation around the glycosidic bond, pseudorotation of the ribose ring, rotation of the exocyclic, rotation around the C_3'-O-P and C_5'-O-P bonds) is fast and can be considered as isotropic. In an early study using an ultrasonic method Rhodes and Schimmel [45] showed that the correlation time of the rotation around the glycosidic bond is of the nanosecond order, similar to that found in polynucleotides.

Concerning the phosphate group whose motion is still the subject of controversy, several models have been proposed recently [43, 46, 47]. In the case of poly U, by using the model of an isotropic motion with a distri-

bution of correlation times, Shindo [46] has obtained good agreement between the observed and calculated values of T_1 and the linewidth of ^{31}P signal. The average correlation time is about 3.3 nsec. On the other hand, Bolton and James [47], on the basis of T_1, NOE, $T_{1\rho}$ measurements, have proposed a motion model with two correlation times for poly A. On increasing temperature from 6° to 20°C, the ratio $T_{1\rho}/T_1$ increases constantly and is almost equal to 1 at 20°C. This seems to indicate that at higher temperature ($t > 25°C$) the use of this motion model is not highly justified. In the present paper, the good linearity of the Arrhenius plots (Figs 6 and 9), the same T_1 ratio for all protons measured at two frequencies, the same $^{13}C-\{^1H\}$ value for all protonated carbons (in the limit of experimental errors), show that our relaxation data can be fairly well interpreted by using a single correlation time.

In the case of nucleosomes and purified DNA, Klevan et al. [33] have also observed short relaxation times T_1 and large $^{31}P-\{^1H\}$NOE values indicating the presence of fast internal motion similar to that observed in poly A [8]. These authors state that the ^{31}P relaxation data are consistent with the dynamic model in which the nucleotide chain rotates freely about the O-P and P-O bonds while the whole molecule is rotating isotropically [43]. However such motion is not allowed by double helix geometry and we agree with them that more sophisticated dynamic models should be examined to explain the ^{31}P-NMR data.

^{13}C spin-lattice relaxation time and $^{13}C-\{^1H\}$NOE measurements have been made recently for calf thymus DNA [47]. It has been shown that the motion of the bases is much slower than the relatively free motion of the sugar. Hogan and Jardetzky [48] have also studied the internal motion in well defined double stranded DNA fragments by ^{31}P and ^1H-NMR spectroscopy. These authors have suggested that the B form helix undergoes substantial fluctuation in deoxyribose sugar puckering that occurs with a relaxation time near 1 nsec.

ACKNOWLEDGEMENTS

^{13}C-NOE experiments were performed on a Bruker CXP-300 during our recent visit to Bruker C° at Karlsruhe (RFA). We wish to thank Dr Forster (Bruker RFA) and Dr Herman (Bruker S.A. France) for their help in obtaining ^{13}C-NMR spectra with and without NOE. We are also indebted to Prof. Guéron (Ecole Polytechnique - Palaiseau - France) for the use of his spectrometer on which ^{31}P relaxation measurements (at 111.6 MHz) were done.

REFERENCES

1. MICHELSON, A.M., MASSOULIE, J. and GUSCHLBAUER, W. (1967) Progress in Nucleic Acid Research, DAVIDSON, T.N. and COHN, W.E., Eds, Academic, New York, p 83.

2. MASSOULIE, J. (1968) Eur. J. Biochem. 3, 428.

3. GIANNONI, G., RICH, A. (1964) Biopolymers 2, 399.

4. THIELE, D. and GUSCHLBAUER, W. (1969) Biopolymers 8, 361.

5. TODD MILES, H. and FRAZIER, J. (1978) Biochem. Soc. 100, 8037.

6. MANTSCH, H.H. and SMITH, I.C.P. (1972) Biochem. Biophys. Res. Commun. 46, 808.

7. SMITH, I.C.P., JENNINGS, H.J. and DESLAURIERS, R. (1975) Accounts of Chem. Res. 8, 306.

8. AKASAKA, K. (1974) Biopolymers 13, 2273.

9. AKASAKA, K., YAMADA, A. and HATANO, H. (1977) Bull. Chem. Soc. Jpn 50, 2858.

10. YAMADA, A., AKASAKA, K. and HATANO, H. (1978) Biopolymers 17, 749.

11. GORENSTEIN, D.G., FINDLAY, J.B., MOMII, R.K., LUXON, P.A. and DEBOJYOTI, K. (1976) Biochemistry 15, 3796.

12. PATEL, D.J. (1978) J. Polym. Sci. Polym. Symp. 62, 117.

13. GLASEL, J.A., HENDLER, S. and SRINIVASAN, P.R. (1968) Proc. Natl. Acad. Sci. USA 60, 1038.

14. Van OSTENBURG, D.O., SPIEWAK, R.L. and DANYLUK, S.S. (1975) Bioinorganic Chem. 4, 225.

15. SOLOMON, I. (1955) Phys. Rev. 99, 559.

16. DODDRELL, D., GLUSHKO, V. and ALLERHAND, A. (1972) J. Chem. Phys. 56, 3683.

17. ABRAGAM, A. (1961) The Principles of Nuclear Magnetism, Oxford University Press, London.

18. LYERLA, J.R. and LEVY, G.C. (1974) Topics in Carbon-13 NMR Spectroscopy, Vol. 1, LEVY, G.C., Ed., Interscience, New York, p. 81.

19. BOVEY, F.A. (1979) Stereodynamic of Molecular Systems, Proceeding of a Symposium held at the State University of New York at Albany, Ap. 23-24, SARMA, R.H., Ed., Pergamon Press. New York, P. 53.

20. HEATLEY, F. (1979) Progress in NMR Spectroscopy, Vol. 13, EMSLEY, J.W., FEENEY, J. and SUTCLIFFE, L.H., Eds., Pergamon Press, New-York, p. 47.

21. MANTSCH, H.H., SAITO, H. and SMITH, I.C.P. (1977) Progress in NMR Spectroscopy, Vol. 11, EMSLEY, J.W., FEENEY, J. and SUTCLIFFE, L.H., Eds, Pergamon Press, New York, p. 212.

22. WOESSNER, D.E. (1962) J. Chem. Phys. 37, 647.

23. WOESSNER, D.E., SNOWDEN, B.S. and MEYER, G.H. (1969) J. Chem. Phys. 59, 719.

24. TSUTSUMI, A., PERLY, B., FORCHIONI, A. and CHACHATY, C. (1978) Macromolecules 11, 977.

25. JONES, A.A. (1977) J. Polym. Sci. Polym. Phys. Ed. 15, 863.

26. IMOTO, T., AKASAKA, K. and HATANO, H. (1975) Chem. Phys. Lett. 32, 86.

27. CHACHATY, C., ZEMB, T., LANGLET, G., TRAN-DINH, S., BUC, H. and MORANGE, M. (1976) Eur. J. Biochem. 62, 45.

28. LÜDEMANN, H.D., WESTHOF, E. and RÖDER, O. (1974) Eur. J. Biochem. 49, 143.

29. NEUMANN, J.M., BORREL, J., THIERY, J.M., GUSCHLBAUER, W. and TRAN-DINH, S. (1977) Biochim. Biophys. Acta 479, 427.

30. GUÉRON, M. and SHULMAN, R.G. (1975) Proc. Natl. Acad. Sci. USA 72, 3482.

31. SALEMINK, P.J.M., SWARTHOF, T. and HILBERS, C.W. (1979) Biochemistry 18, 3477.

32. GORENSTEIN, D.G. (1978) Nuclear Magnetic Resonance Spectroscopy in Molecular Biology, Pullman, B., Ed., Academic Press, New-York, p. 1.

33. KLEVAN, L., ARMITAGE, I.M. and CROTHERS, D.M. (1979) Nucl. Acids Res. 6, 1607.

34. PATEL, D.J. (1978) Eur. J. Biochem. 83, 453.

35. WRIGHT, D.A., AXELSON, D.E. and LEVY, G.C. (1979) Topics in Carbon-13 NMR Spectroscopy, Vol. 3, LEVY, G.C., Ed., Intersience, New York, p. 118.

36. EVANS, F.E. and SARMA, R.H. (1975) J. Am. Chem. Soc. 97, 3215.

37. PATEL, D.J., CANUEL, L.L. and POHL, F.M. (1979) Proc. Natl. Acad. Sci. USA 76, 2508.

38. DORMAN, D.E. and ROBERTS, J.D. (1970) Proc. Natl. Acad. Sci. USA 65, 19.

39. GOVIL, G. and SMITH, I.C.P. (1973) Biopolymers 12, 2589.

40. EZRA, F.S., LEE, C.H., KONDO, N.S., DANYLUK, S.S. and SARMA, R.H. (1977) Biochemistry 16, 1977.

41. NEUMANN, J.M., GUSCHLBAUER, W. and TRAN-DINH, S. (1979) Eur. J. Biochem. 100, 141.

42. TRAN-DINH, S., NEUMANN, J.M., THIERY, J.M., HUYNH-DINH, T., IGOLEN, J. and GUSCHLBAUER, W. (1977) J. Am. Chem. Soc. 99, 3267.

43. DAVANLOO, P., ARMITAGE, I.M. and CROTHERS, D.M. (1979) Biopolymers 18, 663.

44. NEUMANN, J.M. and TRAN-DINH, S. unpublished data.

45. RHODES, L.M. and SCHIMMEL, P.R. (1971) Biochemistry 10, 4426.

46. SHINDO, H. (1980) Biopolymers 19, 509.

47. BOLTON, P.H. and JAMES, T.L. (1979) J. Phys. Chem. 83, 3359.

48. HOGAN, M.E. and JARDETZKY, O. (1979) Proc. Natl. Acad. Sci. USA 76, 6341.

B. ^{1}H-NMR COMPARATIVE STUDIES OF POLYNUCLEOTIDES : CONFORMATION AND DYNAMIC STRUCTURE OF POLY U AND POLY C IN NEUTRAL SOLUTION

NEUMANN, J.M. and TRAN-DINH, S.

(1982) Biopolymers 21, 383.

It was been shown by optical techniques (CD, ORD, UV ...) [1-6] that the hydrodynamic properties of the two homopolyribonucleotides containing a single naturally occurring pyrimidine base poly U and poly C are quite different. Above 15°C, poly U exhibits only a small temperature dependence as far as its optical properties are concerned and behaves as a random coil [4-5]. In the case of poly C in neutral solution, Brahms [2] suggested from the CD results that at neutral pH, poly C possesses a helical or partially helical conformation in agreement with the conclusion of Chou and Thomas [6]. Fasman et al. [3] using the ORD technique claimed to prove the presence of a highly ordered secondary structure and observed a gradual transition between the helix and random coil forms on raising the temperature. Michelson et al. [1] considered poly C to be a random coil with continuously fluctuating regions of helicity arising from base-base interactions in constant change. In brief, in neutral aqueous solution and at room temperature the structure of poly C is more ordered than that of poly U and the formation of a single stranded helix is highly probable for poly C. From the above discussion, we can expect a substantial difference in conformation and dynamic structure between poly U and poly C in neutral solution.

Recently Akasaka et al. [7] have studied the molecular motion of the phosphate moiety in poly U, poly C and poly A and found that mobility increases in the order poly A → poly C → poly U. However no fundamental difference between these polynucleotides has been stated. This is due to the fact that the information obtained from ^{31}P-NMR spectroscopy can not describe either the conformation or the mobility of the ribose and the base. Similarly, owing to the small intrinsic sensibility of ^{13}C and its low natural abundance, ^{13}C-NMR spectroscopy does not lead to many successful applications for the investigation of nucleic acid [8] and polynucleotide [9-10] structures. In contrast, ^{1}H-NMR has already provided a considerable amount of information about the ribose and base conformations of nucleoside monophosphates [11]. However proton relaxation has not been efficiently applied to study the dynamic structure of large and flexible molecules. This is because proton relaxation depends on other neighbouring protons and is very sensitive, due to the r^{-6} dependence, to conformational changes. In a very recent paper [12], we have shown that this difficulty can be avoided by measuring proton relaxation times at different frequencies and temperatures.

In addition to the choice of NMR techniques, another problem which should be considered is the choice of molecular motion models to interpret the relaxation data. Various motion models [13] involving either a correlation time distribution [14-15] or two or several correlation times [16-19] have already been used whenever the single correlation time model was found to be inconsistent with the data. The case of an equilibrium between two forms, with different correlation times for example isolated and complex forms or coiled and ordered forms, which however is frequently observed for biological molecules in aqueous solution has not been examined so far.

In the present paper, the conformation and the dynamic structure of poly U and poly C have been investigated by ^{1}H-NMR spectroscopy at two different frequencies (90 MHz and 250 MHz) and at various temperatures. We show how the conformational and dynamical properties of these two polynucleotides differ. In some cases, the relaxation data have been interpreted in terms of an equilibrium between two different forms.

B.I. THEORETICAL BACKGROUND

The longitudinal relaxation of the magnetization I_{zi} in a system of N protons (spin 1/2) can be written in a generalized form as :

$$\frac{d}{dt} I_{zi} = -R_1(i)(I_{zi} - I_o) - \sum_j \sigma_{ij} (I_{zi} - I_{zj}) \qquad (1)$$

$$R_1(i) = -\frac{1}{T_1(i)} = \frac{\gamma^4 \hbar^2}{10} \sum_j r_{ij}^{-6} f(\omega) \qquad (2)$$

$$\sigma_{ij} = \frac{\gamma^4 \hbar^2}{10} r_{ij}^{-6} g(\omega) \qquad (3)^{*}$$

where γ and $\hbar$ have their usual meanings, r_{ij} is the interatomic distance between the i and j protons. $R_1(i)$ is the local spin-lattice relaxation rate of the i^{th} proton and σ_{ij} is the term governing the cross relaxation between the i and j protons [20], and

$$f(\omega) = 3J(\omega) + 12J(2\omega) \qquad (4)$$

$$g(\omega) = J(o) - 6J(2\omega) \qquad (5)$$

$J(\omega)$ refers to the spectral density. In the simplest case where the rotational reorientation of the internuclear ij vector is isotropic characterized by a correlation time τ_c , $J(\omega)$ is given by

$$J(\omega) = \tau_c/(1 + \omega^2\tau_c^2) \qquad (6)$$

---

*Pour la commodité du traitement suivant, σ_{ij} a le signe opposé à l'expression (8) du chapitre I, section B.III.

The initial slope of the Log $(I_o - I_{zi}) = f(t)$ curve for the i^{th} proton is given by $R_1(i)$. When the cross relaxation is negligeable i.e. $\sigma_{ij} \ll R_1(i)$, this curve is practically linear and coincides with the tangent at t = o with a slope equal to $R_1(i)$. In the opposite case where $\sigma_{ij} \gg R_1(i)$, the longitudinal relaxation rate of all protons tends to the same mean value $\overline{R_1}$ given by [21-22]

$$\overline{R_1} = \frac{1}{N} \sum_i R_1(i) \tag{7}$$

where N is the total number of interacting protons.

In the intermediate cases, the shape of the magnetization decay curves depends on the relative values of R_1 and $\overline{R_1}$: the curve exhibits a concavity if $R_1(i)$ is greater than $\overline{R_1}$ and a convexity in the opposite case. In order to characterize these non linear curves, one usually uses the time constant T_o corresponding to the time t_o for the zero passage $I_z(t_o) = 0$ and $T_o = 1/R_o = t_o/\text{Log}2$. In this way, $T_o = T_1$ when the cross relaxation is negligeable and the magnetization decay is exponential.

For a given proton system in which the average interatomic distances between protons remain constant, an increase in the cross relaxation effect (by varying ω and τ_c) is correlated with an increase in the ratio g/f

$$\frac{g}{f} = \frac{J(o) - 6J(2\omega)}{3J(\omega) + 12J(2\omega)} \tag{8}$$

For $\omega \tau_c \gg 1$, $J(\omega)$ and $J(2\omega)$ become much smaller than $J(o)$.

The relaxation rate of the transverse magnetization of the i^{th} proton can be expressed as follows [20]

$$\frac{dI_{xi}}{dt} = - R_2(i) \, I_{xi} \tag{9}$$

where $R_2(i)$ is the transverse relaxation rate

$$R_2(i) = \frac{1}{T_2(i)} = \frac{\gamma^4 \hbar^2}{20} \sum_j r_{ij}^{-6} \, h(\omega) \tag{10}$$

For the alike spin system

$$h(\omega) = 9J(o) + 15J(\omega) + 6J(2\omega) \qquad (11)$$

In the case of an unlike spin system (polynucleotide protons with a high magnetic field) where the difference in chemical shift is generally large compared with the linewidth and the scalar coupling constants

$$h(\omega) = 5J(o) + 9J(\omega) + 6J(2\omega) \qquad (12)$$

By measuring the transverse relaxation rate $R_2(i)$, the correlation time τ_c can be determined if the sum $\sum_j r_{ij}^{-6}$ is known. It is of interest to not that apart from the $\omega\tau_c \approx 1$ region, the transverse relaxation rate is practically independent of frequency.

B.I.1. Cross relaxation in isolated single stranded polynucleotides in the randomly coiled state

An interesting problem to study is the cross relaxation effect on proton relaxation rates when $\omega\tau_c >> 1$ and when the local motion of isolated single stranded polynucleotides in solution is assumed to be isotropic and can be characterized by a single correlation time τ_c as in the case of poly I [12] and poly U (see Section B.IV). This problem has theoretically been studied for the case of poly C, the *anti* conformation ($\gamma = 210°$ or $\chi = 30°$) for the base, the N conformation for the ribose and the gg conformation for the exocyclic group ; these conformations have been observed in solution (see Sections B.III and B.IV). In figure 1 the T_o values of the poly C protons obtained from the calculated magnetization decay curves are plotted versus the ratio g/f. The results show that : i) The discrepancies between the $T_o(i)$ values are maximum when the cross relaxation is negligeable i.e. the ratio g/f < 1. ii) When the ratio g/f increases, the T_o values tend to the mean value $1/\overline{R_1}$ given by equation (7). iii) The relaxation rate R_o of H_6 , H_2, and H_3, is very close to the mean $\overline{R_1}$ value and is slightly affected by the cross relaxation even when its contribution is large.

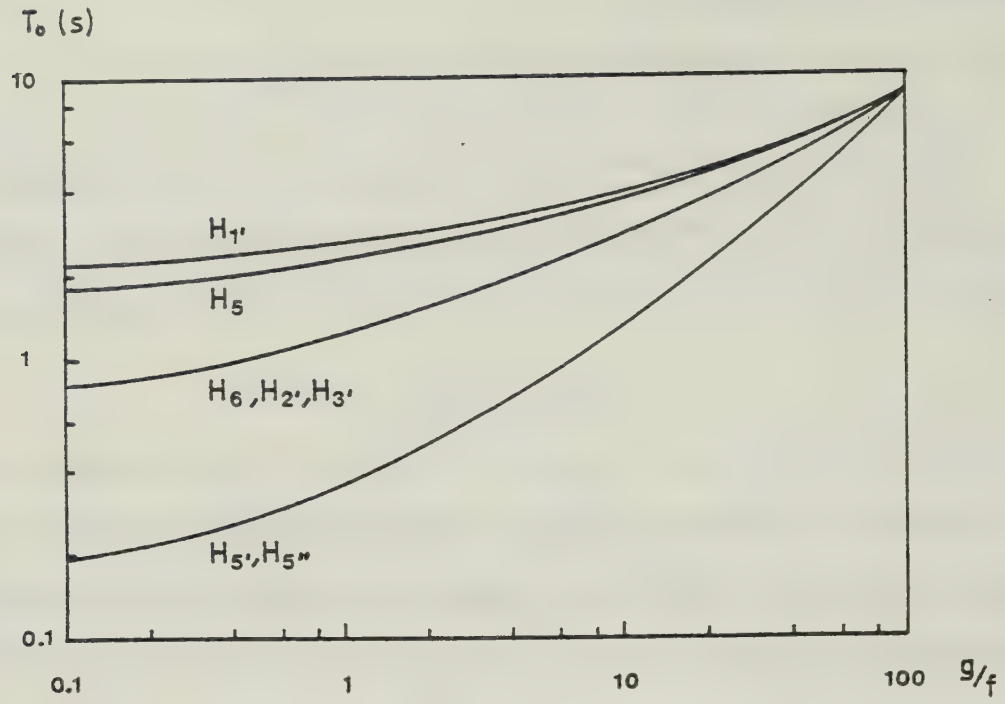

Fig. 1 - Log-Log plot of T_o versus the g/f ratio determined for the poly C protons (see text).

We can therefore expect the Log $(I_o - I_z) = f(t)$ curve of these protons to be linear and slightly deviated from the tangent to the relaxation curves at t = o.

B.I.2. Longitudinal and transverse relaxation of polynucleotide protons in the case of an equilibrium between two forms with different correlation times

In a previous paper [23] we showed that for the case of mononucleotides in solution, the proton Overhauser enhancement can be substantially reduced by the presence of a small amount of large aggregates. Similarly, as a result of the well known possibility for polynucleotides to adopt ordered forms (single or multistranded helices) in solution, proton relaxation rates are expected to depend strongly on the equilibrium between randomly coiled and ordered forms.

The cross relaxation behaviour in the commonly met case of a fast exchange between the randomly coiled and the ordered states whose population and correlation time are p, τ_c and p', τ_c' respectively, is studied by assuming that the conformation of the sugar-base unit is the same and that the isotropic model is applicable to both forms. If $\omega\tau_c' >> 1$ and the lifetime of each form is long compared with the corresponding correlation times, equation (1) remains valid at any given time. Furthermore, if the exchange rate is fast compared with relaxation rates, a time average of equation (1) can be made :

$$\frac{dI_{zi}}{dt} = - \langle R_1(i) \rangle (I_{zi} - I_o) - \sum_j \langle \sigma_{ij} \rangle (I_{zi} - I_{zj}) \qquad (13)$$

Where

$$\langle R_1(i) \rangle = \frac{\gamma^4 \hbar^2}{10} \sum_j r_{ij}^{-6} [3\langle J(\omega) \rangle + 12\langle J(2\omega) \rangle] \qquad (14)$$

$$\langle \sigma_{ij} \rangle = \frac{\gamma^4 \hbar^2}{10} r_{ij}^{-6} [\langle J(o) \rangle - 6\langle J(2\omega) \rangle] \qquad (15)$$

The spectral density functions J(ω) and J(o) in equations (14) and (15) are replaced by :

$$\langle J(\omega) \rangle = pJ(\omega, \tau_c) + p'(\omega, \tau_c')$$

$$= p \frac{\tau_c}{1 + \omega^2 \tau_c^2} + p' \frac{\tau_c'}{1 + \omega_c^2 \tau_c'^2} \qquad (16)$$

$$\langle J(o) \rangle = p\tau_c + p'\tau_c' \qquad (17)$$

with $p + p' = 1$.

The average ratio $\langle g \rangle / \langle f \rangle$ which reflects the cross relaxation contribution is given by

$$\frac{\langle g \rangle}{\langle f \rangle} = \frac{pg + p'g'}{pf + p'f'} \qquad (18)$$

where f' and g' are given by equations (4) and (5) respectively in which τ_c is replaced by τ_c'.

In the case where $\omega\tau_c \approx 1$ and $\tau_c \ll \tau_c'$, $J(\omega,\tau_c) \gg J(\omega,\tau_c')$ while $J(o,\tau_c) \ll J(o,\tau_c')$. Consequently, if the ordered state proportion, p', is relatively small, the time average value of $\langle R_1(i)\rangle$ remains close to the $R_1(i)$ value of the randomly coiled form. In contrast, under the same conditions, the cross relaxation term $\langle\sigma_{ij}\rangle$ which contains J(o) increases substantially and hence the ratio $\langle g\rangle/\langle f\rangle$.

Ex : When τ_c = 1 nsec, τ_c' = 100 nsec and p' = 10%, $\langle R_1(i)\rangle$ decreases only by 10% while J(o) increases by about 1000% and the ratio $\langle g\rangle/\langle f\rangle$ is equal to 6 instead of 0.24 for the randomly coiled form.

As far as the transverse relaxation rate is concerned, in the case of a fast exchange between randomly coiled and ordered forms, a time average of equation (10) can be taken

$$\langle R_2(i)\rangle = \frac{\gamma^4 h^2}{20} \sum_j r_{ij}^{-6} \left[5\langle J(o)\rangle + 9\langle J(\omega)\rangle + 6\langle J(2\omega)\rangle\right] \qquad (19)$$

Unlike $R_1(i)$, $R_2(i)$ contains J(o) and will therefore be strongly affected by the presence of a small population or ordered state with a long correlation time τ_c'. Under the conditions mentioned in the above example, the average transverse relaxation rate $\langle R_2(i)\rangle$ is about six times greater than $R_2(i)$ for the randomly coiled form while the ratio $\langle R_1(i)\rangle/R_1(i)$ is close to 1. The linewidth at half height of the H_6 proton for example is about 6 Hz instead of 1 Hz in the case of isolated single stranded polynucleotides in the randomly coiled state.

B.II. EXPERIMENTAL SECTION

Poly U and poly C containing no free salt were purchased from GIPEP (France). According to the supplier, its average molecular weight, estimated from the sedimentation velocity measurements is about 300,000. The products were either dialysed extensively against a solution of 5.10^{-4} M EDTA, 5×10^{-3} M NaCl, pH ≃ 7 using the flow dialysis method or dissolved directly in water containing ≃ 10^{-3} M EDTA and the pH was adjusted to 7-8 by addition of a small amount of NaOH. The NMR results obtained are practically independent of the sample preparation method.

The samples were lyophilized twice in ^2H_2O and redissolved in ^2H_2O at a final concentration of 0.01 M in monomer units. These solutions were introduced into NMR tubes, degassed in a vacuum line and sealed.

^{1}H-NMR spectra were recorded at 250 MHz on a CAMECA-TSN 250 and at 90 MHz on a Bruker WH 90. Proton relaxation times, T_1, were obtained by the inversion recovery method (180°-τ-90°) and the chemical shifts were measured with an accuracy better than 0.005 ppm from 3-(trimethylsilyl)-($^2H_4$) propionic acid (TMP)

B.III. RESULTS

B.III.1. Temperature effects on chemical shifts and coupling constants

The chemical shifts and coupling constants J_{H-H} of poly U and poly C were measured versus temperature at 250 MHz. In Tables I and II are summarized the results obtained at two extreme temperature values 25°C and 72°C.

The results clearly show that in this temperature range, $J_{1',2'}$ of poly U is considerably higher than $J_{1',2'}$ of poly C : this indicates that the ribose conformations of these two polynucleotides are quite different. The temperature effect on δ and J_{HH} is relatively strong for poly C and negligeable for poly U. The $H_{5'}$, $H_{1'}$, $H_{3'}$ signals of poly C are shifted to

Table I - ^{1}H chemical shifts (in ppm from TMP) of poly U and poly C in $^{2}H_2O$ at neutral pH.

Compounds	H_6	H_5	$H_{1'}$	$H_{2'}$	$H_{3'}$	$H_{4'}$	$H_{5'}$	$H_{5''}$
Poly U 25°C	7.881	5.929	5.959	4.434	4.670	4.470	4.249	4.143
Poly U 72°C	7.841	5.932	5.952	4.431	4.671	4.455	4.227	4.135
Δδ	-0.040	0.003	-0.007	-0.003	0.001	-0.015	-0.022	-0.008
Poly C 25°C	7.778	5.785	5.641	4.355	4.422	4.394	4.180	4.110
Poly U 72°C	7.835	5.959	5.823	4.312	4.546	4.398	4.200	4.113
Δδ	0.057	0.174	0.182	-0.043	0.124	0.004	0.020	0.003

Table II - ^{1}H-^{1}H and ^{31}P-^{1}H coupling constants (in Hz) of poly U and poly C in $^{2}H_2O$ at neutral pH.

Compounds	J_{56}	$J_{1'2'}$	$J_{2'3'}$	$J_{3'4'}$	$J_{4'5'}$	$J_{4'5''}$	$J_{5'5''}$	$J_{3'P}$	$J_{5'5''P}$
Poly U 25°C	8.0	5.5	5.2	3.5	2.0	3.0	10.5	7.5	4.5
Poly U 72°C	8.0	5.5	5.3	3.5	2.3	4.2	11.5	7.8	4.8
Poly C 25°C	7.5	1.0	a)	a)	a)	a)	a)	a)	a)
Poly C 72°C	7.6	2.7	5.0	6.5	3.0	3.0	12.0	8.5	~2.5

a) unresolved resonance signals at 25°C.

lower fields by about 0.1 ppm and $J_{1'2'}$ increases from 1.0 to 2.7 Hz when the temperature increases from 25°C to 72°C. These effects were observed to remain practically unchanged with a fourfold dilution and therefore seem to be due to the interaction between residues of the same strand.

B.III.2. Effects of temperature and frequency on relaxation times

Proton relaxation times of poly U and poly C were measured as a function of temperature at 90 and 250 MHz.

a) Poly U

The longitudinal magnetization decay curves of all protons are practically linear whatever the temperature and frequency. The longitudinal relaxation times T_1 calculated from the initial slope of these curves are plotted versus temperature in figure 2.

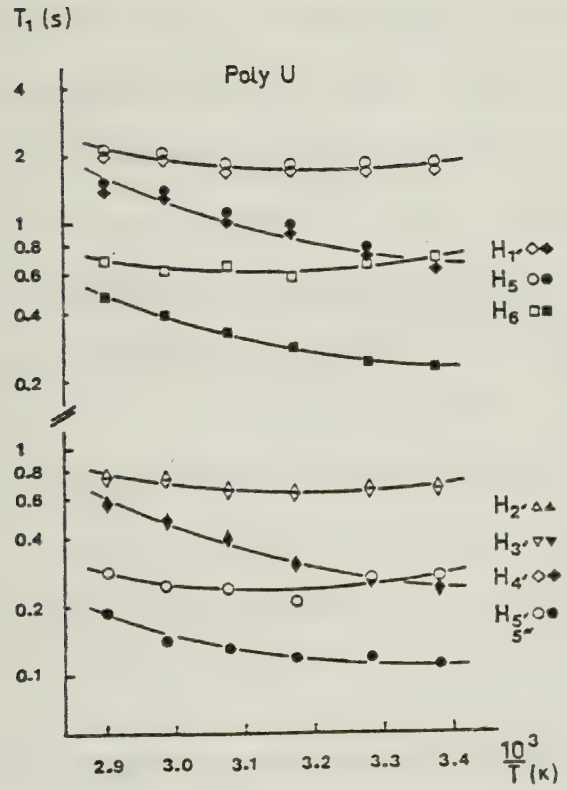

Figure 2

Temperature dependence of longitudinal relaxation times T_1 of poly U protons measured at 90 and 250 MHz (filled and opened symbols respectively).

As expected, the proton relaxation times T_1 are frequency dependent : $T_1(250) > T_1(90)$ whatever the temperature. Inspection of the data in figure 2 reveals three important points :

i) The ratio $T_1(90)/T_1(250)$ at a given temperature is practically the same for all protons and increases by about 100% as the temperature increases from 22°C to 72°C

$$T_1(90)/T_1(250) = 0.37 \pm 0.06 \quad \text{at} \quad 22°C$$
$$T_1(90)/T_1(250) = 0.73 \pm 0.09 \quad \text{at} \quad 72°C$$

ii) The variation of T_1 with temperature is less pronounced at 250 MHz than at 90 MHz.

iii) The extreme narrowing conditions are far from being satisfied even at low frequency (90 MHz).

b) Poly C

The longitudinal magnetization decay of protons does not always exhibit a simple exponential behaviour for all temperatures in the interval between 25°C and 72°C. Figure 3 shows the typical curves of poly C protons obtained at 25°C for frequencies of 90 and 250 MHz. Curves corresponding to H_6 , H_2' , H_3' are found to be fairly straight line as expected (see section B.I) while the H_5 and H_1' curves are convex and the H_5' , H_5'' curve is concave. This behaviour is clearly observed for $t < 52°C$ at 250 MHz and $t < 37°C$ at 90 MHz.

In figure 4, the longitudinal relaxation times T_o corresponding to the zero passage $I_z = 0$ (see section B.I) of the poly C protons versus temperature are plotted at both frequencies (90 and 250 MHz). Some interesting remarks can be made about the data in fig. 4 :

i) When $t > 52°C$, the ratio $T_1(90)/T_1(250)$ is almost constant for all protons, similar to the case of poly U. At 72°C, this ratio is smaller for poly C (= 0.48) than for poly U (= 0.73) indicating that the mobility of these polynucleotides is not the same.

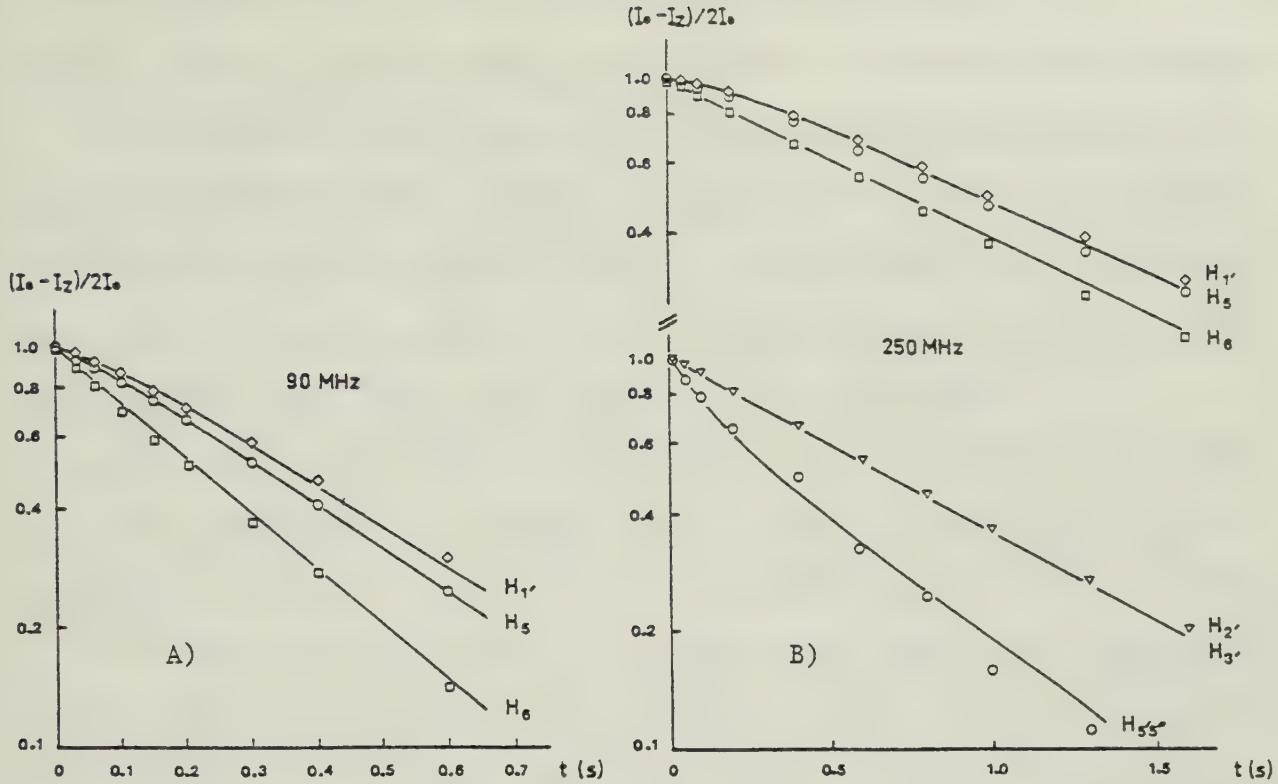

Fig. 3 - Longitudinal magnetization decay of poly C protons at 25°C. Experimental results and simulated curves. A) at 90 MHz ; B) at 250 MHz.

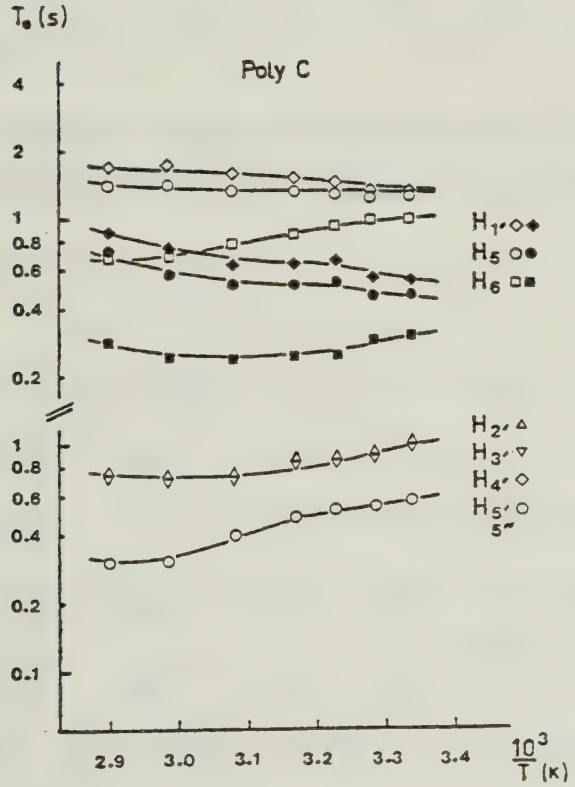

Figure 4

Temperature dependence of longitudinal relaxation times T_0 of poly C protons measured at 90 and 250 MHz (filled and opened symbols respectively).

ii) On lowering the temperature from 52°C to 22°C, the T_o values measured at 250 MHz tend to converge to the same mean value : the T_o value of H_5 and $H_{1'}$ decreases while that of $H_{5'}$, $H_{5''}$ increases, they all tend to approach the average value of H_6 , $H_{2'}$ and $H_{3'}$. This behaviour which remains practically unchanged with a fourfold dilution has also been observed at 90 MHz but at lower temperatures (t < 37°C).

It is important to note that while the longitudinal relaxation times are similar for the two polynucleotides studied, the proton linewidths are much larger in poly C (4-8 Hz whatever the frequency) than in poly U (≃ 1 Hz) at room temperature. On increasing the temperature, the proton linewidths decrease and above 42°C, they are almost the same for both polynucleotides. Table III summarizes the transverse relaxation times T_2 of the poly C protons for temperatures less than 42°C. The ratio of the longitudinal relaxation times of $H_{1'}$ and H_6 , $T_o(H_{1'})/T_o(H_6)$, determined from the proton relaxation data in figure 4 was found to be close to 1 ; in contrast the ratio $T_2(H_{1'})/T_2(H_6)$ is about twice as high as the previous ratio for given temperatures less than 42°C. The latter ratio corresponds very well with that of the calculated sum $\sum_j r_{ij}^{-6}$ of these two protons.

Table III - Temperature dependence of transverse relaxation times T_2 (in ms) of poly C protons measured at 90 and 250 MHz. The values in brackets correspond to the linewidths at half-height (in Hz).

T°	H_6				H_5		$H_{1'}$	
	250 MHz		90 MHz		250 MHz		250 MHz	
25°C	40	(8.0)	45	(7.0)	65	(5.0)	80	(4.0)
32°C	50	(6.0)	70	(4.5)	110	(3.0)	160	(2.0)
42°C	110	(3.0)	110	(3.0)	320	(1.0)	320	(1.0)

B.IV. DISCUSSION

B.IV.1. Poly U and poly C conformations

It is surprising that the S conformer proportion of the poly U ribose calculated from the coupling constants $J_{1'2'}$ and $J_{3'4'}$ (S = 60%) is higher than for the corresponding mononucleotides (S = 44%) 3'UMP and (55%) for 5'UMP [11] and the difference in S proportion is even more substantial when compared with dinucleotide monophosphates containing a U residue (S = 32% in ApU, 38% in GpU and 44% in UpU [11, 24, 25]). Furthermore, in contrast with dimers, the S proportion of poly U remains unchanged with temperature.

Poly C manifests a quite different behaviour : the N conformation is strikingly predominant (> 90%) and is much larger than that observed with monomers (51% in 5'CMP, 59% in 3'CMP) and in unstacked dimers such as CpA (66%) and CpG (58%) [11, 25, 26]. Dimers, which exhibit strong intra- and intermolecular interactions such as ApC and GpC also favour the N conformation (74% and 71% respectively). The ribose conformation of poly C is therefore very similar to that of RNA [27]. On the basis of this similarity and the temperature effect on proton chemical shifts and coupling constants, we suggest that single stranded poly C probably possesses a helical or partially helical structure while poly U exhibits a clear preference for the random coil in agreement with optical results [1, 2, 3].

The relaxation time T_1 ratio between two sugar protons $H_{1'}$ and $H_{3'}$ at a given frequency $T_1(H_{1'})/T_1(H_{3'})$ is found to be about 2.5 for both poly U and poly C ; the base proton H_6 is thus far from the sugar protons $H_{1'}$; this indicates that the *anti* conformation is favoured in these two polynucleotides. The mean interatomic distance $\langle r_{1'-6} \rangle$ (= 3.6 Å) computed from the T_1 values (eq. (2)) confirms this conclusion.

B.IV.2. Dynamic structure of poly U and poly C

a) Poly U

From information obtained in ^{1}H-NMR relaxation studies at two different frequencies (90 and 250 MHz) (Fig. 2), very similar relaxation behaviours are shown to exist for poly U and poly I [12]. The correlation time τ_c distribution can therefore be considered as uniform within the sugar-base unit undergoing isotropic motion and the reorientation of H-H vectors may be characterized by a single correlation time τ_c.

The τ_c values deduced from the ratio $T_1(90)/T_1(250)$ using the method described in a recent paper [12] are plotted versus reciprocal absolute temperature (Fig. 5). A straight line is obtained suggesting that the motion of the ribose-base unit of poly U in the temperature interval between 22°C and 72°C is governed by a single process in accordance with the isotropic model. The activation energy is found to be 4 kcal/mole in agreement with the values (5.1 kcal/mole) given by Aksaka et al. [7].

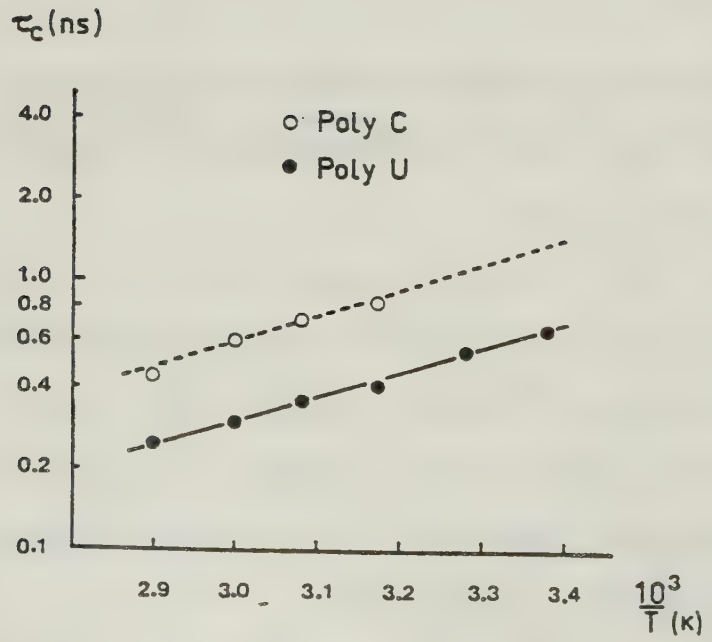

Figure 5

Temperature dependence of correlation times τ_c for poly U -●-●- and poly C --- o ---.

b) Poly C

Above 52°C, the linearity of the Log $(I_o - I_z) = f(t)$ curves and the constant value of the ratio $T_1(90)/T_1(250)$ for all poly C protons at a given temperature indicate very similar dynamic structures for the three polynucleotides : poly C ($t > 52°C$), poly U and poly I [12]. The longitudinal relaxation data can therefore be interpreted using a single correlation time τ_c , characteristic of the local motion of an isolated single strand in the randomly coiled state in solution. It should be noted that the τ_c values obtained from the ratio $T_1(90)/T_1(250)$ are in good agreement with those obtained from T_2 measurements and the sum $\sum_j r_{ij}^{-6}$ computed for the *anti* N and gg conformation ($\gamma = 210°$ or $\chi = 30°$). As a result, the τ_c values for $37°C < t < 52°C$ have been calculated from the T_1 data obtained at 90 MHz using the latter method since in this temperature interval the longitudinal magnetization decay of all poly C protons exhibits a simple exponential behaviour at 90 MHz but not at 250 MHz. The results are reported in figure 5. The τ_c values of poly C between 72°C and 37°C are about twice as high as those of poly U but the Log $\tau_c = f(1/T)$ curves of both polymers are practically parallel.

Below 37°C, the non linearity of the longitudinal magnetization decay curves and the convergence of T_o toward the same mean value whatever the frequency indicate that the cross relaxation mechanism becomes very active in poly C under these experimental conditions. In a very recent communication, Broido and Kearns [28] have also observed an important cross relaxation effect between H_5 and $H_{1'}$. By using an isotropic model with a single correlation time, these authors have found a very short internuclear distance $r_{5-1'}$ (< 2.9 Å) however attempts to build right handed helical models for poly C consistent with the X ray data [29] have been unsuccessful. In the light of our relaxation data, the strong cross relaxation effect observed for all poly C protons is somewhat surprising since this sort of mean T_o value (≃ 1 sec) at 250 MHz corresponds, in an isotropic model, to relatively

small τ_c values ($\simeq$ 1 nsec) for which the cross relaxation effect is weak at 250 MHz and quite negligible at 90 MHz. In an isotropic model, the τ_c value should be at least 10 nsec and the mean T_o value five times greater for such a convergence in T_o be observed. The fact that the ratio of the longitudinal relaxation times $T_o(H_1')/T_o(H_6)$ is close to 1 while the ratio $T_2(H_1')/T_2(H_6)$ is at least twice as high as the previous ratio (see the result section) and corresponds very well with that of the calculated sum $\sum_j r_{ij}^{-6}$ of these two protons for a monomer unit, rules out the possibility of a short distance between H_5 and H_1'. On the other hand, the transverse relaxation times calculated from the linewidths of the poly C protons correspond to a τ_c value of about 15 to 20 nsec much higher than the above mentioned value deduced from the longitudinal relaxation times. Therefore, in contrast to poly U and poly I, the single correlation time model is not suitable for poly C in the 22°C - 37°C temperature interval.

A priori, other models involving either a correlation time distribution [14,15] (a τ_c distribution for the backbone and a single τ_c for the sugar-base unit) or two or several correlation times [16-19] (for the ribose and the base) may be considered. Nevertheless, these two models are found to be inconsistent with the relaxation data for the following reasons :

i) On the basis of the proton T_1 ratios, $T_1(90)/T_1(250)$ the motion of the ribose-base unit in poly U and poly I can be described using a single correlation time model even at room temperature.

ii) Similarly for poly C above 52°C, the relaxation data can be interpreted using the same model ; whereas in a two or several correlation time model, the difference in correlation times (between the backbone and side groups) generally increases with temperature.

iii) The base (H_5) and ribose (H_1') protons whose sums $\sum_j r_{ij}^{-6}$ are practically the same, exhibit a similar longitudinal relaxation behaviour (same T_o values and similar magnetization decay curves), indicating that the base and the ribose have the same mobility.

We have tested a model involving two correlation times, the one, τ_c, corresponding to a fast motion as in the case of a random coil and the other, τ_c', to a slow motion with $\tau_c' \gg \tau_c$. However we were not able to fit the 3 parameters, $R_1(i)$, σ_{ij} and $R_2(i)$ simultaneously and explain why on the one hand the longitudinal relaxation rates correspond to a short τ_c ($\approx$ 1 nsec) and on the other the cross relaxation effect and the transverse relaxation rates are compatible with a much longer correlation time. In fact, it has been shown in the theoretical section that this apparent contradiction resulting from the T_1 and T_2 data can simply be explained by considering the case of an equilibrium in solution of two forms whose population and correlation time are p, τ_c and p', τ_c' respectively : $R_1(i)$, σ_{ij} and $R_2(i)$ become the average values. Since only the two last terms contain $J(o)$ (equations (3) and (10)) and when $\omega\tau_c \approx 1$ and $\tau_c' \gg \tau_c$, a small population p' can cause (via the $\langle J(o) \rangle$ term) a great variation for σ_{ij} and $R_2(i)$ but not for $R_1(i)$

Owing to the well known ability of poly C to adopt helical or partially helical conformations [2, 3, 6, 29] or to be in a randomly coiled form with continuously fluctuating regions of helicity [1], it appears reasonable to consider at low temperature the case of an equilibrium between the random coil with a relatively small τ_c and the single stranded helix with a much longer correlation time τ_c'. Furthermore, Fasman et al. [3] observed a gradual transition between the helix and the random coil and in the present paper, the poly C proton linewidths were found to decrease on raising the temperature indicating a fast exchange between these two forms. Under these conditions the proton relaxation rates thus depend on τ_c, τ_c' and the proportions of the randomly coiled (p) and ordered (p') forms ; the cross relaxation effect and the proton line broadening become substantial even with a small p' proportion while the longitudinal relaxation times are slightly affected. It is important noting that the

following data processing is still valuable for the case of an equilibrium between the random coil and the associated form involving two or more than two strands.

. Calculation of τ_c , τ_c' and p, p'

The linearity of the Log $\tau_c = f(1/T)$ curve (Fig. 5) for t > 37°C suggests that, in the temperature interval between 37°C and 25°C, the τ_c value of poly C in the randomly coiled form can be obtained by extrapolation of the straight line in figure 5. A τ_c value of 1.25 nsec has been obtained at 25°C.

The longitudinal relaxation rates of H_6 , H_2, and H_3, measured at 25°C (Fig. 4) correspond to an apparent correlation time of about 1 to 2 nsec which is close to the above mentioned value (1.25 nsec) for the random coil. Therefore, we can suppose without going into details about the calculation that the randomly coiled form is still largely predominant in the temperature interval between 25°C and 37°C and that τ_c' should be longer than 15 nsec to cause such an observed cross relaxation effect and line-broadening.

The ratio p/p' can be calculated from equation (18) :

$$\frac{p}{p'} = \frac{g' - \frac{\langle g \rangle}{\langle f \rangle} f'}{\frac{\langle g \rangle}{\langle f \rangle} f - g} \qquad (20)$$

where f' and g' are obtained by replacing τ_c with τ_c' in $f(\omega,\tau_c)$ and $g(\omega,\tau_c)$ respectively.

$g(\omega,\tau_c)$ and $f(\omega,\tau_c)$ can be computed by replacing the ω and τ_c (1.25 nsec) values in equations (4) and (5). By using the curve in figure 1, the ratio $\langle g \rangle / \langle f \rangle$ can be approximately determined from the ratio of the longitudinal relaxation times T_o between poly C protons at a given frequency and temperature : $T_o(H_1,)$: $T_o(H_5)$: $T_o(H_6)$: $T_o(H_2,$ or $H_3,)$: $T_o(H_5,$, $H_5,,)$ in figure 3. The following results were obtained at 25°C :

Frequency	g	f	g/f	<g>/<f>
90 MHz	-1.25	7.4	-0.17	1.8
250 MHz	0.8	1.7	0.47	10.0

It is worth noting that the ratio <g>/<f> is much greater than the ratio g/f for the randomly coiled form and that the difference between these two ratios increases with frequency.

As it can be seen from equation (20), each value of τ_c' (and hence of $g'(\omega,\tau_c')$ and $f'(\omega,\tau_c')$) corresponds to a single value of p'. Table IV sums up the pair of value of τ_c' and p' in the τ_c' interval between 20 and 100 nsec for the two frequencies (90 and 250 MHz). We have found very good agreement between two sets of data computed independently from the T_o measurements at two different frequencies.

Table IV - Proportions p' of poly C single stranded helix calculated from equation (20) with various correlation times, τ_c', between 20 and 100 ns at 90 and 250 MHz.

τ_c'	p' (90 MHz)	p' (250 MHz)
20	0.44	0.45
30	0.34	0.35
40	0.28	0.29
50	0.22	0.24
60	0.20	0.22
70	0.18	0.19
80	0.16	0.18
90	0.14	0.16
100	0.13	0.15

The solution found to equation (13) and the comparison between the simulated and experimental magnetization decay curves at 90 and 250 MHz (Fig. 3) are in favour of an equilibrium involving :

$$p = 77\% \qquad \tau_c = 1.25 \text{ nsec}$$
$$p' = 23\% \qquad \tau_c' = 50 \text{ nsec} \qquad \text{at } 25°C$$

This τ_c' value of 50 nsec for the ordered form is in good agreement with that given by Early and Kearns [30] for high molecular weight DNA's and by Yamada et al. [31] for poly G where the multistranded complex is highly predominant at room temperature.

The same method has been used to determine p' for temperatures below 52°C for which the effect of the ordered form on the proton relaxation is significant (Table V).

Table V - Calculated and experimental values of H_6 proton transverse relaxation time T_2 (in ms) at 250 and 90 MHz. The p' proportions of poly C single stranded helix (with a τ_c' value of 50 ns) were determined from the proton longitudinal relaxation time measurements.

T°	p'	T_2 (250 MHz)		T_2 (90 MHz)	
		Exp. value	Calc. value	Exp. value	Calc. value
25°C	0.23	40	48	45	44
32°C	0.18	50	65	70	60
42°C	0.07	110	127	110	114

By replacing in equation (19) the values of p, p', τ_c , τ_c' determined from the longitudinal relaxation data, the transverse relaxation times obtained are found to be very consistent with the experimental T_2 values at the same temperature (Table V).

c) Mobility in polynucleotides

At relatively high temperatures t > 52°C, all the relaxation data of poly I, poly U, poly A and poly C can be correctly interpreted using an isotropic model involving a single correlation time. All these polynucleotides show a random coil behaviour with a correlation time of less than one nanosecond for the local motion of the ribose-base unit. However the degree of mobility is slightly different for the different polynucleotides and can be classified, on the basis of correlation time, in the following order : Poly U > poly I > poly A > poly C (Table VI).

Table VI - Correlation times (in ns) of polynucleotides and DNA's in $^{2}H_2O$ deduced from ^{13}C-, ^{1}H- and ^{2}H-NMR relaxation data.

Compounds	τ_c at 22°C	τ_c at 62°C
Poly I a)	0.7	0.4
Poly U	0.7	0.3
Poly A b) c)	1.5	0.5
Poly C	1.2/50	0.6
Poly G d)	50	
DNA e)	> 50	

a) Ref. [12] ; b) Ref. [32] ;
c) Neumann and Tran-Dinh unpublished results ;
d) Ref. [29] ; e) Ref. [28].

At room temperature, either the randomly coiled or the ordered forms (single or multistranded helices) or an equilibrium between these two forms can be observed ; this depends on the polymer studied. The small τ_c values and the linearity of the Log τ_c = f(1/T) curve in the 22°C - 72°C temperature interval indicate that in solution poly U and poly I [12]

exist in the random coil state. In contrast, poly A shows the behaviour of a single stranded partially ordered molecule in which the bases tend to be st acked up one upon another [32-34]. In the case of poly C, the relaxation data in the present paper clearly indicate that for t < 52°C the random coil is in equilibrium with a proportion of the single stranded helix. Poly G represents a particular case where the multistranded complex is highly predominant at room temperature. The τ_c value of the ordered form is found to be the same for poly C and poly G [31] and similar to that observed for high molecular weight DNA's [30].

REFERENCES

1. MICHELSON, A.M., MASSOULIE, J. and GUSCHLBAUER, W. (1967) Progress in Nucleic Acid Research, DAVIDSON, T.N. and COHN, W.E., Eds, Academic, New York, p. 83.

2. BRAHMS, J. (1963) J. Am. Chem. Soc. 85, 3298.

3. FASMAN, G.D., LINDBLOW, C. and GROSSMAN, L. (1964) Biochemistry 3, 1015.

4. RICHARDS, E.G., FLESSEL, C.P. and FRESCO, J.R. (1963) Biopolymers 1, 431.

5. DANIEL INNERS, L. and FELSENFELD, G. (1970) J. Mol. Biol. 50, 373.

6. CHOU, C.H. and THOMAS, Jr., G.J. (1977) Biopolymers 16, 765.

7. AKASAKA, K., YAMADA, A. and HATANO, H. (1977) Bull. Chem. Soc. Jpn. 50 2858.

8. SMITH, I.C.P., JENNINGS, H.J. and DESLAURIERS, R. (1975) Accounts of Chem. Res. 8, 306.

9. MANTSCH, H.H. and SMITH, I.C.P. (1972) Biochem. Biophys. Res. Commun. 46, 808.

10. GOVIL, G. and SMITH, I.C.P. (1975) Biopolymers 12, 2589.

11. DAVIES, D.B. (1978) Progress in NMR Spectroscopy, Pergamon Press, Oxford, 12, 135.

12. NEUMANN, J.M. and TRAN-DINH, S. (1981) Biopolymers 20, 89.

13. HEATLEY, F. (1979) Progress in NMR Spectroscopy, Vol. 13, EMSLEY, J.W., FEENEY, J. and STUCLIFFE, L.H., Eds, Pergamon Press, New York, p. 212.

14. SHAEFER, J. (1973) Macromolecules 6, 881.

15. SHINDO, H. (1980) Biopolymers 19, 509.

16. WOESSNER, D.E., SNOWDEN, B.S. and MEYER, G.H. (1969) J. Chem. Phys. 59, 719.

17. JONES, A.A. (1977) J. Polym. Sci. Polym. Phys. Ed. 15, 863.

18. LAUPRÊTRE, F., NOËL, C. and MONNERIE, L. (1977) J. Polym. Sci. Polym. Phys. Ed., 15, 2127.

19. BOLTON, P.H. and JAMES, T.L. (1979) J. Phys. Chem. 83, 3359.

20. SOLOMON, I. (1955) Phys. Rev. 99, 559.

21. KALK, A. and BERENDSEN, H.J.C. (1976) J. of Mag. Res. 24, 343.

22. CAMPBELL, I.D. and FREEMAN, R. (1973) J. of Mag. Res. 11, 143.

23. TRAN-DINH, S., GUSCHLBAUER, W. and GUERON, M. (1972) J. Am. Chem. Soc. 94, 7903.

24. LEE, C.H., EZRA, F.S., KONDO, N.S., SARMA, F.H. and DANYLUK, S.S. (1976) Biochemistry 15, 3627.

25. EZRA, F.S., LEE, C.H., KONDO, N.S., DANYLUK, S.S. and SARMA, R.H. (1977) Biochemistry 16, 1977.

26. TRAN-DINH, S., NEUMANN, J.M. and BORREL, J. (1981) Biochim. Biophys. Acta 655, 167.

27. ARNOTT, S., DOVER, S.D. and WONACOTT, A.J. (1969) Acta Cryst. B25, 2192.

28. BROIDO, M.S. and KEARNS, D.R. (1980) J. Magn. Reson. 41, 496.

29. ARNOTT, S., CHANDRASEKARAN, R. and LESLIE, A.G.W. (1976) J. Mol. Biol. 106, 735.

30. EARLY, T.A. and KEARNS, D.R. (1979) Proc. Natl. Acad. Sci. USA, 76, 4165.

31. YAMADA, A., AKASAKA, K. and HATANO, H. (1978) Biopolymers 17, 749.

32. LENG, M. and FELSENFELD, G. (1966) J. Mol. Biol. 15, 455.

33. BRAHMS, J., MICHELSON, A.M. and Van HOLDE, K.E. (1966) J. Mol. Biol. 15, 467.

34. AKASAKA, K. (1974) Biopolymers 13, 2273.

CONCLUSION

La plupart de nos études en RMN de la conformation et de la structure dynamique des mono-, oligo- et polynucléotides en solution ont été effectuées en résonance du proton, qui est présent sur la base et sur le sucre des résidus nucléotides, intrinsèquement plus sensible que le ^{13}C et dont l'abondance isotopique naturelle avoisine 100%.

Cependant, l'analyse spectrale en RMN-^{1}H est souvent complexe à cause du nombre des signaux de résonance observés et l'interprétation des mesures de relaxation, difficile, parce qu'influencées par différents facteurs (variations de conformation, de mobilité). C'est pourquoi nous avons été conduits à développer plusieurs méthodes d'étude tant au niveau des spectres que de celui de la relaxation.

En particulier, la mise au point de procédures d'analyse des spectres en proton des fragments d'ADN en solution nous permet d'obtenir des informations sur la conformation du cycle du déoxyribose des différents résidus dont on sait qu'elle est directement reliée au type de structure réalisée (A, B, Z). L'étude de l'évolution des déplacements chimiques des protons non échangeables, en fonction de la température, complète celle des protons des groupes NH et NH_2 et constitue un moyen simple d'évaluer les paramètres thermodynamiques de la transition hélice-pelote statistique (constante de dissociation, enthalpie).

Par ailleurs, l'interprétation, par différentes méthodes, de l'effet Overhauser proton-proton et des temps de relaxation des protons, combinée à la deutération sélective, nous renseigne sur l'équilibre *syn/anti* de la conformation de la base par rapport au sucre des mono-, oligo- et polynucléotides en solution. Dans ces molécules, les mesures des temps de relaxation des protons, mais aussi dans certains cas du ^{13}C, ^{31}P et ^{2}H, à plusieurs fréquences et en fonction de la température, constituent la base de l'étude de leur structure dynamique. Le cas d'un mélange de conformations (plusieurs temps de corrélation) et son effet sur la relaxation a été étudié et appliqué à plusieurs exemples. L'ensemble de ces méthodes ont un caractère général et restent valables pour les études à venir sur des composés similaires ou d'autres produits.

L'ensemble des mono-, oligo- et polynucléotides étudiés dans ce travail présentent une grande variété de conformations possibles inhérentes aux mouvements *syn* $\leftrightharpoons$ *anti* et N $\leftrightharpoons$ S en particulier.

Nous avons montré que la structure chimique de la base des résidus et leur séquence conditionnent la flexibilité et la conformation, de sorte que leurs variations constituent, sans doute, un mode d'expression de l'information biologique. Par exemple, l'orientation principale de la base de la pseudouridine (ψU) et de ses dérivés est *syn* alors que celle de l'uridine et de ses dérivés est *anti* ; les conformations *anti*, N et gg sont largement plus favorisées dans les résidus de ApC et ApU que dans ceux de CpA et UpA. Plus généralement, les dérivés à base purique apparaissent plus flexibles que ceux à base pyrimidique (des considérations stériques le montrent par ailleurs).

Depuis plusieurs années, la question a été soulevée de savoir s'il existe ou non des corrélations entre les conformations *syn/anti* et N/S. En particulier, Sundaralingam a observé à partir de données cristallographiques de telles corrélations entre les conformations du ribose et celle de

la base par rapport au ribose : association S, *syn* et N, *anti*. Dans ce travail, les résultats obtenus indiquent que des molécules peuvent présenter des conformations du sucre similaires alors que l'orientation de leur base est très différente : la conformation *syn* de la base est plus probable pour les dérivés puriques que pour les dérivés pyrimidiques. Le cas de la pseudouridine et de l'uridine cité plus haut en est un autre exemple.

Hormis les facteurs liés à la structure chimique des molécules, des causes extérieures sont susceptibles de modifier la conformation et la flexibilité, et tout au long de ce travail, l'influence des conditions physicochimiques (concentration, température, pH, etc ...) a été analysée et comparée aux résultats des études antérieures. Parmi l'ensemble de ces facteurs, la température et le pH sont apparus les plus importants. L'effet de température, négligeable au niveau monomère, est sensible dans les oligo- et polynucléotides : d'une manière générale, l'augmentation de la température tend à égaliser les proportions des conformations en équilibre ; l'effet de pH se manifeste notablement, par exemple, avec les résidus à base guanine dont la conformation du sucre change lorsqu'il y a protonation en N_7 de la base.

Si, en ce qui concerne la flexibilité base-sucre, les résidus déoxyribonucléotides présentent, en général, des caractéristiques analogues à celles des résidus ribonucléotides, en particulier l'influence différente d'une purine ou d'une pyrimidine, par contre nous n'avons pas observé (à faible concentration de sel) de variations significatives de la conformation moyenne du déoxyribose comme celles rencontrées avec le ribose. Quelle que soit la nature de la base ou de la séquence et malgré les changements de température ou de concentration, la forme S est toujours prédominante dans les molécules dont le sucre des résidus est le déoxyribose. Parmi celles-ci, l'hexamère à séquence auto-complémentaire dACATGT forme en solution un complexe bicaténaire de type B.

Ce dernier résultat s'inscrit dans l'étude que nous avons poursuivie pour relier la conformation locale des résidus et la structure générale des chaînes et dont l'intérêt est bien évident. Nous avons montré en particulier que l'augmentation des proportions des conformations *anti*, N et gg des résidus des diribonucléosides monophosphates s'associe à des interactions intramoléculaires base-base plus importantes (les interactions intermoléculaires n'affectent pas la conformation dans ce cas) ; la différence de conformation locale entre d'une part poly I, poly U (forme N/S équivalentes) et d'autre part poly C (forme N prédominante) est correlée à une différence de structure : en solution aqueuse neutre, les deux premiers polynucléotides sont sous forme de pelote statistique tandis que poly C présente un mélange forme hélicoïdale-pelote statistique à température ambiante. D'une manière générale, dans les structures les plus ordonnées, la conformation N est favorisée lorsque le sucre est le ribose alors que la conformation S est prédominante lorsque le sucre est le déoxyribose ; cette situation est similaire à celle rencontrée dans les ARN et ADN standards.

Enfin, l'étude de la transition hélice-pelote statistique de dACATGT montre que les paires de base GC contrôlent le processus de dissociation des petits fragments d'ADN : ainsi dans le cas de dATGCAT, la paire GC est en position centrale et l'ouverture des paires de base s'effectue séquentiellement des extrémités vers le centre en trois étapes distinctes, alors que dans le cas de dACATGT, les paires AT extrêmes s'ouvrent en premier, suivies simultanément des paires GC et AT centrales.